NEAR-INFRARED FLUORESCENCE IMAGING IN COLORECTAL CANCER AND ITS METASTASES

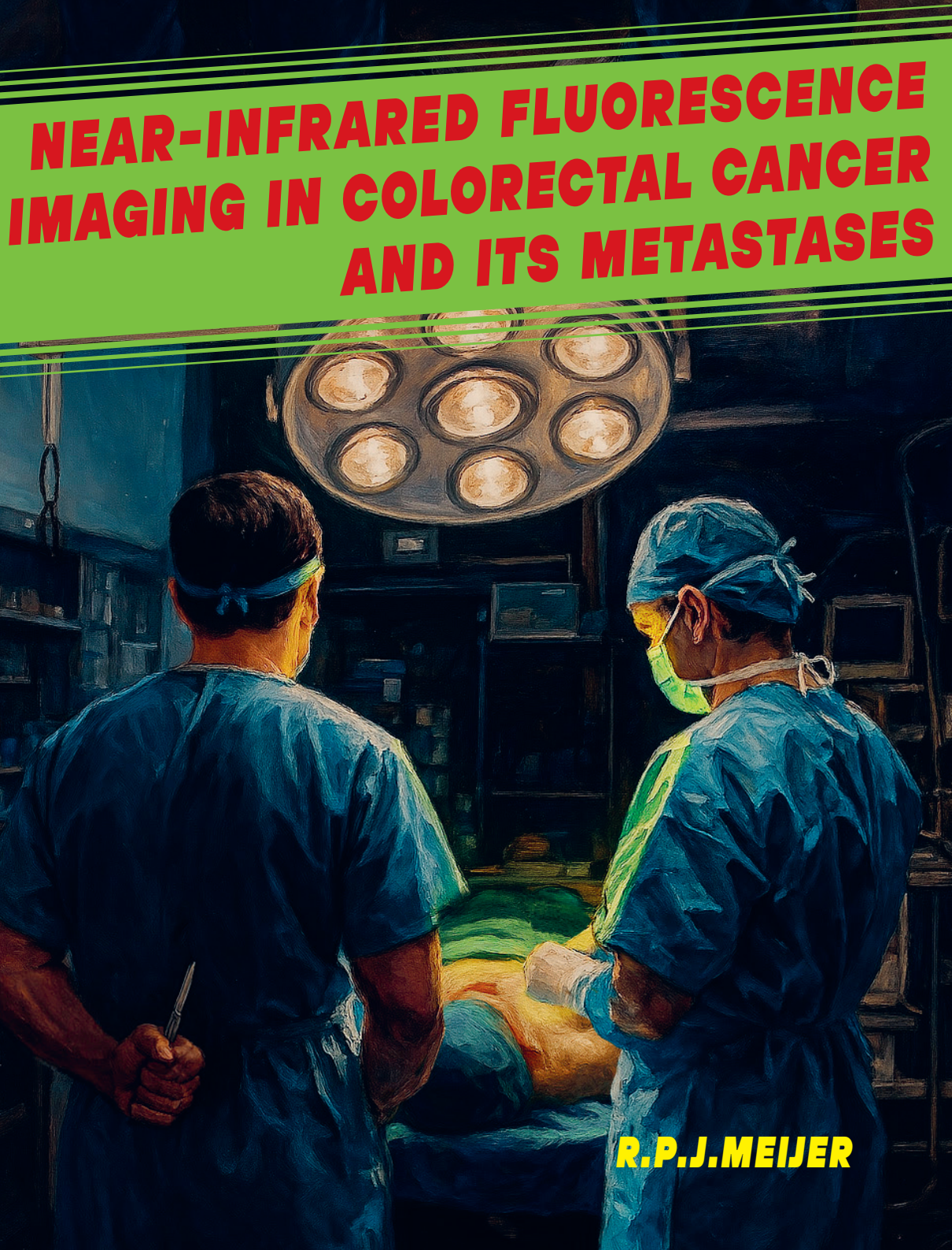

R.P.J.MEIJER

Voor Roos, Mees en Sef

COVER IMAGE
Creative mind: Wineke Cramer, Leiden
Design: Caroline de Lint, Den Haag

DESIGN THESIS
Caroline de Lint, Den Haag

FINANCIAL SUPPORT
The publication of this thesis was financially supported by the foundation Centre for Human Drug Research (CHDR, Leiden, The Netherlands), and Stichting Beroepsopleiding Huisartsen (SBOH).

NEAR-INFRARED FLUORESCENCE IMAGING IN COLORECTAL CANCER AND ITS METASTASES

Proefschrift

ter verkrijging van
de graad van doctor aan de Universiteit Leiden,
op gezag van rector magnificus prof.dr.ir. H. Bijl,
volgens besluit van het college voor promoties
te verdedigen op dinsdag 24 juni 2025
klokke 13:00 uur

door
Ruben Petrus Johannes Meijer
geboren te Voorburg
in 1990

PROMOTORES
Prof. dr. J. Burggraaf
Prof. dr. A.L. Vahrmeijer

CO-PROMOTOR
Dr. D.E. Hilling

LEDEN PROMOTIECOMMISSIE
Prof. dr. V.T.H.B.M. Smit
Dr. L.S. Boogerd *(Antoni van Leeuwenhoek, Amsterdam, NL)*
Prof. dr. E.C.J. Consten *(Meander Medisch Centrum, Amersfoort, NL)*
Prof. dr. P.H.A. Quax

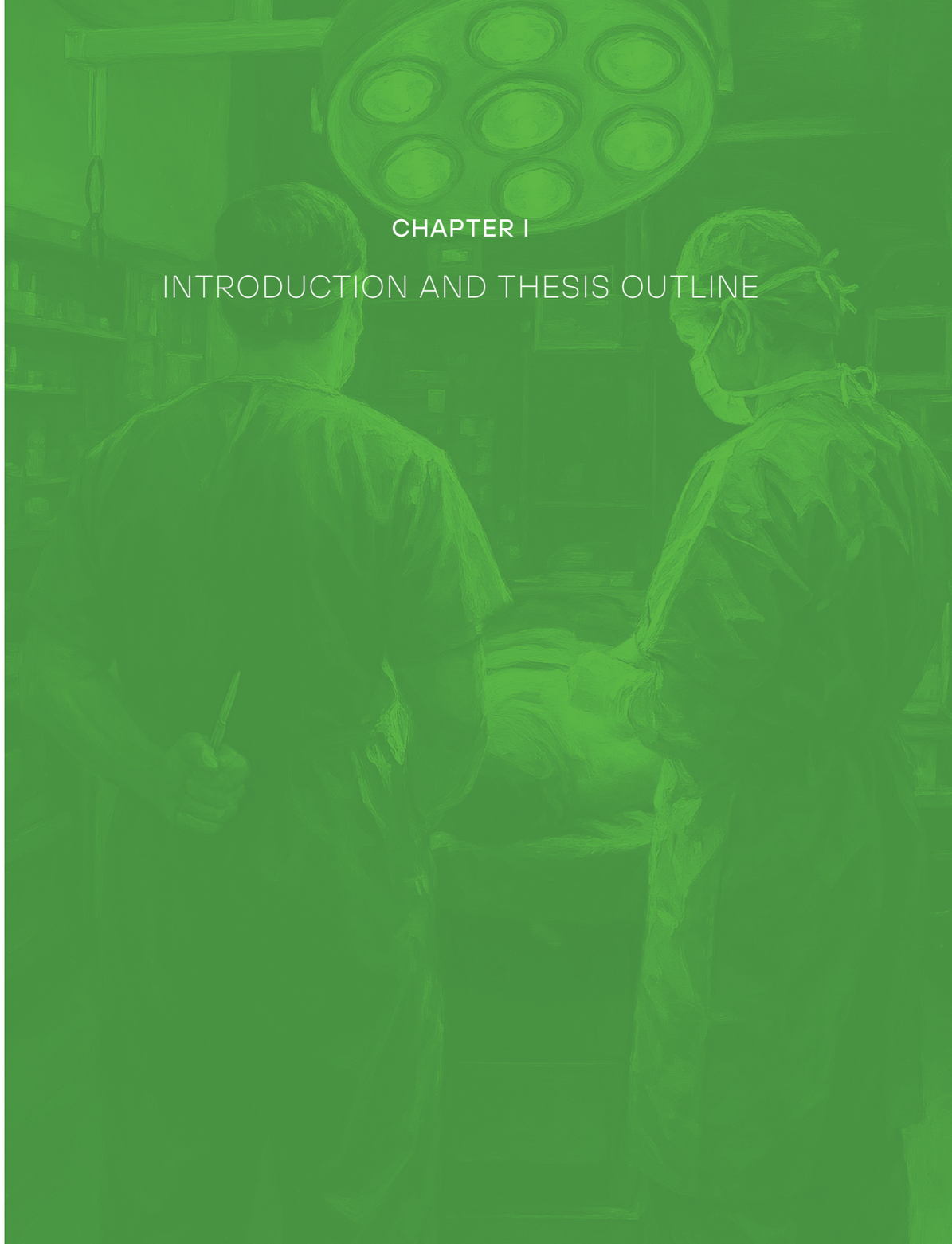

CHAPTER I

INTRODUCTION AND THESIS OUTLINE

Colorectal cancer

With almost 2 million new cases annually worldwide, colorectal cancer (CRC) is one of the most frequent diagnosed malignancies and the second cause of cancer related deaths.[1] Despite implemented screening programs and improved non-invasive treatment options, surgery is still the primary approach for colorectal cancer. Surgical success is based on two major outcome measures: complete tumor resection (including metastases) and surgical complications. Ensuring tumor-negative resection margins is of utmost importance, as tumor-positive resection margins are associated with a significant decrease in overall survival.[2,3] In addition, surgical complications, like anastomotic leakage (AL) and nerve damage are dreaded because of their impact on quality of life and, in the case of AL, the risk of reoperations, with increased mortality.[4,5] Therefore, it is crucial to identify comprised tissue perfusion at the anastomosis site and to differentiate between tumor tissue and vital structures. Although, the integration of minimally invasive and robotic surgery had great advantages, it came at the expense of this differentiation, given the absence of tactile feedback.

Moreover, identifying tumor tissue becomes even more challenging in cases that have undergone prior resection or neoadjuvant treatment. This results from the development of scar tissue, making it challenging to distinguish between fibrosis and remaining tumor tissue, both visually and tactically. Novel intraoperative identification techniques could provide the surgeon with a solution.

Near-infrared fluorescence imaging

Near-infrared (NIR) fluorescence imaging offers the potential of improved visual feedback during surgery. By employing fluorescence imaging principles, it enhances surgical outcomes by providing real-time intraoperative visual feedback of the surgical field. This technology can aid surgeons in discriminating malignant tissue from healthy tissue effectively. It can potentially improve oncological outcome and protect vital structures. NIR fluorescence imaging relies on the administration or application of a fluorescent contrast agent that selectively accumulates in the target tissue. NIR fluorescence imaging is a real-time imaging technique that combines a NIR fluorescent agent with a specialized imaging system (figure 1). These systems can capture light emitted by a fluorescent agent after excitation with an appropriate light source. NIR light (650-900 nm) is favorable for intraoperative imaging compared to visible light because of its better depth penetration in tissue (up to 10 mm). Moreover, the fluorescent agents will not interfere with the standard surgical field, as the human eye is unable to detect light within these NIR wavelengths. During surgical procedures a NIR light source can be strategically placed above the patient or be integrated within the laparoscopic system. The resulting fluorescence can be instantly visualized in real-time on the camera system screens in the form of images with color, overlay, and NIR representations, allowing surgeons to interpret the information seamlessly. NIR fluorescent agents are predominantly injected intravenously and can be divided into two groups: targeted (binding to a specific ligand or activated by the tumor-specific environment) and non-targeted. Currently, various targeted fluorescent agents are tested in phase I-III clinical trials.[6] In this thesis the focus was on SGM-101.

FIGURE 1 The basics of near-infrared fluorescence imaging.
Near-infrared (NIR) fluorescent agents can be administered either intravenously or locally, and their imaging is conducted using a specialized fluorescence imaging system. This system comprises a white light source, a standard camera, a dedicated NIR excitation light, collection optics and filtration, and a camera specifically for capturing NIR fluorescence emission. The NIR fluorescence output is displayed on a screen in the operating theatre. Ideally, a simultaneous visible light image is captured and can be merged with the NIR fluorescence image for enhanced visualization.

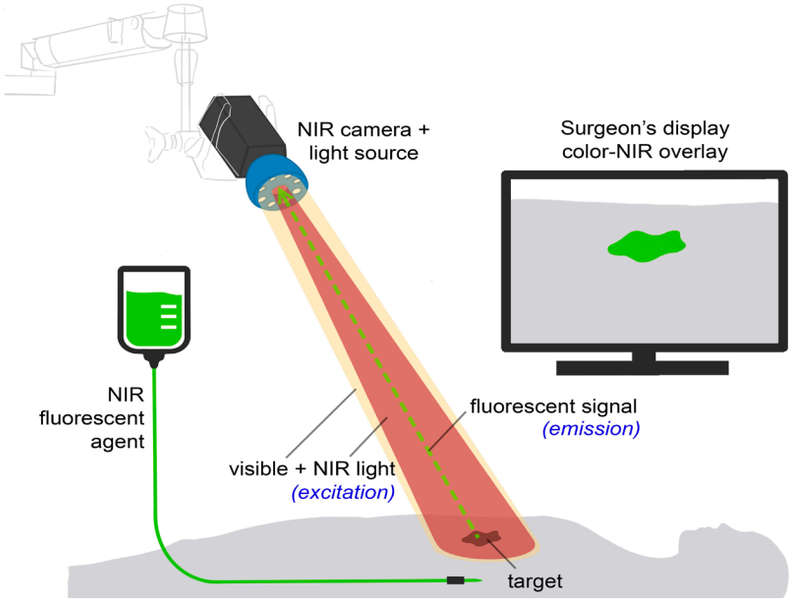

Only a handful of tumor-targeted fluorescent agents have been tested in early phase clinical trials for colorectal cancer. One of these agents is SGM-101, a monoclonal antibody targeting the carcinoembryonic antigen (CEA) bound to the fluorophore BM-104.[7] CEA is notably overexpressed in numerous solid tumors. Specifically, CEA expression is observed in approximately 90% of colorectal adenocarcinomas and 70% of pancreatic adenocarcinomas.[8,9] A phase II study, consisting of 37 patients, showed the first promising clinical results of SGM-101.[10] Based on fluorescence assessment, the surgical plan was changed in nine (24%) patients. In seven patients, fluorescence led to resection of malignant lesions that were not identified with white light only. In two patients, clinically suspected but non-fluorescent tissue was proven to be benign, which resulted in a less extensive resection. These promising results are the basis of the multiple clinical trials described in this thesis.

PERFUSION ASSESSMENT

AL is among the most serious complications in CRC surgery, frequently necessitating additional surgical or radiological interventions, leading to a prolonged hospital stay. AL is reported up to 20% of patients undergoing CRC surgery with associated mortality rates as high as 27%.[11,12]

Inadequate bowel perfusion is considered a significant contributing factor to AL.[13,14] Indocyanine green (ICG) fluorescence-angiography can provide real-time feedback of bowel perfusion and aid to determine in the optimal location for the anastomosis.[15] During the procedure ICG is injected intravenously, and its fluorescence allows for dynamic monitoring of blood flow. This information helps surgeons identify regions with compromised blood supply, which may indicate areas at risk of ischemia or necrosis. By incorporating NIR fluorescence perfusion assessment into standard of care, surgeons could optimize surgical outcomes by preserving well-perfused tissues and minimizing the risk of postoperative complications like anastomotic leakage. Pooled analysis of cohort studies has demonstrated that ICG fluorescence angiography reduces anastomotic leakage, but high-quality evidence is currently lacking. This has led to our initiation of a Dutch multicenter randomized controlled trial assessing the influence of NIR fluorescence perfusion assessment on AL, the AVOID trial.

LYMPH NODE ASSESSMENT

In CRC patients, accurate lymph node staging is crucial for determining prognosis and treatment decisions. Especially the sentinel lymph node (SLN), the first lymph node draining the tumor, seems important for nodal staging because it is believed to be the first place for lymphogenic metastases. Moreover, approximately one-third of patients with stage I and II colon cancer, who are staged as lymph node-negative, still develop distant metastases.[16] This may result from understaging by histopathology, attributed to the presence of lymph nodes with occult malignant cells and micrometastases. Current routine histopathological analysis typically involves the examination of a single paraffin-embedded slide per lymph node, which increases the likelihood of missing tumor cells not located at the slide's cutting surface. More extensive histopathological analysis of all resected lymph nodes could enhance nodal staging, but this process is time-consuming and costly.[17-19] However, extensive analysis of only the SLN is feasible, and thus unfolds a niche for SLN mapping in CRC. Fluorescent dyes like ICG, offer promise for SLN mapping, both *in vivo* and *ex vivo*.[20,21]

Though techniques like ICG mapping show high success rates, they also face issues such as false negatives due to skip metastases.[22] Despite these challenges, fluorescence-guided SLN mapping shows potential for improving staging and guiding treatment decisions in CRC, warranting further exploration and optimization of techniques.

Over the past decade NIR fluorescence-guided surgery has developed from the preclinical stage to initial small-scale (first-in-human) clinical trials. A significant challenge now lies in transitioning these promising results to more extensive clinical trials, as presented in this thesis. These large-scale trials must unequivocally demonstrate patient benefit, such as enhanced complete tumor resections and reduced complication rates, for the technique to be integrated into standard care surgical practices.

Thesis outline

In this thesis, clinical applications of fluorescence guided surgery in colorectal cancer and its metastases are described. It focusses on the clinical use of both targeted and non-targeted fluorescent agents with the use of dedicated open and minimal invasive NIR camera systems. As a result, this thesis will provide insights into the future development and implementation of this technology within the realm of colorectal surgery. Part I of this thesis starts with a review of the current status of fluorescence-guided surgery in colorectal cancer **(chapter 2)**. Subsequently the use of ICG in sentinel node detection **(chapter 3)** and perfusion assessment **(chapter 4, chapter 5)** in colorectal cancer surgery will be

explored. In part II several clinical studies using the CEA-targeted fluorescence tracer SGM-101 will be highlighted. The first chapter **(chapter 6)** will be an outline of the development of this targeted fluorescent agent. This will be followed by chapters about the detection of distant liver metastases of colorectal and pancreatic cancer **(chapter 7)**, the detection of colorectal lung metastases **(chapter 8)** and the detection of both primary lung cancer and colorectal lung metastases **(chapter 9)**. In part III a study for the identification of novel targets for fluorescence-guided lung surgery with the use of data driven software was performed **(chapter 10)**.

REFERENCES

1 Sung H, Ferlay J, Siegel RL, Laversanne M, Soerjomataram I, Jemal A, *et al.* Global Cancer Statistics 2020: GLOBOCAN Estimates of Incidence and Mortality Worldwide for 36 Cancers in 185 Countries. CA Cancer J Clin. 2021;71(3):209-49.

2 Amri R, Bordeianou LG, Sylla P, Berger DL. Association of Radial Margin Positivity With Colon Cancer. JAMA Surg. 2015;150(9):890-8.

3 Nagtegaal ID, Quirke P. What is the role for the circumferential margin in the modern treatment of rectal cancer? J Clin Oncol. 2008;26(2):303-12.

4 Bakker IS, Grossmann I, Henneman D, Havenga K, Wiggers T. Risk factors for anastomotic leakage and leak-related mortality after colonic cancer surgery in a nationwide audit. Br J Surg. 2014;101(4):424-32; discussion 32.

5 Buchs NC, Gervaz P, Secic M, Bucher P, Mugnier-Konrad B, Morel P. Incidence, consequences, and risk factors for anastomotic dehiscence after colorectal surgery: a prospective monocentric study. Int J Colorectal Dis. 2008;23(3):265-70.

6 Hernot S, van Manen L, Debie P, Mieog JSD, Vahrmeijer AL. Latest developments in molecular tracers for fluorescence image-guided cancer surgery. Lancet Oncol. 2019;20(7):e354-e67.

7 Gutowski M, Framery B, Boonstra MC, Garambois V, Quenet F, Dumas K, *et al.* SGM-101: An innovative near-infrared dye-antibody conjugate that targets CEA for fluorescence-guided surgery. Surg Oncol. 2017;26(2):153-62.

8 de Geus SW, Boogerd LS, Swijnenburg RJ, Mieog JS, Tummers WS, Prevoo HA, *et al.* Selecting Tumor-Specific Molecular Targets in Pancreatic Adenocarcinoma: Paving the Way for Image-Guided Pancreatic Surgery. Mol Imaging Biol. 2016;18(6):807-19.

9 Tiernan JP, Perry SL, Verghese ET, West NP, Yeluri S, Jayne DG, *et al.* Carcinoembryonic antigen is the preferred biomarker for *in vivo* colorectal cancer targeting. Br J Cancer. 2013;108(3):662-7.

10 de Valk KS, Deken MM, Schaap DP, Meijer RP, Boogerd LS, Hoogstins CE, *et al.* Dose-Finding Study of a CEA-Targeting Agent, SGM-101, for Intraoperative Fluorescence Imaging of Colorectal Cancer. Ann Surg Oncol. 2021;28(3):1832-44.

11 Sparreboom CL, Komen N, Rizopoulos D, Verhaar AP, Dik WA, Wu Z, *et al.* A multicentre cohort study of serum and peritoneal biomarkers to predict anastomotic leakage after rectal cancer resection. Colorectal Dis. 2020;22(1):36-45.

12 Angeramo CA, Dreifuss NH, Schlottmann F, Bun ME, Rotholtz NA. Postoperative outcomes in patients undergoing colorectal surgery with anastomotic leak before and after hospital discharge. Updates Surg. 2020;72(2):463-8.

13 Vignali A, Gianotti L, Braga M, Radaelli G, Malvezzi L, Di Carlo V. Altered microperfusion at the rectal stump is predictive for rectal anastomotic leak. Dis Colon Rectum. 2000;43(1):76-82.

14 Kologlu M, Yorganci K, Renda N, Sayek I. Effect of local and remote ischemia-reperfusion injury on healing of colonic anastomoses. Surgery. 2000;128(1):99-104.

15 van Manen L, Handgraaf HJM, Diana M, Dijkstra J, Ishizawa T, Vahrmeijer AL, *et al.* A practical guide for the use of indocyanine green and methylene blue in fluorescence-guided abdominal surgery. J Surg Oncol. 2018;118(2):283-300.

16 Figueredo A, Coombes ME, Mukherjee S. Adjuvant therapy for completely resected stage II colon cancer. Cochrane Database Syst Rev. 2008;2008(3):CD005390.

17 Doekhie FS, Mesker WE, Kuppen PJ, van Leeuwen GA, Morreau H, de Bock GH, *et al.* Detailed examination of lymph nodes improves prognostication in colorectal cancer. Int J Cancer. 2010;126(11):2644-52.

18 Liefers GJ, Cleton-Jansen AM, van de Velde CJ, Hermans J, van Krieken JH, Cornelisse CJ, *et al.* Micrometastases and survival in stage II colorectal cancer. N Engl J Med. 1998;339(4):223-8.

19 Yamamoto H, Murata K, Fukunaga M, Ohnishi T, Noura S, Miyake Y, *et al.* Micrometastasis Volume in Lymph Nodes Determines Disease Recurrence Rate of Stage II Colorectal Cancer: A Prospective Multicenter Trial. Clin Cancer Res. 2016;22(13):3201-8.

20 Chand M, Keller DS, Joshi HM, Devoto L, Rodriguez-Justo M, Cohen R. Feasibility of fluorescence lymph node imaging in colon cancer: FLICC. Tech Coloproctol. 2018;22(4):271-7.

21 Nishigori N, Koyama F, Nakagawa T, Nakamura S, Ueda T, Inoue T, *et al.* Visualization of Lymph/Blood Flow in Laparoscopic Colorectal Cancer Surgery by ICG Fluorescence Imaging (Lap-IGFI). Ann Surg Oncol. 2016;23 Suppl 2:S266-74.

22 Bao F, Zhao LY, Balde AI, Liu H, Yan J, Li TT, *et al.* Prognostic impact of lymph node skip metastasis in Stage III colorectal cancer. Colorectal Dis. 2016;18(9):O322-9.

PART 1

NIR FLUORESCENCE IMAGING IN COLORECTAL CANCER SURGERY

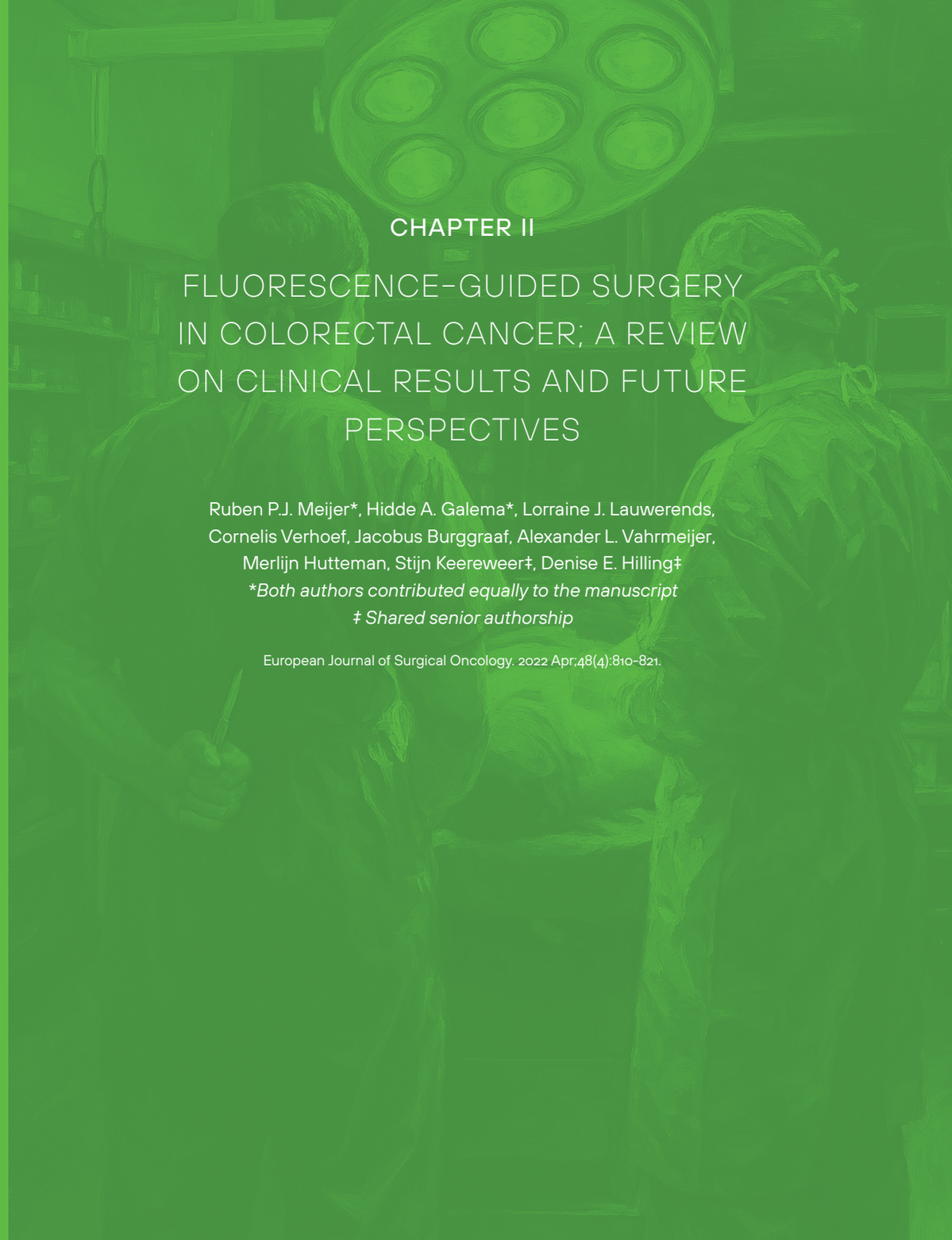

CHAPTER II

FLUORESCENCE-GUIDED SURGERY IN COLORECTAL CANCER; A REVIEW ON CLINICAL RESULTS AND FUTURE PERSPECTIVES

Ruben P.J. Meijer*, Hidde A. Galema*, Lorraine J. Lauwerends, Cornelis Verhoef, Jacobus Burggraaf, Alexander L. Vahrmeijer, Merlijn Hutteman, Stijn Keereweer‡, Denise E. Hilling‡

**Both authors contributed equally to the manuscript*

‡ Shared senior authorship

European Journal of Surgical Oncology. 2022 Apr;48(4):810-821.

Abstract

BACKGROUND Colorectal cancer is the fourth most diagnosed malignancy worldwide and surgery is one of the cornerstones of the treatment strategy. Near-infrared (NIR) fluorescence imaging is a new and upcoming technique, which uses an NIR fluorescent agent combined with a specialised camera that can detect light in the NIR range. It aims for more precise surgery with improved oncological outcomes and a reduction in complications by improving discrimination between different structures.

METHODS A systematic search was conducted in the Embase, Medline and Cochrane databases with search terms corresponding to 'fluorescence-guided surgery', 'colorectal surgery', and 'colorectal cancer' to identify all relevant trials.

RESULTS The following clinical applications of fluorescence guided surgery for colorectal cancer were identified and discussed: (1) tumour imaging, (2) sentinel lymph node imaging, (3) imaging of distant metastases, (4) imaging of vital structures, (5) imaging of perfusion. Both experimental and FDA/EMA approved fluorescent agents are debated. Furthermore, promising future modalities are discussed.

CONCLUSION Fluorescence-guided surgery for colorectal cancer is a rapidly evolving field. The first studies show additional value of this technique regarding change in surgical management. Future trials should focus on patient related outcomes such as complication rates, disease free survival, and overall survival.

Introduction

Colorectal cancer (CRC) is globally the fourth most common malignancy and the second cause of cancer related mortality with over 550 000 deaths annually.[1] In most CRC patients, surgery remains the cornerstone of treatment. Complete surgical resection of the tumour is associated with better overall survival and lower recurrence rates.[2,3] Minimal invasive surgery, laparoscopic or robot-assisted, is increasingly used in the last two decades. Despite it its advantages, this application also brought new technical challenges as it lacks tactile feedback for tumour identification and identification of vital structures. These challenges sparked the interest in novel intraoperative visualisation techniques, such as near-infrared (NIR) fluorescence imaging.

FIGURE 1 The basic principles of fluorescence-guided surgery.
NIR fluorescent agents are administered intravenously or locally. Imaging of the agent is performed using a fluorescence imaging system. Besides a white light source and camera, this system includes a dedicated NIR excitation light, collection optics and filtration, and a camera dedicated to NIR fluorescence emission light. NIR fluorescence output is displayed on a screen in the operating theatre. A simultaneous visible light image, which can be merged with the NIR fluorescence image, is desirable.

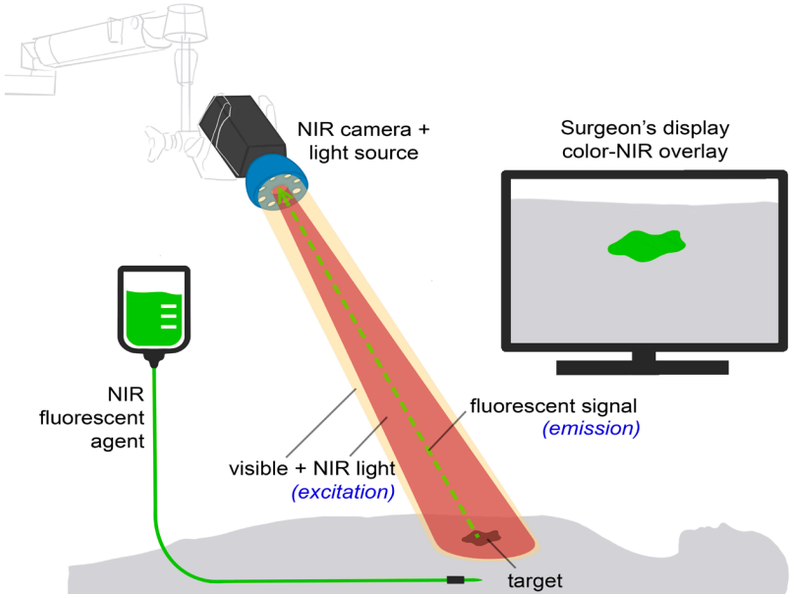

fluorescent agent with a specialised imaging system (figure 1). These systems can capture light emitted by a fluorescent agent after excitation with an appropriate light source (figure 2). NIR light (650-900 nm) is favourable for intraoperative imaging compared to visible light because of its better depth penetration in tissue (up to 10 mm). Moreover, the fluorescent agents will not interfere with the standard surgical field, as the human eye is unable to detect light within these NIR wavelengths.

FIGURE 2 The basic principles of fluorescence.
NIR fluorescent agents are administered intravenously or locally. Imaging of the agent is performed using a fluorescence imaging system. Besides a white light source and camera, this system includes a dedicated NIR excitation light, collection optics and filtration, and a camera dedicated to NIR fluorescence emission light. NIR fluorescence output is displayed on a screen in the operating theatre. A simultaneous visible light image, which can be merged with the NIR fluorescence image, is desirable.

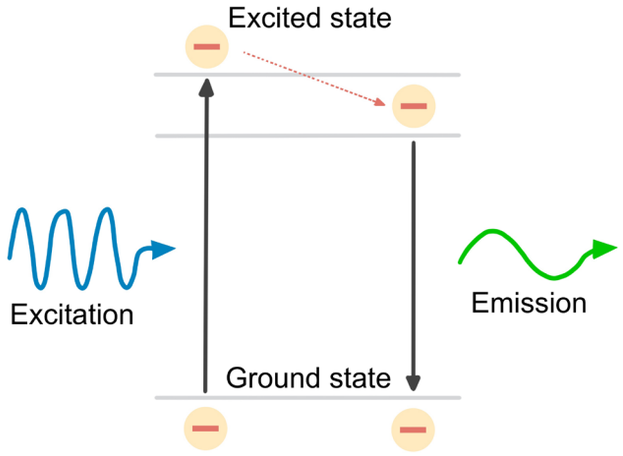

NIR fluorescent agents are predominantly injected intravenously and can be divided into two groups: targeted (binding to a specific ligand or activated by the tumour-specific environment) and non-targeted. Currently, various targeted fluorescent agents are tested in phase I-III clinical trials.[4] In the group of non-targeted agents, indocyanine green (ICG) and methylene blue (MB) are approved by the United States Food and Drug Administration (FDA) and the European Medicines Agent (EMA), for other purposes. ICG was first used in 1957 to determine hepatic function, but its fluorescent properties (excitation peak around 800 nm), and hence other applications, became known decades later.[5] MB on the other hand, is predominantly cleared renally and has its excitation peak around 700 nm.[6] Both agents have been proven to be safe for fluorescence utilisation.

There are many applications for NIR fluorescence imaging during colorectal surgery. This review provides an overview of the currently available clinical applications and promising future modalities of fluorescence-guided surgery in the treatment of CRC patients.

Methods

Due to heterogeneity in available literature and study phases between the several subjects, this study was not fully conducted according to the PRISMA guidelines.

LITERATURE SEARCH AND SELECTION CRITERIA

A systematic search was conducted in the Embase, Medline and Cochrane databases with search terms corresponding to 'fluorescence-guided surgery', 'colorectal surgery', and 'colorectal cancer'. The search strategy was expanded with terms to identify articles reporting on vital structure imaging and colorectal metastases. Supplement 1 shows the search strategies per database and its corresponding hits. The last search was conducted on December 21st, 2020. All articles were independently screened based on title and abstract by two authors (HG and RM). Next, full article screening and reference screening was performed. Inconsistencies were discussed with an additional author (DH). Regarding experimental fluorescent agents, all clinical studies were included in the final reference list. Regarding ICG and MB, the final reference list was generated based on the quality of the article and the amount of scientific evidence available per subject. Articles on the following subjects were included: fluorescence-guided surgery for CRC for the imaging of the primary tumour, lymph nodes, metastases (peritoneal, liver, extra-abdominal), vital structures (nerve, ureter, urethra), and perfusion (anastomosis, omentoplasty). Only articles in English and published after the year 2000 were considered.

DATA EXTRACTION

The following data was extracted: tumour type, fluorescent agent, fluorescence imaging application, (optimal) dose, (optimal) dosing interval, optimal tumour-to-background (TBR), sensitivity, specificity, change in surgical management, and other outcomes.

QUALITY ASSESSMENT

Quality assessment was performed for all studies assessing experimental fluorescent agents. The Methodological index for non-randomized studies (MINORS score) was used for quality assessment. A total score of 16 (for non-comparative studies) or 24 (for comparative studies) could be obtained.[7]

Results

A total of 14 completed clinical studies (supplement 2) and 8 ongoing trials (supplement 3) assessing experimental fluorescent agents for CRC surgery were identified. Figure 3 gives an overview of all clinical applications of fluorescence-guided surgery (FGS) for CRC, with the assessed fluorescent agents (table 1). All 14 clinical studies regarding experimental fluorescence agents had a MINORS score of 11 or higher (supplement 4).

FIGURE 3 A schematic overview of all clinical applications of fluorescence guided surgery for colorectal cancer.

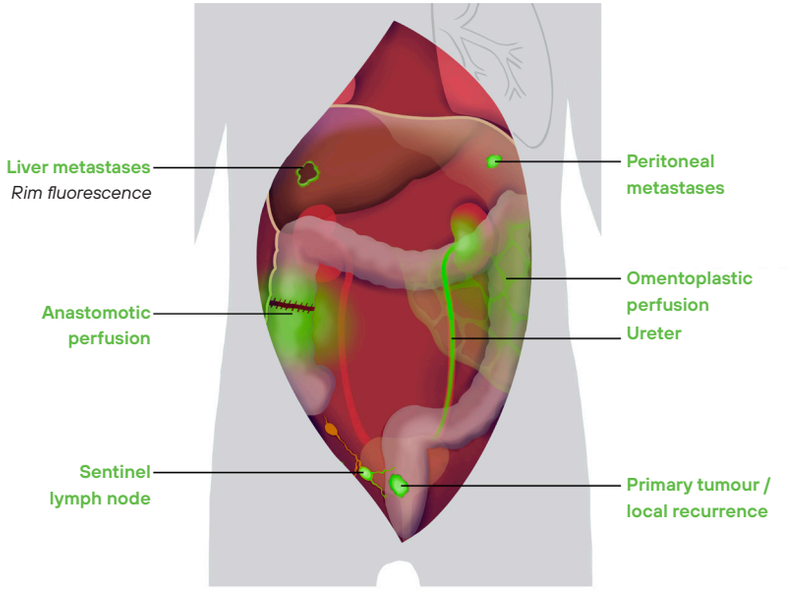

Abbreviations: ICG Indocyanine Green | MB: Methylene blue

IMAGING OF THE PRIMARY TUMOUR AND LOCAL RECURRENCE

Achieving tumour-negative resection margins is of utmost importance in the surgical treatment of CRC patients, as tumour-positive resection margins are associated with a significant decrease in overall survival.[2,8] Tumour-positive resection margins are reported in 5% of all colon cancer cases, but occur more frequently with increasing tumour stage, with an occurrence of up to 14% in T4 colon cancer.[2] Moreover, in primary locally advanced rectal cancer the proportion of tumour-positive resection margins is reported up to 28%.[8] This rate is even higher in patients with recurrent rectal cancer, where up to 50% tumour-positive resection margins are reported.[9] These high rates in recurrent rectal cancer are likely a consequence of the distorted anatomy and treatment related fibrosis after previous resection and (re-)neoadjuvant treatment. Tumour identification is challenging in these cases due to the difficult distinction (both visual and tactile) between fibrosis and residual tumour tissue.

Preoperative endoscopic tattooing with India ink, a permanent marker injected distal to the tumour, is the current standard of care for intraoperative tumour identification in CRC, with an accuracy rate of 70-88%.[10,11] However, India ink can leak into the abdominal cavity and thereby interfere with the surgical procedure.

TABLE 1 Overview of all fluorescent agents used for colorectal cancer surgery and their optical properties.

Fluorescent Agent	Molecular target	Fluorophore	~Peak absorbance wavelength	~Peak emission wavelength	Reference
Bevacizumab-800CW	VEGF-A	IRDye-800CW	778 NM	794 NM	21
cRGD-ZW800-1	Integrins (αvβ6, αvβ3, αvβ5)	ZW800-1	785 NM	805-850 NM	69
HSA800	NA	IRDye-800CW	778 NM	795 NM	21
ICG	NA	ICG	780 NM	830 NM	5
IRDye-800BK	NA	IRDye-800BK	774 NM	790 NM	72
IS-001	NA	IS-001	780 NM	815 NM	70
LUM015	Cathepsins (K,L,S,B)	Cy5	650 NM	675 NM	22
MB	NA	MB	667 NM	685 NM	6
ONM-100	Metabolic acidosis*	ICG	780 NM	830 NM	5
SGM-101	CEA	BM-104	685 NM	705 NM	19
ZW800-1	NA	ZW800-1	785 NM	805-850 NM	69

*Activated in a tumour-specific pH-environment
Abbreviations: VEGF-A vascular endothelial growth factor alpha | NM nanometre | ICG indocyanine green | MB methylene blue | CEA carcinoembryonic antigen | NA not applicable

In 2009, the first NIR fluorescence imaging technique to identify the primary tumour in CRC was introduced by injecting ICG peritumoural via endoscopy. It has a high tumour identification rate (100%) and minimal adverse events.[12,13] However, a major drawback is the relatively rapid clearance of ICG, as detection rates tend to decrease two to seven days after injection.[12] Therefore, patients must undergo an additional endoscopy in the week before surgery, in contrast to the conventional injection of India ink that can be administered at the initial, diagnostic colonoscopy. Because of these drawbacks, peritumoural ICG injection has not been widely implemented for tumour identification. Moreover, this technique will not improve the tumour-negative resection margin rates because it does not differentiate between tumour tissue and benign surrounding tissue, nor does it enable the detection of additional lesions. A potential solution is the use of fluorescent agents that specifically bind to tumour cells.

The number of tumour-targeted fluorescent agents has substantially increased in the past two decades. The use of these agents is aimed to achieve complete tumour resection. This should lead to a decrease in the number of tumour-positive resection margins, detection of additional lesions and avoid unnecessary removal of benign tissue. To quantify fluorescence intensity, most studies use the signal-to-background ratio (SBR) or TBR. This is a ratio of the mean fluorescence intensity of the tumour and the surrounding tissue (background). A TBR of at least 1.5 and preferably 2.0 is deemed sufficient for tumour identification. Currently, four tumour-targeted fluorescent agents have been tested in early phase clinical studies for CRC and have shown promising results: SGM-101, cRGD-ZW800-1, bevacizumab-800CW, and ONM-100.[14–18]

SGM-101 consists of a monoclonal antibody targeting the carcinoembryonic antigen (CEA) bound to the fluorophore BM-104.[19] A phase II study of 37 patients showed an intraoperative TBR of 1.9. Importantly, based on fluorescence assessment, the surgical plan was changed in 9 (24%) patients. In 7 patients, fluorescence led to resection of malignant lesions that were not identified with white light only. In two patients, clinically suspected but non-fluorescent tissue was proven to be benign, which resulted in a less extensive resection (18). These promising results have led to the initiation of 2 phase III trials using SGM-101 (NCT03659448, NCT04642924).

cRGD-ZW800-1 is a cyclic pentapeptide (cRGD) conjugated to the 800 nm zwitterionic NIR fluorophore ZW800-1. It targets various integrins that have been shown to be overexpressed on colorectal tumour cells. In the first-in-human study, 12 colon cancer patients were included. Intraoperative fluorescence imaging of the primary tumour was feasible in both open and minimal invasive surgeries (figure 4). The highest mean TBR of 1.6 was found in the highest dosing of 0.05 mg/kg.[15]

FIGURE 4 Fluorescence imaging results of primary colon cancer.
Intraoperative fluorescence imaging result of an adenocarcinoma of the ascending colon (TBR 1.6) using cRGD-ZW800-1. Imaging was performed using the Quest Spectrum laparoscopic imaging system. It shows an image in white light (A), near-infrared (B) and merge of A and B (C).

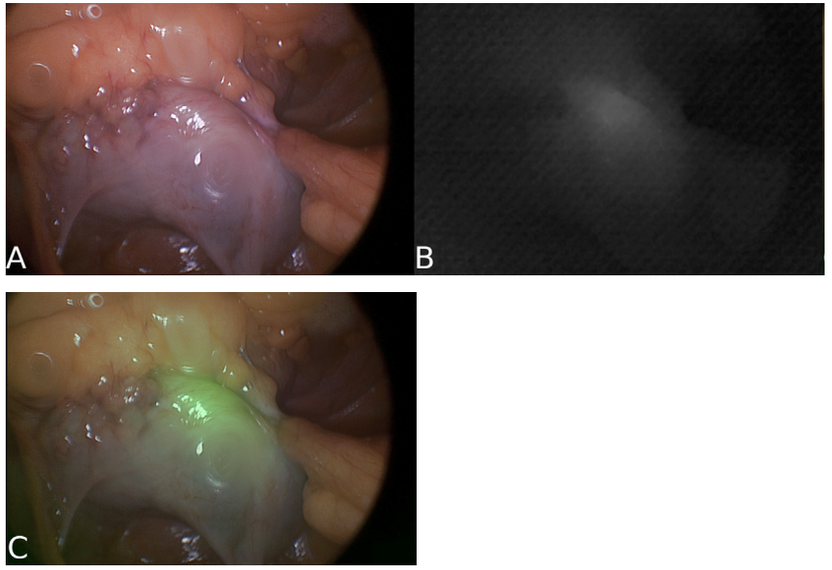

Bevacizumab-800CW consists of a monoclonal antibody targeting vascular endothelial growth factor A (VEGF-A), bound to IRDye800CW.[20,21] Bevacizumab-800CW has been studied in eight rectal cancer patients.[16] During back table fluorescence assessment of the resection margins on the surgical specimen, a tumour-positive margin was correctly identified in one out of two patients. In the six patients with a tumour-negative resection margin, one (17%) showed a false-positive signal.

ONM-100 is a pH-activatable fluorescent agent that exploits the metabolic microenvironment of solid tumours.[17] It does not bind to specific tumour receptors but is activated in the acidic tumour environment. It is a conjugation of a pH-sensitive nanoparticle to ICG, which becomes fluorescent in environments with a pH below 6.9. Thirty patients were studied with this agent, of which three

underwent surgery for CRC. All three CRC patients showed a sharply demarcated fluorescent signal during back table imaging. Currently, a phase II study using ONM-100 is ongoing in which patients undergoing surgery for CRC are also included (NCT03735680).

A phase I/II trial will be conducted using LUM015, a novel PEGylated protease-activated fluorescent imaging agent targeting cathepsins, which play a crucial role in mammalian cell turnover.[22] The first results of this study, which focuses on intraoperative imaging of CRC, are expected in 2021 (NCT02584244).

Altogether, these early phase clinical trials have shown that tumour-targeted fluorescence imaging is a feasible addition to CRC surgery. The fluorescent agents detected most of the known tumours and SGM-101 even detected additional lesions, which were not detected in white light. To assess the impact on patient related outcomes, future studies should focus on clinical endpoints like tumour-negative resection margin rate and change in surgical management.

IMAGING OF THE SENTINEL LYMPH NODE

Adequate lymph node staging in CRC patients is crucial; it is an important prognostic feature and determines the need for (neo)adjuvant chemotherapy and/or radiotherapy. The sentinel lymph node (SLN) may be crucial in nodal staging, as it is defined as the first lymph node draining the tumour and is believed to be the first place for lymphogenic metastases. Moreover, one in three patients with stage I and II colon cancer, who are staged as lymph node-negative, still develop distant metastases.[23] This might be a consequence of understaging by histopathology, due to lymph nodes with occult malignant cells and micrometastases. Currently, a single paraffin embedded slide per lymph node is reviewed during routine histopathological analysis, increasing the chance of missing tumour cells away from the slide's cutting edge. More extensive histopathological analysis of all resected lymph nodes would improve nodal staging, but this process is time-consuming and expensive.[24]Extensive analysis of only the SLN is feasible, and thus unfolds a niche for SLN mapping in CRC. Moreover, tumour-negative SLNs create an opportunity for endoscopic or local resection of early stage tumours.[25]

A reason for the absence of SLN mapping in the routine treatment of CRC patients might be a consequence of so-called skip metastases that are reported in up to 22% the patients.[26] In these cases, malignant cells are absent in the SLN, but present in other regional lymph nodes. Moreover, the use of blue dye for SLN mapping in CRC appears limited due to its minimal depth penetration in the mesocolic and mesorectal fat.[27] Therefore, the interest in fluorescent dyes, especially the peritumoural injection of ICG, has increased. These fluorescent dyes have already shown to be of additional value for the identification of complete lymph drainage patterns, including aberrant flow.[28,29] Nevertheless, the identification of only the SLN would be a valuable addition.

Various techniques have been used in studies assessing fluorescence-guided SLN mapping in CRC. Agent administration and SLN mapping can be performed before or during the procedure (*in vivo*) or after resection (*ex vivo*). Although *ex vivo* imaging might be easier to adapt in the current surgical or pathological workflow, it has drawbacks. Most importantly, *ex vivo* injection of an agent and identification of the SLN lacks the possibility of finding SLNs in patients with aberrant lymph node drainage patterns.[30] Another technical consideration is the site of injection. For *in vivo* SLN mapping, submucosal injection is done endoscopically, prior to surgery. Alternatively, subserosal injection can be performed during surgery, which in laparoscopic surgery demands transcutaneous needle placement. Submucosal injection is preferred over subserosal injection because of better accuracy of injection near the tumour and easier endoscopic needle positioning.[31]

ICG is the only fluorescent dye that has been reported for *in vivo* SLN mapping in CRC with cohorts up to 48 patients and success rates of SLN detection ranging from 65.5 to 100%.[31–35] The accuracy of this technique seems to diminish with increasing tumour stage.[34,36] Which is most likely a result of the distorted drainage patterns caused by transmural growth of advanced tumours.

Ex vivo SLN mapping facilitates the use of experimental agents, like HSA800 (IRDye 800CW conjugated to human serum albumin). HSA800 has shown a potential advantage over ICG, due to its bigger hydrodynamic diameter that results in better retention in the SLN.[37] HSA800 has demonstrated successful identification of the SLN in 95-100% of 96 patients.[38–40]

Despite high fluorescence-guided SLN identification rates, the SLN itself was associated with a relatively low negative predictive value (74-100%) in general, mainly as a result of high false-negative rates (when the SLN did not contain tumour tissue, but other regional lymph nodes did).[31–35,38,39] This can be a result of the occurrence of skip metastases.[26]

Correct staging is essential for treatment planning in CRC patients and may be improved with SLN mapping. A patient is upstaged when no tumour deposits were seen during conventional histopathology of all lymph nodes, but the SLN showed malignant cells at advanced histopathological analysis using serial sectioning and immunohistochemistry. SLN mapping with ICG and subsequent advanced histopathology resulted in upstaging in 6-23% of the patients.[31–33]

Although plausible, it is yet unknown whether upstaged patients with micrometastatic lymph nodes will benefit from subsequent neoadjuvant treatment.

Overall, it can be concluded that fluorescence-guided identification of the SLN is feasible and potentially of additional clinical value. However, a wide variety of techniques for fluorescence-guided SLN identification are currently used. It is recommended to first determine the optimal agent, injection technique and patient population. The high false-negative rate (tumour-negative SLN with tumour-positive regional nodes) remains a major drawback for SLN mapping in CRC in general. Nevertheless, its value in terms of upstaging and the consequence of adjuvant treatment seems enough reason to further explore this field.

IMAGING OF DISTANT METASTASES

PERITONEAL METASTASES

Approximately 10% of all CRC patients develop peritoneal metastases during the course of the disease.[41] In the past, this diagnosis was considered non-curable with a median overall survival of approximately 12 months.[42] These survival rates have improved with the introduction of cytoreductive surgery followed by intraoperative hyperthermic intraperitoneal chemotherapy (HIPEC).[3,43] Studies have shown that in particular complete cytoreduction plays a major role as it prolongs the long-term survival of patients with peritoneal metastases.[3] However, identification of small peritoneal lesions can be challenging, especially after previous abdominal surgery or neoadjuvant therapy with subsequent fibrosis. An accurate peritoneal cancer index (PCI) is essential as this score plays a crucial role in the decision to perform a HIPEC procedure or not.[44] Fluorescence imaging can potentially lead to more complete cytoreductive surgery by more accurately identifying peritoneal lesions.

Intravenous injection of ICG and subsequent fluorescence imaging of peritoneal metastases is primarily based on the enhanced permeability and retention (EPR) effect. The EPR effect is dependent on the porous nature of tumour vasculature and the extended circulation of the fluorescent agent, leading to accumulation in the tumour.[45] ICG is administered at the start of the surgical procedure and has shown good intraoperative imaging of peritoneal metastases, which has led to a modification of the surgical plan in 4 out of 14 patients (29%) solely based on the fluorescence assessment.[46] Nevertheless, the authors reported limited ability to assess fluorescence in areas with high physiological ICG accumulation such as the liver, as well as a sensitivity of 0% in patients with mucinous tumours (46). Moreover, neoadjuvant treatment resulted in a higher false-negative rate (53.8% vs. 42.9%) and lower sensitivity (65.0% vs 76.3%) compared to patients who did not receive neoadjuvant treatment.[47]

To date, two tumour-targeted agents have been used for *in vivo* detection of peritoneal metastases in CRC: bevacizumab-800CW and SGM-101. Bevacizumab-800CW was the first tumour-targeted fluorescent agent that was reported to yield promising results, identifying additional peritoneal metastases in two out of seven (29%) patients.[48] Similar results were achieved in a study with SGM-101, where fluorescence imaging led to a change in PCI in 5 out of 12 (42%) patients (figure 5). Four patients had a higher PCI and one patient a lower PCI, all confirmed by histopathology.[49] It is noteworthy that both studies reported a high false-positive rate (38% and 47%, respectively). This could be a result of non-specific localisation of the fluorescent agent or autofluorescence of collagen-rich structures and calcifications.[50]

FIGURE 5 Fluorescence imaging result of colorectal peritoneal metastases.
Intraoperative fluorescence imaging result of peritoneal metastases of a mucinous carcinoma with signet ring cell differentiation (TBR 1.8) using SGM-101. Imaging was performed using the Quest Spectrum open imaging system. It shows an image in white light (A), near-infrared (B) and merge of A and B (C).

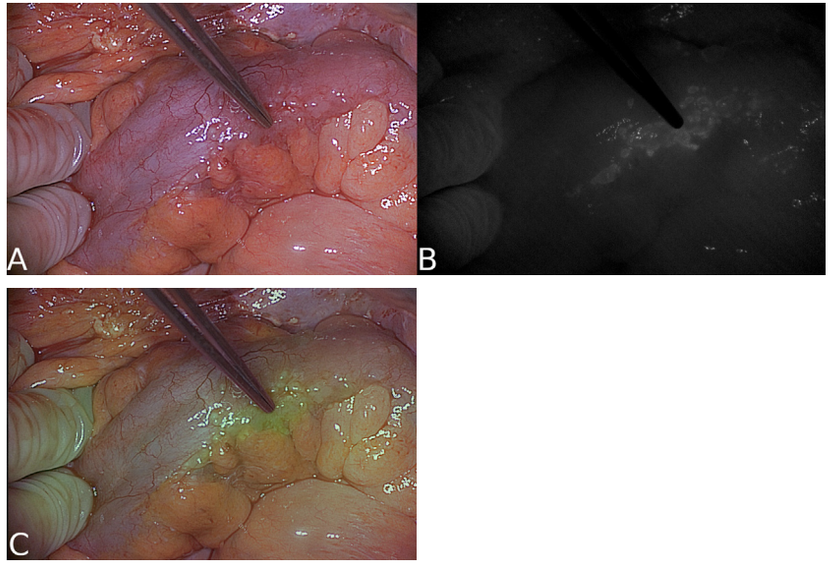

One clinical trial is currently ongoing using LUM015, including patients with peritoneal metastases of gastrointestinal cancer, ovarian cancer, and mesothelioma (NCT03834272). The aforementioned phase III study with SGM-101 will also include patients with peritoneal metastases (NCT03659448).

The feasibility of fluorescence-guided detection of peritoneal metastases has been demonstrated, allowing for detection of peritoneal deposits and potentially also of occult lesions. This is especially valuable knowing that treatment success is primarily determined by complete cytoreduction.

LIVER METASTASES

Over the course of the disease, 20-30% of CRC patients develop liver metastases (CRLM).[51] Complete resection of these metastases is an important treatment option, with positive resection margins being associated with a two- to three-fold decrease in 5-year survival compared to negative margins. However, positive resection margins occur in approximately 13% of patients.[52] In the past, the hepatic surface was palpated for superficial lesions during surgery. With minimal invasive surgery this has become challenging. Nowadays, preoperative magnetic resonance imaging (MRI), computed tomography (CT) and intraoperative ultrasound (IOUS) are the most frequently used imaging modalities for the identification of CRLM.[53] Fluorescence imaging offers surgeons another tool for detecting CRLM. It is suitable for detecting small superficial metastases (up to eight mm deep), but also for resection margin assessment. Intravenous ICG doses between 10-50 mg are described with injection windows of 1-14 days prior to surgery.[54] After intravenous injection, ICG is exclusively cleared by the liver. Immature hepatocytes, located at the transition zone between healthy and malignant liver cells, are unable to excrete ICG into bile due to down-regulation of anion transporters, resulting in an accumulation of ICG. This causes CRLM to show a rim of fluorescence (figure 6).[55]

Various studies have reported on fluorescence imaging with ICG for the detection of occult CRLM, but none were randomized.[55-57] In one systematic review, six out of nine studies reported a sensitivity exceeding 94%.[54] Furthermore, when fluorescence imaging was added to conventional imaging, extra metastases were found and resected in 20 out of 148 patients (13.5%). Tumour-targeted fluorescence identification of CRLM was previously reported in one study using SGM-101. SGM-101 provided visualisation of all 12 malignant lesions in eight patients with a mean *in vivo* TBR of 1.7.[58]

It is widely debated if additional resection of small superficial CRLM improves overall survival. One study has retrospectively assessed (disease-free) survival of 86 patients after ICG-guided resection of CRLM.[59] Significantly more additional lesions were found when fluorescence-guided resection with ICG was added compared to standard care (25% vs. 13%, p=0.04). However, this was not associated with a significant decrease in local recurrence-free survival (HR: 0.74; 95% CI: 0.42-1.28), and overall survival (HR: 0.94; 95% CI: 0.50-1.76).

FIGURE 6 Fluorescence imaging result of a liver metastasis.
A colorectal liver metastasis showing clear 'rim fluorescence' after intravenous injection of 10 mg indocyanine green 24 hours prior to surgery. Imaging was performed using the Quest Spectrum open imaging system.

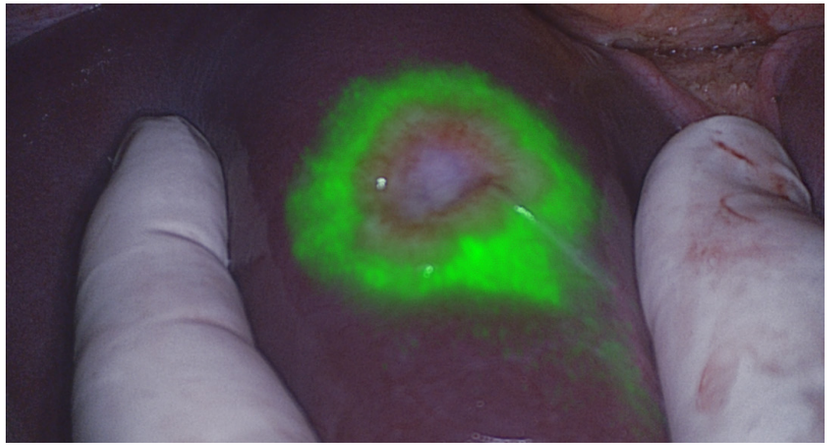

assessment and aiding in tumour delineation for CRLM resection. Two small case series with a total of 52 patients achieved 100% tumour-negative resection margins using ICG to determine the precise tumour border.[56,57] Recently, a systematic workflow was proposed to detect or prevent tumour positive margins in CRLM surgery.[60] In a selected group of eight patients with initial tumour positive resection margins, the surgeons were able to correctly identify seven out of eight positive margins by using the proposed surgical workflow. The currently ongoing prospective MIMIC-trial will assess whether this surgical workflow can lead to a decrease of tumour-positive resection margins in 186 patients with CRLM (Netherlands trial register: NL7674).

Fluorescence imaging with ICG has been demonstrated to improve intraoperative detection of CRLM. It can also be used for margin assessment and aiding in tumour delineation for CRLM resection. Future trials must confirm this potential and demonstrate whether this technique will improve patient survival.

EXTRA-ABDOMINAL METASTASES

A feasibility study with SGM-101 to identify colorectal lung metastases is currently recruiting (NCT04737213). A similar study with SGM-101 to identify colorectal brain metastases will be conducted soon (NCT04755920).

IMAGING OF VITAL STRUCTURES

URETERS

Iatrogenic ureteral injury is a severe complication in abdominal surgery and has an incidence of up to 5.7% in colorectal surgery. Surgeries on the distal colon and rectum bear the highest risk for ureteral injury.[61] Depending on the time of diagnosis, location, and extent of the injury, treatment ranges from minimal invasive transurethral procedures to complex surgical reconstruction. Consequences of (undiagnosed) iatrogenic ureteral injury include kidney failure, sepsis, ureteral stenosis, urinoma, and fistulas.[62] The ureter is usually identified through visual inspection and palpation, which can be difficult due to its retroperitoneal location. The introduction of minimal invasive surgery in the last decades has further increased this challenge.[61] Intraoperative fluorescence imaging can guide the surgeon in identification of the ureter, which could result in less ureteral injury. ICG and MB have both been studied for ureteral identification. Due to the hepatic clearance of ICG, retrograde intra-ureteral injection is needed, which makes ureteral identification with ICG a complex procedure.[63] Successful ureteral identification using ICG is reported in 94-100% of procedures.[63-65] As MB is cleared renally, intravenous injection is possible for intraoperative identification of ureters. Outcomes of intravenous MB administration for ureteral identification show variable results.[66-68] Fluorescence of the ureters is reported in 50-100% of cases and usually between 10-90 minutes after injection of MB. Optimal visualisation is achieved with doses between 0.5 mg/kg and 1.0 mg/kg. Most important, in most cases, the ureter could only be identified with fluorescence after it was already adequately identified in white light, thus the clinical benefit was minimal. Overall, MB appears to be suboptimal for ureteral identification.

To date, three experimental fluorophores have been used in clinical studies to image the ureter: ZW800-1, IS-001, and IRDye800BK.[69-71] These experimental fluorophores are all fluorescent dyes with peak emission around 800 nm. ZW800-1 is a zwitterionic molecule that shows low non-specific binding and is exclusively renally cleared. ZW800-1 was intravenously administered during abdominopelvic surgery in 12 patients. Using ZW800-1, all ureters became fluorescent within 10 minutes, without dissecting the peritoneum.[69] The SBR was 2.7 in the group with 2.5 mg throughout the first hour. The ureters remained visible with NIR during the whole procedure, with the longest procedure being over 3.5 hours. The first clinical study assessing the safety and efficacy of IS-001 included 24 patients who underwent laparoscopic gynaecological surgery[70]. The ureters could be identified in all patients, the highest SBR (3.6) was observed with a dose of 20 mg. Signal intensity decreased rapidly over time, with the peak SBR occurring 30 minutes after injection. The third experimental fluorescent dye that was studied for ureter identification is IRDye800BK, a hydrophilic dye.[72] In this trial, the optimal dose of 0.06 mg/kg was administered in 25 patients.[71] In all patients, the ureter was visualised within ten minutes. After 90 minutes the ureter was still visible in 89% of the patients. Currently, another clinical trial is ongoing using IRDye800BK, including 40 patients undergoing laparoscopic surgery (NCT03387410).

ZW800-1, IS-001, and IRDye-800BK appear suitable for ureter identification with NIR fluorescence imaging and have advantages over MB and ICG. Future clinical trials are needed to confirm the promising early results of these experimental fluorescent agents. However, large sample sizes are required for such studies due to relatively low incidence of iatrogenic ureteral injury. Therefore, phase III studies should focus on patients with high risk for intraoperative ureteral injury.

URETHRA

Besides ureteral injury, the urethra is also at risk for injury during pelvic surgery. Perineal dissection in (low) rectal surgery is an especially high-risk step for urethral injury. One clinical study with urethral administration of ICG during prostatectomies in 12 patients has been published.[73] No intraoperative urethra injury occurred. In another study, ICG was injected in the urethra during a transanal total mesorectal excision in one patient, resulting in successful identification of the urethra.[74]

NERVES

Sexual and urological dysfunction due to iatrogenic nerve injury are complications of rectal surgery, significantly affecting quality of life. Up to 79% of the patients

undergoing rectal surgery acquire some sort of sexual or urological dysfunction.[75] The hypogastric, splanchnic, and levator ani nerves are at risk during (colo) rectal surgery.[76] Nerve targeted fluorescence-guided surgery has the potential to improve nerve identification, and therefore prevent injury. Although promising pre-clinical results of nerve specific fluorescence imaging have been reported, the translation to clinical studies has yet to be made.[77-79] The main difficulties include fluorescent agents not being able to pass the nerve-blood barrier, and relatively high nonspecific uptake of nerve targeted agents by fat and muscle.[79]

IMAGING OF PERFUSION

ANASTOMOTIC PERFUSION

Anastomotic leakage is one of the most severe complications in CRC surgery. It often requires additional surgical or radiological intervention, leading to a prolonged hospital stay. Anastomotic leakage is reported up to 13% of patients undergoing CRC surgery with subsequent mortality rates of up to 27%.[80,81] Poor bowel perfusion is thought to play an important role in anastomotic leakage. ICG fluorescence-angiography can provide real-time feedback of bowel perfusion and aid the surgeon in determining the optimal location for the anastomosis. ICG doses between 2-20 mg have been reported.[82,83] In general, bowel perfusion can be assessed within 60 seconds after intravenous injection.

Over the years, several cohort studies have been published on the effect of ICG fluorescence angiography use on anastomotic leakage. Studies specifically addressing colonic anastomoses are sporadic and fail to show a significant decrease in anastomotic leakage rates when using ICG fluorescence angiography.[84,85] More data has been reported on rectal surgery. Song *et al*. published the most recent and complete meta-analysis on rectal anastomoses including 2088 patients from nine retrospective studies.[86] Their pooled analysis showed an odds ratio for anastomotic leakage of 0.34 (95% CI: 0.22-0.52) in favour of ICG fluorescence angiography over standard of care.

Recently, the first randomised controlled trials (RCTs) on ICG fluorescence angiography have been published. One study included 240 patients undergoing left-sided colon or rectal resection and failed to show a significant difference in anastomotic leakage rate between the ICG fluorescence angiography group and the control group (5% vs 9%; p = 0.2).[87] The second study investigated the value of ICG fluorescence angiography on the occurrence of anastomotic leakage in 377 patients undergoing sigmoid or rectal resection. A significantly lower anastomotic leakage rate was found in the ICG fluorescence angiography group (9.1% vs 16.3%; p = 0.04).[88] However, this difference was predominantly based on the occurrence of anastomotic leakage grade A, which does not alter patient management.[89] Thus, minimal clinical benefit was demonstrated as no difference was observed in the number of re-operations or the length of postoperative hospital stay. The third RCT also failed to report a significant decrease of anastomotic leakage in the ICG fluorescence angiography group compared to the control group (9.0% vs 9.6%; p = 0.37).[90] It should be noted that the pre-determined sample size was not achieved due to a decrease in accrual rates. More RCTs have been registered that will include similar or higher amount of patients (NCT02598414, NCT04012645). Noteworthy are the INTACT-trial and the AVOID-trial, both planning to include up to 1000 patients (ISCRN: 13334746, NCT04712032). Also, the prospective IMARI trial is assessing a series of interventions, including ICG fluorescence angiography, and its influence on anastomotic leakage in rectal cancer surgery (Netherlands trial register: NL8261).

In conclusion, ICG fluorescence angiography has potential in the prevention of anastomotic leakage in a safe and simple way. Pooled analysis of cohort studies has demonstrated that ICG fluorescence angiography reduces anastomotic leakage, but high-quality evidence is currently lacking. RCTs with inclusion up to 1000 patients are currently ongoing and might provide with the answer if ICG fluorescence angiography prevents anastomotic leakage in CRC surgery.

OMENTOPLASTIC PERFUSION

Perineal wound bed complications occur in almost 50% of the patients undergoing abdominoperineal resection (APR) and carry major morbidity.[91] Omentoplasty can be performed for the prevention and management of these complications. It is hypothesised that the transferred omentum prevents dead space formation, has an anti-inflammatory and antibacterial effect, and provides excellent vascularisation to the wound bed.[92] However, its clinical benefit in rectal cancer surgery has been disputed. A meta-analysis of 1894 patients showed that omentoplasty did not reduce the risk of postoperative presacral abscesses or perineal complications.[93] ICG fluorescence angiography of the transferred omentum was recently assessed in a pilot study.[94] Remarkably, ICG fluorescence angiography led to a change in surgical management in 80% of the patients. A follow up study by the same group showed a decrease in pelviperineal non-healing in the ICG group compared to the control group (22% vs 42%; p = 0.051).[95] However non-significant, this study showed a trend towards improved outcomes after ICG

fluorescence angiography guided omentoplasty. The reported alteration of the surgical plan in 80% of cases suggests that 'standard' omentoplasty is vulnerable to poor omental perfusion. Further research on ICG fluorescence angiography for omentoplasty is therefore warranted.

Discussion and future perspectives

NIR fluorescence-guided surgery is a rapidly evolving technique with various clinical applications in CRC surgery. This review provides an overview of the clinical applications of all fluorescent agents for CRC surgery. ICG, the nonspecific FDA/EMA approved fluorescent agent is already used in a variety of clinical applications of which CRLM resection and ICG fluorescence angiography show the most potential. However, no unequivocal benefits in relevant outcome measures have yet been reported. Over the past years, promising experimental fluorescent agents (targeted and non-targeted) have been investigated. These agents could potentially improve intraoperative fluorescence imaging, ultimately leading to improved detection of tumour tissue, vital structures, and vascularisation. Improving intraoperative detection of tumour could not only lead to more complete resections, but can also lead to better patient selection, as unnecessary surgery could be prevented if the disease is found to be too advanced. On the other hand, false-positive lesions would lead to unnecessary resection of healthy tissue which makes tumour-binding specificity of the fluorescent agent crucial.

Quantification of the fluorescence signal is challenging, with numerous factors such as scattering, absorption, camera angulation and distance, and background light influencing the signal intensity.[96] The latest studies on ICG fluorescence angiography for the prevention of anastomotic leakage focus on less subjective perfusion assessment by analysing time-dependent inflow parameters.[97,98] Real-time quantification of the fluorescence signal of tumour-targeted agents, aiding surgeons in deciding whether tissue is malignant or not, has not been reported yet. Most clinical studies report the SBR (or TBR) and change in surgical management as the main parameters in early phase studies. Eventually, trials should report on clinically significant events such as the tumour-negative resection margin rate, detection of occult lesions, surgical complications, and (disease free) survival.[99]

Nowadays, a variety of fluorescence camera systems is available in clinical practice. It is important to keep in mind that these camera systems can influence imaging results.[21] This also counts for the difference between open- and laparoscopic cameras. Most laparoscopes that are currently clinically available are optimised for ICG at 830 nm. This wavelength is slightly too high for optimal imaging of most experimental fluorescent agents, which have peak emission wavelengths around 800 nm (table 1). Therefore, there is a need for high-quality laparoscopes that are optimised for imaging of specific tumour-targeted fluorescent agents. Fluorescence imaging could account for the lack of tactile feedback in minimal invasive surgery, as it has the potential to improve visualisation of vital structures (e.g. the ureter, nerves) and tumours. Moreover, fluorescence imaging can be integrated in the laparoscopic field with an overlay view, which is an advantage over open surgery, where an additional handheld camera is needed. Especially in rectal surgery, in the conically shaped (male) pelvis, difficulties are experienced with optimal positioning due to the size of most open cameras. A laparoscope is much smaller and therefore easier to manoeuvre towards an optimal imaging angle.

Conclusion

In conclusion, the field of fluorescence-guided surgery is rapidly evolving with already several clinical applications in CRC surgery. ICG is widely used, and its use appears to be beneficial in specific applications. Many experimental fluorescent agents have been developed and several of these agents are currently being assessed in late phase clinical studies. The most promising applications of these experimental fluorescent agents in CRC surgery are distinguishing between fibrotic and tumour tissue after neo-adjuvant treatment, improving the rate of tumour-negative resection margins in locally advanced and recurrent rectal cancer, detection of occult metastases in cytoreductive surgery for peritoneal metastases, and ureteral imaging in high-risk cases. An essential next step for the implementation of these agents in clinical practice is to show direct patient benefit in terms of change in surgical management, surgical complications, recurrence-free survival, and overall survival.

REFERENCES

1 Bray F, Ferlay J, Soerjomataram I, Siegel RL, Torre LA, Jemal A. Global cancer statistics 2018: GLOBOCAN estimates of incidence and mortality worldwide for 36 cancers in 185 countries. *CA Cancer J Clin* 2018;68(6): 394-424.

2 Amri R, Bordeianou LG, Sylla P, Berger DL. Association of Radial Margin Positivity With Colon Cancer. *JAMA Surg* 2015;150(9): 890-898.

3 Elias D, Gilly F, Boutitie F, Quenet F, Bereder JM, Mansvelt B, Lorimier G, Dube P, Glehen O. Peritoneal colorectal carcinomatosis treated with surgery and perioperative intraperitoneal chemotherapy: retrospective analysis of 523 patients from a multicentric French study. *J Clin Oncol* 2010;28(1): 63-68.

4 Hernot S, van Manen L, Debie P, Mieog JSD, Vahrmeijer AL. Latest developments in molecular tracers for fluorescence image-guided cancer surgery. *Lancet Oncol* 2019;20(7): e354-e367.

5 Fox IJ, Brooker LG, Heseltine DW, Essex HE, Wood EH. A tricarbocyanine dye for continuous recording of dilution curves in whole blood independent of variations in blood oxygen saturation. *Proc Staff Meet Mayo Clin* 1957;32(18): 478-484.

6 Ginimuge PR, Jyothi SD. Methylene blue: revisited. *J Anaesthesiol Clin Pharmacol* 2010;26(4): 517-520.

7 Slim K, Nini E, Forestier D, Kwiatkowski F, Panis Y, Chipponi J. Methodological index for non-randomized studies (minors): development and validation of a new instrument. *ANZ J Surg* 2003;73(9): 712-716.

8 Nagtegaal ID, Quirke P. What is the role for the circumferential margin in the modern treatment of rectal cancer? *J Clin Oncol* 2008;26(2): 303-312.

9 Holman FA, Bosman SJ, Haddock MG, Gunderson LL, Kusters M, Nieuwenhuijzen GA, van den Berg H, Nelson H, Rutten HJ. Results of a pooled analysis of IOERT containing multimodality treatment for locally recurrent rectal cancer: Results of 565 patients of two major treatment centres. *Eur J Surg Oncol* 2017;43(1): 107-117.

10 Conaghan PJ, Maxwell-Armstrong CA, Garrioch MV, Hong L, Acheson AG. Leaving a mark: the frequency and accuracy of tattooing prior to laparoscopic colorectal surgery. *Colorectal Dis* 2011;13(10): 1184-1187.

11 Feingold DL, Addona T, Forde KA, Arnell TD, Carter JJ, Huang EH, Whelan RL. Safety and reliability of tattooing colorectal neoplasms prior to laparoscopic resection. *J Gastrointest Surg* 2004;8(5): 543-546.

12 Satoyoshi T, Okita K, Ishii M, Hamabe A, Usui A, Akizuki E, Okuya K, Nishidate T, Yamano H, Nakase H, Takemasa I. Timing of indocyanine green injection prior to laparoscopic colorectal surgery for tumour localization: a prospective case series. *Surg Endosc* 2020.

13 Watanabe M, Tsunoda A, Narita K, Kusano M, Miwa M. Colonic tattooing using fluorescence imaging with light-emitting diode-activated indocyanine green: A feasibility study. *Surg Today* 2009;39(3): 214-218.

14 Boogerd LSF, Hoogstins CES, Schaap DP, Kusters M, Handgraaf HJM, van der Valk MJM, Hilling DE, Holman FA, Peeters KCMJ, Mieog JSD, van de Velde CJH, Farina-Sarasqueta A, van Lijnschoten I, Framery B, Pèlegrin A, Gutowski M, Nienhuijs SW, de Hingh IHJT, Nieuwenhuijzen GAP, Rutten HJT, Cailler F, Burggraaf J, Vahrmeijer AL. Safety and effectiveness of SGM-101, a fluorescent antibody targeting carcinoembryonic antigen, for intraoperative detection of colorectal cancer: a dose-escalation pilot study. *Lancet Gastroenterol Hepatol* 2018;3(3): 181-191.

15 de Valk KS, Deken MM, Handgraaf HJM, Bhairosingh SS, Bijlstra OD, van Esdonk MJ, Terwisscha van Scheltinga AG, Valentijn R, March TL, Vuijk J, Peeters KC, Holman FA, Hilling DE, Mieog JSD, Frangioni JF, Burggraaf J, Vahrmeijer AL. First-in-Human Assessment of cRGD-ZW800-1, a Zwitterionic, Integrin-Targeted, Near-Infrared Fluorescent Peptide in Colon Carcinoma. *Clin Cancer Res* 2020.

16 de Jongh SJ, Tjalma JJJ, Koller M, Linssen MD, Vonk J, Dobosz M, Jorritsma-Smit A, Kleibeuker JH, Hospers GAP, Havenga K, Hemmer PHJ, Karrenbeld A, van Dam GM, van Etten B, Nagengast WB. Back-Table Fluorescence-Guided Imaging for Circumferential Resection Margin Evaluation Using Bevacizumab-800CW in Patients with Locally Advanced Rectal Cancer. *J Nucl Med* 2020;61(5): 655-661.

17 Voskuil FJ, Steinkamp PJ, Zhao T, van der Vegt B, Koller M, Doff JJ, Jayalakshmi Y, Hartung JP, Gao J, Sumer BD, Witjes MJH, van Dam GM, group Ss. Exploiting metabolic acidosis in solid cancers using a tumour-agnostic pH-activatable nanoprobe for fluorescence-guided surgery. *Nat Commun* 2020;11(1): 3257.

18 de Valk KS, Deken MM, Schaap DP, Meijer RP, Boogerd LS, Hoogstins CE, van der Valk MJ, Kamerling IM, Bhairosingh SS, Framery B, Hilling DE, Peeters KC, Holman FA, Kusters M, Rutten HJ, Cailler F, Burggraaf J, Vahrmeijer AL. Dose-Finding Study of a CEA-Targeting Agent, SGM-101, for Intraoperative Fluorescence Imaging of Colorectal Cancer. *Ann Surg Oncol* 2020.

19 Gutowski M, Framery B, Boonstra MC, Garambois V, Quenet F, Dumas K, Scherninski F, Cailler F, Vahrmeijer AL, Pèlegrin A. SGM-101: An innovative near-infrared dye-antibody conjugate that targets CEA for fluorescence-guided surgery. *Surg Oncol* 2017;26(2): 153-162.

20 Lv W, Gao T, Wang S, Hou J, Liu M, Yang J, Du T, Chen Z, Chen Z, Feng X, Zeng W. Long-term tracking of cancer cell nucleus and identification of colorectal cancer with an aggregation-induced emission-based fluorescent probe. *J Biomed Nanotechnol* 2019;15(5): 1033-1042.

21 Zhu B, Sevick-Muraca EM. A review of performance of near-infrared fluorescence imaging devices used in clinical studies. *Br J Radiol* 2015;88(1045): 20140547.

22 Whitley MJ, Cardona DM, Lazarides AL, Spasojevic I, Ferrer JM, Cahill J, Lee CL, Snuderl M, Blazer DG, 3rd, Hwang ES, Greenup RA, Mosca PJ, Mito JK, Cuneo KC, Larrier NA, O'Reilly EK, Riedel RF, Eward WC, Strasfeld DB, Fukumura D, Jain RK, Lee WD, Griffith LG, Bawendi MG, Kirsch DG, Brigman BE. A mouse-human phase 1 co-clinical trial of a protease-activated fluorescent probe for imaging cancer. *Sci Transl Med* 2016;8(320): 320ra324.

23 Figueredo A, Coombes ME, Mukherjee S. Adjuvant therapy for completely resected stage II colon cancer. *Cochrane Database Syst Rev* 2008(3): CD005390.

24 Yamamoto H, Murata K, Fukunaga M, Ohnishi T, Noura S, Miyake Y, Kato T, Ohtsuka M, Nakamura Y, Takemasa I, Mizushima T, Ikeda M, Ohue M, Sekimoto M, Nezu R, Matsuura N, Monden M, Doki Y, Mori M. Micrometastasis Volume in Lymph Nodes Determines Disease Recurrence Rate of Stage II Colorectal Cancer: A Prospective Multicenter Trial. *Clin Cancer Res* 2016;22(13): 3201-3208.

25 Cahill RA, Leroy J, Marescaux J. Localized resection for colon cancer. *Surg Oncol* 2009;18(4): 334-342.

26 Bao F, Zhao LY, Balde AI, Liu H, Yan J, Li TT, Chen H, Li GX. Prognostic impact of lymph node skip metastasis in Stage III colorectal cancer. *Colorectal Dis* 2016;18(9): O322-329.

27 Bembenek AE, Rosenberg R, Wagler E, Gretschel S, Sendler A, Siewert JR, Nahrig J, Witzigmann H, Hauss J, Knorr C, Dimmler A, Grone J, Buhr HJ, Haier J, Herbst H, Tepel J, Siphos B, Kleespies A, Koenigsrainer A, Stoecklein NH, Horstmann O, Grutzmann R, Imdahl A, Svoboda D, Wittekind C, Schneider W, Wernecke KD, Schlag PM. Sentinel lymph node biopsy in colon cancer: a prospective multicenter trial. *Ann Surg* 2007;245(6): 858-863.

28 Chand M, Keller DS, Joshi HM, Devoto L, Rodriguez-Justo M, Cohen R. Feasibility of fluorescence lymph node imaging in colon cancer: FLICC. *Tech Coloproctol* 2018;22(4): 271-277.

29 Nishigori N, Koyama F, Nakagawa T, Nakamura S, Ueda T, Inoue T, Kawasaki K, Obara S, Nakamoto T, Fujii H, Nakajima Y. Visualization of Lymph/Blood Flow in Laparoscopic Colorectal Cancer Surgery by ICG Fluorescence Imaging (Lap-IGFI). *Ann Surg Oncol* 2016;23 Suppl 2: S266-274.

30 Tuech JJ, Pessaux P, Regenet N, Bergamaschi R, Colson A. Sentinel lymph node mapping in colon cancer. *Surg Endosc* 2004;18(12): 1721-1729.

31 Ankersmit M, Bonjer HJ, Hannink G, Schoonmade LJ, van der Pas MHGM, Meijerink WJHJ. Near-infrared fluorescence imaging for sentinel lymph node identification in colon cancer: a prospective single-center study and systematic review with meta-analysis. *Tech Coloproctol* 2019;23(12): 1113-1126.

32 Andersen HS, Bennedsen ALB, Burgdorf SK, Eriksen JR, Eiholm S, Toxværd A, Riis LB, Rosenberg J, Gögenur I. *In vivo* and *ex vivo* sentinel node mapping does not identify the same lymph nodes in colon cancer. *Int J Colorectal Dis* 2017;32(7): 983-990.

33 Hirche C, Mohr Z, Kneif S, Doniga S, Murawa D, Strik M, Hünerbein M. Ultrastaging of colon cancer by sentinel node biopsy using fluorescence navigation with indocyanine green. *Int J Colorectal Dis* 2012;27(3): 319-324.

34 Nagata K, Endo S, Hidaka E, Tanaka JI, Kudo SE, Shiokawa A. Laparoscopic sentinel node mapping for colorectal cancer using infrared ray laparoscopy. *Anticancer Res* 2006;26(3 B): 2307-2311.

35 Cahill RA, Anderson M, Wang LM, Lindsey I, Cunningham C, Mortensen NJ. Near-infrared (NIR) laparoscopy for intraoperative lymphatic road-mapping and sentinel node identification during definitive surgical resection of early-stage colorectal neoplasia. *Surg Endosc Interv Tech* 2012;26(1): 197-204.

36 Burghgraef TA, Zweep AL, Sikkenk DJ, van der Pas M, Verheijen PM, Consten ECJ. *In vivo* sentinel lymph node identification using fluorescent tracer imaging in colon cancer: A systematic review and meta-analysis. *Crit Rev Oncol Hematol* 2021;158: 103149.

37 Ohnishi S, Lomnes SJ, Laurence RG, Gogbashian A, Mariani G, Frangioni JV. Organic alternatives to quantum dots for intraoperative near-infrared fluorescent sentinel lymph node mapping. *Mol Imaging* 2005;4(3): 172-181.

38 Schaafsma BE, Verbeek FPR, Van Der Vorst JR, Hutteman M, Kuppen PJK, Frangioni JV, Van De Velde CJH, Vahrmeijer AL. *Ex vivo* sentinel node mapping in colon cancer combining blue dye staining and fluorescence imaging. *J Surg Res* 2013;183(1): 253-257.

39 Hutteman M, Choi HS, Mieog JSD, Van Der Vorst JR, Ashitate Y, Kuppen PJK, Van Groningen MC, Löwik CWGM, Smit VTHBM, Van De Velde CJH, Frangioni JV, Vahrmeijer AL. Clinical translation of *ex vivo* sentinel lymph node mapping for colorectal cancer using invisible near-infrared fluorescence light. *Ann Surg Oncol* 2011;18(4): 1006-1014.

40 Weixler B, Rickenbacher A, Raptis DA, Viehl CT, Guller U, Rueff J, Zettl A, Zuber M. Sentinel Lymph Node Mapping with Isosulfan Blue or Indocyanine Green in Colon Cancer Shows Comparable Results and Identifies Patients with Decreased Survival: A Prospective Single-Center Trial. *World J Surg* 2017;41(9): 2378-2386.

41 Koppe MJ, Boerman OC, Oyen WJ, Bleichrodt RP. Peritoneal carcinomatosis of colorectal origin: incidence and current treatment strategies. *Ann Surg* 2006;243(2): 212-222.

42 Razenberg LG, Lemmens VE, Verwaal VJ, Punt CJ, Tanis PJ, Creemers GJ, de Hingh IH. Challenging the dogma of colorectal peritoneal metastases as an untreatable condition: Results of a population-based study. *Eur J Cancer* 2016;65: 113-120.

43 Simkens GA, van Oudheusden TR, Nieboer D, Steyerberg EW, Rutten HJ, Luyer MD, Nienhuijs SW, de Hingh IH. Development of a Prognostic Nomogram for Patients with Peritoneally Metastasized Colorectal Cancer Treated with Cytoreductive Surgery and HIPEC. *Ann Surg Oncol* 2016;23(13): 4214-4221.

44 Faron M, Macovei R, Goere D, Honore C, Benhaim L, Elias D. Linear Relationship of Peritoneal Cancer Index and Survival in Patients with Peritoneal Metastases from Colorectal Cancer. *Ann Surg Oncol* 2016;23(1): 114-119.

45 Maeda H. Tumour-selective delivery of macromolecular drugs via the EPR effect: background and future prospects. *Bioconjug Chem* 2010;21(5): 797-802.

46 Liberale G, Vankerckhove S, Gomez Caldon M, Ahmed B, Moreau M, El Nakadi I, Larsimont D, Donckier V, Bourgeois P. Fluorescence imaging after indocyanine green injection for detection of peritoneal metastases in patients undergoing cytoreductive surgery for peritoneal carcinomatosis from colorectal cancer: A pilot study. *Ann Surg* 2016;264(6): 1110-1115.

47 Filippello A, Porcheron J, Klein JP, Cottier M, Barabino G. Affinity of Indocyanine Green in the Detection of Colorectal Peritoneal Carcinomatosis. *Surg Innov* 2017;24(2): 103-108.

48 Harlaar NJ, Koller M, de Jongh SJ, van Leeuwen BL, Hemmer PH, Kruijff S, van Ginkel RJ, Been LB, de Jong JS, Kats-Ugurlu G, Linssen MD, Jorritsma-Smit A, van Oosten M, Nagengast WB, Ntziachristos V, van Dam GM. Molecular fluorescence-guided surgery of peritoneal carcinomatosis of colorectal origin: a single-centre feasibility study. *Lancet Gastroenterol Hepatol* 2016;1(4): 283-290.

49 Schaap DP, de Valk KS, Deken MM, Meijer RPJ, Burggraaf J, Vahrmeijer AL, Kusters M, Kusters M, Boogerd LSF, Schaap DP, Voogt ELK, Nieuwenhuijzen GAP, Rutten HJT, de Hingh IHJT, Burger JWA, Nienhuijs SW, de Valk KS, Meijer RPJ, Burggraaf J, Brandt-Kerkhof ARM, Verhoef C, Madsen EVE, van Kooten JP, Framery B, Gutowski M, A PM-h, Cailler F, van Lijnschoten I, Vahrmeijer AL, Hoogstins CES, Boogerd LSF, de Valk KS, Deken MM, Meijer RPJ. Carcinoembryonic antigen-specific, fluorescent image-guided cytoreductive surgery with hyperthermic intraperitoneal chemotherapy for metastatic colorectal cancer. *Br J Surg* 2020;107(4): 334-337.

50 Kobayashi H, Watanabe R, Choyke PL. Improving conventional enhanced permeability and retention (EPR) effects; what is the appropriate target? *Theranostics* 2013;4(1): 81-89.

51 Manfredi S, Lepage C, Hatem C, Coatmeur O, Faivre J, Bouvier AM. Epidemiology and management of liver metastases from colorectal cancer. *Ann Surg* 2006;244(2): 254-259.

52 Nierop PMH, Höppener DJ, van der Stok EP, Galjart B, Buisman FE, Balachandran VP, Jarnagin WR, Kingham TP, Allen PJ, Shia J, Vermeulen PB, Groot Koerkamp B, Grünhagen DJ, Verhoef C, D'Angelica MI. Histopathological growth patterns and positive margins after resection of colorectal liver metastases. HPB *(Oxford)* 2020;22(6): 911-919.

53 Elfrink AKE, Pool M, van der Werf LR, Marra E, Burgmans MC, Meijerink MR, den Dulk M, van den Boezem PB, Te Riele WW, Patijn GA, Wouters M, Leclercq WKG, Liem MSL, Gobardhan PD, Buis CI, Kuhlmann KFD, Verhoef C, Besselink MG, Grünhagen DJ, Klaase JM, Kok NFM, the Dutch Hepato-Biliary Audit G. Preoperative imaging for colorectal liver metastases: a nationwide population-based study. *BJS Open* 2020;4(4): 605-621.

54 Liberale G, Bourgeois P, Larsimont D, Moreau M, Donckier V, Ishizawa T. Indocyanine green fluorescence-guided surgery after IV injection in metastatic colorectal cancer: A systematic review. *Eur J Surg Oncol* 2017;43(9): 1656-1667.

55 Van Der Vorst JR, Schaafsma BE, Hutteman M, Verbeek FPR, Liefers GJ, Hartgrink HH, Smit VTHBM, Löwik CWGM, Van De Velde CJH, Frangioni JV, Vahrmeijer AL. Near-infrared fluorescence-guided resection of colorectal liver metastases. *Cancer* 2013;119(18): 3411-3418.

56 Peloso A, Franchi E, Canepa MC, Barbieri L, Briani L, Ferrario J, Bianco C, Quaretti P, Brugnatelli S, Dionigi P, Maestri M. Combined use of intraoperative ultrasound and indocyanine green fluorescence imaging to detect liver metastases from colorectal cancer. HPB 2013;15(12): 928-934.

57 Aoki T, Murakami M, Koizumi T, Matsuda K, Fujimori A, Kusano T, Enami Y, Goto S, Watanabe M, Otsuka K. Determination of the surgical margin in laparoscopic liver resections using infrared indocyanine green fluorescence. *Langenbecks Arch Surg* 2018;403(5): 671-680.

58 Meijer RPJ, de Valk KS, Deken MM, Boogerd LSF, Hoogstins CES, Bhairosingh SS, Swijnenburg RJ, Bonsing BA, Framery B, Fariña Sarasqueta A, Putter H, Hilling DE, Burggraaf J, Cailler F, Mieog JSD, Vahrmeijer AL. Intraoperative detection of colorectal and pancreatic liver metastases using SGM-101, a fluorescent antibody targeting CEA. *Eur J Surg Oncol* 2020.

59 Handgraaf HJM, Boogerd LSF, Höppener DJ, Peloso A, Sibinga Mulder BG, Hoogstins CES, Hartgrink HH, van de Velde CJH, Mieog JSD, Swijnenburg RJ, Putter H, Maestri M, Braat AE, Frangioni JV, Vahrmeijer AL. Long-term follow-up after near-infrared fluorescence-guided resection of colorectal liver metastases: A retrospective multicenter analysis. *Eur J Surg Oncol* 2017;43(8): 1463-1471.

60 Achterberg FB, Sibinga Mulder BG, Meijer RPJ, Bonsing BA, Hartgrink HH, Mieog JSD, Zlitni A, Park SM, Farina Sarasqueta A, Vahrmeijer AL, Swijnenburg RJ. Real-time surgical margin assessment using ICG-fluorescence during laparoscopic and robot-assisted resections of colorectal liver metastases. *Ann Transl Med* 2020;8(21): 1448.

61 Gild P, Kluth LA, Vetterlein MW, Engel O, Chun FKH, Fisch M. Adult iatrogenic ureteral injury and stricture-incidence and treatment strategies. *Asian J Urol* 2018;5(2): 101-106.

62 Blackwell RH, Kirshenbaum EJ, Shah AS, Kuo PC, Gupta GN, Turk TMT. Complications of Recognized and Unrecognized Iatrogenic Ureteral Injury at Time of Hysterectomy: A Population Based Analysis. *J Urol* 2018;199(6): 1540-1545.

63 White LA, Joseph JP, Yang DY, Kelley SR, Mathis KL, Behm K, Viers BR. Intraureteral indocyanine green augments ureteral identification and avoidance during complex robotic-assisted colorectal surgery. *Colorectal Dis* 2020.

64 Mandovra P, Kalikar V, Patankar RV. Real-Time Visualization of Ureters Using Indocyanine Green During Laparoscopic Surgeries: Can We Make Surgery Safer? *Surg Innov* 2019;26(4): 464-468.

65 Cabanes M, Boria F, Hernández Gutiérrez A, Zapardiel I. Intra-operative identification of ureters using indocyanine green for gynecological oncology procedures. *Int J Gynecol Cancer* 2019.

66 Al-Taher M, Van Den Bos J, Schols RM, Bouvy ND, Stassen LPS. Fluorescence Ureteral Visualization in Human Laparoscopic Colorectal Surgery Using Methylene Blue. *J Laparoendosc Adv Surg Techn* 2016;26(11): 870-875.

67 Barnes TG, Hompes R, Birks J, Mortensen NJ, Jones O, Lindsey I, Guy R, George B, Cunningham C, Yeung TM. Methylene blue fluorescence of the ureter during colorectal surgery. 2018;32(9): 4036-4043.

68 Verbeek FPR, Van Der Vorst JR, Schaafsma BE, Swijnenburg RJ, Gaarenstroom KN, Elzevier HW, Van De Velde CJH, Frangioni JV, Vahrmeijer AL. Intraoperative near infrared fluorescence guided identification of the ureters using low dose methylene blue: A first in human experience. *J Urol* 2013;190(2): 574-579.

69 de Valk KS, Handgraaf HJ, Deken MM, Sibinga Mulder BG, Valentijn AR, Terwisscha van Scheltinga AG, Kuil J, van Esdonk MJ, Vuijk J, Bevers RF, Peeters KC, Holman FA, Frangioni JV, Burggraaf J, Vahrmeijer AL. A zwitterionic near-infrared fluorophore for real-time ureter identification during laparoscopic abdominopelvic surgery. *Nat Commun* 2019;10(1).

70 Farnam RW, Arms RG, Klaassen AH, Sorger JM. Intraoperative ureter visualization using a near-infrared imaging agent. *J Biomed Opt* 2019;24(6): 1-8.

71 Huh WK, Johnson JL, Elliott E, Boone JD, Leath CA, Kovar JL, Kim KH. Fluorescence Imaging of the Ureter in Minimally Invasive Pelvic Surgery. *J Minimally Invasive Gynecol* 2020.

72 Al-Taher M, van den Bos J, Schols RM, Kubat B, Bouvy ND, Stassen LPS. Evaluation of a novel dye for near-infrared fluorescence delineation of the ureters during laparoscopy. *BJS Open* 2018;2(4): 254-261.

73 Simone G, Misuraca L, Anceschi U, Minisola F, Ferriero M, Guaglianone S, Tuderti G, Gallucci M. Urethra and Ejaculation Preserving Robot-assisted Simple Prostatectomy: Near-infrared Fluorescence Imaging-guided Madigan Technique. *Eur Urol* 2019;75(3): 492-497.

74 Nitta T, Tanaka K, Kataoka J, Ohta M, Ishii M, Ishibashi T, Okuda J. Novel technique with the IRIS U kit to prevent urethral injury in patients undergoing transanal total mesorectal excision. *Ann Med Surg* 2019;46: 1-3.

75 Lange MM, Marijnen CA, Maas CP, Putter H, Rutten HJ, Stiggelbout AM, Meershoek-Klein Kranenbarg E, van de Velde CJ, Cooperative clinical investigators of the D. Risk factors for sexual dysfunction after rectal cancer treatment. *Eur J Cancer* 2009;45(9): 1578-1588.

76 Lange MM, van de Velde CJ. Urinary and sexual dysfunction after rectal cancer treatment. *Nat Rev Urol* 2011;8(1): 51-57.

77 Gonzales J, Pirovano G, Chow CY, de Souza Franca PD, Carter LM, Klint JK, Guru N, Lewis JS, King GF, Reiner T. Fluorescence labeling of a NaV1.7-targeted peptide for near-infrared nerve visualization. *EJNMMI Res* 2020;10(1).

78 Hingorani DV, Whitney MA, Friedman B, Kwon JK, Crisp JL, Xiong Q, Gross L, Kane CJ, Tsien RY, Nguyen QT. Nerve-targeted probes for fluorescence-guided intraoperative imaging. *Theranostics* 2018;8(15): 4226-4237.

79 Wang LG, Barth CW, Kitts CH, Mebrat MD, Montaño AR, House BJ, McCoy ME, Antaris AL, Galvis SN, McDowall I, Sorger JM, Gibbs SL. Near-infrared nerve-binding fluorophores for buried nerve tissue imaging. *Sci Transl Med* 2020;12(542).

80 Sparreboom CL, Komen N, Rizopoulos D, Verhaar AP, Dik WA, Wu Z, van Westreenen HL, Doornebosch PG, Dekker JWT, Menon AG, Daams F, Lips D, van Grevenstein WMU, Karsten TM, Bayon Y, Peppelenbosch MP, Wolthuis AM, D'Hoore A, Lange JF. A multicentre cohort study of serum and peritoneal biomarkers to predict anastomotic leakage after rectal cancer resection. *Colorectal Dis* 2020;22(1): 36-45.

81 Angeramo CA, Dreifuss NH, Schlottmann F, Bun ME, Rotholtz NA. Postoperative outcomes in patients undergoing colorectal surgery with anastomotic leak before and after hospital discharge. *Updates Surg* 2020;72(2): 463-468.

82 van Manen L, Handgraaf HJM, Diana M, Dijkstra J, Ishizawa T, Vahrmeijer AL, Mieog JSD. A practical guide for the use of indocyanine green and methylene blue in fluorescence-guided abdominal surgery. *J Surg Oncol* 2018;118(2): 283-300.

83 Watanabe J, Ishibe A, Suwa Y, Suwa H, Ota M, Kunisaki C, Endo I. Indocyanine green fluorescence imaging to reduce the risk of anastomotic leakage in laparoscopic low anterior resection for rectal cancer: a propensity score-matched cohort study. *Surg Endosc* 2020;34(1): 202-208.

84 Kin C, Vo H, Welton L, Welton M. Equivocal effect of intraoperative fluorescence angiography on colorectal anastomotic leaks. *Dis Colon Rectum* 2015;58(6): 582-587.

85 Kudszus S, Roesel C, Schachtrupp A, Höer JJ. Intraoperative laser fluorescence angiography in colorectal surgery: a noninvasive analysis to reduce the rate of anastomotic leakage. *Langenbeck's Arch Surg* 2010: 1-6.

86 Song M, Liu J, Xia D, Yao H, Tian G, Chen X, Liu Y, Jiang Y, Li Z. Assessment of intraoperative use of indocyanine green fluorescence imaging on the incidence of anastomotic leakage after rectal cancer surgery: a PRISMA-compliant systematic review and meta-analysis. *Tech Coloproctol* 2020.

87 De Nardi P, Elmore U, Maggi G, Maggiore R, Boni L, Cassinotti E, Fumagalli U, Gardani M, De Pascale S, Parise P, Vignali A, Rosati R. Intraoperative angiography with indocyanine green to assess anastomosis perfusion in patients undergoing laparoscopic colorectal resection: results of a multicenter randomized controlled trial. *Surg Endosc* 2020;34(1): 53-60.

88 Alekseev M, Rybakov E, Shelygin Y, Chernyshov S, Zarodnyuk I. A study investigating the perfusion of colorectal anastomoses using fluorescence angiography: results of the FLAG randomized trial. *Colorectal Dis* 2020.

89 Rahbari NN, Weitz J, Hohenberger W, Heald RJ, Moran B, Ulrich A, Holm T, Wong WD, Tiret E, Moriya Y, Laurberg S, den Dulk M, van de Velde C, Buchler MW. Definition and grading of anastomotic leakage following anterior resection of the rectum: a proposal by the International Study Group of Rectal Cancer. *Surgery* 2010;147(3): 339-351.

90 Jafari MD, Pigazzi A, McLemore EC, Mutch MG, Haas E, Rasheid S, Wait AD, Paquette IM, Bardakcioglu O, Safar B, Landmann RG, Varma M, Maron DJ, Martz J, Bauer J, George VV, Fleshman JW, Steele SR, Stamos MJ. Perfusion Assessment in Left-Sided/Low Anterior Resection (PILLAR III): A Randomized, Controlled, Parallel, Multicenter Study Assessing Perfusion Outcomes with PINPOINT Near-Infrared Fluorescence Imaging in Low Anterior Resection. *Dis Colon Rectum* 2021.

91 Musters GD, Klaver CEL, Bosker RJI, Burger JWA, van Duijvendijk P, van Etten B, van Geloven AAW, de Graaf EJR, Hoff C, Leijtens JWA, Rutten HJT, Singh B, Vuylsteke R, de Wilt JHW, Dijkgraaf MGW, Bemelman WA, Tanis PJ. Biological Mesh Closure of the Pelvic Floor After Extralevator Abdominoperineal Resection for Rectal Cancer: A Multicenter Randomized Controlled Trial (the BIOPEX-study). *Ann Surg* 2017;265(6): 1074-1081.

92 Chandra A, Srivastava RK, Kashyap MP, Kumar R, Srivastava RN, Pant AB. The anti-inflammatory and antibacterial basis of human omental defense: selective expression of cytokines and antimicrobial peptides. *PLoS One* 2011;6(5): e20446.

93 Blok RD, Hagemans JAW, Klaver CEL, Hellinga J, van Etten B, Burger JWA, Verhoef C, Hompes R, Bemelman WA, Tanis PJ. A Systematic Review and Meta-analysis on Omentoplasty for the Management of Abdominoperineal Defects in Patients Treated for Cancer. *Ann Surg* 2020;271(4): 654-662.

94 Slooter MD, Blok RD, Wisselink DD, Buskens CJ, Bemelman WA, Tanis PJ, Hompes R. Near-infrared fluorescence angiography for intra-operative assessment of pedicled omentoplasty for filling of a pelvic cavity: a pilot study. *Tech Coloproctol* 2019;23(8): 723-728.

95 Slooter MD, Blok RD, de Krom MA, Buskens CJ, Bemelman WA, Tanis PJ, Hompes R. Optimizing omentoplasty for management of chronic pelvic sepsis by intra-operative fluorescence angiography: a comparative cohort study. *Colorectal Dis* 2020;22(12): 2252-2259.

96 Keereweer S, Van Driel PB, Snoeks TJ, Kerrebijn JD, Baatenburg de Jong RJ, Vahrmeijer AL, Sterenborg HJ, Löwik CW. Optical image-guided cancer surgery: challenges and limitations. *Clin Cancer Res* 2013;19(14): 3745-3754.

97 Lütken CD, Achiam MP, Svendsen MB, Boni L, Nerup N. Optimizing quantitative fluorescence angiography for visceral perfusion assessment. *Surg Endosc* 2020;34(12): 5223-5233.

98 Goncalves LN, van den Hoven P, van Schaik J, Leeuwenburgh L, Hendricks CHF, Verduijn PS, van der Bogt KEA, van Rijswijk CSP, Schepers A, Vahrmeijer AL, Hamming JF, van der Vorst JR. Perfusion Parameters in Near-Infrared Fluorescence Imaging with Indocyanine Green: A Systematic Review of the Literature. *Life* 2021;11(5): 433.

99 Lauwerends LJ, van Driel P, Baatenburg de Jong RJ, Hardillo JAU, Koljenovic S, Puppels G, Mezzanotte L, Löwik C, Rosenthal EL, Vahrmeijer AL, Keereweer S. Real-time fluorescence imaging in intraoperative decision making for cancer surgery. *Lancet Oncol* 2021.

Supplementaries

SUPPLEMENT 1 Search strategies per database and the corresponding hits after removal of duplicates.

Database	Full search strategy
Embase (1123 articles)	('fluorescence guided surgery'/de OR (('fluorescence angiography'/de OR 'fluorescence imaging system'/de OR 'indocyanine green angiography'/de OR 'indocyanine green'/de OR 'near infrared spectroscopy'/exp OR 'near infrared imaging system'/de OR 'fluorescence imaging'/de) AND ('surgery'/exp OR surgery:lnk OR 'laparoscope'/exp)) OR (((fluorescen* OR indocyanine-green* OR ICG OR near-infrared* OR near-infra-red*) NEAR/9 (surg* OR operat* OR intraoperat* OR resect* OR microsurg* OR laparoscop*))):ab,ti,kw) AND ('large intestine tumour'/exp OR 'large intestine cancer'/exp OR 'large intestine carcinoma'/exp OR 'colorectal surgery'/exp OR 'ureter'/de OR 'ureter injury'/de OR 'ureter surgery'/exp OR 'urethra'/exp OR 'urethra injury'/de OR 'urethra surgery'/exp OR 'peripheral nerve'/de OR (((rect* OR colorect* OR colon* OR appendi* OR anal* OR anus OR cecum OR caecum OR large-intestin* OR sigmoid* OR bowel*) NEAR/3 (carcinoma* OR neoplas* OR tumour* OR tumour* OR cancer* OR surger* OR resect*)) OR ureter* OR urethr* OR (nerve* NEAR/3 (imag* OR detect* OR locali*))):ab,ti,kw) NOT (conference abstract)/lim AND (english)/lim
Medline (198 articles)	(((Fluorescein Angiography/ OR Optical Imaging/ OR Indocyanine Green/ OR Spectroscopy, Near-Infrared/) AND (exp Surgical Procedures, Operative/ OR surgery.fs. OR Laparoscopy/)) OR (((fluorescen* OR indocyanine-green* OR ICG OR near-infrared* OR near-infra-red*) ADJ9 (surg* OR operat* OR intraoperat* OR resect* OR microsurg* OR laparoscop*))).ab,ti,kf.) AND (exp Colorectal Neoplasms/ OR Colorectal Surgery/ OR Urethra/ OR Ureter/ OR Peripheral Nerves/ OR (((rect* OR colorect* OR colon* OR appendi* OR anal* OR anus OR cecum OR caecum OR large-intestin* OR sigmoid* OR bowel*) ADJ3 (carcinoma* OR neoplas* OR tumour* OR tumour* OR cancer* OR surger* OR resect*)) OR ureter* OR urethr* OR (nerve* ADJ3 (imag* OR detect* OR locali*))).ab,ti,kf.) NOT (letter* OR news OR comment* OR editorial* OR congres* OR abstract* OR book* OR chapter* OR dissertation abstract*).pt. AND english.lg.
Cochrane (73 articles)	((((fluorescen* OR indocyanine-green* OR ICG OR "near-infrared*" OR "near-infra-red*") NEAR/9 (surg* OR operat* OR intraoperat* OR resect* OR microsurg* OR laparoscop*))):ab,ti,kw) AND ((((rect* OR colorect* OR colon* OR appendi* OR anal* OR anus OR cecum OR caecum OR large-intestin* OR sigmoid* OR bowel*) NEAR/3 (carcinoma* OR neoplas* OR tumour* OR tumour* OR cancer* OR surger* OR resect*)) OR ureter* OR urethr* OR (nerve* NEAR/3 (imag* OR detect* OR locali*))):ab,ti,kw)

SUPPLEMENT 2 Overview of all clinical studies on colorectal cancer surgery assessing experimental fluorescent agents.

PRIMARY TUMOUR

First author	Tumour type	Year	Fluorescent agent	Study design	Fluorescence imaging application	Nr of patients	(Optimal) dose	(Optimal) adm. interval	Optimal TBR (mean)	Sensitivity	Specificity	Change in surgical management	Other outcomes
Boogerd (14)	CC + RC	2018	SGM-101	Open-label, dose escalation	*In vivo* and PEARL MSI	26*	10 mg	4 days	1.64 (*in vivo*) 6.1 (*ex vivo*: PEARL MSI)	98%	62%	35%	ppv: 81% | npv: 94% | acc: 84%
De Jongh (16)	RC	2020	Bevacizumab-800CW	Open-label, fixed dose, pilot study	1 = Back table imaging for CRM evaluation 2 = Odyssey imaging to determine sens / spec for tumour detection	1 = 8 2 = 17	4.5 mg	2-3 days	4.7 (*ex vivo*: Odyssey)	96.19%**	80.39%**	na	Tumour positive correctly identified in 1 out of 2 patients (50%)
De Valk (15)	CC	2020	cRGD-ZW800-1	Open-label, dose escalation	*In vivo* and PEARL MSI	12	0.05 mg/kg	18 hours	1.6 (*in vivo*) 6.2 (*ex vivo*: PEARL MSI)	nr	nr	nr	Lymph nodes: sens 100% | spec: 87% | ppv: 33% | npv: 100% | acc: 88%
De Valk (18)	CC + RC	2020	SGM-101	Open-label, dose escalation	*In vivo* and back table	37*	10 mg	4 days	1.9 (*in vivo*) 3.5 (*ex vivo*: back table)	96%	63%	24%	ppv: 70% | npv: 94% | acc: 78%
Voskuil (17)	nr***	2020	ONM-100	Open-label, dose escalation	PEARL MSI	3	1.2 mg/kg	24 hours	nr***	nr***	nr***	nr***	-

(B) SENTINEL LYMPH NODE

First author	Year	Fluorescent agent	Study design	Fluorescence imaging application	Nr of patients	(Optimal) dose	(Optimal) adm. interval	SBR	Sensitivity	Specificity	Change in surgical management	Other outcomes
Hutteman (39)	2011	HSA800	Pilot study	Ex vivo	24	1cc 50 µM	post-operative in specimen	nr	nr	na	nr	SLN's detected: 100% | avg SLN's: 3
Schaafsma (38)	2013	HSA800	Pilot study	Ex vivo	22	1cc 50 µM	post-operative in specimen	nr	80%	na	nr	SLN's detected: 95% | avg SLN's: 3.5
Weixler (40)	2017	HSA800	Prospective single-centre	Ex vivo	50	1cc 50 µM	post-operative in specimen	nr	64%	na	10%	SLN's detected: 100% | avg SLN's: 4.4

(C) PERITONEAL METASTASES

First author	Year	Fluorescent agent	Study design	Fluorescence imaging application	Nr of patients	(Optimal) dose	(Optimal) adm. interval	Optimal TBR (mean)	Sensitivity	Specificity	Change in surgical management	Other outcomes
Harlaar (48)	2016	Bevacizumab-800CW	Open-label, feasibility study	*In vivo* and back table	7	4.5 mg	2 days	6.92 (*ex vivo*: back table)	nr	nr	29%	ppv: 53% | npv: 100%
Schaap (49)	2020	SGM-101	Open-label, pilot study	*In vivo* and back table	14	10-15 mg	4-6 days	nr	98.5%	62.2%	50%	ppv: 82.3%| npv: 95.8%| acc: 85.4%

(D) LIVER METASTASES

First author	Year	Fluorescent agent	Study design	Fluorescence imaging application	Nr of patients	Optimal dose	(Optimal) adm. interval	Optimal TBR (median)	Sensitivity	Specificity	Change in surgical management	Other outcomes
Meijer (58)	2020	SGM-101	Open label, dose finding	*In vivo* (occult lesions and resection margin)	8	10 mg	4 days	2.0 (*in vivo*)	nr	nr	0%	ppv: 89% | positive : 9%

(E) URETER

First author	Year	Fluorescent agent	Study design	Fluorescence imaging application	Nr of patients	Optimal dose	Adm. interval	Optimal SBR	Ureters identified	Duration of visualisation
De Valk (69)	2019	ZW800-1	Open label, dose finding	In vivo	12	2.5 mg	per-operative	2.7	100%	3.5 hours
Farnam (70)	2019	IS-001	Open label, dose finding	In vivo	24	20-40 mg	per-operative	3.6	100%	nr
Huh (71)	2020	IRDye-800BK	Open label, dose finding	In vivo	41	0.06 mg/kg	per-operative	nr	100%	1.5 hours

* 21 out of 26 patients from Boogerd et al were also included in the study by de Valk *et al.*

** Based on microscopy determined optimal mean fluorescence intensity cut off values for tumour detection

*** Results of interest not separately specified for colorectal cancer patientsw

SUPPLEMENT 3 overview of all ongoing clinical trials on colorectal cancer surgery assessing experimental fluorescent agents.

Principal investigator	Fluorescent agent	Study phase	Imaging target	Tumour type	Planned inclusion FLI (n)	Control group (n)	Recruitment status	(Estimated) study completion date	NCT number
Barnes, T.G.	IRDYe-800BK	Phase I/II	Ureter	na	40	na	Completed	nov-18	NCT03387410
Chan, A.T.	LUM015	Phase I	Primary tumour	All stage colorectal cancer	11	na	Recruiting	dec-20	NCT02584244
Cusack, J.C.	LUM015	nr	Peritoneal metastases	Peritoneal metastases of CRC	nr*	na	Not yet recruiting	feb-21	NCT03834272
OncoNano Medicine, Inc.	ONM-100	Phase II	Primary tumour	Colorectal cancer, not specified	nr*	na	Recruiting	dec-20	NCT03735680
Vahrmeijer, A.L.	SGM-101	Phase III	Primary tumour and peritoneal metastases	LARC & LRRC, T4 colon cancer, locally recurrent colon cancer, and peritoneal metastases of CRC	240	60	Recruiting	dec-21	NCT03659448
Vahrmeijer, A.L	SGM-101	Phase II	Extra abdominal metastases	Colorectal lung metastases	10	na	Recruiting	dec-21	NCT04737213
Vahrmeijer, A.L	SGM-101	Phase II	Extra abdominal metastases	Colorectal brain metastases	10	na	Not yet recruiting	dec-22	NCT04755920
Vahrmeijer, A.L	SGM-101	Phase III	Primary tumour	LARC & LRRC	203	na	Recruiting	oct-23	NCT04642924

* Study assessing various tumour types, amount of patient undergoing surgery for colorectal cancer is not specified.

SUPPLEMENT 4 MINORS score per study assessing experimental fluorescent agents.

First author	MINORS score	Maximum MINORS score	Clearly stated aim	Consecutive patients	Prospective data collection	Appropriate endpoint	Unbiased evaluation of endpoints	Appropriate follow-up	Loss to follow-up	Prospective calculation of sample size	Gold Standard control	Contemporary groups	Baseline equivalence of groups	Statistical analysis adapted to study design
Boogerd (14)	14	16	2	2	2	2	0	2	2	2	NA	NA	NA	NA
De Jongh (16)	11	16	2	2	1	2	0	2	2	0	NA	NA	NA	NA
De Valk (15)	14	16	2	2	2	2	2	2	2	0	NA	NA	NA	NA
De Valk (18)	14	16	2	2	2	2	0	2	2	2	NA	NA	NA	NA
Voskuil (17)	14	16	2	2	2	2	2	2	2	0	NA	NA	NA	NA
Hutteman (39)	11	16	1	2	2	2	0	2	2	0	NA	NA	NA	NA
Schaafsma (38)	18	24	2	2	2	2	0	2	2	0	2	2	0	2
Weixler (40)	13	24	2	0	1	2	0	2	0	0	2	0	2	2
Harlaar (48)	14	16	2	2	2	2	2	2	2	0	NA	NA	NA	NA
Schaap (49)	12	16	2	2	2	2	0	2	2	0	NA	NA	NA	NA
Meijer (58)	12	16	2	2	2	2	0	2	2	0	NA	NA	NA	NA
De Valk (69)	14	16	2	2	2	2	2	2	2	0	NA	NA	NA	NA
Farnam (70)	14	16	2	2	2	2	0	2	2	2	NA	NA	NA	NA
Huh (71)	12	16	2	2	2	2	0	2	2	0	NA	NA	NA	NA

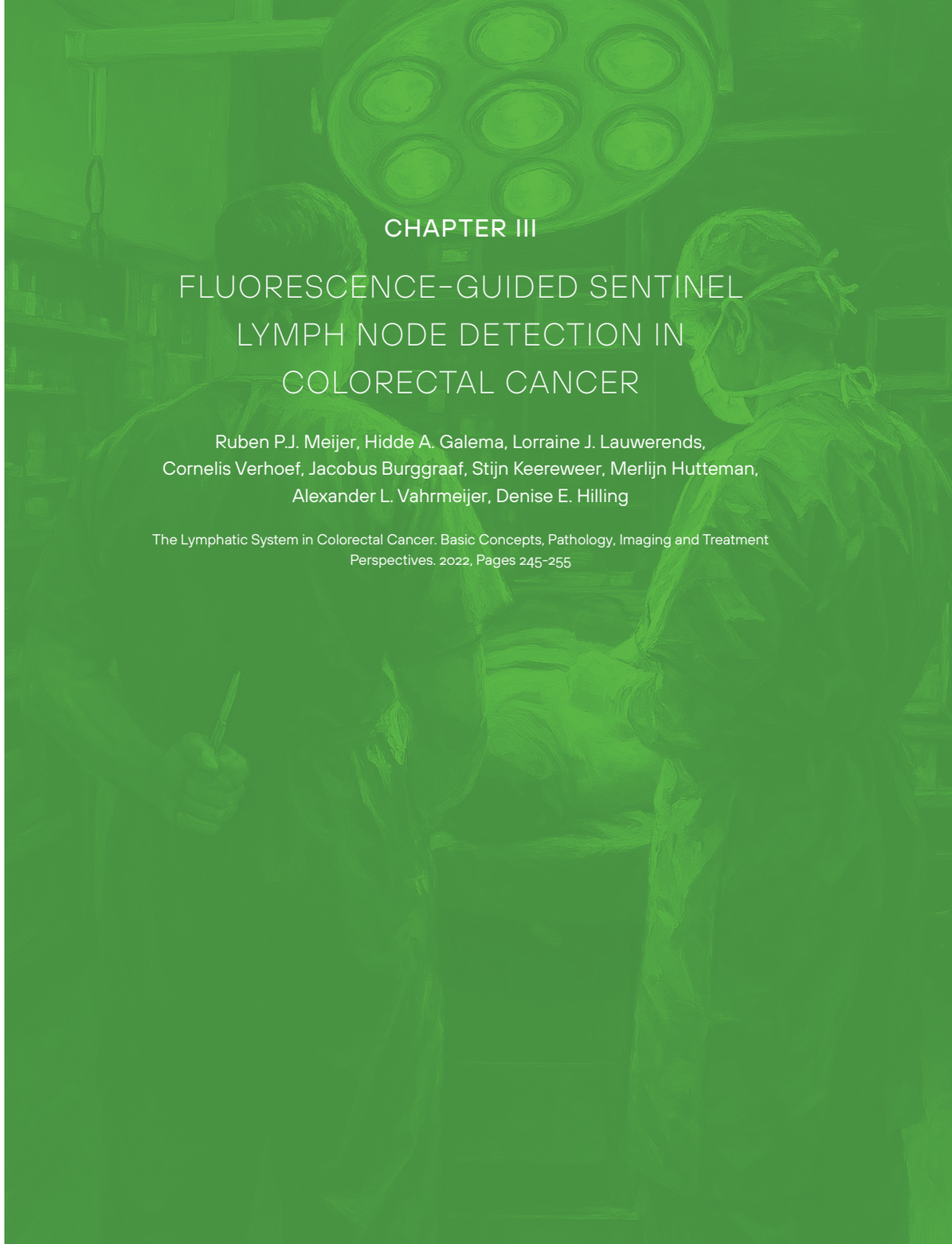

CHAPTER III

FLUORESCENCE-GUIDED SENTINEL LYMPH NODE DETECTION IN COLORECTAL CANCER

Ruben P.J. Meijer, Hidde A. Galema, Lorraine J. Lauwerends, Cornelis Verhoef, Jacobus Burggraaf, Stijn Keereweer, Merlijn Hutteman, Alexander L. Vahrmeijer, Denise E. Hilling

The Lymphatic System in Colorectal Cancer. Basic Concepts, Pathology, Imaging and Treatment Perspectives. 2022, Pages 245-255

Abstract

Sentinel lymph node (SLN) mapping can be a valuable addition to the treatment of colorectal cancer patients. Nevertheless, conventional lymph node mapping methods using blue dye are limited due to inadequate depth penetration, and the use of a radiocolloid tracer has its logistic hurdles. With near-infrared (NIR) fluorescence imaging, the SLN can be accurately identified in most patients resulting in more accurate lymph node staging. Current technical challenges and the low negative predictive value of the SLN withhold surgeons from its use in daily practice.

Concept of sentinel lymph node mapping

Adequate lymph node staging is important in colorectal cancer (CRC) treatment, as lymph node metastases are an important determinant for patient prognosis and an indication for adjuvant systemic treatment. The sentinel lymph node (SLN) is defined as the first group of lymph node(s) draining a tumour. The identification, removal, and analysis of these SLNs (SLN mapping) can therefore be of added value for the staging of CRC patients, and subsequent treatment. SLN mapping was first described in 1960 for parotid cancer and is nowadays standard of care in breast cancer and melanoma patients.[1-3]

The SLN concept could also be of added value in CRC patients. Patients with stage I and II diseases (with no lymph node involvement) still develop distant metastases in up to 30% of cases.[4] This could be the result of, among others, understaging of these patients due to missed lymph nodes with occult tumour cells and micrometastases during routine histopathological examination, or inadequate lymph node harvesting at the time of primary treatment. Routine histopathological examination currently exists of reviewing a single paraffin-embedded slide per lymph node, with the chance of missing tumour cells away from the slide's cutting edge. Extensive histopathological analysis of all lymph nodes using serial sectioning or reverse transcriptase polymerase chain reaction could result in more accurate lymph node staging. However, both methods are expensive and time consuming.[5-7] As the SLN procedure identifies the lymph node(s) with the highest chance of containing metastases, more extensive histopathological analysis of only these lymph nodes is feasible. Furthermore, tumour-negative SLNs create an opportunity for local or endoscopic resection of CRC, especially in early-stage tumours.[8]

Conventional methods for SLN mapping include the use of either blue dye, a radiocolloid tracer, or the combination of both.[2,3] The use of blue dye for SLN mapping in CRC is limited due to inadequate depth penetration and the utilization of radiocolloid tracers has some logistic hurdles.[9] A nuclear medicine physician and an endoscopist are required for tracer injection. Moreover, the gamma probe used for localization does not enable real-time visualization. These shortcomings have increased the interest in novel techniques, such as near-infrared (NIR) fluorescence imaging.

Fluorescence-guided surgery

NIR fluorescence imaging provides the surgeon with real-time information of the surgical field and can aid in differentiation between malignant and healthy tissue during surgery.[10] NIR light (700-900 nm) is not visible to the human eye and has relatively deep (up to 10 mm) tissue penetration. Human tissue itself has low autofluorescence in the NIR light spectrum, resulting in a high signal-to-background ratio.[11] NIR fluorescence-guided surgery requires two components: an NIR camera system and a fluorescent agent (figure 1). These NIR camera systems are composed of an NIR excitation light source, collection optics (including optical filtration), and a camera that can detect emitted NIR light. These systems emit photons with a specific wavelength, which are absorbed by the fluorescent agent. Electrons within these agent's molecules transit to an excited state and fall back to their ground state (figure 2). This will release the stored energy in an emitted photon with a longer wavelength than the exciting light of the NIR camera system, the so-called Stokes shift. This emitted photon is subsequently captured by the camera system. The camera output is usually displayed on a monitor including a merged image of the fluorescence signal and the white light image. Both the camera systems and fluorescent agents have shown great improvements in the last decades and have resulted in the clinical use of NIR fluorescence for different purposes during surgery (e.g., bile duct detection, tissue perfusion).[12-14]

Several dedicated NIR fluorescence imaging systems are clinically used for open, laparoscopic, and robotic surgery. On the other hand, only two fluorescent agents, indocyanine green (ICG) and methylene blue, have been approved for clinical use by the US Food and Drug Administration (FDA) and European Medicines Agency (EMA). Both are nontargeted fluorescent agents, meaning these agents do not bind to a specific target. ICG, first described in 1957 for the determination of cardiac output, is the most used agent for fluorescence-guided SLN mapping in various cancer types and can also be used for the visualization of vital structures (e.g., bile ducts), liver tumours, and assessment of tissue perfusion.[14-15]

FIGURE 1 Fluorescence-guided surgery.
NIR fluorescent agents are administered intravenously or locally. NIR fluorescence is visualized using a specialized imaging system for intraoperative imaging. The imaging system uses dedicated NIR excitation light to excite the fluorophore. Collection optics, emission filters, and an image sensor capable of detecting NIR fluorescence emission light. The NIR fluorescence signal is displayed on a monitor in the surgical theater. A simultaneous white light image, which can be merged with the NIR fluorescence image, is desirable.

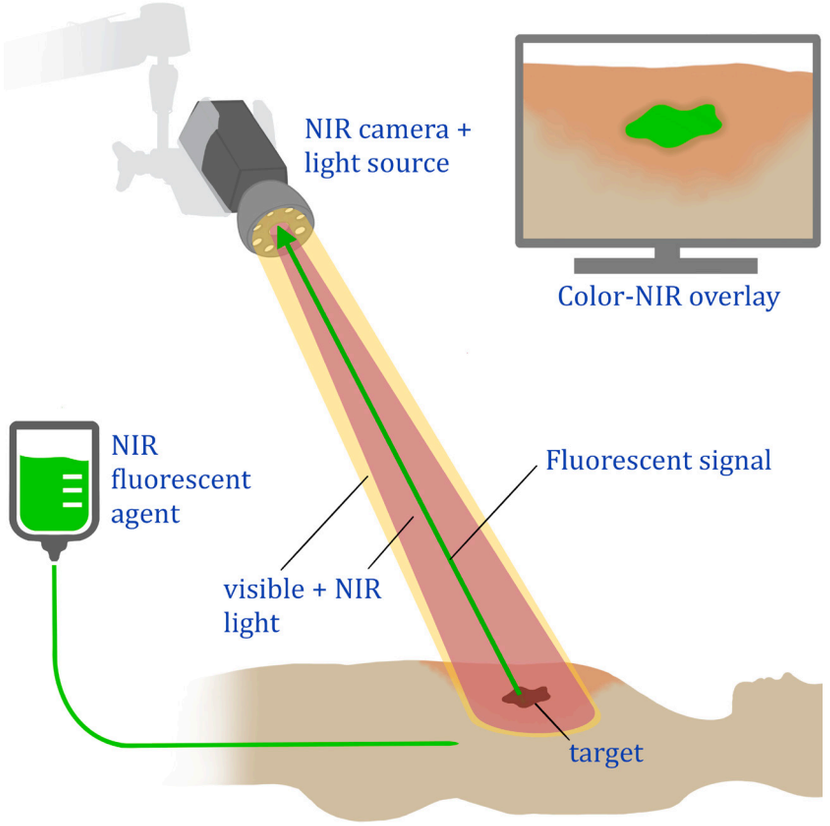

FIGURE 2 Schematic overview of the principle of fluorescence.
A photon in the appropriate wavelength (excitation light) is absorbed by the fluorophore, elevating an electron to an excited state. When the electron transitions back to its ground state, a photon is emitted. This emitted photon is of a longer wavelength and lower energy.

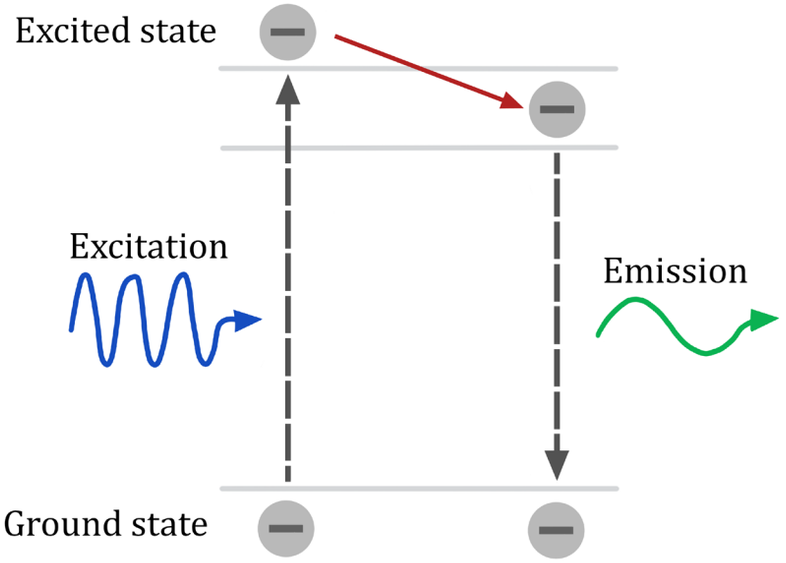

Fluorescence-guided sentinel lymph node detection in colorectal cancer

While peritumoural injection of ICG is the most used technique for NIR fluorescence guided SLN mapping, alternative fluorescent dyes have also been assessed (figure 3). In addition, different injection sites and variable timing of the injection have been investigated.

The injection site of ICG can be either subserosal or submucosal, with a slight preference for the latter.[16-18] The submucosa houses an important part of the intestinal lymphatic system, which might improve the lymphatic uptake of the fluorescent agent from the tumour surrounding tissue.[19] Submucosal injection is performed prior to or during surgery, via endoscopy. Subserosal injection, on the other hand, is performed intraoperatively by the surgeon. In minimally invasive surgery, this requires transcutaneous injection of the fluorescent agent. Correct positioning of the needle and maintaining this position during injection of the fluorescent agent is easier with the submucosal technique and therefore leads to less spillage of ICG.[16-17]

Timing of fluorescent dye administration and assessment has been assessed directly pre- or intraoperatively (both referred to as *in vivo*), and postoperatively (*ex vivo*). *In vivo* administration has some practical drawbacks, particularly for the preferred submucosal injection. For *in vivo* submucosal injection, an endoscopy in the operating room is required directly before or during surgery, which poses a logistical challenge. Furthermore, bowel insufflation might alter the surgical field and therefore hamper the surgical procedure. The alternative, *ex vivo* imaging, is logistically simpler and enables the use of experimental agents. *Ex vivo* imaging also has some disadvantages. Lymphatic flow may be disrupted after resection, and altering the surgical plan (i.e., perform a more limited resection) based on histopathological analysis of the harvested lymph nodes is not possible. Moreover, *ex vivo* fluorescent agent injection and lymph node identification does not facilitate identifying SLNs in patients with aberrant lymph node drainage patterns.[20]

Table 1 summarizes studies that describe fluorescence-guided SLN mapping in CRC patients. A procedure is defined as successful if one or more lymph nodes were identified by fluorescence (the SLN). An upstaged patient is defined as a patient who was staged as No (all lymph nodes being tumour-negative) using conventional histopathology but showed tumour-positive SLNs after additional extensive histopathological assessment of the SLNs. These patients can consequently change from stage I or II CRC to stage III. The percentage of upstaged patients was calculated by dividing the number of upstaged patients by all lymph node-negative patients before extensive histopathological assessment of the SLN.

In all studies, intraoperative identification of the SLNs was performed using ICG and this was successful in most cases. Andersen *et al.* had a remarkably lower success rate of 65.5% in their multicenter trial, with all other studies being single center.[16] This could be explained by a learning curve, which is suggested by Bembenek *et al.* to be more than 22 cases per center, a number none of their centers had reached.[9] The sensitivity of SLN identification with ICG ranged from 0.33 to 1, and the negative predictive value was relatively low, with only three (33%) studies reporting an NPV above 0.9.

FIGURE 3 Intraoperative results of sentinel lymph node mapping using with indocyanine green.

Three patients (I-III) demonstrating NIR fluorescence-guided sentinel lymph node mapping with indocyanine green (A, a white light image; B, an NIR image without filter; and C, a filtered NIR image). (I) Two bright spots in the mesocolon were identified in the filtered view, consistent with sentinel lymph nodes. (II) A bright spot is seen in the filtered view, consistent with a paraaortic sentinel lymph node. (III) A bright spot is seen in the filtered view, alongside the right iliac artery, consistent with a sentinel lymph node. The injection site of the rectal tumour is clearly visible, as well as an efferent channel in the sigmoid mesentery which was found to lead to another sentinel lymph node.

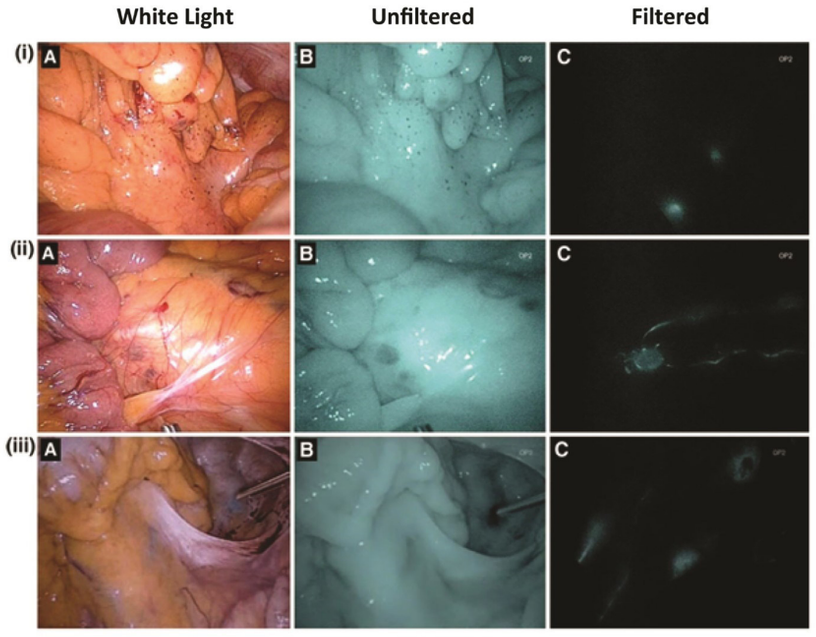

Source: Reproduced by permission from Cahill, R. A., Anderson, M., Wang, L. M., Lindsey, I., Cunningham, C., Mortensen, N. J. (2012) (40). Near-infrared (NIR) laparoscopy for intraoperative lymphatic road-mapping and sentinel node identification during definitive surgical resection of early-stage colorectal neoplasia. Surgical Endoscopy, 26(1), 197-204.

TABLE 1 Results of clinical trials assessing fluorescence-guided SLN mapping for CRC.

	Agent	Patients	Diagnosis	Procedure	Injection site	Number SLNs	Success rate	Sensitivity	NPV	Upstaged patients* (%)
INTRAOPERATIVE										
Andersen (16)	ICG:HA	29	CC	L	SS	1 (0-3)*	65.50%	0.33	0.76	1 (12%)
Ankersmit (17)	ICG:HA	29	CC	L	14 SS; 15 SM	2 (0-6)*	89.70%	0.44	0.8	3 (13%)
Cahill (39)	ICG	18	CRC	L	SM	3.6 (1-5)**	100%	1	1	0 (0%)
Carrara (40)	ICG	95	CRC	L	SS	1.5 (1-5)**	96.8	0.73	0.96	1 (1%)
Currie (41)	ICG	30	CC	L	SM	3 (1-4)***	90%	0.33	0.75	1 (5%)
Hirche (42)	ICG	26	CC	O	SS	1.7 (0-5)**	96%	0.82	0.87	3 (21%)
Kusano (43)	ICG	26	CRC	O	SS	2.6 (± 2.4)****	88.50%	0.5	0.81	NR
Nagata (44)	ICG	48	CRC	L	SS	3.5 (± 1.7) ****	97.90%	0.44	0.89	NR
Noura (45)	ICG	25	RC	O	SM	2.1 (± 0.8)****	92%	1	1	NR
Watanabe (46)	ICG	31	CC	L	SS	10.4 (± 4.73)****	100%	0.67	0.93	NR
POSTOPERATIVE										
Hutteman (18)	HSA800	24	CRC	NA	SM	3 (1-5)*	100%	0.89	0.94	NR
Liberale (47)	ICG	20	CC	NA	SS	1 (0-4)*	95%	0.57	0.81	3 (23%)
Schaafsma (48)	HSA800	22	CC	NA	SM	3.5 (± 1.9)****	95%	0.8	0.94	NR
Weixler (49)	HSA800	50	CC	NA	SS	4.4 (± 2.2)****	98%	0.64	0.74	5 (17%)

The number of detected SLNs are presented as: *median with range, **mean with range, ***median with interquartile range, ****mean with standard deviation. The sensitivity is calculated by dividing the number of procedures with a tumour-positive SLN (true positives) by the sum of true positive and false negative procedures. The negative predictive value is determined by dividing the amount of true negative procedures by the sum of true negative and false negative procedures. Upstaged patients are defined as patients with no tumour involvement on conventional histopathology of all lymph nodes, but a tumour-positive SLN at advanced histopathology. The percentage of upstaged patients is calculated as: upstaged patients/upstaged patients + true negatives. Abbreviations: CC = Colon cancer; CRC = colorectal cancer; HA = human albumin; ICG = indocyanine green; L = laparoscopic; NA = not applicable; NPV = negative predictive value; NR = not reported; O = open; RC = rectal cancer; SLN = sentinel lymph nodes; SM = submucosal; SS = subserosal.

HSA800 (IRDye 800CW conjugated to human serum albumin) is another fluorescent agent used for *ex vivo* SLN mapping in CRC patients, which has not been approved by the FDA or EMA yet. Preclinical studies have shown an advantage of HSA800 over ICG regarding lymphatic entry, flow, fluorescence yield, and reproducibility. This is most likely a result of its bigger hydrodynamic diameter, resulting in improved retention in the SLN.[21] Clinical *ex vivo* studies with HSA800 have shown comparable results to *in vivo* assessment with ICG with a wide range in sensitivity (0.64-0.89) and negative predictive value (0.74-0.94).

Future perspectives

Fluorescence-guided SLN mapping has the potential to improve adequate staging in CRC patients. Despite its advantages and several published clinical studies, it is not used in common day practice. This might be the result of technical and logistic hurdles. Moreover, it is unknown if the upstaging of patients with micrometastatic lymph nodes and subsequent adjuvant treatment will lead to improved patient outcomes.

The number of early-stage CRC patients is expected to increase in the coming years, due to the introduction of nationwide screening programs.[22,23] With this increasing number of early-stage CRC patients, the number of lymph node-negative patients is also expected to rise, since 90% of the T1 tumours are No.[24,25] Especially in these patients SLN mapping might be valuable. Because of the low incidence of lymph node metastases in these patients, a reliable SLN procedure showing a tumour-negative SLN enables the possibility for local excision without an extensive lymphadenectomy, thereby potentially lowering perioperative morbidity.[8]

The relatively low negative predictive value of the SLNs (the probability that in case of a tumour-negative SLN, all other regional lymph nodes are tumour negative) is an important reason that this procedure is not yet implemented in daily practice. It withholds surgeons from performing a local excision and omitting an oncological resection based on a tumour-negative SLN. The low NPV is mainly a consequence of a high false negative rate (tumour-negative SLNs in the presence of a tumour-positive regional lymph node). One explanation for this high false negative rate is the occurrence of the so-called skip metastases, which are reported in 10-22% of the cases.[26,27] Tumour size could be another reason for this high false negative rate. T3-T4 tumours showed false negative results in 23% of the cases compared to 2% of the T1-T2 tumours.[28] It is suggested that these more invasive tumours (T3-T4) alter the lymphatic flow, resulting in skip metastases.

Based on the promising preliminary results, the interest in neoadjuvant treatment for colon cancer has increased in recent years.[29,30] This novel treatment strategy could influence the success rate of SLN mapping, as research in other tumour types suggest altered lymphatic flow after neoadjuvant treatment.[31] As a result, it could be preferable to perform SLN mapping prior to neoadjuvant therapy.

A meta-analysis by Ankersmit *et al.* showed a pooled upstaging (no tumour involvement on conventional histopathology, but a tumour-positive SLN at advanced histopathology) in 15% of the patients.[17] This means that roughly one out of seven patients is wrongly classified as No without the use of fluorescence imaging and extensive histopathological assessment of the SLN. These patients would not have been upstaged to stage III and wrongfully been withheld adjuvant therapy, which theoretically leads to worse survival.

As emphasized, the use of fluorescence-guided SLN mapping with ICG increases the detection rate of SLNs in CRC patients and can result in upstaging in a substantial number of patients. Nevertheless, this concept still requires postoperative histopathological analysis. Direct intraoperative feedback regarding the malignancy status of any lymph node could be provided with the use of tumour-targeted fluorescence-guided surgery. Tumour-targeted agents consist of a fluorophore conjugated to a targeting component and therefore possess strong binding affinity for a specific cancer-associated molecular target or biomarker.[32] Unfortunately, tumour-targeted tracers tend to show a relatively high false positive rate (fluorescent lymph node without tumour localization) of 7%-33% for lymph node imaging, due to aspecific tracer localization.[33-35] On the other hand, it is still debated whether a small tumour load (micrometastases and lymph nodes with isolated tumour cells) accumulate enough volume of the tracer to produce a sufficiently enhanced fluorescent signal. Nevertheless, tumour-targeted agents do not only allow for the identification of lymph node metastases but also other metastases, the primary tumour and tumour-positive resection margins.[36] Several tumour-targeted agents are currently studied in phase II and III trials (SGM-101 in Locally Advanced and Recurrent Rectal Cancer.[37,38]

Conclusions

Fluorescence-guided SLN mapping in CRC can be a valuable addition to detect micrometastases and occult metastases in locoregional lymph nodes. It can result in upstaging in a significant part of the patients, whom otherwise would not have received adjuvant therapy. The low negative predictive value appears to be an important reason for the delayed introduction to current standard of care. Tumour-targeted fluorescent agents might overcome these shortcomings in the future.

REFERENCES

1 Gould EA, Winship T, Philbin PH, Kerr HH. Observations on a "sentinel node" in cancer of the parotid. Cancer. 1960;13:77-8.

2 He PS, Li F, Li GH, Guo C, Chen TJ. The combination of blue dye and radioisotope versus radioisotope alone during sentinel lymph node biopsy for breast cancer: a systematic review. BMC Cancer. 2016;16:107.

3 Valsecchi ME, Silbermins D, de Rosa N, Wong SL, Lyman GH. Lymphatic mapping and sentinel lymph node biopsy in patients with melanoma: a meta-analysis. J Clin Oncol. 2011;29(11):1479-87.

4 Figueredo A, Coombes ME, Mukherjee S. Adjuvant therapy for completely resected stage II colon cancer. Cochrane Database Syst Rev. 2008;2008(3):CD005390.

5 Doekhie FS, Mesker WE, Kuppen PJ, van Leeuwen GA, Morreau H, de Bock GH, *et al.* Detailed examination of lymph nodes improves prognostication in colorectal cancer. Int J Cancer. 2010;126(11):2644-52.

6 Liefers GJ, Cleton-Jansen AM, van de Velde CJ, Hermans J, van Krieken JH, Cornelisse CJ, *et al.* Micrometastases and survival in stage II colorectal cancer. N Engl J Med. 1998;339(4):223-8.

7 Yamamoto H, Murata K, Fukunaga M, Ohnishi T, Noura S, Miyake Y, *et al.* Micrometastasis Volume in Lymph Nodes Determines Disease Recurrence Rate of Stage II Colorectal Cancer: A Prospective Multicenter Trial. Clin Cancer Res. 2016;22(13):3201-8.

8 Cahill RA, Leroy J, Marescaux J. Localized resection for colon cancer. Surg Oncol. 2009;18(4):334-42.

9 Bembenek AE, Rosenberg R, Wagler E, Gretschel S, Sendler A, Siewert JR, *et al.* Sentinel lymph node biopsy in colon cancer: a prospective multicenter trial. Ann Surg. 2007;245(6):858-63.

10 Vahrmeijer AL, Hutteman M, van der Vorst JR, van de Velde CJ, Frangioni JV. Image-guided cancer surgery using near-infrared fluorescence. Nat Rev Clin Oncol. 2013;10(9):507-18.

11 Frangioni JV. New technologies for human cancer imaging. J Clin Oncol. 2008;26(24):4012-21.

12 Griffiths M, Chae MP, Rozen WM. Indocyanine green-based fluorescent angiography in breast reconstruction. Gland Surg. 2016;5(2):133-49.

13 van den Hoven P, Ooms S, van Manen L, van der Bogt KEA, van Schaik J, Hamming JF, *et al.* A systematic review of the use of near-infrared fluorescence imaging in patients with peripheral artery disease. J Vasc Surg. 2019;70(1):286-97 e1.

14 van Manen L, Handgraaf HJM, Diana M, Dijkstra J, Ishizawa T, Vahrmeijer AL, *et al.* A practical guide for the use of indocyanine green and methylene blue in fluorescence-guided abdominal surgery. J Surg Oncol. 2018;118(2):283-300.

15 Fox IJ, Brooker LG, Heseltine DW, Essex HE, Wood EH. A tricarbocyanine dye for continuous recording of dilution curves in whole blood independent of variations in blood oxygen saturation. Proc Staff Meet Mayo Clin. 1957;32(18):478-84.

16 Andersen HS, Bennedsen ALB, Burgdorf SK, Eriksen JR, Eiholm S, Toxværd A, *et al. In vivo* and *ex vivo* sentinel node mapping does not identify the same lymph nodes in colon cancer. Int J Colorectal Dis. 2017;32(7):983-90.

17 Ankersmit M, Bonjer HJ, Hannink G, Schoonmade LJ, van der Pas M, Meijerink W. Near-infrared fluorescence imaging for sentinel lymph node identification in colon cancer: a prospective single-center study and systematic review with meta-analysis. Tech Coloproctol. 2019;23(12):1113-26.

18 Hutteman M, Choi HS, Mieog JS, van der Vorst JR, Ashitate Y, Kuppen PJ, *et al.* Clinical translation of *ex vivo* sentinel lymph node mapping for colorectal cancer using invisible near-infrared fluorescence light. Ann Surg Oncol. 2011;18(4):1006-14.

19 Miller MJ, McDole JR, Newberry RD. Microanatomy of the intestinal lymphatic system. Ann N Y Acad Sci. 2010;1207 Suppl 1(Suppl 1):E21-8.

20 Tuech JJ, Pessaux P, Regenet N, Bergamaschi R, Colson A. Sentinel lymph node mapping in colon cancer. Surg Endosc. 2004;18(12):1721-9.

21 Ohnishi S, Lomnes SJ, Laurence RG, Gogbashian A, Mariani G, Frangioni JV. Organic alternatives to quantum dots for intraoperative near-infrared fluorescent sentinel lymph node mapping. Mol Imaging. 2005;4(3):172-81.

22 Cardoso R, Guo F, Heisser T, Hackl M, Ihle P, De Schutter H, *et al.* Colorectal cancer incidence, mortality, and stage distribution in European countries in the colorectal cancer screening era: an international population-based study. Lancet Oncol. 2021;22(7):1002-13.

23 Navarro M, Nicolas A, Ferrandez A, Lanas A. Colorectal cancer population screening programs worldwide in 2016: An update. World J Gastroenterol. 2017;23(20):3632-42.

24 Fields AC, Lu P, Hu F, Hirji S, Irani J, Bleday R, *et al.* Lymph Node Positivity in T1/T2 Rectal Cancer: a Word of Caution in an Era of Increased Incidence and Changing Biology for Rectal Cancer. J Gastrointest Surg. 2021;25(4):1029-35.

25 Ricciardi R, Madoff RD, Rothenberger DA, Baxter NN. Population-based analyses of lymph node metastases in colorectal cancer. Clin Gastroenterol Hepatol. 2006;4(12):1522-7.

26 Bao F, Zhao LY, Balde AI, Liu H, Yan J, Li TT, *et al.* Prognostic impact of lymph node skip metastasis in Stage III colorectal cancer. Colorectal Dis. 2016;18(9):O322-9.

27 Saha S, Sehgal R, Patel M, Doan K, Dan A, Bilchik A, *et al.* A multicenter trial of sentinel lymph

node mapping in colorectal cancer: prognostic implications for nodal staging and recurrence. Am J Surg. 2006;191(3):305-10.
28 Burghgraef TA, Zweep AL, Sikkenk DJ, van der Pas M, Verheijen PM, Consten ECJ. *In vivo* sentinel lymph node identification using fluorescent tracer imaging in colon cancer: A systematic review and meta-analysis. Crit Rev Oncol Hematol. 2021;158:103149.
29 Karoui M, Rullier A, Piessen G, Legoux JL, Barbier E, De Chaisemartin C, *et al.* Perioperative FOLFOX 4 Versus FOLFOX 4 Plus Cetuximab Versus Immediate Surgery for High-Risk Stage II and III Colon Cancers: A Phase II Multicenter Randomized Controlled Trial (PRODIGE 22). Ann Surg. 2020;271(4):637-45.
30 Seymour MT, Morton, D. FOxTROT: an international randomised controlled trial in 1052 patients (pts) evaluating neoadjuvant chemotherapy (NAC) for colon cancer. Journal of Clinical Oncology. 2019;37(15).
31 Kuehn T, Bauerfeind I, Fehm T, Fleige B, Hausschild M, Helms G, *et al.* Sentinel-lymph-node biopsy in patients with breast cancer before and after neoadjuvant chemotherapy (SENTINA): a prospective, multicentre cohort study. Lancet Oncol. 2013;14(7):609-18.
32 Hernot S, van Manen L, Debie P, Mieog JSD, Vahrmeijer AL. Latest developments in molecular tracers for fluorescence image-guided cancer surgery. Lancet Oncol. 2019;20(7):e354-e67.
33 de Valk KS, Deken MM, Handgraaf HJM, Bhairosingh SS, Bijlstra OD, van Esdonk MJ, *et al.* First-in-Human Assessment of cRGD-ZW800-1, a Zwitterionic, Integrin-Targeted, Near-Infrared Fluorescent Peptide in Colon Carcinoma. Clin Cancer Res. 2020;26(15):3990-8.
34 Lu G, van den Berg NS, Martin BA, Nishio N, Hart ZP, van Keulen S, *et al.* Tumour-specific fluorescence-guided surgery for pancreatic cancer using panitumumab-IRDye800CW: a phase 1 single-centre, open-label, single-arm, dose-escalation study. Lancet Gastroenterol Hepatol. 2020;5(8):753-64.
35 Rosenthal EL, Moore LS, Tipirneni K, de Boer E, Stevens TM, Hartman YE, *et al.* Sensitivity and Specificity of Cetuximab-IRDye800CW to Identify Regional Metastatic Disease in Head and Neck Cancer. Clin Cancer Res. 2017;23(16):4744-52.
36 de Valk KS, Deken MM, Schaap DP, Meijer RP, Boogerd LS, Hoogstins CE, *et al.* Dose-Finding Study of a CEA-Targeting Agent, SGM-101, for Intraoperative Fluorescence Imaging of Colorectal Cancer. Ann Surg Oncol. 2021;28(3):1832-44.
37 SGM-101 in Locally Advanced and Recurrent Rectal Cancer (SGM-LARRC) [Internet]. clinicaltrials.gov. 2020. Available from: https://clinicaltrials.gov/ct2/show/NCT04642924.
38 Performance of SGM-101 for the Delineation of Primary and Recurrent Tumour and Metastases in Patients Undergoing Surgery for Colorectal Cancer [Internet]. Clinicaltrials.gov. 2018. Available from: https://clinicaltrials.gov/ct2/show/NCT03659448.
39 Cahill RA, Anderson M, Wang LM, Lindsey I, Cunningham C, Mortensen NJ. Near-infrared (NIR) laparoscopy for intraoperative lymphatic road-mapping and sentinel node identification during definitive surgical resection of early-stage colorectal neoplasia. Surg Endosc. 2012;26(1):197-204.
40 Carrara A, Motter M, Amabile D, Pellecchia L, Moscatelli P, Pertile R, *et al.* Predictive value of the sentinel lymph node procedure in the staging of non-metastatic colorectal cancer. Int J Colorectal Dis. 2020;35(10):1921-8.
41 Currie AC, Brigic A, Thomas-Gibson S, Suzuki N, Moorghen M, Jenkins JT, *et al.* A pilot study to assess near infrared laparoscopy with indocyanine green (ICG) for intraoperative sentinel lymph node mapping in early colon cancer. Eur J Surg Oncol. 2017;43(11):2044-51.
42 Hirche C, Mohr Z, Kneif S, Doniga S, Murawa D, Strik M, *et al.* Ultrastaging of colon cancer by sentinel node biopsy using fluorescence navigation with indocyanine green. Int J Colorectal Dis. 2012;27(3):319-24.
43 Kusano M, Tajima Y, Yamazaki K, Kato M, Watanabe M, Miwa M. Sentinel node mapping guided by indocyanine green fluorescence imaging: a new method for sentinel node navigation surgery in gastrointestinal cancer. Dig Surg. 2008;25(2):103-8.
44 Nagata K, Endo S, Hidaka E, Tanaka J, Kudo SE, Shiokawa A. Laparoscopic sentinel node mapping for colorectal cancer using infrared ray laparoscopy. Anticancer Res. 2006;26(3B):2307-11.
45 Noura S, Ohue M, Seki Y, Tanaka K, Motoori M, Kishi K, *et al.* Feasibility of a lateral region sentinel node biopsy of lower rectal cancer guided by indocyanine green using a near-infrared camera system. Ann Surg Oncol. 2010;17(1):144-51.
46 Watanabe J, Ota M, Suwa Y, Ishibe A, Masui H, Nagahori K. Evaluation of lymph flow patterns in splenic flexural colon cancers using laparoscopic real-time indocyanine green fluorescence imaging. Int J Colorectal Dis. 2017;32(2):201-7.
47 Liberale G, Vankerckhove S, Galdon MG, Larsimont D, Ahmed B, Bouazza F, *et al.* Sentinel Lymph Node Detection by Blue Dye Versus Indocyanine Green Fluorescence Imaging in Colon Cancer. Anticancer Res. 2016;36(9):4853-8.
48 Schaafsma BE, Verbeek FP, van der Vorst JR, Hutteman M, Kuppen PJ, Frangioni JV, *et al. Ex vivo* sentinel node mapping in colon cancer combining blue dye staining and fluorescence imaging. J Surg Res. 2013;183(1):253-7.
49 Weixler B, Rickenbacher A, Raptis DA, Viehl CT, Guller U, Rueff J, *et al.* Sentinel Lymph Node Mapping with Isosulfan Blue or Indocyanine Green in Colon Cancer Shows Comparable Results and Identifies Patients with Decreased Survival: A Prospective Single-Center Trial. World J Surg. 2017;41(9):2378-86.

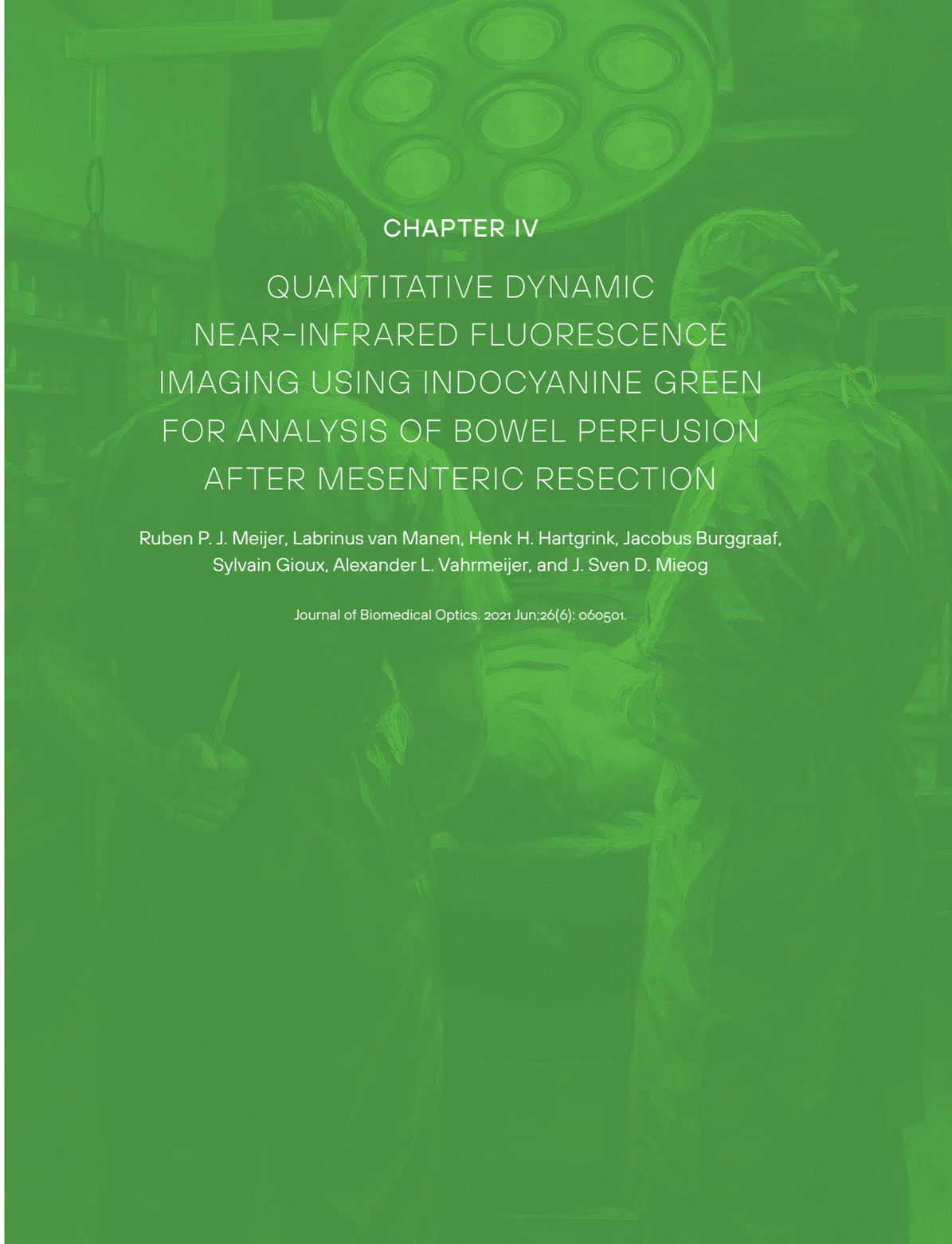

CHAPTER IV

QUANTITATIVE DYNAMIC NEAR-INFRARED FLUORESCENCE IMAGING USING INDOCYANINE GREEN FOR ANALYSIS OF BOWEL PERFUSION AFTER MESENTERIC RESECTION

Ruben P. J. Meijer, Labrinus van Manen, Henk H. Hartgrink, Jacobus Burggraaf, Sylvain Gioux, Alexander L. Vahrmeijer, and J. Sven D. Mieog

Journal of Biomedical Optics. 2021 Jun;26(6): 060501.

Abstract

SIGNIFICANCE Near-infrared (NIR) fluorescence imaging using indocyanine green (ICG) has proven to be a feasible application for real-time intraoperative assessment of tissue perfusion, although quantification of NIR fluorescence signals is pivotal for standardized assessment of tissue perfusion.

AIM Four patients are described with possible compromised bowel perfusion after mesenteric resection. Based on these patients we want to emphasize the difficulties in the quantification of NIR fluorescence imaging for perfusion analysis.

APPROACH During image-guided fluorescence assessment, 5 mg of ICG (2.5 mg/ml) was intravenously administered by the anesthesiologist. NIR fluorescence imaging was done with the open camera system of Quest Medical Imaging. Fluorescence data taken from the regions of interest (bowel at risk, transition zone of bowel at risk and adjacent normally perfused bowel, and normally perfused reference bowel) were quantitatively analyzed after surgery for fluorescence intensity- and perfusion time-related parameters.

RESULTS Bowel perfusion, as assessed clinically by independent surgeons based on NIR fluorescence imaging, resulted in different treatment strategies, three with excellent clinical outcome, but one with a perfusion related complication. Post-surgery quantitative analysis of fluorescence dynamics showed different patterns in the affected bowel segment compared to the unaffected reference segments for the four patients.

CONCLUSIONS Similar intraoperative fluorescence results could lead to different surgical treatment strategies, which demonstrated the difficulties in interpretation of uncorrected fluorescence signals. Real-time quantification and standardization of NIR fluorescence perfusion imaging could probably aid surgeons in the nearby future.

Introduction

Extensive oncological abdominal surgery occasionally includes removal of part of the mesentery containing blood vessels supplying the associated bowel. Because mesenteric resection can result in compromised bowel perfusion leading to necrosis, it is commonly combined with bowel resection and subsequent anastomosis formation. However, anastomosis formation harbors the risk of an anastomotic leakage, which is the most feared complication of bowel resections and accounts for considerable morbidity and mortality.[1-3] Indirect perfusion of adjacent bowel segments with intact mesenterial blood supply could be sufficient to avoid bowel resection and subsequent anastomosis after partial mesenteric resection. For decades, surgeons rely on the use of tactile and visual feedback to determine the perfusion state, which has certain limitations. Near-infrared (NIR) fluorescence imaging using indocyanine green (ICG) has proven to be a feasible and reproducible application for real-time intraoperative quantification of tissue perfusion.[4-6] Surgical procedures in which part of the mesentery is resected can benefit from NIR fluorescence imaging with ICG. However, quantification of NIR fluorescence signals is pivotal for standardized assessment of tissue perfusion. This report aims to demonstrate the current shortcomings in intraoperative quantification of NIR fluorescence imaging for bowel perfusion assessment after mesenterial disruption without a planned bowel resection.

Methods and case reports

METHODS

Four patients underwent standard-of-care NIR fluorescence imaging using ICG for intraoperative bowel perfusion assessment after mesenteric resection. Informed consent for publication of this work was obtained from the patients. For the surgical procedures, 25 mg of ICG (Pulsion Medical Systems, Munich, Germany) was diluted in 10 ml sterile water to obtain a 2.5 mg/ml concentration. During image-guided fluorescence assessment, 5 mg of ICG was intravenously administered by the anesthesiologist. NIR fluorescence imaging was done with the open-camera system of Quest Medical Imaging (Middenmeer, The Netherlands).

Fluorescence data were quantitatively analyzed after surgery for fluorescence intensity- and perfusion time-related parameters according to Son *et al.*[7] Snapshots were taken every 2 s after ICG injection from the video recording,

and fluorescence intensities of each image were sequentially analyzed using Mevislab (MeVis Medical Solutions AG, Bremen, Germany). Five regions of interest were taken: one from the part of the bowel at risk, two from the margin of adjacent normally perfused bowel to bowel at risk (the transition zone), and two from normally perfused bowel adjacent to the bowel at risk. Results were averaged in case of two regions per zone. The following fluorescence parameters were analyzed: Half of difference between baseline and maximum fluorescence intensity ($F_{½\ max}$), difference between baseline and maximum fluorescence intensity (F_{max}), time from first fluorescence increase to maximum intensity (T_{max}), slope of the fluorescence inflow (slope = F_{max}/T_{max}), slope in 10 s after the rise of fluorescence intensity ($slope_{10}$), time from first fluorescence increase to half of maximum intensity ($T_{½\ max}$), and the ratio of $T_{½}$ max over T_{max} (TR = $T_{½\ max}/T_{max}$).

CASE I

A 25-year-old man, who underwent several resections for recurrent osteosarcoma, was referred for resection of a progressively growing abdominal nodule of 21 mm in size detected on routine computed tomography that was suspected to be a metastatic lesion. At explorative midline laparotomy, no other metastases were found. The lesion was situated in the mesocolon adjacent to the descending colon and consequently a mesenteric resection sparing the left colic artery was performed. Visual assessment of the colon showed slight discoloration at the resection side over a trajectory of 4 cm. Intraoperative subjective fluorescence assessment of the bowel perfusion showed slightly slower increase of fluorescence intensity of the bowel segment at risk (figure 1), but this part became as fluorescent as the reference bowel within one minute. The perfusion was judged as being sufficient and it was decided to not perform a bowel segment resection. The postoperative period was uneventful, and discharge was at postoperative day 3.

Postoperative quantitative fluorescence analysis showed lower maximum fluorescence intensities (27.3 versus 39.2 versus 50.8 arbitrary units (AU)), inflow slope (0.76 versus 1.56 versus 2.56 AU/s), and $slope_{10}$ (1.05 versus 2.04 versus 3.74 AU/s) in the affected bowel compared to the transition zone and reference bowel (Table 1). Furthermore, T_{max} (36 versus 25 versus 19 s), $T_{½\ max}$ (12 versus 9.5 versus 7.5 s) and TR (0.33 versus 0.38 versus 0.39) were lower at the transition zone and directly perfused reference bowel segments.

FIGURE 1 Overview of ICG inflow and quantitative perfusion analyses.
(a), (d), and (j) Case I, II, and IV showed a delayed fluorescence inflow; (b), (e), and (k) lower maximum fluorescence intensity levels in the affected bowel, which is illustrated by (c), (f), and (l) quantitative analysis. Case III showed minimal difference in (g) fluorescence inflow or (h) maximum fluorescence intensity. ROIs were taken in the affected bowel with compromised perfusion (red), transition zone with possible impaired perfusion (yellow), and reference bowel with normal perfusion (blue).

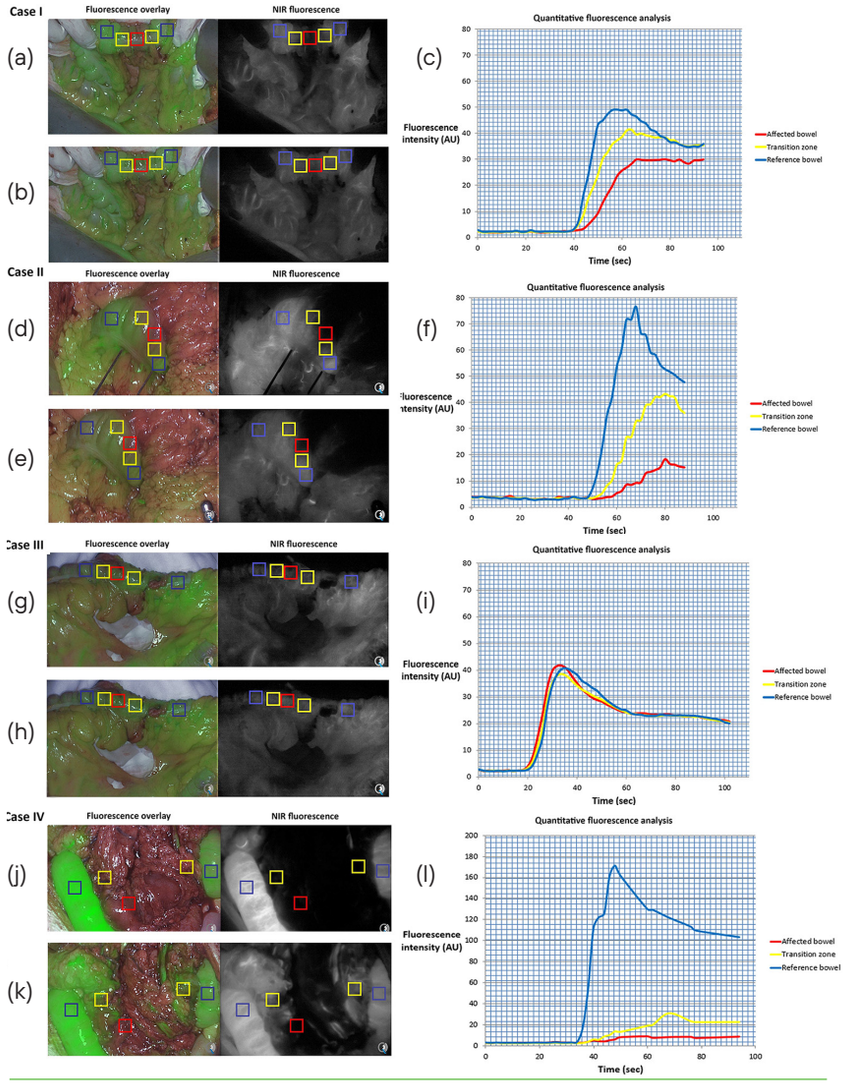

Abbreviations: ICG: indocyanine green; ROI: region of interest; AU: arbitrary units

CASE II

A 71-year-old man, without any relevant other diagnosis in his medical history, was referred because of esophageal cancer, eligible for resection after neoadjuvant treatment. During the dissection of the greater gastric curvature, iatrogenic injury of the mesocolon occurred. Visual assessment of the colon showed an area of about 3 cm that was slightly darker than the surrounding bowel. Intraoperative fluorescence assessment of the bowel perfusion showed decreased fluorescence intensity adjacent to the aperture in the mesocolon (figure 1, lower panel). It was concluded that perfusion of this part of the bowel was inadequate and therefore the two well-perfused parts were approximated with serosal sutures, thereby folding the less perfused part intraluminally. The postoperative recovery was uneventful, and discharge was at postoperative day 7.

Postoperative quantitative fluorescence analysis showed a difference in F_{max} (14.8 versus 40.4 versus 73.0 AU), slope (0.57 versus 1.35 versus 3.65 AU/s), and slope$_{10}$ (0.51 versus 1.27 versus 3.82 AU/s) between the bowel segment at risk, the transition zone, and the unaffected bowel segment (Table 1). T_{max} was higher at the transition zone compared to the affected bowel and reference bowel (30 versus 26 versus 20 s). $T_{½\ max}$ was higher for the affected bowel compared to the transition zone and reference bowel (17 versus 15 versus 10 s). TR was equal between the transition zone and reference bowel (0.50), although TR was higher (0.65) for the affected bowel segment.

CASE III

A 53-year-old female patient underwent a pylorus-preserving pancreaticoduodenectomy because of an adenocarcinoma of the duodenum. A partial resection of the mesentery of the transverse colon including the right colonic artery was unavoidable due to tumor involvement. Visually, no problems were suspected regarding the perfusion of the adjacent bowel segment. Assessment of the perfusion using ICG-guided fluorescence showed clear and equal fluorescence in all parts of the bowel (affected and unaffected zones). As a result, no further intraoperative intervention was deemed necessary. During her recovery the patient did not develop any symptoms of inadequate bowel perfusion.

Postoperative quantitative fluorescence analysis showed similar maximum fluorescence intensities (38.9 versus 36.15 versus. 38.3 AU), inflow slope (2.43 versus 2.15 versus 2.30 AU/s), and slope$_{10}$ (3.11 versus 2.67 versus 2.42 AU/s) in the affected bowel compared to the transition zone and reference bowel (Table 1). Furthermore, T_{max} (16 versus 17 versus 17 s), $T_{½\ max}$ (8 versus 8.5 versus 10 s) and TR (0.5 versus 0.5 versus 0.59) did not show any clinical significant difference at three different zones of the bowel.

TABLE 1 Quantitative perfusion analysis of described cases compared to literature for anastomotic leakage.

	Case I			Case II			Case III			Case IV			Literature comparison
	Affected bowel	Transition zone	Reference bowel	Affected bowel	Transition zone	Reference bowel	Affected bowel	Transition zone	Reference bowel	Affected bowel	Transition zone	Reference bowel	Suggested cutoff values for poor perfusion
FLUORESCENCE INTENSITY RELATED FACTORS													
$F_{½\ max}$ (AU)	13.7	19.5	24.2	7.4	20.2	36.5	19.5	18.1	19.2	2.75	16.5	84.9	NA
F_{max} (AU)	27.3	39.2	50.8	14.8	40.4	73.0	38.9	36.2	38.3	5.5	32.9	169.8	<528
Slope or ingress rate (AU/s)	0.76	1.56	2.56	0.57	1.35	3.65	2.43	2.15	2.30	0.23	0.97	12.13	<0.77; <2.18
Slope10 (AU/s)	1.05	2.04	3.74	0.51	1.28	3.82	3.11	2.67	2.42	0.21	0.97	12.02	NA
PERFUSION TIME-RELATED FACTORS													
T_{max} (s)	36	25	19	26	30	20	16	17	17	24	35	14	>578
$T_{½\ max}$ (s)	12	9.5	7.5	17	15	10	8	8.5	10	12	14.5	7.5	>187; >148; >109
TR	0.33	0.38	0.39	0,65	0.50	0.50	0.50	0.50	0.59	0.5	0.43	0.54	>0.67

Abbreviations: $F_{½\ max}$: half of difference between baseline and maximum fluorescence intensity; NA: not available; F_{max}: difference between baseline and maximum fluorescence intensity; AU: arbitrary units; slope: slope of the fluorescence inflow; slope10: slope in 10 s after the rise of fluorescence intensity, T_{max}: time from first fluorescence increase to maximum intensity; $T_{½\ max}$: time from first fluorescence increase to half of maximum intensity; TR: ratio of $T_{½\ max}$ and T_{max}.

CASE IV

A 76-year-old male patient, diagnosed with gastric cancer, underwent residual stomach resection, because of a tumor-positive resection margin after previous distal gastrectomy 3 months before. During the current surgical procedure part of the mesentery of the transverse colon had to be resected, due to extensive adhesions, as the patient had multiple abdominal surgeries in the past. At visual inspection the adjacent transverse colon was darker than the assumed healthy bowel segments and arterial pulsations were weak. Subjective intraoperative fluorescence assessment of the bowel perfusion showed delayed fluorescence inflow of a 3-cm long transverse colon segment. Subjective fluorescence intensity seemed equal at all bowel sites 3 min after ICG administration. It was decided not to intervene, based on doubtful palpable pulsations and fluorescence signals after 3 min. Two days postoperative a relaparotomy was performed, which

showed an ischemic part of the transverse colon of 3 cm and poor perfusion over 10 cm, which was resected and subsequently an anastomosis was created. The patient recovered and was discharged 2 weeks after the initial surgery.

Postoperative quantitative fluorescence analysis showed decreased maximum fluorescence intensities (8.8 versus 36.1 versus. 173.25 AU), inflow slope (0.23 versus 0.97 versus

12.13 AU/s), and slope10 (0.21 versus 0.97 versus 12.02 AU/s) in the affected bowel and transition zone compared to reference bowel (Table 1). T_{max} (24 versus 35 versus 14 s), $T_{½\ max}$ (12 versus 14.5 versus 7.5 s) and TR (0.5 versus 0.43 versus 0.54) did not show any clinical significant difference at three different zones of the bowel.

Discussion

In this report, four patients with clinically suspect compromised bowel perfusion after mesenteric resection are described. Bowel perfusion, as assessed by independent surgeons based on NIR fluorescence imaging, resulted in different treatment strategies, which are supported for case I, II, and III by quantitative fluorescence analysis as compared to current literature. The affected bowel in patient I and II showed slightly impaired perfusion parameters, which was more pronounced in the second patient. The third patient did not show any impaired perfusion parameters and might therefore be considered as a negative control in patients with normal bowel perfusion after mesenteric resection. Patient IV showed distinct poor perfusion parameters. Unfortunately, conventional methods, including interpretation of the unquantified NIR fluorescence imaging withheld the surgeon from doing a resection with subsequent anastomosis. Patient IV also emphasizes an important drawback of subjective NIR fluorescence assessment. After time, ICG tends to distribute even to ischemic zones which possibly leads to overestimation of the perfusion quality at the end of ICG distribution.

Quantification of NIR fluorescence signals is pivotal for standardized assessment of tissue perfusion. Currently, available fluorescence imaging systems lack the capacity to perform real-time quantitative imaging during surgery. Therefore, surgeons have to assess the fluorescence signal in a qualitative manner using the perceived intensity and inflow as the only parameters. This can easily lead to misinterpretation as fluorescence intensities vary greatly with the experimental conditions and do not take into account the time-dependent diffusion of ICG. More precisely, fluorescent intensity is dependent on type and amount of injected tracer, the camera-target distance, the local tissue absorption, and scattering properties and camera system specific settings including, but not limited to the excitation light delivery mode and fluorescence light collection.[10–13]

Quantitative fluorescence parameters are categorized in time-dependent and fluorescence intensity-related that have already been investigated during reconstructive, vascular, and intestinal surgery in several studies.[7,10,13–15] For bowel surgery, fluorescence parameters have mainly been correlated to the occurrence of anastomotic leakage and have to our knowledge not yet been described in patients with mesenteric resection, in which collateral vessels provide perfusion to the affected bowel segment. It has been suggested that a smaller fluorescence inflow slope (arterial inflow) and a low F_{max} are important predictors for poor vascular perfusion.[8,10] Three studies described cutoff values for these fluorescence parameters to determine higher risk of either colorectal or free jejunal graft anastomotic leakage, even though these studies used different cutoff values and demonstrated contradictory results.[7–9] Slope (<0.7 AU/s; <2.1 AU/s)[7,8] and $T_{½\ max}$ (>18 s; >10 s)[7,9] were significantly associated with anastomotic leakage in two out of three studies, whereas F_{max} (<52 AU)[8] and TR (>0.6)[7] were significantly associated in one out of three studies. Although these cutoff values are not directly applicable to our cases, it provides a general indication of bowel perfusion.

According to the flow chart proposed by Son *et al.*,[7] the affected bowel segment in the second case could be described as a zone with an acceptable perfusion, to which surgeons should pay extra attention. In the current cases, the surgeons decided on different treatment strategies after subjective fluorescence assessment. Post-surgical analysis showed mildly compromised tissue perfusion of the affected bowel segments in patient I and II, but more pronounced in the second case. One could say that the surgeons interpreted the fluorescence images sufficiently, as the surgeon of the second case decided for a small intervention. Moreover, good clinical outcome in case I indicates sufficient indirect perfusion of adjacent bowel segments, justifying the decision not to intervene.

As the area of the resected mesenteric layers was quite small in the four cases (~5×5 cm), it would be worthwhile to further investigate the effect of the size of the resected mesentery on the perfusion fluorescence parameters at certain distances on the bowel and correlate this to serum lactate levels in more controlled circumstances.[10,13] Moreover, patient-related factors, such as

smoking or hypertension,[16] could also influence the bowel perfusion and should also be considered when analyzing the bowel perfusion using NIR fluorescence imaging.

Current quantification methods include temporal analysis of the fluorescence dynamic signal,[13] such as in this study, ratiometric imaging using an additional reflectance channel to normalize the fluorescence signal,[17] and quantitative fluorescence imaging using spectral, or spatial modulation of light.[12] It is important to acknowledge both benefits and disadvantages of each quantification method. The analysis of the fluorescence dynamics in time allows to quantify the temporal properties of the contrast agent diffusion within the tissues. Though this is a powerful method to assess adequacy of perfusion, the advantage may be off-set as it necessitates point measurements precluding real-time availability of results or a complex acquisition and processing methodology to gather all the necessary information and display results as a quantitative heatmap. Ratiometric imaging has the advantage of being simple to implement and allows to eliminate variation factors such as distance or illumination inhomogeneity, but it has to be acknowledged that tissue optical properties (absorption and scattering) are not fully addressed.[17]

Soon, improvements in imaging devices and quantitative imaging methods will provide more reliable and interpretable information content in real-time during surgery. Both quantitative fluorescence and dynamic fluorescence imaging are demonstrating the potential of optical imaging to augment the capacity for surgeons to observe objectively and identify problems during the surgery. Systems able to display the dynamic evolution of the fluorescent signal, such as fluorescence-based enhanced reality (FLER) provide a quantitative and reproducible estimation of the bowel perfusion in augmented reality.[18] FLER is independent from the distance, since it is time-dependent and independent from the camera-to-target distance. Nevertheless, improvement in quantification methods are necessary to move the field forward. It is suggested that correcting for arterial input function by pulse dye densitometry could improve the currently used quantification methods by reducing the intra- and inter-subject variability.[19] Furthermore, fluorescence imaging can be combined with other methods such as endogenous functional imaging of oxygenation or blood perfusion to increase the capabilities of optical imaging to guide surgery reliably and in real time.[20,21]

Conclusion

This report demonstrates the difficulties of visual assessment of fluorescence perfusion imaging in patients with potentially compromised bowel segment following partial mesenteric excision. In the presented cases, a bowel resection with subsequent anastomosis was not planned, which makes it difficult to compare our results with existing literature. Moreover, the currently available quantitative fluorescence parameters are sparsely studied, and their cutoffs differ significantly among studies warranting validation in large clinical trials. More fundamental studies are needed on underlying kinetic mechanisms causing the variance in these parameters.

REFERENCES

1 C. Y. Kang *et al.*, "Risk factors for anastomotic leakage after anterior resection for rectal cancer," JAMA Surg. 148(1), 65-71 (2013).

2 R. Sauer *et al.*, "Adjuvant vs. neoadjuvant radiochemotherapy for locally advanced rectal cancer: the German trial CAO/ARO/AIO-94," Colorectal Dis. 5(5), 406-415 (2003).

3 N. Hyman *et al.*, "Anastomotic leaks after intestinal anastomosis: it's later than you think," Ann. Surg. 245(2), 254-258 (2007).

4 L. van Manen *et al.*, "A practical guide for the use of indocyanine green and methylene blue in fluorescence-guided abdominal surgery," J. Surg. Oncol. 118(2), 283-300 (2018).

5 A. L. Vahrmeijer *et al.*, "Image-guided cancer surgery using near-infrared fluorescence," Nat. Rev. Clin. Oncol. 10(9), 507-518 (2013).

6 M. L. Landsman *et al.*, "Light-absorbing properties, stability, and spectral stabilization of indocyanine green," J. Appl. Physiol. 40(4), 575-583 (1976).

7 G. M. Son *et al.*, "Quantitative analysis of colon perfusion pattern using indocyanine green (ICG) angiography in laparoscopic colorectal surgery," Surg. Endosc. 33(5), 1640-1649 (2019).

8 T. Wada *et al.*, "ICG fluorescence imaging for quantitative evaluation of colonic perfusion in laparoscopic colorectal surgery," Surg. Endosc. 31(10), 4184-4193 (2017).

9 K. Kamiya *et al.*, "Quantitative assessment of the free jejunal graft perfusion," J. Surg. Res.194(2), 394-399 (2015).

10 M. Diana *et al.*, "Intraoperative fluorescence-based enhanced reality laparoscopic real-time imaging to assess bowel perfusion at the anastomotic site in an experimental model," Br. J. Surg. 102(2), e169-e176 (2015).

11 J. V. Frangioni, "*In vivo* near-infrared fluorescence imaging," Curr. Opin. Chem. Biol. 7(5), 626-634 (2003).

12 P. A. Valdes *et al.*, "qF-SSOP: real-time optical property corrected fluorescence imaging," Biomed. Opt. Express 8(8), 3597-605 (2017).

13 M. Diana *et al.*, "Real-time navigation by fluorescence-based enhanced reality for precise estimation of future anastomotic site in digestive surgery," Surg. Endosc. 28(11), 3108-3118 (2014).

14 P. van den Hoven *et al.*, "A systematic review of the use of near-infrared fluorescence imaging in patients with peripheral artery disease," J. Vasc. Surg. 70(1), 286-297.e1 (2019).

15 A. Matsui *et al.*, "Quantitative assessment of perfusion and vascular compromise in perforator flaps using a near-infrared fluorescence-guided imaging system," Plast. Reconstr. Surg. 124(2), 451-460 (2009).

16 A. Fawcett *et al.*, "Smoking, hypertension, and colonic anastomotic healing; a combined clinical and histopathological study," Gut 38(5), 714-718 (1996).

17 V. Ntziachristos *et al.*, "Planar fluorescence imaging using normalized data," J. Biomed. Opt.10(6), 064007 (2005).

18 A. D'Urso *et al.*, "Computer-assisted quantification and visualization of bowel perfusion using fluorescence-based enhanced reality in left-sided colonic resections," Surg. Endosc. (2020).

19 J. T. Elliott *et al.*, "Intraoperative fluorescence perfusion assessment should be corrected by a measured subject-specific arterial input function," J. Biomed. Opt. 25(6), 066002 (2020).

20 S. Gioux *et al.*, "First-in-human pilot study of a spatial frequency domain oxygenation imaging system," J. Biomed. Opt. 16(8), 086015 (2011).

21 M. Ghijsen *et al.*, "Quantitative real-time optical imaging of the tissue metabolic rate of oxygen consumption," J. Biomed. Opt. 23(3), 036013 (2018).

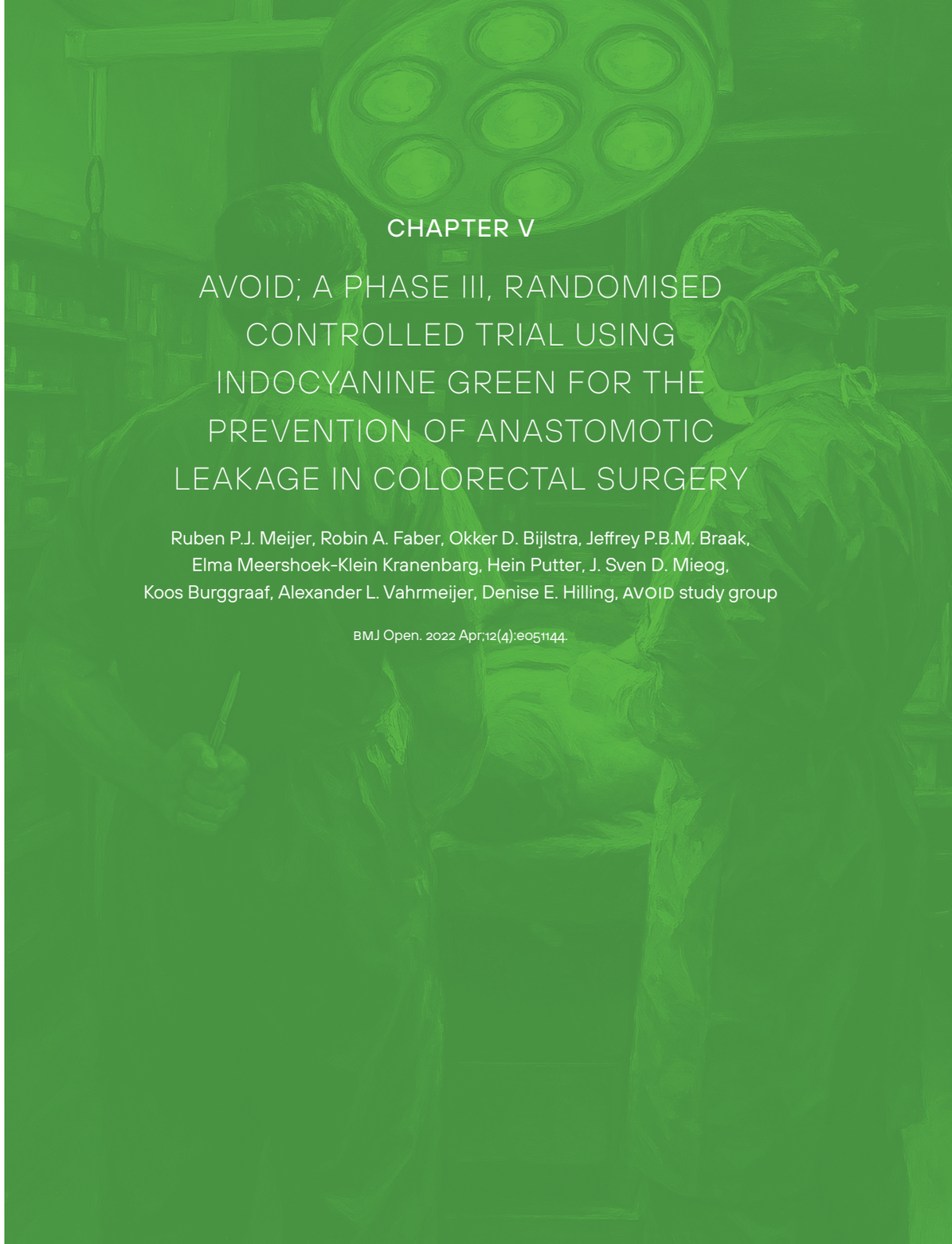

CHAPTER V

AVOID; A PHASE III, RANDOMISED CONTROLLED TRIAL USING INDOCYANINE GREEN FOR THE PREVENTION OF ANASTOMOTIC LEAKAGE IN COLORECTAL SURGERY

Ruben P.J. Meijer, Robin A. Faber, Okker D. Bijlstra, Jeffrey P.B.M. Braak,
Elma Meershoek-Klein Kranenbarg, Hein Putter, J. Sven D. Mieog,
Koos Burggraaf, Alexander L. Vahrmeijer, Denise E. Hilling, AVOID study group

BMJ Open. 2022 Apr;12(4):e051144.

Abstract

INTRODUCTION Anastomotic leakage (AL) is one of the major complications after colorectal surgery. Compromised tissue perfusion at the anastomosis site increases the risk of AL. Several cohort studies have shown that indocyanine green (ICG) combined with fluorescent near-infrared imaging is a feasible and reproducible technique for real-time intraoperative imaging of tissue perfusion, leading to reduced leakage rates after colorectal resection. Unfortunately, these studies were not randomised. Therefore, we propose a randomised controlled trial to assess the value of ICG-guided surgery in reducing AL after colorectal surgery.

METHODS AND ANALYSIS A multicentre, randomised controlled clinical trial will be conducted to assess the benefit of ICG-guided surgery in preventing AL. A total of 978 patients scheduled for colorectal surgery will be included. Patients will be randomised between the Fluorescence Guided Bowel Anastomosis group and the Conventional Bowel Anastomosis group. The primary endpoint is clinically relevant AL (defined as requiring active therapeutic intervention or reoperation) within 90 days after surgery. Among the secondary endpoints are 30-day clinically relevant AL, all-cause postoperative complications, all-cause and AL-related mortality, surgical and non-surgical reinterventions, total surgical time, length of hospital stay and all-cause and AL-related readmittance.

ETHICS AND DISSEMINATION This protocol has been approved by the Medical Ethical Committee Leiden-Den Haag-Delft (METC-LDD) and is registered at ClinicalTrials.gov and trialregister.nl. The results of this study will be reported through peer-reviewed publications and conference presentations.

TRIAL REGISTRATION NUMBERS NCT04712032 and NL7502

Introduction

Anastomotic leakage (AL) is a major complication after colorectal surgery, accounting for considerable morbidity and mortality.[1-6] The incidence of AL in colorectal surgery ranges from 2.4 to 11% in colon cases and up to 23.3% in rectal cancer surgery.[4-15] The occurrence of AL often has a multifactorial cause, including risk factors such as tumour location, level of anastomosis, male gender, high ASA score, comorbidities, smoking, obesity and (neoadjuvant) radiotherapy.[3,4,6,11,13,14,16]

Most risk factors for AL can no longer be changed at the time of surgery. Therefore, it is important to focus on the few factors that can be influenced, such as compromised tissue perfusion at the anastomosis site. It has been reported that this factor significantly increases the risk of AL.[17-19] Perfusion is commonly assessed by palpating the mesenteric arterial pulsations, inspection of the bowel colour, and bleeding at the anastomosis sides. Other intraoperative tests to prove the integrity of the anastomosis are the air leak test and inspection of the resection doughnuts.[20] Though useful, these clinical assessments have proven to have a low predictive value for AL which emphasises the urge for a better diagnostic test.[21]

A promising diagnostic tool is intraoperative near-infrared (NIR) fluorescence imaging. This technique combines a fluorescent contrast agent, e.g. indocyanine green (ICG), and a dedicated NIR imaging system.[22] The intravenous injection of ICG has proven to be a feasible and reproducible application for real-time perfusion assessment.[23-25] ICG was introduced by Fox *et al.* in 1957 and is currently used for a variety of diagnostic indications.[26] Diluted and intravenously injected ICG, with a peak emission at 820 nm, is invisible for the naked eye and will therefore not interfere with the surgical field.[27] Moreover, it is cleared quickly by the liver and has low toxicity.[28]

Several cohort studies have investigated the benefit of NIR fluorescence imaging with ICG for intraoperative assessment of bowel perfusion. Some of these studies have shown that this technique enables clear visualisation of bowel perfusion within minutes after intravenous injection of ICG, resulting in reduced leakage rates and hospital stay.[29-32] Moreover, several systematic reviews support this promising results concerning the prevention of AL.[33-34] This has already led to the start of two randomised controlled trials (ICG-COLORAL; NCT03602677 and InTACT trial; ISCRN 13334746) which are currently recruiting patients. On the other hand, Kin *et al.* have shown no benefit by using ICG in preventing AL.[35] Major drawbacks of these cohort studies are that they were

not randomised and did not use clinically relevant AL as the primary endpoint. Therefore, we propose AVOID: '*Anastomotic leakage and Value Of Indocyanine green in Decreasing leakage rates*', a randomised controlled trial to investigate the benefit of intraoperative imaging with ICG for the reduction of AL rate in colorectal surgery.

Methods and analysis

PRIMARY AIM

The main objective of this study is to assess if ICG-guided perfusion assessment will result in a reduction of the AL rate within 90 days after surgery. ICG-guided perfusion assessment will be an adjunct to conventional laparoscopic imaging versus conventional laparoscopic imaging alone.

HYPOTHESIS

It is hypothesised that intraoperative assessment of bowel perfusion using NIR fluorescence imaging with ICG will lower the incidence of clinically relevant AL within 90 days after colorectal resection.

STUDY DESIGN

In this multicentre randomised controlled trial, patients will be allocated to two groups: the Fluorescence Guided Bowel Anastomosis group (FGBA) or the Conventional Bowel Anastomosis group (CBA). Patients in the FGBA group will receive at least one dose of 5 milligram ICG, up to a maximum of 3 doses, to assess bowel perfusion. Patients in the CBA group will not receive any study related interventions and will be treated according to standard of care. The allocated treatment result is not blinded for the surgeon performing the procedure. Patients will be unblinded after the procedure.

SETTING

This national study will take place in multiple academic and large teaching hospitals in the Netherlands. More Dutch hospitals will be added during the course of the study.

PARTICIPANTS

All patients scheduled for laparoscopic or robotic-assisted colorectal surgery (malignant and benign indications) with primary anastomosis will be screened for eligibility during multidisciplinary team meetings and, when eligible for participation, informed about the study by their attending physician. It will be emphasized that a patient can withdraw from the study at any given moment without having to offer any reason. The fundamental concepts outlined in the Declaration of Helsinki will be followed during the execution of the trial.[36]

SAMPLE SIZE CALCULATION

The power analysis was performed based on Dutch national AL percentages, derived from the Dutch ColoRectal Audit (DCRA).[37] It is hypothesized that the use of ICG will decrease the AL rate in colorectal surgery from 7 to 3%. With a significance of 0.0492 (adjusted for the interim analysis using the O'Brien-Flemming approach), power of 80%, drop-out of 5% and a control-intervention ratio of 1:1, a sample size of 978 (489:489) patients is needed.[38]

INCLUSION CRITERIA

In order to be eligible to participate in this study, a patient must meet all of the following criteria: aged 18 years and above, scheduled for laparoscopic or robotic-assisted colorectal resection with primary anastomosis, able to communicate in the Dutch language and willing to comply with the study restrictions, and signed informed consent prior to any study-mandated procedure.

EXCLUSION CRITERIA

A potential patient who meets any of the following criteria will be excluded from participation in this study: known allergy or history of adverse reaction to ICG, iodine or iodine dyes, severe liver or kidney insufficiency, hyperthyroidism or a benign thyroid tumour, pregnant or breastfeeding women, scheduled for emergency surgery, palliative surgery or terminally ill, scheduled for a defunctioning stoma, taking phenobarbital, phenylbutazone, primidone, phenytoin, haloperidol, nitrofurantoin, and probenecid, or any other condition that the investigator considers to be potentially jeopardizing the patients well-being or the study objectives (following a detailed medical history and physical examination).

RANDOMISATION

After inclusion in the study (i.e., after written informed consent is obtained), patients will be randomised to the FGBA or the CBA group. Randomisation will be performed online via Castor EDC (Castor, Amsterdam, the Netherlands) with variable block sizes and stratified by institute. The allocated treatment result is not blinded for the surgeon performing the procedure. Patients will be unblinded after the surgical procedure.

FIGURE 1 Surgical flowchart.

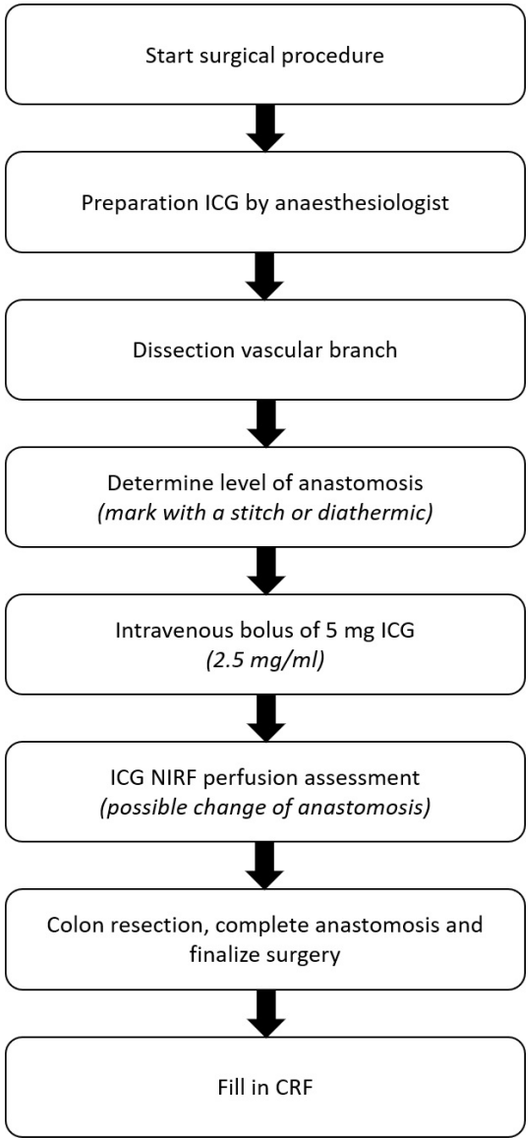

Abbreviations: CRF, case report form; ICG, indocyanine green; NIRF, near-infrared fluorescence.

INTERVENTION

Patients in the CBA group will undergo laparoscopic or robotic colorectal resection according to standard of care using conventional methods to assess the integrity and viability of the anastomosis. Patients in the FGBA group will undergo the same standard of care surgical procedure as patients in the CBA group; however, in addition to the conventional methods, NIR fluorescence imaging with ICG will be performed to assess the bowel perfusion at the anastomosis side. All surgeries, in both arms, will be performed by an attending surgeon. NIR fluorescence imaging with ICG will be performed as follows (Figure 1): after dissection of the vascular branch, the preferred level of anastomoses (proximally and distally) will be highlighted by a stitch or diathermic mark in the adjacent mesocolon or mesorectum. Then, 5 mg ICG (2.5 mg/ml, Diagnostic Green, Aschheim, Germany), followed by 10 ml saline flush, will be injected intravenously by the anaesthesiologist. Within a few minutes, the anastomotic microvascularisation of both bowel ends will be assessed using the Olympus Medical Imaging Video System and Laparoscope (Olympus, Leiderdorp, the Netherlands) or Da Vinci Firefly (Intuitive Inc., Sunnyvale, CA, United States of America). The green overlay setting of these systems will be used for perfusion assessment. The level of resection and subsequent anastomosis may be changed accordingly (with the mesocolic stitch serving as the baseline). During the procedure, the ICG injection (5 mg) may be repeated for a second or third time with a 15 minute wash-out period between each administration. Repeated doses may be applicable when, for example, both anastomosis sides do not fit into the optical field, or when perfusion seems compromised after anastomosis finalisation. All injections, including the reason(s) for repeated injection(s), and the consequences of administration, will be documented in the case report form (CRF).

The 90-day follow-up is a standard of care follow-up moment in all participating hospitals. It will be done either by phone, by videoconference or in person, according to standard of care in the participating hospital. Patients who, for any reason, do not visit the hospital 90 days after resection, will be contacted by phone and asked for any postoperative complications or reinterventions.

OUTCOME MEASURES

PRIMARY OUTCOME

The primary outcome is the rate of clinically relevant AL within 90 days after surgery. This will be compared between the FGBA group using ICG for perfusion assessment and the standard of care surgery, CBA group. The definition

of clinically relevant AL is derived from the definition of Rahbari *et al.*[39] Grade B (requiring active therapeutic intervention but manageable without re-operation) and C AL (requiring re-operation) will be considered clinically relevant. There is no central study protocol for the detection of AL. No routine CT scans will be performed for AL assessment. Post-operative blood tests, radiologic assessment and subsequent assessment of AL will be based on local protocols and the judgement of the local surgical team.

SECONDARY OUTCOMES

30-day clinically relevant AL
30- and 90-day all-cause postoperative complications
30- and 90-day mortality; all-cause and AL related
30- and 90-day reinterventions; surgical and non-surgical
Total surgical time of primary surgery
Postoperative length of hospital stay; primary stay and readmittance within 90 days
Readmittance; all-cause and AL related

TRAINING

Prior to their first inclusion, surgeons and other involved hospital staff of the participating center will be trained during a site initiation visit by the principal investigator or one of the coordinating investigators. If needed, training with the Olympus Medical Imaging Video System and Laparoscope or Da Vinci Firefly will be provided by either Olympus or Intuitive. Surgeons are invited to observe surgical procedures, using NIR fluorescence imaging with ICG for intraoperative assessment of bowel perfusion, in the Leiden University Medical Centre (LUMC). One of the coordinating investigators, with a broad experience in fluorescence-guided surgery, will assist all participating surgeons during their first number of cases to ensure standardization of the technique.

This study is performed in collaboration with Olympus. In order to keep the study data as homogenous as possible, the use of camera system has been limited to the Olympus Medical Imaging Video System and the Da Vinci Firefly in case of robotic-assisted surgery.

DATA COLLECTION

A CRF will be filled in during surgery by trained local research staff. This CRF captures baseline characteristics, basic surgical data and study specific data. For patients in the FGBA group it will be documented whether the resection margins have been adjusted and, if so, which margin (distal or proximal margin) and the extent of adjustment in centimetres. In addition, in case of a non-planned de-functioning stoma, it will be recorded whether ICG-guidance contributed to this decision. All clinical data will be prospectively registered via an electronic CRF (ECRF) in a digital database of Castor EDC. We will not transfer or collect imaging data (video or pictures) for postoperative analysis.

DATA VALIDATION AND MANAGEMENT

Patient data will be registered coded and analysed by comparing the FGBA group with the CBA group. Only the local investigators will have access to local source data after informed consent is given. The research group from LUMC will have access to all coded data in the Castor EDC database.

STUDY TIMELINE

Patients have been included in the study from July 2020, starting in the LUMC. As per August 1st 2021, 352 patients were included in 6 different hospitals. With a mean inclusion rate of 40 patients per month the anticipated last inclusion will be in the final quarter of 2022. There is no maximum for the number of centres nor the number of inclusions per centre.

STATISTICAL ANALYSIS

The most recent version of SPSS (IBM, Armonk, New York, USA) will be used for statistical analysis. Categorical variables of the FGBA and CBA group will be compared by the Chi-Square test. Numerical variables will be compared by the independent sample T-test or the Mann-Whitney U test, depending on distribution. All p-values will be 2-sided. A p-value of less than 0.0492 will indicate a statistically significant difference. All data will be analysed on an intention-to-treat principle and, when applicable, on a per protocol analysis.

The primary outcome measure, clinically relevant AL within 90 days after surgery, will be compared using the Mantel-Haenszel test, stratified by centre.

An interim analysis will be conducted after 489 patients have been randomised and reached the last day of follow-up (day 90). This interim analysis will aim at stopping the study for futility, if the conditional power for the primary endpoint (clinically relevant AL within 90 days after surgery) with the planned sample size, based on the observed results at the interim analysis, using the original settings of null and alternative hypothesis, is less than 10%.

If this interim analysis shows efficacy based on the primary endpoint with a nominal alpha level of 0.0054, the study will be stopped as well. Already included

patients will be followed until the last follow-up moment. Sub-group analysis will be conducted by separately assessing patients with 1. colon and rectal resections, 2. left and right sided resections, 3. malignant and benign pathology, 4. laparoscopic and robotic-assisted surgery.

DATA MONITORING

The study will be monitored for quality and regulatory compliance, by study-independent LUMC staff. Monitoring frequency will be at least annually, but may be increased depending on findings.

ADVERSE EVENTS

All adverse events related to indocyanine green will be reported. Furthermore, all events that are serious adverse events will be registered in the online Dutch database, toetsingonline.nl, and in the ECRF of Castor EDC.

PATIENT AND PUBLIC INVOLVEMENT

Patients or public were neither involved in the development of the research questions and outcome measures nor the planning of the study design. Patients are not involved in the recruitment or conduct of the study. Results of the study will be published in peer-reviewed journals, no other information of the results of the study are provided to the patients. Patients will not take part in assessment regarding possible burden of the interventions of this study.

Expected limitations and difficulties

Intraoperative fluorescence assessment of bowel perfusion is currently a subjective tool. This will most likely influence our results as over 30 different surgeons will interpret the fluorescence output. Quantification of the NIR fluorescence signal would improve standardized assessment of tissue perfusion.

Using different NIR platforms (the Olympus Medical Imaging Video System and Laparoscope, and the Da Vinci Firefly) will have some influence on our results as well. Nevertheless, both systems are optimized for the detection of ICG, we therefore think its effect on our study results is minimal.

AL after colorectal surgery is a multifactorial complication. It is unclear which percentage of AL is solely based on compromised perfusion. It is especially questionable if compromised perfusion plays a role in late AL (> 7 days after surgery).

REFERENCES

1 Buchs NC, Gervaz P, Secic M, *et al.* Incidence, consequences, and risk factors for anastomotic dehiscence after colorectal surgery: a prospective monocentric study. Int J Colorectal Dis 2008;23(3):265-70. doi: 10.1007/s00384-007-0399-3

2 Chambers WM, Mortensen NJ. Postoperative leakage and abscess formation after colorectal surgery. Best Pract Res Clin Gastroenterol 2004;18(5):865-80. doi: 10.1016/j.bpg.2004.06.026

3 Bakker IS, Grossmann I, Henneman D, *et al.* Risk factors for anastomotic leakage and leak-related mortality after colonic cancer surgery in a nationwide audit. Br J Surg 2014;101(4):424-32; discussion 32. doi: 10.1002/bjs.9395

4 Walker KG, Bell SW, Rickard MJ, *et al.* Anastomotic leakage is predictive of diminished survival after potentially curative resection for colorectal cancer. Ann Surg 2004;240(2):255-9.

5 Isbister WH. Anastomotic leak in colorectal surgery: a single surgeon's experience. ANZ J Surg 2001;71(9):516-20.

6 Kang CY, Halabi WJ, Chaudhry OO, *et al.* Risk factors for anastomotic leakage after anterior resection for rectal cancer. JAMA Surg 2013;148(1):65-71. doi: 10.100½013.jamasurg.2

7 Platell C, Barwood N, Dorfmann G, *et al.* The incidence of anastomotic leaks in patients undergoing colorectal surgery. Colorectal Dis 2007;9(1):71-9. doi: 10.1111/j.1463-1318.2006.01002.x

8 Vignali A, Fazio VW, Lavery IC, *et al.* Factors associated with the occurrence of leaks in stapled rectal anastomoses: a review of 1,014 patients. J Am Coll Surg 1997;185(2):105-13.

9 Single-stage treatment for malignant left-sided colonic obstruction: a prospective randomized clinical trial comparing subtotal colectomy with segmental resection following intraoperative irrigation. The SCOTIA Study Group. Subtotal Colectomy versus On-table Irrigation and Anastomosis. Br J Surg 1995;82(12):1622-7.

10 Kockerling F, Rose J, Schneider C, *et al.* Laparoscopic colorectal anastomosis: risk of postoperative leakage. Results of a multicenter study. Laparoscopic Colorectal Surgery Study Group (LCSSG). Surg Endosc 1999;13(7):639-44.

11 Frasson M, Flor-Lorente B, Rodriguez JL, *et al.* Risk Factors for Anastomotic Leak After Colon Resection for Cancer: Multivariate Analysis and Nomogram From a Multicentric, Prospective, National Study With 3193 Patients. Ann Surg 2015;262(2):321-30. doi: 10.1097/SLA.0000000000000973

12 Senagore A, Lane FR, Lee E, *et al.* Bioabsorbable staple line reinforcement in restorative proctectomy and anterior resection: a randomized study. Dis Colon Rectum 2014;57(3):324-30. doi: 10.1097/DCR.0000000000000065

13 Law WL, Chu KW. Anterior resection for rectal cancer with mesorectal excision: a prospective evaluation of 622 patients. Ann Surg 2004;240(2):260-8.

14 Yeh CY, Changchien CR, Wang JY, *et al.* Pelvic drainage and other risk factors for leakage after elective anterior resection in rectal cancer patients: a prospective study of 978 patients. Ann Surg 2005;241(1):9-13.

15 Hyman N, Manchester TL, Osler T, *et al.* Anastomotic leaks after intestinal anastomosis: it's later than you think. Ann Surg 2007;245(2):254-8. doi: 10.1097/01.sla.0000225083.27182.85

16 Snijders HS, Henneman D, van Leersum NL, *et al.* Anastomotic leakage as an outcome measure for quality of colorectal cancer surgery. BMJ Qual Saf 2013;22(9):759-67. doi: 10.1136/bmjqs-2012-001644

17 Vignali A, Gianotti L, Braga M, *et al.* Altered microperfusion at the rectal stump is predictive for rectal anastomotic leak. Dis Colon Rectum 2000;43(1):76-82.

18 Kologlu M, Yorganci K, Renda N, *et al.* Effect of local and remote ischemia-reperfusion injury on healing of colonic anastomoses. Surgery 2000;128(1):99-104. doi: 10.1067/msy.2000.107414

19 Sheridan WG, Lowndes RH, Young HL. Tissue oxygen tension as a predictor of colonic anastomotic healing. Dis Colon Rectum 1987;30(11):867-71.

20 Hirst NA, Tiernan JP, Millner PA, *et al.* Systematic review of methods to predict and detect anastomotic leakage in colorectal surgery. Colorectal Dis 2014;16(2):95-109. doi: 10.1111/codi.12411 [published Online First: 2013/09/03]

21 Karliczek A, Harlaar NJ, Zeebregts CJ, *et al.* Surgeons lack predictive accuracy for anastomotic leakage in gastrointestinal surgery. Int J Colorectal Dis 2009;24(5):569-76. doi: 10.1007/s00384-009-0658-6 [published Online First: 2009/02/18]

22 van Manen L, Handgraaf HJM, Diana M, *et al.* A practical guide for the use of indocyanine green and methylene blue in fluorescence-guided abdominal surgery. Journal of surgical oncology 2018;118(2):283-300. doi: 10.1002/jso.25105 [published Online First: 2018/06/26]

23 Jafari MD, Wexner SD, Martz JE, *et al.* Perfusion assessment in laparoscopic left-sided/anterior resection (PILLAR II): a multi-institutional study. J Am Coll Surg 2015;220(1):82-92 e1. doi: 10.1016/j.jamcollsurg.2014.09.015

24 van den Hoven P, Ooms S, van Manen L, *et al.* A systematic review of the use of near-infrared fluorescence imaging in patients with peripheral artery disease. J Vasc Surg 2019;70(1):286-97 e1. doi: 10.1016/j.jvs.2018.11.023 [published Online First: 2019/06/25]

25 Griffiths M, Chae MP, Rozen WM. Indocyanine green-based fluorescent angiography in breast reconstruction. Gland Surg 2016;5(2):133-49. doi: 10.3978/j.issn.2227-684X.2016.02.01 [published Online First: 2016/04/06]
26 Fox IJ, Brooker LG, Heseltine DW, *et al*. A tricarbocyanine dye for continuous recording of dilution curves in whole blood independent of variations in blood oxygen saturation. Proc Staff Meet Mayo Clin 1957;32(18):478-84. [published Online First: 1957/09/04]
27 Sauda K, Imasaka T, Ishibashi N. Determination of protein in human serum by high-performance liquid chromatography with semiconductor laser fluorometric detection. Anal Chem 1986;58(13):2649-53.
28 Landsman ML, Kwant G, Mook GA, *et al*. Light-absorbing properties, stability, and spectral stabilization of indocyanine green. J Appl Physiol 1976;40(4):575-83. doi: 10.1152/jappl.1976.40.4.575
29 Kudszus S, Roesel C, Schachtrupp A, *et al*. Intraoperative laser fluorescence angiography in colorectal surgery: a noninvasive analysis to reduce the rate of anastomotic leakage. Langenbecks Arch Surg 2010;395(8):1025-30. doi: 10.1007/s00423-010-0699-x
30 Boni L, Fingerhut A, Marzorati A, *et al*. Indocyanine green fluorescence angiography during laparoscopic low anterior resection: results of a case-matched study. Surg Endosc 2017;31(4):1836-40. doi: 10.1007/s00464-016-5181-6
31 Kim JC, Lee JL, Yoon YS, *et al*. Utility of indocyanine-green fluorescent imaging during robot-assisted sphincter-saving surgery on rectal cancer patients. Int J Med Robot 2016;12(4):710-17. doi: 10.1002/rcs.1710
32 Jafari MD, Lee KH, Halabi WJ, *et al*. The use of indocyanine green fluorescence to assess anastomotic perfusion during robotic assisted laparoscopic rectal surgery. Surg Endosc 2013;27(8):3003-8. doi: 10.1007/s00464-013-2832-8
33 Song M, Liu J, Xia D, *et al*. Assessment of intraoperative use of indocyanine green fluorescence imaging on the incidence of anastomotic leakage after rectal cancer surgery: a PRISMA-compliant systematic review and meta-analysis. Tech Coloproctol 2021;25(1):49-58. doi: 10.1007/s10151-020-02335-1 [published Online First: 2020/09/05]
34 Chan DKH, Lee SKF, Ang JJ. Indocyanine green fluorescence angiography decreases the risk of colorectal anastomotic leakage: Systematic review and meta-analysis. Surgery 2020;168(6):1128-37. doi: 10.1016/j.surg.2020.08.024 [published Online First: 2020/10/05]
35 Kin C, Vo H, Welton L, *et al*. Equivocal effect of intraoperative fluorescence angiography on colorectal anastomotic leaks. Dis Colon Rectum 2015;58(6):582-7. doi: 10.1097/DCR.0000000000000320
36 World Medical A. World Medical Association Declaration of Helsinki: ethical principles for medical research involving human subjects. JAMA 2013;310(20):2191-4. doi: 10.1001/jama.2013.281053 [published Online First: 2013/10/22]
37 Dupont WD, Plummer WD, Jr. Power and sample size calculations. A review and computer program. Control Clin Trials 1990;11(2):116-28. doi: 10.1016/0197-2456(90)90005-m [published Online First: 1990/04/01]
38 O'Brien PC, Fleming TR. A multiple testing procedure for clinical trials. Biometrics 1979;35(3):549-56.
39 Rahbari NN, Weitz J, Hohenberger W, *et al*. Definition and grading of anastomotic leakage following anterior resection of the rectum: a proposal by the International Study Group of Rectal Cancer. Surgery 2010;147(3):339-51. doi: 10.1016/j.surg.2009.10.012 [published Online First: 2009/12/17]

PART 2

INTRAOPERATIVE IMAGING USING SGM-101; A TUMOR TARGETED NIR FLUOROPHORE

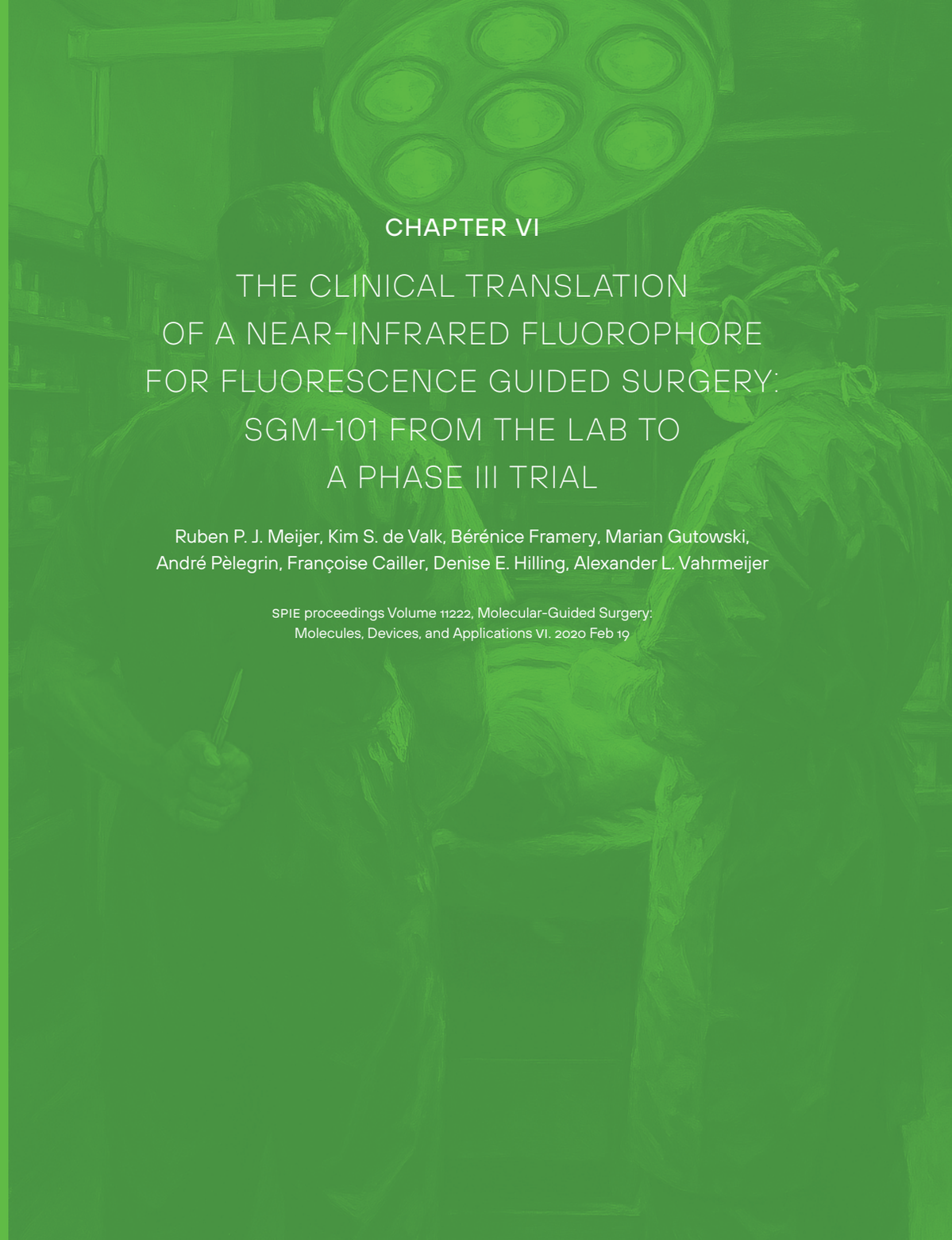

CHAPTER VI

THE CLINICAL TRANSLATION OF A NEAR-INFRARED FLUOROPHORE FOR FLUORESCENCE GUIDED SURGERY: SGM-101 FROM THE LAB TO A PHASE III TRIAL

Ruben P. J. Meijer, Kim S. de Valk, Bérénice Framery, Marian Gutowski, André Pèlegrin, Françoise Cailler, Denise E. Hilling, Alexander L. Vahrmeijer

SPIE proceedings Volume 11222, Molecular-Guided Surgery: Molecules, Devices, and Applications VI. 2020 Feb 19

Abstract

Near-infrared (NIR) fluorescence imaging is a promising intraoperative technique for real-time visualization of tumor tissue during surgery. The process of clinical translation of novel fluorescent agents is an essential part in the evolution of NIR fluorescence guided surgery. Poor visualization of tumors during surgery is one of the major challenges surgeons often face in oncologic patients, mainly due to the improved neo-adjuvant treatment patients receive. In these cases, NIR fluorescence imaging with the use of tumor-targeted fluorescent agents can play an essential role and help provide better oncologic results or patient outcomes. However, before this technique can be implemented in standard of care, optimal tumor-targeted fluorescent agents need to be developed and novel fluorescent agents need to undergo a successful process of clinical translation. Here we describe the clinical translation of SGM-101, a fluorescent anti-CEA monoclonal antibody.

Introduction

Surgery is the most important therapy for patients with colon, rectum or pancreas cancer. Complete resection, which is a crucial factor for patient prognosis, is challenging as surgeons have to rely on the visual appearance and palpation of tissue to discriminate between tumor and normal tissue. Consequently, incomplete resection of malignant tissue or unnecessary removal of healthy tissue may occur. This problem may become bigger as open surgery is increasingly replaced by minimal invasive surgery. In these cases, or complex open surgeries, NIR intraoperative imaging techniques can be of added value. Intraoperative NIR fluorescence imaging is an evolving technique that combines the use of a fluorescent agent with a dedicated NIR camera system, to allow real-time visualization of lymph nodes, tumor tissue and/or vital anatomic structures for surgical guidance.[1] Particularly the use of tumor-specific markers coupled to fluorescent imaging moieties show great potential to improve the intraoperative tumor staging and possibly allow more radical tissue resections.

Carcinoembryonic antigen (CEA) is a tumor-specific marker that is highly expressed in several tumors of epithelial origin (such as colorectal and pancreas cancer) while it is minimally expressed in normal tissue. Anti-CEA monoclonal antibodies have been used in more than 100 clinical studies without any toxicity concerns. In addition, it has been shown that it is possible to link an anti-CEA monoclonal antibody to a NIR fluorophore. The compound that will be discussed in this paper is SGM-101, a CEA-specific antibody conjugated to the fluorophore BM104, developed by SurgiMab (Montpellier, France). The hypothesis is that, following preoperative intravenous (IV) administration of SGM-101 in patients with colon, rectum or pancreas cancer, SGM-101 will bind to CEA expressing cancer cells, consequently enhancing malignant tissue with the use of a NIR fluorescence imaging system. Due to this, surgeons will be able to visualize tumors in real-time during surgery and thereby increase the chance of complete resections.

This article gives an overview of the clinical translation of SGM-101, starting with the preclinical work all the way to the currently enrolling phase III studies.

Clinical translation of sgm-101

In the past years SGM-101 has successfully been translated from the preclinical setting to a currently enrolling international phase III study. As one of the first tumor specific fluorescent antibodies, this path towards clinical approval is still new and lacking standardization. The translational route of SGM-101 can serve

as a platform for discussion about standardizing the clinical methodology in fluorescence-guided surgery research.

PRECLINICAL WORK

Preclinical studies are of great importance, as it acts as a preliminary study to determine whether further studies are consequential. Most importantly, they are crucial in the step towards the clinic (i.e. humans) as the preclinical data is needed to validate and determine the toxicity of a novel agent before it gets exposed to humans. The studies provide useful information regarding the toxicology, as well as the initial diagnostic value of a new agent. Once the novel agent has passed the validation process of whether it is useful for further employment, it will undergo the Good Manufacturing Practice (GMP) production and release by a qualified person so that it can be used in humans. The GMP batch will yet again undergo, more extensive, toxicity testing in animals.

The preclinical work of SGM-101 has demonstrated SGM-101's efficacy in binding CEA *in vitro* and *in vivo* in human CEA expressing mouse models. Stability testing showed no amounts of the dye used for SGM-101 released after up to 96 hours of incubation. Furthermore, biodistribution studies showed high values of SGM-101 at the tumor site and almost none in normal tissue. Moreover, the injection of SGM-101 was well tolerated in all mouse models, Wistar rats and beagle dogs during the *in vivo* pharmacology studies. The lowest NOAEL (no observed adverse effect level) was determined in dogs at 5 mg/kg per day (which corresponds to a 15-fold the intended maximum clinical dose).[2]

The final preclinical study of SGM-101 showed the detection of tumor nodules in three different colon cancer models. Positive predictive values ranged from 90.24 (nodules <1 mg) to 99.04% (nodules >10mg). Free BM105 dye (BM104 with an activated ester for conjugation to the antibody) and an irrelevant conjugate did not induce any NIR fluorescence.[3]

These preclinical data formed the solid base for conducting the first clinical studies with SGM-101 in CEA-expressing tumors.

FIRST-IN-HUMAN

After completion of the preclinical studies and approval by the medical ethics committee, the first major step in the clinic could be performed, which is the exposure of the agent in humans. First-in-human studies with novel fluorescent agents can be performed in either healthy volunteers or in a selected group of the target patient population. SGM-101 was first injected in 18 patients with peritoneal metastasized cancer. All doses, including the maximal dose of 15 mg, were well tolerated; no dose-limiting toxicity has been recorded during the dose escalation phase and none of the adverse events observed have been considered related to the investigational medicinal product.

COLORECTAL CANCER

After first-in-human studies it is important to determine the right dose and dosing interval, respecting the maximum dose tested in previous studies. Nowadays, the only quantitative endpoint for (tumor) visibility using NIR fluorescence is the tumor-to-background ratio (TBR). Nevertheless, there is no consensus about the cut-off points for a sufficient TBR.

Boogerd *et al.* included 26 patients in a multicenter trial, to assess the safety, tolerability and feasibility of SGM-101 in detecting colorectal cancer. SGM-101 did not cause any treatment-related adverse events and showed good intraoperative results (Figure 1). A mean intraoperative TBR of 1.6 was found and the surgeons changed their initial surgical plan, based on SGM-101 NIR assessment, in 6 patients. They reported a sensitivity of 98%, specificity of 62% and accuracy of 84%.[4]

In order to find the optimal dose and dosing time to surgery the study by Boogerd *et al.* got expanded by de Valk *et al.* (Unpublished data). The optimal dose of 10 mg, 4 days prior to surgery, was determined in 36 patients. Moreover, comparable intraoperative results were found.

PERITONEAL METASTASES

An exploratory multicenter pilot study was performed in 14 patients with peritoneal metastasized colorectal cancer who were scheduled for hyperthermic intraperitoneal chemotherapy (HIPEC).[5] Due to too extensive disease, two patients only underwent explorative laparotomy, without HIPEC.

In the remaining 12 patients, a total of 103 lesions were resected. Sixty-five of the 66 malignant lesions were fluorescent (true positive) and 23 of the 37 benign lesions showed no fluorescence (true negative), resulting in a sensitivity of 98.5% and a specificity of 62.2%. The study demonstrated a positive predictive value of 82.3%, a negative predictive value of 95.8% and an accuracy of SGM-101 of 85.4%.

The peritoneal cancer index (PCI) changed in 7 out of 12 patients due to fluorescence imaging. In six patients the PCI increased under fluorescence, which was accurate in four, confirmed by histopathological analysis. In those four patients the score increased with 1 or 2 points, but did not result in termination of the surgical procedure. According to Dutch guidelines, a planned surgical procedure is terminated when a PCI of more than 20 is determined or more than 5 regions are affected. The one case with a decrease in PCI (PCI 5 to 4) due to fluorescence was correct, but definitive pathological analysis concluded a PCI of 3.

Although the detection of extra tumor tissue might not influence the PCI or alter the surgery, SGM-101 still showed additional benefit in 5 out of 12 patients. Detection of those extra lesions still resulted in a more complete cytoreduction, which might be beneficial on the oncologic outcome.

FIGURE 1 Intraoperative images from NIR detected additional lesions.
All lesions were undetected or not suspicious for malignancy in white light, but detected by NIR fluorescence and confirmed malignant by histopathological analysis. (A) Fluorescent hotspot in the bowel mesentery. (B) Two small tumor hotspots in the omentum. (C) Intense fluorescent signal in the right ovary. (D) Retroperitoneal lymph nodes, visible below a layer of overlying tissue.

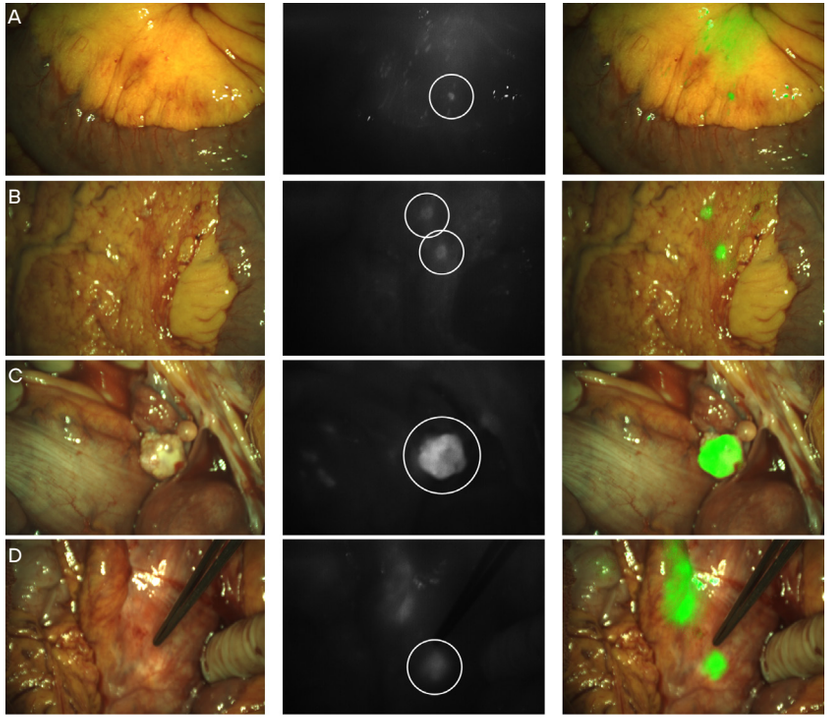

LIVER METASTASES

In total, 11 patients with liver metastases were included (Unpublished data, Meijer *et al.*). Eight patients had liver metastases from colorectal origin and three patients from pancreatic origin. In those 11 patients all malignant lesions were fluorescent. This study showed no additional lesions or alterations due to SGM-101. Nevertheless, these results are promising since all malignant liver lesions were fluorescent and only a very limited number of patients were studied for the visualization of liver metastases with SGM-101. One possible benefit of SGM-101 might be lowering the number of positive resection margins in liver matastasectomies, since recent reports still show 28% resection margin positivity.[6]

PANCREATIC CANCER

Twelve patients were included in the first study using SGM-101 for pancreatic cancer.[7] *In vivo* results showed a mean TBR of 1.6 and *ex vivo* with the Pearl imager (LI-COR, Lincoln, USA) a mean TBR of 3.2 was measured. Only 7 tumors were resected and six were confirmed as adenocarcinomas. One lesion was deemed false-positive since pathological assessment showed a premalignant lesion (intraductal papillary mucinous neoplasm with low-grade dysplasia). In the remaining patients the surgical procedure was abandoned due to irresectability or metastases.

Future perspectives

The abovementioned results offer a great basis for new projects, both confirming the previous results in phase III studies, as well as extending them to new oncological fields. During the preparation of phase III studies in fluorescence-guided surgery, new challenges emerge. One of the biggest challenges is choosing proper endpoints, in the constantly changing field of oncology. Not only the procedures themselves change (i.e. robot-assisted surgery), but also other treatment strategies, like (neo)adjuvant therapy are subject to change. With this perspective, multiple follow-up studies are being executed with SGM-101.

PHASE III

Currently two large phase III studies are enrolling colorectal cancer patients; 1) "The performance of SGM-101 for the delineation of primary, recurrent and metastatic colorectal cancer (SGM-CLIN03; EudraCT# 2018-000151-40 and IND# 134725)" and 2) "SGM-101 in Locally Advanced and Recurrent Rectal Cancer (SGM-LARRC; EudraCT# 2019-001748-23)".

SGM-CLIN03 is an international, semi-blinded, randomized, controlled clinical study including patients with different advanced staged colorectal cancer (T4 colon, T3/4 rectal, peritoneal metastasized and recurrent colorectal cancer). In total 300 patients will be randomized (4:1 for SGM-101:placebo) in 10 centers in Germany, Italy, the Netherlands and the United States. The primary objective is to show benefit in terms of additional resections only identified by fluorescence and confirmed malignant by histopathological analysis.

SGM-LARRC is a Dutch national multicenter study, supported by the Dutch Cancer Society (KWF), including patients with locally advanced or recurrent rectal cancer in parallel arms. In these patients, clear resection margins are key in terms of overall and disease-free survival. Despite the introduction of neoadjuvant therapy, a positive resection margin is found in 25% of the locally advanced and 50% of the recurrent rectal cancer cases.[8-14] Therefore, the primary endpoint is based on the clinical benefit of fluorescence-guided surgery combined with SGM-101 as the intraoperative imaging agent. The corresponding endpoint is the rate of patients with R0 resections.

LUNG CANCER

In addition, new areas for the use of SGM-101 are being explored. This has led to the development of two studies in lung cancer; "SGM-101 in colorectal lung metastases (SGM-CLM; EudraCT# 2019-002044-24)" and "SGM-101 in primary lung cancer (SGM-CLIN06; IND# 145137)".

Despite novel therapeutic developments curative surgery is still an important treatment option for patients with colorectal lung metastases. Complete resection (R0) is crucial, leading to 46% 5-year overall survival versus 20% in the R1 group. Unfortunately, one in 10 patients will belong to the R1 group.[15] SGM-CLM will enroll patients scheduled for the resection of colorectal lung metastasis in multiple Dutch hospitals. In this feasibility study a maximum of 15 patients will be included in different dosing groups. The primary endpoint will be the concordance between the pathology result with respect to the presence of malignancy and the intraoperative fluorescence assessment. This multicenter Dutch study is expected to start enrolling patients in mid-2020.

Up to 72% of the lung and pleural malignancies express CEA, therefore making it an interesting application for SGM-101.[16] As a proof of concept, SGM-CLIN06 will aim to include 10 to 20 patients in a single-center study, to determine the sensitivity of SGM-101 in the detection of lung nodules. Inclusion is expected to start in the first half of 2020, at the University of Pennsylvania (Philadelphia, USA).

Conclusion

SGM-101 is the first fluorescent agent being tested in phase III studies for colorectal cancer. The promising results in primary, recurrent and metastasized colorectal cancer formed the base for this important step. Moreover, the use of standardized methodology in the field of fluorescence-guided surgery will be of added value for regulatory approval.

REFERENCES

1 Vahrmeijer AL, Hutteman M, van der Vorst JR, van de Velde CJ, Frangioni JV. Image-guided cancer surgery using near-infrared fluorescence. Nat Rev Clin Oncol. 2013;10(9):507-18.

2 Framery B, Gutowski M, Dumas K, Evrard A, Muller N, Dubois V, *et al.* Toxicity and pharmacokinetic profile of SGM-101, a fluorescent anti-CEA chimeric antibody for fluorescence imaging of tumors in patients. Toxicol Rep. 2019;6:409-15.

3 Gutowski M, Framery B, Boonstra MC, Garambois V, Quenet F, Dumas K, *et al.* SGM-101: An innovative near-infrared dye-antibody conjugate that targets CEA for fluorescence-guided surgery. Surg Oncol. 2017;26(2):153-62.

4 Boogerd LSF, Hoogstins CES, Schaap DP, Kusters M, Handgraaf HJM, van der Valk MJM, *et al.* Safety and effectiveness of SGM-101, a fluorescent antibody targeting carcinoembryonic antigen, for intraoperative detection of colorectal cancer: a dose-escalation pilot study. Lancet Gastroenterol Hepatol. 2018;3(3):181-91.

5 Schaap DP, de Valk KS, Deken MM, Meijer RPJ, Burggraaf J, Vahrmeijer AL, *et al.* Carcinoembryonic antigen-specific, fluorescent image-guided cytoreductive surgery with hyperthermic intraperitoneal chemotherapy for metastatic colorectal cancer. Br J Surg. 2020.

6 Fretland AA, Dagenborg VJ, Bjornelv GMW, Kazaryan AM, Kristiansen R, Fagerland MW, *et al.* Laparoscopic Versus Open Resection for Colorectal Liver Metastases: The OSLO-COMET Randomized Controlled Trial. Ann Surg. 2018;267(2):199-207.

7 Hoogstins CES, Boogerd LSF, Sibinga Mulder BG, Mieog JSD, Swijnenburg RJ, van de Velde CJH, *et al.* Image-Guided Surgery in Patients with Pancreatic Cancer: First Results of a Clinical Trial Using SGM-101, a Novel Carcinoembryonic Antigen-Targeting, Near-Infrared Fluorescent Agent. Ann Surg Oncol. 2018;25(11):3350-7.

8 Debove C, Maggiori L, Chau A, Kanso F, Ferron M, Panis Y. Risk factors for circumferential R1 resection after neoadjuvant radiochemotherapy and laparoscopic total mesorectal excision: a study in 233 consecutive patients with mid or low rectal cancer. Int J Colorectal Dis. 2015;30(2):197-203.

9 Gebhardt C, Meyer W, Ruckriegel S, Meier U. Multivisceral resection of advanced colorectal carcinoma. Langenbecks Arch Surg. 1999;384(2):194-9.

10 Frykholm GJ, Pahlman L, Glimelius B. Combined chemo- and radiotherapy vs. radiotherapy alone in the treatment of primary, nonresectable adenocarcinoma of the rectum. Int J Radiat Oncol Biol Phys. 2001;50(2):427-34.

11 Dresen RC, Gosens MJ, Martijn H, Nieuwenhuijzen GA, Creemers GJ, Daniels-Gooszen AW, *et al.* Radical resection after IORT-containing multimodality treatment is the most important determinant for outcome in patients treated for locally recurrent rectal cancer. Ann Surg Oncol. 2008;15(7):1937-47.

12 Dresen RC, Kusters M, Daniels-Gooszen AW, Cappendijk VC, Nieuwenhuijzen GA, Kessels AG, *et al.* Absence of tumor invasion into pelvic structures in locally recurrent rectal cancer: prediction with preoperative MR imaging. Radiology. 2010;256(1):143-50.

13 Palmer G, Martling A, Cedermark B, Holm T. A population-based study on the management and outcome in patients with locally recurrent rectal cancer. Ann Surg Oncol. 2007;14(2):447-54.

14 Heriot AG, Byrne CM, Lee P, Dobbs B, Tilney H, Solomon MJ, *et al.* Extended radical resection: the choice for locally recurrent rectal cancer. Dis Colon Rectum. 2008;51(3):284-91.

15 Casiraghi M, De Pas T, Maisonneuve P, Brambilla D, Ciprandi B, Galetta D, *et al.* A 10-year single-center experience on 708 lung metastasectomies: the evidence of the "international registry of lung metastases". J Thorac Oncol. 2011;6(8):1373-8.

16 Wang J, Ma Y, Zhu ZH, Situ DR, Hu Y, Rong TH. Expression and prognostic relevance of tumor carcinoembryonic antigen in stage IB non-small cell lung cancer. J Thorac Dis. 2012;4(5):490-6.

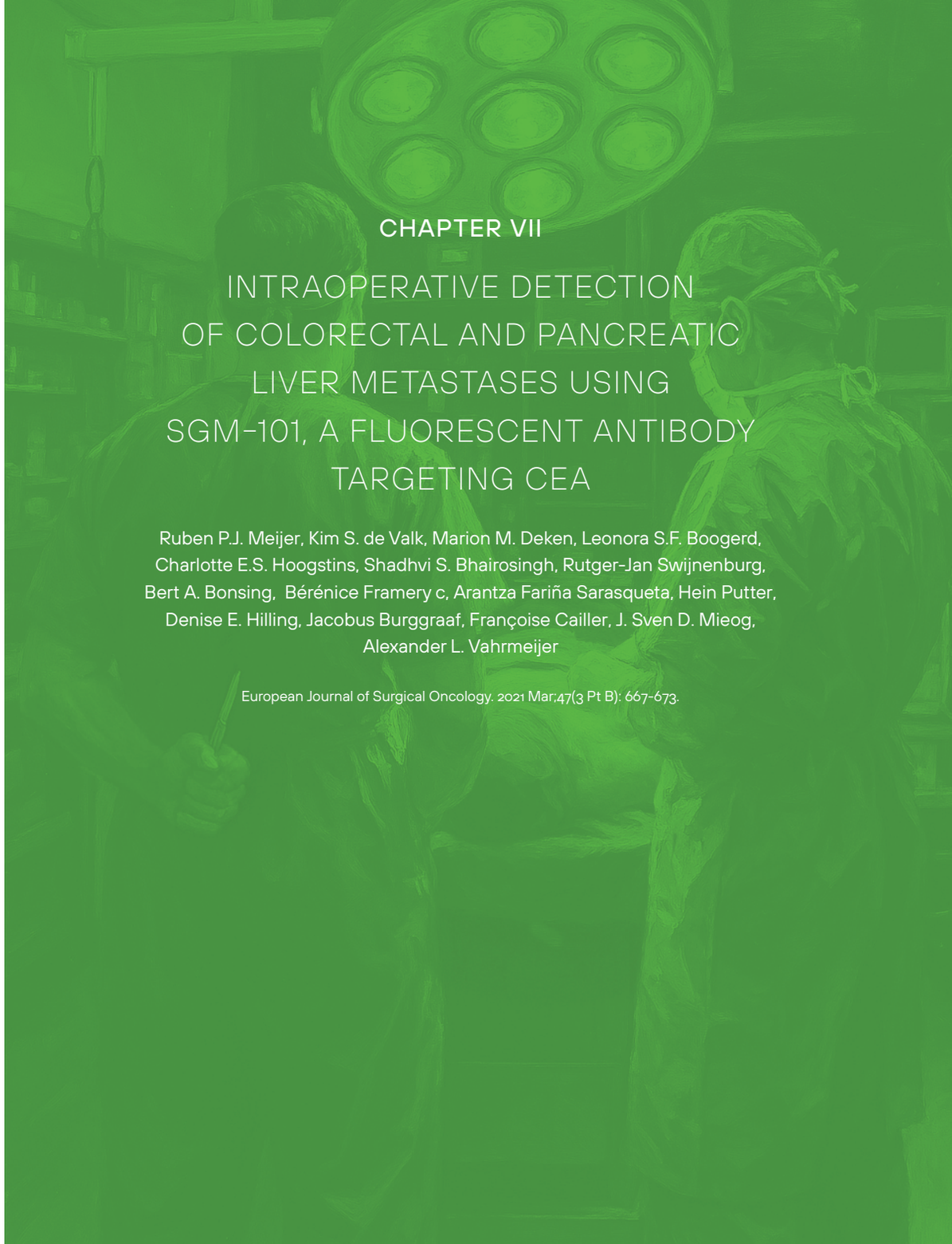

CHAPTER VII

INTRAOPERATIVE DETECTION OF COLORECTAL AND PANCREATIC LIVER METASTASES USING SGM-101, A FLUORESCENT ANTIBODY TARGETING CEA

Ruben P.J. Meijer, Kim S. de Valk, Marion M. Deken, Leonora S.F. Boogerd, Charlotte E.S. Hoogstins, Shadhvi S. Bhairosingh, Rutger-Jan Swijnenburg, Bert A. Bonsing, Bérénice Framery c, Arantza Fariña Sarasqueta, Hein Putter, Denise E. Hilling, Jacobus Burggraaf, Françoise Cailler, J. Sven D. Mieog, Alexander L. Vahrmeijer

European Journal of Surgical Oncology. 2021 Mar;47(3 Pt B): 667-673.

Abstract

BACKGROUND Fluorescence-guided surgery can provide surgeons with an imaging tool for real-time intraoperative tumor detection. SGM-101, an anti-CEA antibody labelled with a fluorescent dye, is a tumor-specific imaging agent that can aid in improving detection and complete resection for CEA-positive tumors. In this study, the performance of SGM-101 for the detection of colorectal and pancreatic liver metastases was investigated.

METHODS In this open-label, non-randomized, single-arm pilot study, patients were included with liver metastases from colorectal origin and intraoperatively detected liver metastases from pancreatic origin (during planned pancreatic surgery). SGM-101 was administered two to four days before the scheduled surgery as a single intravenous injection. Intraoperative fluorescence imaging was performed using the Quest Spectrum® imaging system. The performance of SGM-101 was assessed by measuring the intra-operative fluorescence signal and comparing this to histopathology.

RESULTS A total of 19 lesions were found in 11 patients, which were all suspected as malignant in white light and subsequent fluorescence inspection. Seventeen lesions were malignant with a mean tumor-to-background ratio of 1.7. The remaining two lesions were false-positives as proven by histology.

CONCLUSION CEA-targeted fluorescence-guided intraoperative tumor detection with SGM-101 is feasible for the detection of colorectal and pancreatic liver metastases.

Introduction

Tumor-targeted near-infrared (NIR) fluorescence imaging is a surgical technique that allows real-time detection of malignant tissue to aid surgeons in the peroperative decision making.[1] The added value of tumor-targeted fluorescence imaging is twofold: identification of novel, mostly small malignant lesions and prevention of tumor-positive resection margins.[2,3]

Achieving a complete resection is of utmost importance during oncologic surgery. Especially for colorectal liver metastases, in which a tumor-positive resection margin (<1 mm) is one of the main factors associated with limited overall survival.[4] Unfortunately, margin-positive resections are found in 12%-28% of the patients after liver metastasectomy.[5-7] In pancreatic cancer, intraoperative detection of occult liver metastases immediately translates into a change in treatment strategy, mostly palliation.[8,9] Therefore, adequate pre- and intraoperative staging is important in this vulnerable patient population to avoid a futile high-risk resection.

Preoperative imaging modalities, such as computed tomography (CT), positron emission tomography (PET), and magnetic resonance imaging (MRI), used for the detection of possible liver metastases lack sensitivity for subcentimeter and (sub)capsular lesions.[10-12] Intraoperative detection, by means of palpation, visual inspection, and ultrasonography (in case of deep-seated tumors) is therefore of great importance. With this in mind, real-time intraoperative fluorescence imaging can be a useful tool for surgeons, as it is known to have a high sensitivity in identifying small, superficially located malignant lesions in the liver.[13-15] Additionally, due to the growing use of minimally-invasive procedures, fluorescence imaging can be beneficial as it enhances the visual inspection, thereby compensating for the lack of tactile feedback.

The carcinoembryonic antigen (CEA) is overexpressed in more than 90% of colorectal and 70% of pancreatic adenocarcinomas.[16,17] SGM-101 (SurgiMab, Montpellier, France) is a chimeric antibody targeting CEA, labelled with a fluorescent dye, making it a promising tumor-targeted agent for imaging of CEA-positive cancers. Recent publications have shown promising results in the field of fluorescence-guided surgery using SGM-101.[3,18,19] In complex colorectal cancer, fluorescence imaging with SGM-101 resulted in the additional identification of malignant lesions in 43% of the patients.[3] These lesions were not detected by preoperative imaging or with the naked eye during surgery and were only detected with fluorescence imaging, resulting in a change in treatment strategy

in 35% of the patients.[3] Moreover, the intravenous injection of SGM-101 was considered safe as no related (serious) adverse events were reported in these patients.[3] SGM-101 was further evaluated in additional patients with pancreatic ductal adenocarcinoma and primary and recurrent colorectal cancer to assess the safety, efficacy and optimal dose of SGM-101. The aim of this study was to assess the performance of SGM-101 for the detection of colorectal and pancreatic liver metastases.

Methods

The study was an open-label, non-randomized, single-arm pilot study performed in eleven patients with colorectal or pancreatic adenocarcinoma metastasized to the liver, to evaluate the performance of SGM-101 for the detection of these liver metastases. In the pancreatic cancer patients, the liver metastases were found during the explorative phase of the surgical procedure and were not diagnosed upfront by routine imaging techniques.

Four of these 11 patients have previously been described.[3,18] The study was a collaborative effort between SurgiMab (Sponsor; Montpellier, France), the Centre for Human Drug Research (CHDR; Leiden, the Netherlands) and the Department of Surgery of Leiden University Medical Center (LUMC; Leiden, the Netherlands). The study was approved by a certified medical ethics review board (Stichting BEBO, Assen, the Netherlands) and performed in accordance with the laws and regulations on drug research in humans of the Netherlands. The study is registered in ClinicalTrials.gov under identifier NCT02973672 and aimed to include patients with primary and recurrent colorectal cancer and primary pancreatic cancer. For the current analysis only patients with liver metastases were subtracted from the total group to determine the potential of CEA-targeted fluorescence imaging for liver metastases.

Patients were included in the study after evaluation in a multidisciplinary team meeting and met the following inclusion criteria: aged over 18 years with elevated serum CEA levels (>3 ng/ ml) and scheduled for a surgical resection of colorectal liver metastases or exploration of pancreatic ductal adenocarcinoma with possible subsequent resection of the primary tumor. The exclusion criteria ruled out pregnancy, history of (severe) allergic reactions, impaired renal or hepatic function, and a diagnosis of another malignancy in the last 5 years. All subjects provided written informed consent to the investigators prior to the start of any study-related procedure.

SGM-101 is a CEA-specific chimeric antibody conjugated to a NIR emitting fluorochrome with a fluorescence peak around 705 nm.[20] Intravenous administration of SGM-101 (5-15 mg over 30 min) was performed at the CHDR, where patients were admitted 2e4 days before their scheduled surgery. After infusion, patients were observed for at least 6 hours for safety and tolerability assessments. Plasma CEA levels were determined before and after administration of SGM-101.

All patients underwent the scheduled surgical procedure at LUMC according to standard of care by certified HPB surgeons who were familiar with fluorescence imaging. First, the surgical field was explored under white light using standard visual and tactile methods and subsequently completed with ultrasound imaging based on the surgeon's preference. Next, fluorescence imaging was performed, using the Quest Spectrum® (Quest Medical Imaging BV, Middenmeer, The Netherlands). This imaging system can measure at two different wavelengths. For this study, the tissue was illuminated with 680 nm laser light and visualized at approximately 710 nm.

Every liver lesion was recorded as 1) suspect or not suspect for malignancy as assessed on preoperative imaging 2) suspect or not suspect for malignancy as assessed with the naked eye under white light during surgery and 3) suspect or not suspect for malignancy as assessed with fluorescence imaging. It was the surgeon's decision whether resection of the suspected liver lesion was feasible (which applied to both fluorescent and non-fluorescent lesions) and if intraoperative frozen sections (e.g. in case of pancreatic cancer) were needed for histologic confirmation.

Images obtained with the Quest Spectrum® were viewed and processed with the use of the Architector Vision Suite (version 1.8.3; Quest Medical Imaging, Middenmeer, the Netherlands). For every fluorescent lesion, an intraoperative tumor-to-background ratio (TBR) was calculated, using ImageJ (version 1.51j8; National Institute of Health, MD, USA). The TBR was calculated by dividing the quotient of the signal intensity of a region of interest (ROI) selected in the tumorous tissue with an ROI located in the directly surrounding liver parenchyma.

Due to the exploratory nature of the study, the sample size was not based on statistical considerations. For statistical analysis, IBM SPSS Statistics (Version 25, La Jolla, CA, USA) was used. To explore a possible TBR difference between the different dosing groups a Kruskal-Wallis test was conducted. $P < 0.05$ was considered as significant.

All resected lesions were assessed at the Department of Pathology using a standardized pathology manual designed for fluorescence-guided surgery

studies, including immunohistochemistry analysis with haematoxylin and eosin (H&E) staining and CEA staining on 4 mm formalin-fixed, paraffin-embedded sections. These tissue sections were scored for expression of CEA using the total immunostaining score (TIS), by multiplying the percentage score (PS) and intensity score (IS) found. The PS represented the percentage of positively stained cells and ranged between 0 and 4 (0: none, 1: <10%, 2: 10-50%, 3: 51-80%, 4: >80%). The IS represented the intensity of the stained cells and ranged between 0 and 3.

(0: no staining, 1: mild, 2: moderate, 3: intense). The calculated TIS was then defined as negative (0), weak (1-4), moderate (6-8) or intense (9-12).

For all lesions, the definitive histological diagnosis was compared with the clinical white light assessment and the fluorescence imaging data to determine concordance. A confirmed malignant lesion which was fluorescent during surgery was considered a true-positive. A malignant lesion without fluorescence during surgery was a false-negative. Benign lesions without fluorescence during surgery were considered as true-negative and finally, benign lesions that emitted fluorescence during surgery were considered as false-positive.

Results

From January 2016 to January 2019, a total of 11 patients (9 males and 2 females; median age 70 years) were included in this study (Table 1). Eight patients had highly suspect liver metastases from colorectal origin and three patients were scheduled for an exploration and potential resection for pancreatic ductal adenocarcinoma. All patients received SGM-101 and underwent the scheduled surgery (10 open procedures, 1 laparoscopic procedure). Patients were scheduled for a liver metastasectomy for colorectal metastases (n = 6), exploration and potential pancreatoduodenectomy (n = 3), sigmoid resection with synchronous liver metastasectomy (n = 1) and low anterior resection with synchronous liver metastasectomy (n = 1; Table 1). All serum CEA-levels decreased after injection with SGM-101. No adverse events (AEs) or serious adverse events (SAEs) were reported that were directly related to SGM-101.

TABLE 1 Patient characteristics.

Demographics				SGM-101 dosing			Diagnosis		
ID	Age	Sex	CEA serum level pre-injection (µg/L)	Dose (mg)	Interval (days)	CEA serum level post-injection (µg/L)	Primary carcinoma	In situ	Executed procedure
1	71	M	10.6	5	2	1.1	Pancreas	Yes	Aborted PS (o)
2	68	M	23.5	7.5	2	1.0	Pancreas	Yes	Aborted PS (l)
3	71	M	41.1	7.5	4	13.9	Pancreas	Yes	Aborted PS (o)
4	64	M	9.1	7.5	4	1.5	Sigmoid	Yes	Sigmoid resection with LM (o)
5	72	M	49.9	10	4	U	Sigmoid	No	LM (o)
6	70	F	5.3	10	4	2.5	Sigmoid	No	LM (o)
7	76	M	5.0	10	4	0.4	Colon	No	LM (o)
8	61	F	46.2	10	4	44.2	Sigmoid	No	Aborted LM (o)
9	59	M	147.8	10	4	30.9	Rectal	Yes	LM (o)
10	44	M	140.7	12.5	4	U	Sigmoid	Yes	Low anterior resection with LM (o)
11	73	M	11.5	15	4	U	Rectal	No	LM (o)

Abbreviations: CEA carcinoembryonic antigen, M Male, PS pancreatic surgery, O open, LM liver metastasectomy, F Female, L laparoscopic, U unknown.

TABLE 2 Intraoperative and pathology results.

		Intraoperative					Pathology				IHC		
ID	Lesion	Location (segment)	WLS	IOUS	NIR	TBR	Histopathology	Size (MM)	Tumor free margin (MM)	Concor-dance	IS	PS	TIS
1	1	2	+	NA	+	1.37	Adenocarcinoma	NA	NA	TP	3	4	12
2	2	2	+	NA	+	1.41	Adenocarcinoma	NA	NA	TP	1	1	1
	3	3	+	NA	+	1.19	Adenocarcinoma	NA	NA	TP	3	4	12
3	4	4	+	NA	+	2.39	Adenocarcinoma	NA	NA	TP	3	4	12
	5	4	+	NA	+	2.00	Adenocarcinoma	NA	NA	TP	3	4	12
4	6	2/3	+	+	+	1.55	Adenocarcinoma	17	4	TP	3	4	12
	7	4B	+	+	+	1.72	Adenocarcinoma	13	15	TP	3	4	12
	8	6	+	+	+	1.43	Adenocarcinoma	11	5	TP	3	4	12
5	9	8	+	+	+	1.55	Calcified nodule	NA	NA	FP	0	1	0
	10	6	+	+	+	1.99	Adenocarcinoma	22	7	TP	3	4	12
	11	6/7	+	+	+	1.46	Adenocarcinoma	14	12	TP	3	4	12
6	12	6	+	+	+	2.03	Adenocarcinoma	38	R1	TP	3	4	12
7	13	7/8	+	+	+	2.10	Adenocarcinoma	28	6	TP	3	4	12
8	14	6	+	+	+	1.31	Adenocarcinoma	NA	NA	TP	3	4	12
9	15	8	+	+	+	1.80	Adenocarcinoma	85	3	TP	3	4	12
	16	8/9	+	+	+	2.04	Adenocarcinoma	32	3	TP	3	4	12
10	17	8	+	+	+	1.32	Adenocarcinoma	7	1	TP	3	4	12
11	18	6	+	+	+	1.31	Liver parenchyma	NA	NA	FP	0	1	0
	19	2/3	+	+	+	1.15	Adenocarcinoma	16	80	TP	3	4	12

Abbreviations: IHC immunohistochemistry, WLS White Light Suspect, IOUS intraoperative ultrasound, NIR Near Infrared Suspect, TBR Tumor-to-background ratio, MM milli- meter, IS *Intensity Score,* PS Percentage Score, TIS Total Immunostaining Score, U unknown, + Positive, NA not applicable, TP true-positive, FP false-positive.

LESIONS

A total of 19 lesions were resected (Table 2). All lesions were suspected for malignancy under white light and with intraoperative ultrasound, as well as with fluorescence imaging (figure 1 and figure 2). Seventeen lesions were confirmed malignant by histological evaluation. These 17 lesions had a mean TBR of 1.7 (range 1.2-2.4) with the highest median TBR of 2.0 found in the group dosed with 10 mg 4 days before surgery (figure 3, p = 0.235). The two false-positive lesions were a calcified nodule with inflammation and steatosis (lesion 5, TBR 1.6) and normal liver parenchyma (Lesion 11, TBR 1.3).

Radicality assessment was possible in 11 lesions, as lesion 1-5 and 14 were intraoperative frozen sections of which radicality could not be evaluated with certainty. Of the evaluated lesions, one lesion was irradically resected with microscopic tumor invasion of the resection margin (Lesion 12). The planned surgical procedure (Whipple or pancreatic tail resection) was aborted in all patients with pancreatic ductal adenocarcinoma immediately after histological confirmation with intraoperative frozen section analysis of the liver metastases. In one patient with colorectal liver metastases (patient ID 8), multiple small lesions in different segments of the liver were detected (both in white light and with fluorescence) and were confirmed malignant at frozen section analysis leading to a non-curative situation as decided by the surgeon.

FIGURE 1 Fluorescence evaluation of a colorectal liver metastasis (Patient 4, Lesion 8).
A. Intraoperative fluorescence imaging shows clear fluorescence at the tumor site (liver segment 6, TBR 1.4). Note the intense auto-fluorescence signal from the surgical gloves. **B.** *Ex vivo* breadloafs from the lesion in A show co-localisation of fluorescence with visual tumor localisation. **C.** Staining with hematoxylin and eosin (H&E) and for carcinoembryonic antigen (CEA). Total immunostaining score (TIS) of 12, the CEA pattern corresponds to the site containing tumor cells visible on H&E staining.

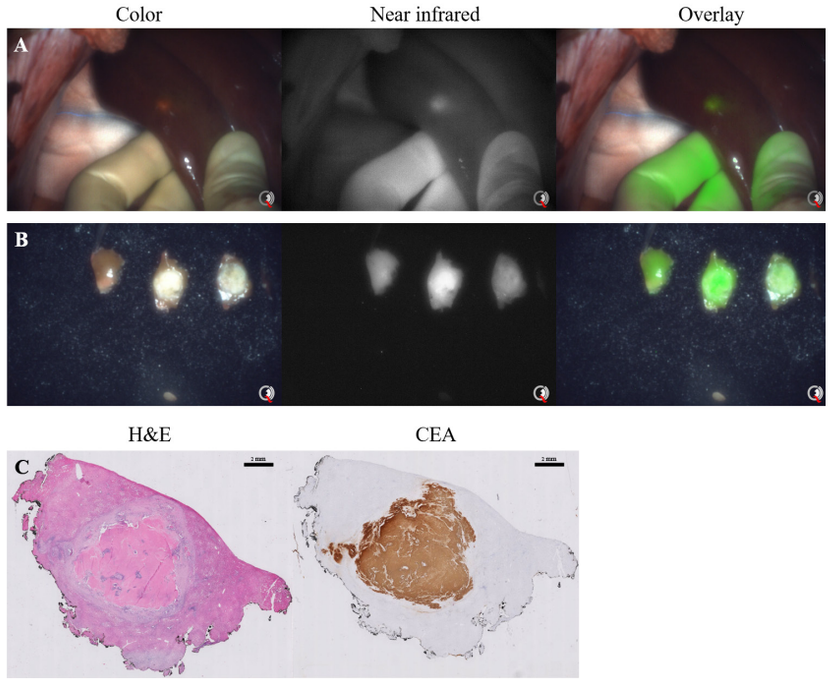

FIGURE 2 Fluorescence evaluation of a liver metastasis from a pancreatic ductal adenocarcinoma (Patient 3, Lesion 4).
A. Intraoperative fluorescence imaging showed clear fluorescence at the tumor site (liver segment 4, TBR 2.4). **B.** *Ex vivo* back table image from the lesion in A shows co-localisation of fluorescence with visual tumor localisation. **C.** Staining with hematoxylin and eosin (H&E) and for carcinoembryonic antigen (CEA). Total immunostaining score (TIS) of 12, the CEA pattern corresponds to the site containing tumor cells visible on H&E staining.

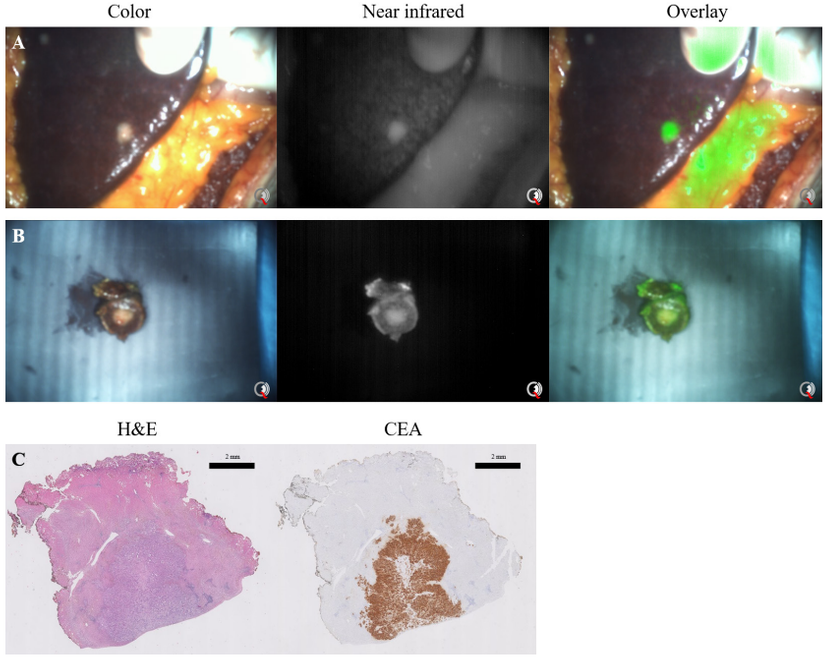

FIGURE 3 Scatter plot of the tumor-to-background ratios of all malignant lesions.
Every true-positive lesion is presented as an individual point. The median per dose is presented with a horizontal line (p ¼ 0.235).

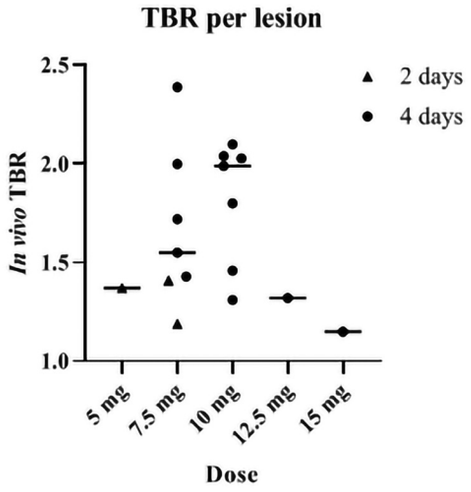

IMMUNOHISTOCHEMISTRY

Sixteen out of 17 true-positive lesions had a maximum TIS of 12 (Table 2). One true-positive lesion was weak for CEA expression (TIS 1, TBR 1.4). Both false-positive liver lesions were negative for CEA-expression (TIS 0, TBR 1.5 and 1.3).

Discussion

This study describes the first series of intraoperative fluorescence imaging for the detection of liver metastases using a tumor-targeted agent. SGM-101 enabled detection of all liver metastases of pancreatic and colorectal origin and resulted in an 89% accuracy rate without any false-negative lesions.

A limitation of this study is the small sample size of 11 patients. This is a consequence of the decision to analyse 2 subgroups (liver metastases and peritoneal metastases) separate from the main study population (primary and recurrent colorectal cancer and primary pancreatic cancer).[3,18,19] Moreover, we decided to combine the results from colorectal and pancreatic liver metastases, as both entities are CEA-positive in most cases, to show the potential of CEA-targeted fluorescence imaging in these patients.

The current marketing information on SGM-101 is insufficient to elaborate on the cost of the procedure and the possible subsequent financial benefit. The costs for fluorescence-guided surgery in general are incurred through the one-time purchase of an imaging system and the use a fluorescent agent. These costs will, most likely, be compensated by a reduction in complications and improved patient outcomes.

The majority of the resected liver metastases in this study were true-positives (17 out of 19). Only two lesions were reported as false-positives but were also suspected as malignant under white light. However, both these false-positive lesions did not show any CEA expression with immunohistochemistry, making it plausible that fluorescence was triggered by other factors, such as auto-fluorescence which is known to be more common for this wavelength (700 nm).[21] Another explanation may be the enhanced permeability retention effect, in which macromolecular drugs (such as antibodies) tend to accumulate in tissue with hypervascularisation and compromised lymphatic drainage.[22]

During fluorescence imaging intraoperative TBR measurements should be considered leading, as tissue resection and decision making occurs during surgery, while the tissue is still inside the patient. However, current commercially available imaging systems cannot calculate the TBR in real-time. Therefore, TBRs are calculated after the procedure. In this study, a mean intraoperative TBR of 1.7 was found, which is relatively high given the fact that SGM-101 is cleared by the liver. This is most likely a consequence of the relatively long interval from injection till surgery, as the mainstream of patients were administered with SGM-101 4 days before surgery, which potentially lowers the background in the liver and thus increases the TBR. Previously, Cetuximab-IRDye800, a NIR fluorescent agent, targeting the epidermal growth factor receptor (EGFR), was used for the intraoperative detection of pancreatic cancer.[23] Interestingly, liver metastases were detected by negative contrast. This might be a consequence of the relative high dye/protein ratio (1.8) of Cetuximab-IRDye800 and a higher EGFR expression in healthy hepatocytes compared to the tumor cells. The dye/protein ratio for SGM-101 is 1.6, which is approximately the same as for Cetuximab-IRDye800. Nevertheless, CEA-expression in the tumor surrounding hepatocytes was not detected, explaining the clear contrast found in our cohort.

Immediate back table imaging of resected liver lesions can be used to identify positive resection margins. Additionally, these images can be compared to the intraoperative images of the wound bed to recognize any remaining fluorescence and thus a potential margin-positive resection, which can be addressed immediately. Given the margin-positive resection rate of up to 28% in liver metastasectomy patients, identification of remaining malignancy at the wound bed can lead to a direct re-resection and change an R1 resection into a R0 resection.[5] In this patient series, in 1 out of 11 assessable lesions, the resection margin was positive for tumor. Unfortunately, assessment of fluorescence at the wound bed was not recorded in this study.

In 2009, Ishizawa *et al.*, described the results of indocyanine green (ICG) for the detection of liver metastases and primary liver malignancies.[24] ICG causes a fluorescent rim, due to the accumulation of ICG in the tumor surrounding hepatocytes. Our group previously reported the identification of additional liver lesions using ICG in approximately 12% of patients.[13-15] The current study with SGM-101 did not show detection of additional liver lesions, which might be a consequence of the small study population and the inclusion of four patients with irresectable disease (patient ID 1-3 and 8). However, SGM-101 is, opposed to ICG, tumor-specific. As a CEA-targeting antibody, SGM-101 has the possibility to detect other types of metastases (eg. peritoneal), as well as the primary tumor. Therefore, SGM-101 seems to be a promising alternative or adjunct to ICG, especially in those patients who still have their primary tumor in situ or have a high probability of synchronous metastases (i.e. liver or peritoneal metastases). A larger study is currently being prepared and expected to start in the first quarter of 2021, to assess the added value of SGM-101 for the detection of additional liver metastases and tumor-positive resection margins, potentially in combination with ICG. A benefit of the combination SGM-101 and ICG, is that these agents work on different wavelengths (700 nm and 800 nm, respectively) and provide tumor detection with a different mechanism. With the use of a NIR camera system that has the ability to image both wavelengths independently, one can switch between those wavelengths without interference.

Conclusion

All liver metastases from colorectal and pancreatic origin were fluorescent with SGM-101, administered 2-4 days prior to surgery. These results warrant further research to determine the added value of this technique.

REFERENCES

1 Vahrmeijer AL, Hutteman M, van der Vorst JR, van de Velde CJ, Frangioni JV. Image-guided cancer surgery using near-infrared fluorescence. Nat Rev Clin Oncol 2013;10(9):507e18.

2 Harlaar NJ, Koller M, de Jongh SJ, van Leeuwen BL, Hemmer PH, Kruijff S, *et al.* Molecular fluorescence-guided surgery of peritoneal carcinomatosis of colorectal origin: a single-centre feasibility study. Lancet Gastroenterol Hepatol 2016;1(4):283e90.

3 Boogerd LSF, Hoogstins CES, Schaap DP, Kusters M, Handgraaf HJM, van der Valk MJM, *et al.* Safety and effectiveness of SGM-101, a fluorescent antibody targeting carcinoembryonic antigen, for intraoperative detection of colorectal cancer: a dose-escalation pilot study. Lancet Gastroenterol Hepatol 2018;3(3): 181e91.

4 Margonis GA, Sergentanis TN, Ntanasis-Stathopoulos I, Andreatos N, Tzanninis IG, Sasaki K, *et al.* Impact of surgical margin width on recurrence and overall survival following Ro hepatic resection of colorectal metastases: a systematic review and meta-analysis. Ann Surg 2018;267(6):1047e55.

5 Fretland AA, Dagenborg VJ, Bjornelv GMW, Kazaryan AM, Kristiansen R, Fagerland MW, *et al.* Laparoscopic versus open resection for colorectal liver metastases: the OSLO-COMET randomized controlled trial. Ann Surg 2018;267(2):199e207.

6 Postriganova N, Kazaryan AM, Rosok BI, Fretland A, Barkhatov L, Edwin B. Margin status after laparoscopic resection of colorectal liver metastases: does a narrow resection margin have an influence on survival and local recurrence? HPB 2014;16(9):822e9.

7 Montalti R, Tomassini F, Laurent S, Smeets P, De Man M, Geboes K, *et al.* Impact of surgical margins on overall and recurrence-free survival in parenchymal-sparing laparoscopic liver resections of colorectal metastases. Surg Endosc 2015;29(9):2736e47.

8 Seufferlein T, Porzner M, Becker T, Budach V, Ceyhan G, Esposito I, *et al.* [S3-guideline exocrine pancreatic cancer]. Z Gastroenterol 2013;51(12): 1395e440.

9 Tempero MA, Malafa MP, Behrman SW, Benson 3rd AB, Casper ES, Chiorean EG, *et al.* Pancreatic adenocarcinoma, version 2.2014: featured up-dates to the NCCN guidelines. J Natl Compr Canc Netw 2014;12(8):1083e93.

10 Niekel MC, Bipat S, Stoker J. Diagnostic imaging of colorectal liver metastases with CT, MR imaging, FDG PET, and/or FDG PET/CT: a meta-analysis of prospective studies including patients who have not previously undergone treatment. Radiology 2010;257(3):674e84.

11 Kaibori M, Matsui K, Ishizaki M, Iida H, Okumura T, Sakaguchi T, *et al.* Intra-operative detection of superficial liver tumors by fluorescence imaging using indocyanine green and 5-aminolevulinic acid. Anticancer Res 2016;36(4): 1841e9.

12 Peloso A, Franchi E, Canepa MC, Barbieri L, Briani L, Ferrario J, *et al.* Combined use of intraoperative ultrasound and indocyanine green fluorescence imaging to detect liver metastases from colorectal cancer. HPB 2013;15(12):928e34.

13 Handgraaf HJM, Boogerd LSF, Hoppener DJ, Peloso A, Sibinga Mulder BG, Hoogstins CES, *et al.* Long-term follow-up after near-infrared fluorescence-guided resection of colorectal liver metastases: a retrospective multicenter analysis. Eur J Surg Oncol 2017;43(8):1463e71.

14 Boogerd LS, Handgraaf HJ, Lam HD, Huurman VA, Farina-Sarasqueta A, Frangioni JV, *et al.* Laparoscopic detection and resection of occult liver tumors of multiple cancer types using real-time near-infrared fluorescence guidance. Surg Endosc 2017;31(2):952e61.

15 van der Vorst JR, Schaafsma BE, Hutteman M, Verbeek FP, Liefers GJ, Hartgrink HH, *et al.* Near-infrared fluorescence-guided resection of colorectal liver metastases. Cancer 2013;119(18):3411e8.

16 Tiernan JP, Perry SL, Verghese ET, West NP, Yeluri S, Jayne DG, *et al.* Carcinoembryonic antigen is the preferred biomarker for *in vivo* colorectal cancer targeting. Br J Canc 2013;108(3):662e7.

17 de Geus SW, Boogerd LS, Swijnenburg RJ, Mieog JS, Tummers WS, Prevoo HA, *et al.* Selecting tumor-specific molecular targets in pancreatic adenocarcinoma: paving the way for image-guided pancreatic surgery. Mol Imag Biol 2016;18(6):807e19.

18 Hoogstins CES, Boogerd LSF, Sibinga Mulder BG, Mieog JSD, Swijnenburg RJ, van de Velde CJH, *et al.* Image-guided surgery in patients with pancreatic cancer: first results of a clinical trial using SGM-101, a novel carcinoembryonic antigen-targeting, near-infrared fluorescent agent. Ann Surg Oncol 2018;25(11):3350e7.

19 Schaap DP, de Valk KS, Deken MM, Meijer RPJ, Burggraaf J, Vahrmeijer AL, *et al.* Carcinoembryonic antigen-specific, fluorescent image-guided cytoreductive surgery with hyperthermic intraperitoneal chemotherapy for metastatic colorectal cancer. Br J Surg 2020;107(4):334e7.

20 Gutowski M, Framery B, Boonstra MC, Garambois V, Quenet F, Dumas K, *et al.* SGM-101: an innovative near-infrared dye-antibody conjugate that targets CEA for fluorescence-guided surgery. Surg Oncol 2017;26(2):153e62.

21 DeLong JC, Hoffman RM, Bouvet M. Current status and future perspectives of fluorescence-guided surgery for cancer. Expert Rev Anticancer Ther 2016;16(1):71e81.

22 Maeda H. Tumor-selective delivery of macromolecular drugs via the EPR effect: background and future prospects. Bioconjugate Chem 2010;21(5): 797e802.

23 Tummers WS, Miller SE, Teraphongphom NT, Gomez A, Steinberg I, Huland DM, *et al.* Intraoperative Pancreatic Cancer Detection using Tumor-Specific Multimodality Molecular Imaging. Ann Surg Oncol. 2018;25(7): 1880e8.

24 Ishizawa T, Fukushima N, Shibahara J, Masuda K, Tamura S, Aoki T, *et al.* Real-time identification of liver cancers by using indocyanine green fluorescent imaging. Cancer 2009;115(11):2491e504.

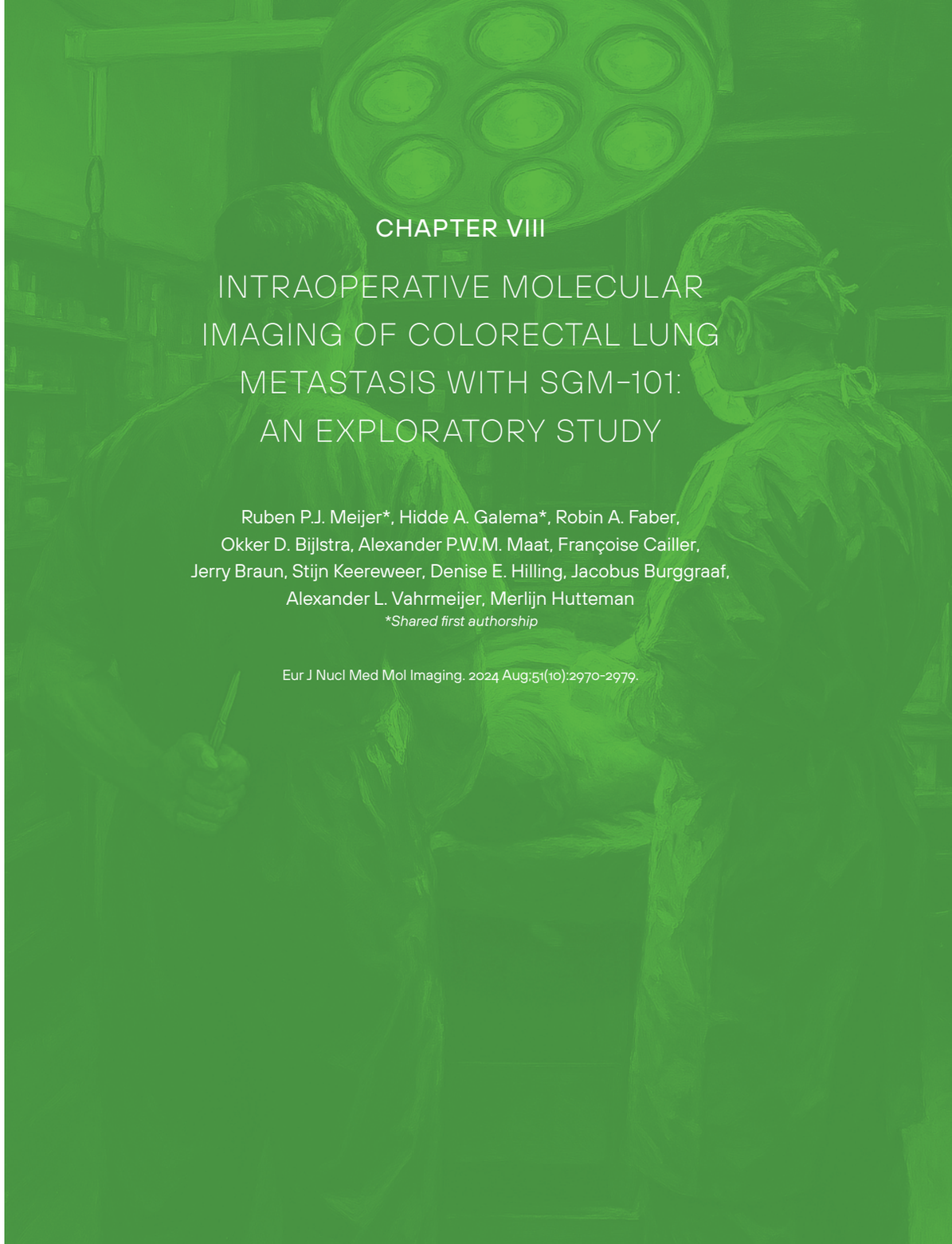

CHAPTER VIII

INTRAOPERATIVE MOLECULAR IMAGING OF COLORECTAL LUNG METASTASIS WITH SGM-101: AN EXPLORATORY STUDY

Ruben P.J. Meijer*, Hidde A. Galema*, Robin A. Faber, Okker D. Bijlstra, Alexander P.W.M. Maat, Françoise Cailler, Jerry Braun, Stijn Keereweer, Denise E. Hilling, Jacobus Burggraaf, Alexander L. Vahrmeijer, Merlijn Hutteman

**Shared first authorship*

Eur J Nucl Med Mol Imaging. 2024 Aug;51(10):2970-2979.

Abstract

PURPOSE Metastasectomy is a common treatment option for patients with colorectal lung metastases (CLM). Challenges exist with margin assessment and identification of small nodules, especially during minimally invasive surgery. Intraoperative fluorescence imaging has the potential to overcome these challenges. The aim of this study was to assess feasibility of targeting CLM with the carcinoembryonic antigen (CEA) specific fluorescent tracer SGM-101.

METHODS This was a prospective, open-label feasibility study. The primary outcome was the number of CLM that showed a true positive fluorescence signal with SGM-101. Fluorescence positive signal was defined as a signal-to-background ratio (SBR) ≥ 1.5. A secondary endpoint was the CEA expression in the colorectal lung metastases, assessed with the immunohistochemistry and scored by the total immunostaining score.

RESULTS Thirteen patients were included in this study. Positive fluorescence signal with *in vivo*, back table and closed-field bread loaf imaging was observed in 31%, 45% and 94% of the tumours respectively. Median SBRs for the three imaging modalities were 1.00 (IQR: 1.00-1.53), 1.45 (IQR: 1.00-1.89) and 4.81 (IQR: 2.70-7.41). All tumour lesions had a maximum total immunostaining score for CEA expression of 12/12.

CONCLUSION This study demonstrated the potential of fluorescence imaging of CLM with SGM-101. CEA expression was observed in all tumours and closed-field imaging showed excellent CEA specific targeting of the tracer to the tumour nodules. The full potential of SGM-101 for *in vivo* detection of the tracer can be achieved with improved minimal invasive imaging systems and optimal patient selection.

Introduction

Around 5% of the patients with colorectal cancer (CRC) develop lung metastases after treatment with curative intent.[1,2] For selected, oligo-metastatic patients, metastasectomy is an important treatment option so long as the primary disease is under control. Tumour identification during metastasectomy is sometimes challenging, as nodules can be small. Positive margins are associated with decreased overall survival, which makes complete removal of the tumour of utmost importance.[3] While the introduction of video-assisted thoracic surgery (VATS) has reduced surgical morbidity, tumour identification has become more challenging. Therefore, interest is growing in other methods for intraoperative detection of colorectal lung metastases (CLM).

Intraoperative, tumour-specific, near-infrared (NIR) fluorescence imaging is developed for several surgical procedures, including lung surgery.[4] To realize NIR fluorescence tumour imaging, patients are administered intravenously with a tumour-specific tracer attached to a fluorophore. Imaging of these agents with a fluorescence imaging system allows for real-time intraoperative visualization of the tumour.[5] SGM-101 is a fluorescent tracer that consists of a monoclonal antibody that targets carcinoembryonic antigen (CEA), labelled with a NIR fluorophore (BM-104). This fluorophore has an excitation and emission wavelength around 700 nm.[6] CEA is overexpressed in >95% of the colorectal cancers and thus an excellent target for molecular imaging of CRC.[7] NIR fluorescence imaging of CLM with SGM-101 may improve intraoperative detection of these tumours and thus increase the chance of a complete resection of the tumour.

Intraoperative NIR fluorescence imaging with SGM-101 has been studied in trials for locally advanced CRC, peritoneal metastases of CRC, colorectal liver metastases, and pancreatic cancer.[8-12] In a phase II rectal cancer trial, NIR fluorescence imaging with SGM-101 resulted in a change in surgical plan in 7 out of 37 patients. Currently, two phase III trials are ongoing with SGM-101 for CRC and peritoneal metastases.[13,14] The aim of this study was to assess the potential of targeting CLM with SGM-101.

Methods

This study was reviewed and approved by the medical ethical committee 'Leiden-Den Haag-Delft' and conducted according to the declaration of Helsinki (10th version, Fortaleza, 2013). Informed consent was obtained from all

study participants. The study was registered in Clinicaltrials.gov under identifier NCT04737213. The study was conducted in the Leiden University Medical Center (LUMC) and the Erasmus MC Cancer Institute (EMC).

STUDY DESIGN

This was a prospective, open-label, non-randomized feasibility study to assess the ability of SGM-101 to target CLM. In this single arm trial, all patients were intravenously administered with SGM-101. SGM-101 was supplied by Surgimab (Montpellier, France). All patients received intravenous administration three to five days prior to surgery, based on earlier study protocols.[10–12] The drug was administered over 30 minutes and patients were observed for three hours after infusion. Patients at least 18 years old, scheduled for resection of (suspected) CLM, and willing and able to give written informed consent were eligible for inclusion. Exclusion criteria were: history of any anaphylactic reaction, other malignancies either currently active or diagnosed in the last 5 years, hepatic or renal insufficiencies, blood count abnormalities, known positive test for HIV, hepatitis B surface antigen or hepatitis C virus antibody or patients with untreated serious infections, patients pregnant or breastfeeding, or any condition that the investigator considered to be potentially jeopardizing the patient's wellbeing or the study objectives.

OUTCOMES

The primary outcome of this study was the number of CLM that showed a true positive fluorescence signal with SGM-101 and a NIR fluorescence imaging system. Secondary endpoints were the optimal dose of SGM-101 for fluorescence imaging of CLM, possible change in surgical management based on fluorescence imaging, and concordance between fluorescence imaging and CEA expression on the corresponding tissue slides.

For the primary outcome, lesions were considered fluorescent (i.e. a positive index test) if the signal-to-background ratio (SBR) was ≥ 1.5.[15] The reference standard for demonstrating CLM was final histopathological assessment. Imaging of the CLM was performed in three settings: *in vivo* imaging, *ex vivo* imaging of the whole specimen on the back table (back table imaging), and *ex vivo* imaging of bread loaf slides in a closed-field imaging device (closed-field imaging). *In vivo* and back table imaging was performed with the Quest spectrum V2 fluorescence camera (Middenmeer, The Netherlands). During VATS, the endoscopic camera of Quest spectrum V2 was used. Closed-field imaging was performed with the PEARL MSI imaging system (Li-Cor ,Lincoln, Nebraska, USA). SBRs were calculated with the 'Quest TBR tool' (Quest Medical Imaging, Middenmeer, The Netherlands) and Image Studio software (Li-Cor, Lincoln, Nebraska, USA). The SBR was defined as the mean fluorescence intensity of the signal derived from the tumour divided by the mean fluorescence intensity of the surrounding normal tissue.

Doses of 7.5, 10, and 12.5 mg were studied. The optimal dose was decided based on closed-field bread loaf imaging. As this was a feasibility study, no direct change in surgical management was performed, based on intraoperative fluorescence imaging alone. However, possible change in surgical management was noted as a secondary outcome measure (type D study).[16] CEA expression was assessed by immunohistochemistry with the monoclonal mouse antibody against CEACAM5 (clone number CI-P83-1, Santa Cruz Biotechnology).[12] Scoring of staining was done by multiplying the intensity score by the proportion score, to calculate the total immunostaining score (TIS).[17] A dedicated pathologist (MD) performed scoring of the immunohistochemistry-stained tissue slides.

STATISTICS

R software (version 4.1.0, R Foundation for statistical computing, Vienna, Austria) was used for statistical analysis. Numerical data was described with median and interquartile range (IQR) or range. To assess SBR differences between dose groups, a Kruskal-Wallis test was performed. To assess the influence of overlying lung parenchyma on fluorescence signal intensity, tumours were categorized as closer or further distanced than 14 mm of the visceral pleura as defined by pre-operative computed tomography (CT). anti-CEACAM5 [18] $P < 0.05$ was considered significant. The sample size is based upon experience with this type of compounds and not on a formal power calculation. Using the 3+3 dose escalation design, a minimum of 9 and a maximum of 15 patients will be included, corresponding to a minimum of 3 patients per dose level. Patients were allocated in a chronological order.

Results

Between January 2021 and September 2022, 13 patients (ten males, three females) with a median age of 56 years (IQR: 54.5-66.5) were included. Patient and surgical characteristics are described in Table 1. There were no (serious) adverse events with any possible relationship to the administration of SGM-101.

TABLE 1 Patient- and surgical characteristics.

		N (%)*
Patients		13 (100)
Sex	Male	10 (77)
	Female	3 (23)
Hospital	LUMC	7 (46)
	EMC	6 (54)
Age (median [IQR])		56 [54.5-66.5]
Serum CEA (µg/ml) (median [IQR])		5.8 [3.33-8.5]
Location metastasis	RUL	5 (28)
	ML	1 (6)
	RLL	6 (33)
	LUL	3 (17)
	LLL	3 (17)
Surgical procedure**	Lobectomy	4 (31)
	Segment resection	2 (15)
	Wedge resection	9 (69)
	Lymphadenectomy	5 (38)
Surgical approach	Thoracotomy	2 (15)
	VATS	9 (70)
	RATS	2 (15)***

* Percentages may not always add up to 100 due to rounding to full numbers
** Multiple patients underwent combined lobectomy and wedge/segment resections
*** One converted to thoracotomy due to haemorrhage

N = number | LUMC = Leiden University Medical Centre | EMC = Erasmus Medical Centre | CEA = carcinoembryonic antigen IQR = interquartile range | RUL = right upper lobe | ML = middle lobe | RLL = right lower lobe | LUL = left upper lobe | LLL = left lower lobe | VATS = video assisted thoracic surgery | RATS = robot assisted thoracic surgery

TUMOUR LESIONS

Eighteen CLM were resected. Characteristics of all lesions are described in Table 2. *In vivo* imaging was performed on 16 lesions, back table imaging on 15 lesions, and closed-field imaging on 18 lesions. A positive fluorescence signal was observed in five lesions (31%) *in vivo*, in seven lesions (47%) with back table imaging and in 17 lesions (94%) with the closed-field imaging. Median SBRs for the three imaging modalities were 1.00 (IQR: 1.00-1.53), 1.45 (IQR: 1.00-2.05) and 4.81 (IQR: 2.70-7.41) respectively. All metastases were detected based on preoperative imaging and white light inspection. No lesions were identified solely based on NIR fluorescence imaging. Five metastases were located > 14 mm of the pleura, none of which showed positive *in vivo* fluorescence (median SBR: 1.00, range 1.00-1.34). For lesions ≤ 14 mm of the pleura, 5 out of 11 (45%) were fluorescent *in vivo* (median SBR: 1.34, range: 1.00-2.15) and 6 out of 11 (64%) lesions on the back table (median SBR: 1.98, range 1.00-3.53). Figure 1 presents an example of *in vivo* and back table imaging (lesion 7).

FIGURE 1 Representative in (A,B) and *ex vivo* (C, D, E, F) fluorescence images of a colorectal lung metastasis (lesion 7).
White light (left panels) and gradient fluorescence overlay (right panels) images.

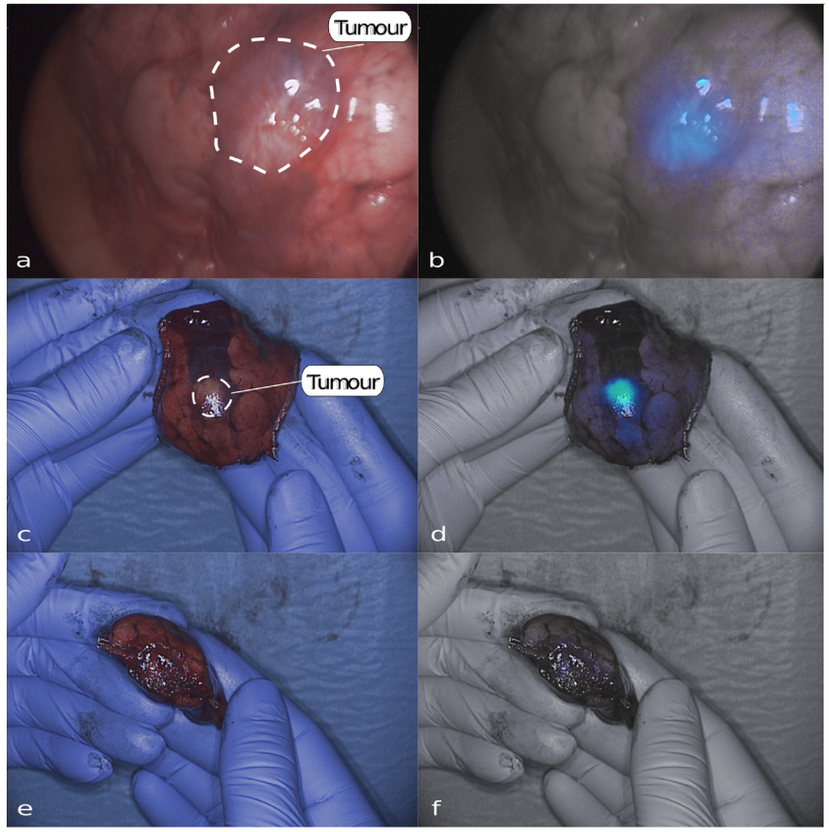

TABLE 2 Characteristics per lesion.

				Preoperative			Intraoperative			Pathology				IHC		
ID	Dose SGM-101	Lesion	Location	Distance to pleura (MM)	CT	WL	SBR (*in vivo*)*	SBR (*ex vivo*)*	Histopathology	Margin (MM)	SBR (bread loaf)*	Concordance **	IS	PS	TIS
1	7.5	1	RLL	6	+	+	2.15	MISS	metastasis CRC	4	6.1	TP	3	4	12
		2	station 11	N/A	-	+	1	MISS	benign LN	N/A	MISS	TN	N/A	N/A	N/A
		3	RLL	17	+	-	1.34	MISS	metastasis CRC	20	5.91	TP	3	4	12
2	7.5	4	RUL	10	+	+	1.62	3.53	metastasis CRC	5	6.43	TP	3	4	12
3	7.5	5	LLL	0	+	+	1.51	1.98	metastasis CRC	10	4.09	TP	3	4	12
		6	LLL	18	+	+	1	1.57	metastasis CRC	23	5.07	TP	3	4	12
4	10	7	RLL	22	+	+	MISS	MISS	metastasis CRC	2	10.44	TP	3	4	12
5	10	8	LUL	0	+	+	1.61	2.19	metastasis CRC	free	4.54	TP	3	4	12
6	10	9	RUL	8	+	+	1	1	fibrosis	N/A	MISS	TN	N/A	N/A	N/A
		10	RUL	2	+	+	1	1	fibrosis	N/A	MISS	TN	N/A	N/A	N/A
		11	RUL	N/A	-	+	1	1	fibrosis	N/A	MISS	TN	N/A	N/A	N/A
		12	RLL	23	+	+	1	1	metastasis CRC	3	1.52	TP	3	4	12
		13	ML	0	+	+	1	1	metastasis CRC	5	2.35	TP	3	4	12
7	12.5	14	RLL	3	+	+	1.34	1.19	metastasis CRC	6	2.99	TP	3	4	12
		15	ML	1	+	+	1	1	metastasis CRC	1	2.01	TP	3	4	12
		16	RUL	15	+	+	1	1	metastasis CRC	10	1.23	FN	3	4	12
		17	station 11	N/A	-	+	MISS	1	benign LN	N/A	MISS	TN	N/A	N/A	N/A
8	12.5	18	RUL	9	+	+	MISS	1.45	metastasis CRC	26	9.93	TP	3	4	12
9	12.5	19	RLL	7	+	-	1	2.04	metastasis CRC	free	3.8	TP	3	4	12
10	7.5	20	LUL	20	+	+	1	1	metastasis CRC	10	8.06	TP	3	4	12
11	7.5	21	LUL	10	+	+	1	2.13	metastasis CRC	free	9.88	TP	3	4	12
12	12.5	22	RUL	2	+	+	1	1.37	metastasis CRC	free	2.49	TP	3	4	12
13	10	23	LLL	0	+	+	1.6	2.06	metastasis CRC	free	7.73	TP	3	4	12
		24	station 7	N/A	-	+	MISS	1	benign LN	N/A	miss	TN	0	0	0
		25	station 8	N/A	-	+	MISS	1.78	malignant LN	N/A	miss	TP	3	4	12
		26	station 9	N/A	-	+	MISS	1	benign LN	N/A	miss	TN	N/A	N/A	N/A
		27	station 10	N/A	+	+	MISS	1.63	malignant LN	N/A	miss	TP	3	4	12
		28	station 11 ventral	N/A	+	+	1.59	1.69	malignant LN	N/A	miss	TP	3	4	12
		29	station 11 dorsal	N/A	-	+	MISS	1	benign LN	N/A	miss	TN	N/A	N/A	N/A

* an SBR of ≥ 1.5 is considered fluorescence positive ** concordance between fluorescence imaging and histopathology. Abbreviations: IHC = *immunohistochemistry* | MM = *millimetre* | CT = *computed tomography* | WL = *white light suspect* | SBR = *signal-to-background ratio* | IS = *intensity score* | PS = *proportion score* | TIS = *total immunostaining score* | RLL = *right lower lobe* | MISS = *missing* | CRC = *colorectal cancer* | TP = *true positive* | N/A = *not applicable* | LN = *lymph node* | TN = *true negative* | RUL = *right upper lobe* | LLL = *left lower lobe* | LUL = *left upper lobe* | ML = *middle lobe* | FN = *False negative*

LYMPH NODES

In patient 1 and 7, two benign lymph nodes were resected based on white light suspicion, but were fluorescence-negative (true negatives). In patient 13, a lymphadenectomy was performed for preoperatively identified hilar lymph node metastases. Three malignant lymph nodes were fluorescent on the back table (lesions 25, 27, 28, true positives). Three other non-fluorescent lesions were resected based on clinical suspicion for tumour involvement. All three contained fibrosis without tumour (lesions 24, 26, 29, true negatives). Figure 2 presents the white light and gradient overlay fluorescence images of three lymph nodes (lesions 25, 26, 28).

SGM-101 DOSE

Five patients (seven lesions) were injected with 7.5 mg SGM-101, four patients (five lesions) with 10 mg, and four patients (six lesions) with 12.5 mg. Median SBRs (closed-field imaging) for the dose levels were 6.1 (IQR: 5.50-7.25), 4.54 (IQR: 2.35-7.73), and 2.9 (IQR: 2.13-4.25) respectively (Figure 3a, p=0.20). There was no difference in absolute tumour or background mean fluorescence intensity (MFI) between the three dose groups (tumour: p=0.14, background: p=0.34, Figure 3b).

POTENTIAL CHANGE IN SURGICAL MANAGEMENT

In one patient, three clinically suspect, *in vivo* non-fluorescent nodules were resected (true negatives, lesions 9, 10, 11). In patient 5, the surgeon was unsure whether a complete removal of the tumour was achieved. Therefore, a small additional resection was performed. Fluorescence back table imaging of the primary specimen showed no tumour involvement of the resection margin (Figure 1, e and f). Final pathology assessment of primary resected specimen confirmed absence of tumour in the resection margin. In patient 9, tumour identification was based on the location on the CT scan and white light inspection. After resection, it was unclear whether the tumour was in the specimen, as the nodule was not palpable. After removing the staples, a clear fluorescent signal was observed in the specimen (Figure 4). The fluorescent tissue was sent for frozen section analysis and confirmed as malignant.

FIGURE 2 Fluorescence images of of malignant (A-D) and benign (E,F) lymph nodes.
White light (left panels) and gradient fluorescence overlay (right panels) images

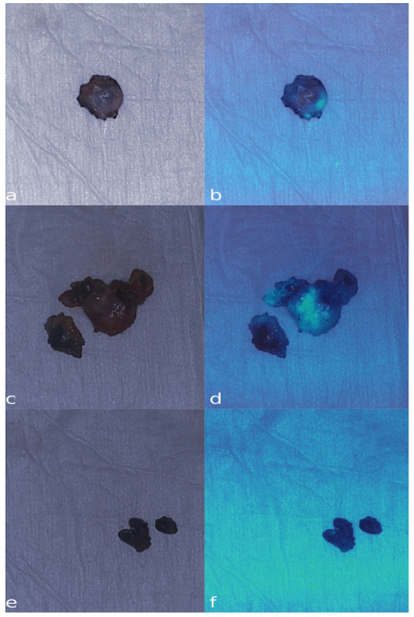

FIGURE 3 The signal-to-background ratios (A) and the mean fluorescence intensities (MFI) for tumour and background tissue per dose group (B) per dose group.
The boxes represent medians with q1 and q3 and the error bars represent the range.

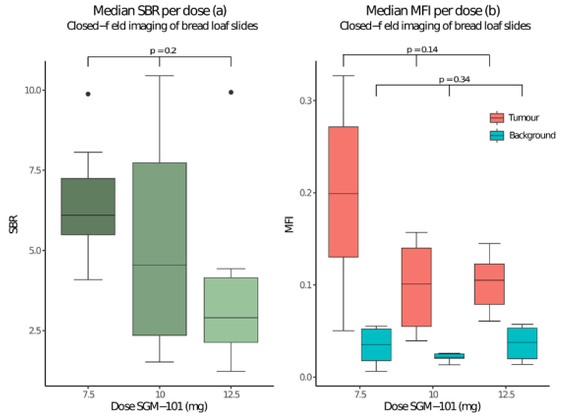

FIGURE 4 Images of an invisible and non-palpable tumour with a clear fluorescence signal (lesion 19).
White light (a) and gradient fluorescence overlay (b) images

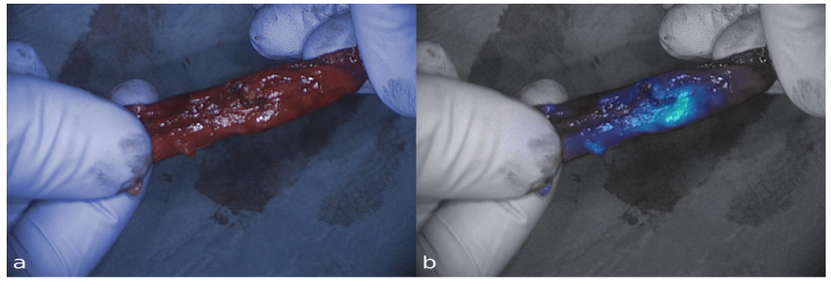

Preoperative serum CEA levels were elevated (> 5.0 µg/L) in 6 out of 11 patients and unknown in the other two patients. CEA expression of all 18 tumor lesions was assessed by immunohistochemistry and all 18 lesions had a total immunostaining score (TIS) of 12 out of 12. Figure 5 presents a bread loaf tissue section of a CLM imaged with several imaging modalities. Figure 6 presents a slide from the same tissue block with the H&E and CEA immunohistochemistry staining. Three tumor containing lymph nodes had maximum CEA expression (TIS: 12). One normal control lymph node had no CEA expression (lesion 24, TIS: 0). CEA expression per lesion is shown in Table 2.

FIGURE 5 A tissue slide of a CLM imaged with the PEARL MSI and Odyssey CLx scanner.

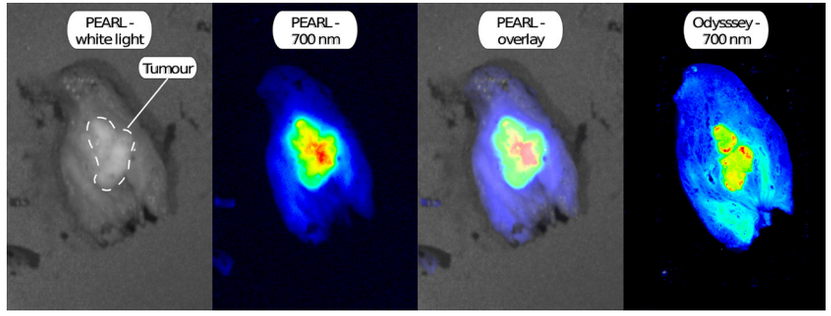

FIGURE 6 H&E staining and CEA immunohistochemistry staining on a tissue slide as demonstrated in Figure 5.

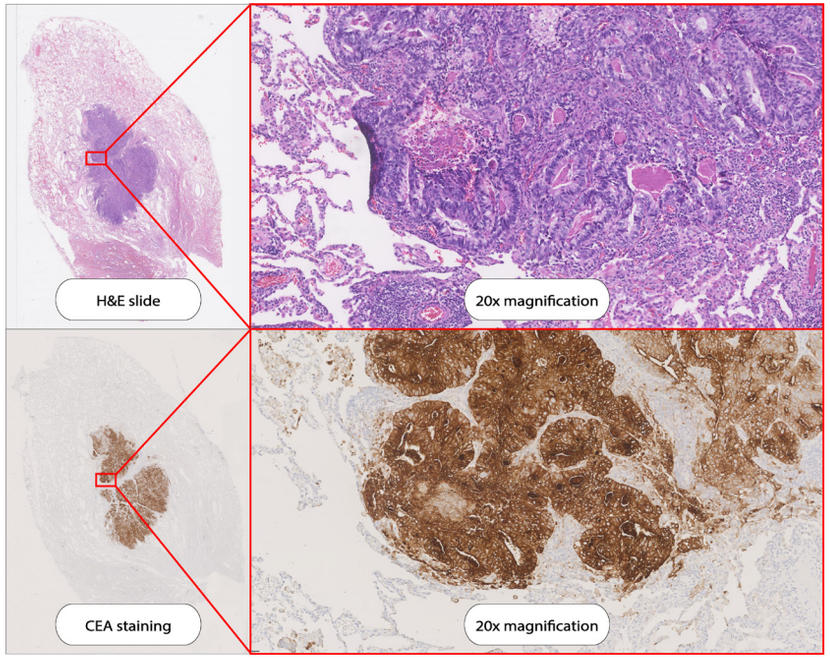

The present study shows that targeting of SGM-101 to CLM was accurate and that CEA is the target of choice for tumour-specific imaging of CLM. Challenges remain with *in vivo* detection of the tumour lesions, especially with the minimally invasive NIR fluorescence imaging system. The full potential of SGM-101 for *in vivo* detection of the tracer may therefore be achieved with improved minimally invasive imaging systems. Optimal patient selection may also further improve the efficacy of SGM-101. If intraoperative identification of the lesion is expected to be challenging, SGM-101 may help for the detection of superficial lesions. Identification of lesions deeper in the lung parenchyma is not expected to be possible with the technique, as overlying lung tissue negatively affects the observed fluorescence signal. An earlier study found a distance from the tumour to pleura of 14 mm as determined by pre-operative CT, to be the maximum tumour depth that can be imaged with an 800 nm fluorophore.[18] For SGM-101 (700 nm) this might be slightly lower.[5,19] In the current study, five lesions had a distance to the pleura of more than 14 mm on CT and none of these were fluorescent *in vivo*. A second application of intraoperative NIR fluorescence imaging is margin assessment. When close or positive resection margins are expected during surgery (e.g. when the tumour infiltrates the chest wall or a bronchus), intraoperative fluorescence imaging with SGM-101 may also be beneficial. For margin assessment, tumour depth is not influential. This is due to the fact that margin assessment is performed by imaging of the resection margin on the specimen on the back table. When positive margins are suspected, the wound bed can also be imaged to assess for residual signal. Given that 94% of the tumour bread loaves showed a positive fluorescence signal, it is expected that when tumour positive margins occur, they can be detected with this technique. Thus, patients with superficial nodules which are expected to be challenging to identify, or patients with tumours with potential tumour positive margins are most likely to benefit from the use of SGM-101.

A secondary objective of this study was to find the optimal dose of SGM-101 for the identification of CLM. For primary colorectal cancer, a dose of 10 mg was found to be the optimal dose.[10] Our study assessed three doses. In all dose groups sufficient SBRs were found. SBRs appeared to decrease with increasing doses but these differences were not significant. Therefore, a dose of 7.5 mg may be sufficient for pulmonary CLM imaging. The lowest dose is also preferable with regard to costs.

Recently, the first results were published on the use of SGM-101 for CLM and primary lung tumours.[20] In this study, ten patients were included, of which four had CLM. A dose of 10 mg of SGM-101 was administered according to the standard dose for primary or recurrent colorectal cancer. In the paper, only SBRs from the closed-field imaging were reported. When comparing SBRs from this trial to our results we find similar results, with mean SBRs of 3-4. For primary lung cancer surgery, several trials have been performed with other fluorescent tracers.[4] OTL-38 is a folate-α targeted fluorescent tracer for pulmonary adenocarcinoma that has been used in several studies for intraoperative imaging of primary lung adenocarcinoma. However, OTL-38 is not a good candidate for imaging of most other adenocarcinomas, including CRC. Less than 30% of the CRCs express folate-α, while CEA is expressed on 95% of tumours.[7,21,22]

Several limitations of this study can be mentioned. The low number of patients might have affected dose finding. In addition, patients were not selected based on tumour location and distance to the pleura. This may explain why several nodules were not fluorescent when imaged intraoperatively. However,

as we asked all eligible patients for participation, we most likely included a clinically representative cohort of patients.

In conclusion, the present study demonstrates the potential of fluorescence imaging of CLM with SGM-101. Closed-field imaging of bread loaves showed excellent targeting of the tracer to the tumour nodules, with maximum target expression on all tumour nodules. Challenges remain with *in vivo* detection of this tracer. Improving minimally invasive fluorescence imaging systems and optimal patient selection most likely enables the optimal efficacy of SGM-101 for CLM surgery.

REFERENCES

1 Meyer Y Olthof PB Grünhagen DJ de Hingh I de Wilt JHW Verhoef C et al. Treatment of metachronous colorectal cancer metastases in the Netherlands: A population-based study. Eur J Surg Oncol. 2021.

2 Riihimäki M Hemminki A Sundquist J Hemminki K. Patterns of metastasis in colon and rectal cancer. Sci Rep. 20166:29765.

3 Hao Z Parasramka S Chen Q Jacob A Huang B Mullett T et al. Neoadjuvant Versus Adjuvant Chemotherapy for Resectable Metastatic Colon Cancer in Non-academic and Academic Programs. Oncologist. 2022.

4 Neijenhuis LKA de Myunck L Bijlstra OD Kuppen PJK Hilling DE Borm FJ et al. Near-Infrared Fluorescence Tumour-Targeted Imaging in Lung Cancer: A Systematic Review. Life (Basel). 202212.

5 Keereweer S Van Driel PB Snoeks TJ Kerrebijn JD Baatenburg de Jong RJ Vahrmeijer AL et al. Optical image-guided cancer surgery: challenges and limitations. Clin Cancer Res. 201319:3745-54.

6 Gutowski M Framery B Boonstra MC Garambois V Quenet F Dumas K et al. SGM-101: An innovative near-infrared dye-antibody conjugate that targets CEA for fluorescence-guided surgery. Surg Oncol. 201726:153-62.

7 Tiernan JP Perry SL Verghese ET West NP Yeluri S Jayne DG et al. Carcinoembryonic antigen is the preferred biomarker for *in vivo* colorectal cancer targeting. Br J Cancer. 2013108:662-7.

8 Meijer RPJ de Valk KS Deken MM Boogerd LSF Hoogstins CES Bhairosingh SS et al. Intraoperative detection of colorectal and pancreatic liver metastases using SGM-101 a fluorescent antibody targeting CEA. Eur J Surg Oncol. 202147:667-73.

9 Schaap DP de Valk KS Deken MM Meijer RPJ Burggraaf J Vahrmeijer AL et al. Carcinoembryonic antigen-specific fluorescent image-guided cytoreductive surgery with hyperthermic intraperitoneal chemotherapy for metastatic colorectal cancer. Br J Surg. 2020107:334-7.

10 de Valk KS Deken MM Schaap DP Meijer RP Boogerd LS Hoogstins CE et al. Dose-Finding Study of a CEA-Targeting Agent SGM-101 for Intraoperative Fluorescence Imaging of Colorectal Cancer. Ann Surg Oncol. 202128:1832-44.

11 Hoogstins CES Boogerd LSF Sibinga Mulder BG Mieog JSD Swijnenburg RJ van de Velde CJH et al. Image-Guided Surgery in Patients with Pancreatic Cancer: First Results of a Clinical Trial Using SGM-101 a Novel Carcinoembryonic Antigen-Targeting Near-Infrared Fluorescent Agent. Ann Surg Oncol. 201825:3350-7.

12 Boogerd LSF Hoogstins CES Schaap DP Kusters M Handgraaf HJM van der Valk MJM et al. Safety and effectiveness of SGM-101 a fluorescent antibody targeting carcinoembryonic antigen for intraoperative detection of colorectal cancer: a dose-escalation pilot study. Lancet Gastroenterol Hepatol. 20183:181-91.

13 Vahrmeijer AL. SGM-101 in Locally Advanced and Recurrent Rectal Cancer (SGM-LARRC). ClinicalTrial.gov.

14 Vahrmeijer AL. Performance of SGM-101 for the Delineation of Primary and Recurrent Tumour and Metastases in Patients Undergoing Surgery for Colorectal Cancer. ClinicalTrials.gov.

15 Azargoshasb S Boekestijn I Roestenberg M KleinJan GH van der Hage JA van der Poel HG et al. Quantifying the Impact of Signal-to-background Ratios on Surgical Discrimination of Fluorescent Lesions. Mol Imaging Biol. 2022.

16 Lauwerends LJ van Driel P Baatenburg de Jong RJ Hardillo JAU Koljenovic S Puppels G et al. Real-time fluorescence imaging in intraoperative decision making for cancer surgery. Lancet Oncol. 202122:e186-e95.

17 Linders D Deken M van der Valk M Tummers W Bhairosingh S Schaap D et al. CEA EpCAM αvβ6 and uPAR Expression in Rectal Cancer Patients with a Pathological Complete Response after Neoadjuvant Therapy. Diagnostics (Basel). 202111.

18 Okusanya OT Holt D Heitjan D Deshpande C Venegas O Jiang J et al. Intraoperative near-infrared imaging can identify pulmonary nodules. Ann Thorac Surg. 201498:1223-30.

19 Kennedy GT Azari FS Chang A Nadeem B Bernstein E Segil A et al. Comparative Experience of Short Versus Long Wavelength Fluorophores for Intraoperative Molecular Imaging of Lung Cancer. Ann Surg. 2022.

20 Azari F Meijer RPJ Kennedy GT Hanna A Chang A Nadeem B et al. Carcinoembryonic Antigen-Related Cell Adhesion Molecule Type 5 Receptor-Targeted Fluorescent Intraoperative Molecular Imaging Tracer for Lung Cancer: A Nonrandomized Controlled Trial. JAMA Netw Open. 20236:e2252885.

21 D'Angelica M Ammori J Gonen M Klimstra DS Low PS Murphy L et al. Folate receptor-α expression in resectable hepatic colorectal cancer metastases: patterns and significance. Mod Pathol. 201124:1221-8.

22 Chen CI Li WS Chen HP Liu KW Tsai CJ Hung WJ et al. High Expression of Folate Receptor Alpha (FOLR1) is Associated With Aggressive Tumour Behavior Poor Response to Chemoradiotherapy and Worse Survival in Rectal Cancer. Technol Cancer Res Treat. 202221:15330338221141795.

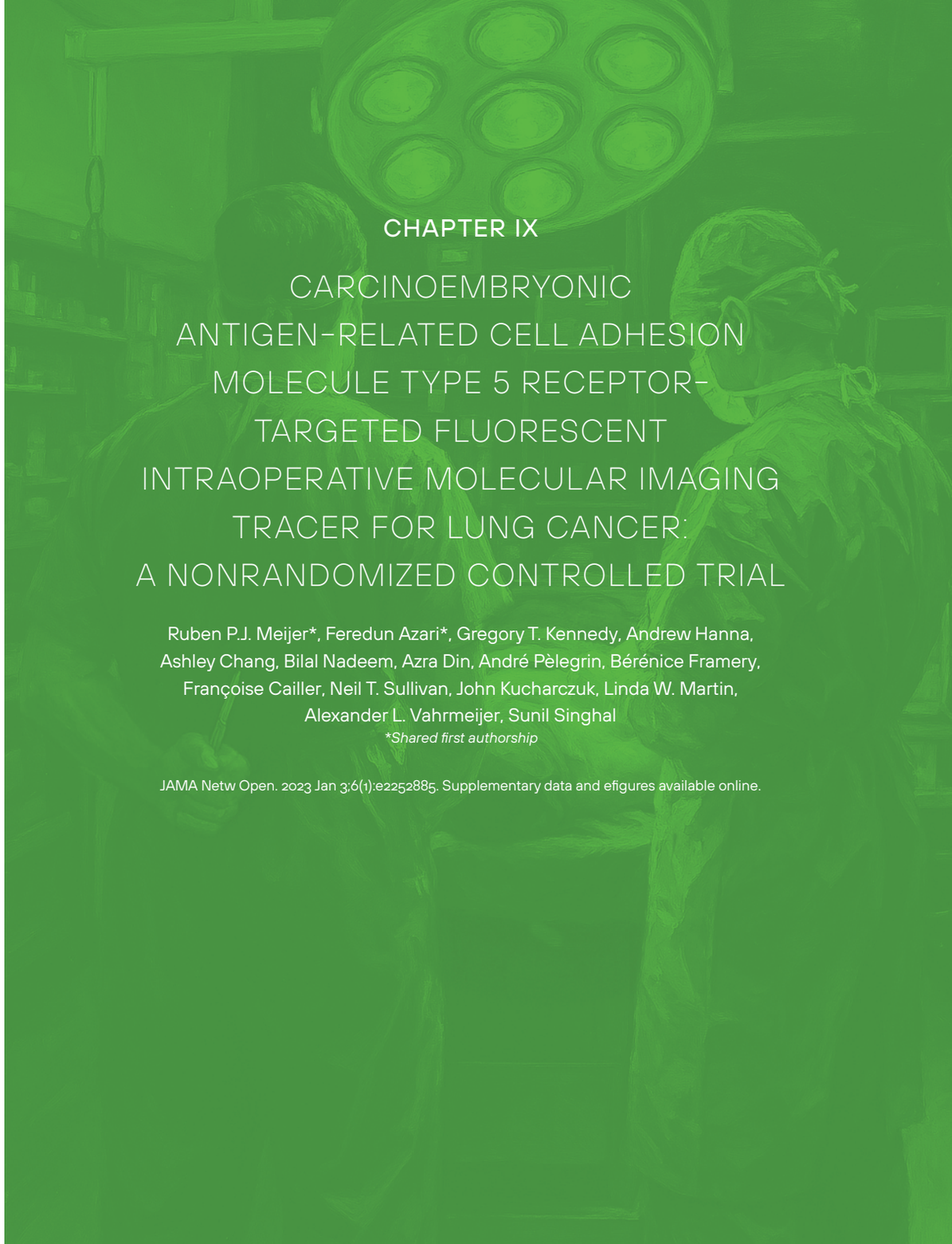

CHAPTER IX

CARCINOEMBRYONIC ANTIGEN-RELATED CELL ADHESION MOLECULE TYPE 5 RECEPTOR-TARGETED FLUORESCENT INTRAOPERATIVE MOLECULAR IMAGING TRACER FOR LUNG CANCER: A NONRANDOMIZED CONTROLLED TRIAL

Ruben P.J. Meijer*, Feredun Azari*, Gregory T. Kennedy, Andrew Hanna, Ashley Chang, Bilal Nadeem, Azra Din, André Pèlegrin, Bérénice Framery, Françoise Cailler, Neil T. Sullivan, John Kucharczuk, Linda W. Martin, Alexander L. Vahrmeijer, Sunil Singhal

**Shared first authorship*

JAMA Netw Open. 2023 Jan 3;6(1):e2252885. Supplementary data and efigures available online.

Abstract

IMPORTANCE Localization of subcentimeter ground glass opacities during minimally invasive thoracoscopic lung cancer resections is a significant challenge in thoracic oncology. Intraoperative molecular imaging has emerged as a potential solution, but the availability of suitable fluorescence agents is a limiting factor.

OBJECTIVE To evaluate the suitability of SGM-101, a carcinoembryonic antigen (CEA)-related cell adhesion molecule type 5 (CEACAM5) receptor-targeted near-infrared fluorochrome, for molecular imaging-guided lung cancer resections, because glycoprotein is expressed in more than 80% of adenocarcinomas.

DESIGN, SETTING, AND PARTICIPANTS For this nonrandomized, proof-of-principal, phase 1 controlled trial, patients were divided into 2 groups between August 1, 2020, and January 31, 2022. Patients with known CEACAM5-positive gastrointestinal tumors suggestive of lung metastasis were selected as proof-of-principle positive controls. The investigative group included patients with lung nodules suggestive of primary lung malignant neoplasms. Patients 18 years or older without significant comorbidities that precluded surgical exploration with suspicious pulmonary nodules requiring surgical biopsy were included in the study.

INTERVENTIONS SGM-101 (10 mg) was infused up to 5 days before index operation, and pulmonary nodules were imaged using a near-infrared camera system with a dedicated thoracoscope.

MAIN OUTCOMES AND MEASURES SGM-101 localization to pulmonary nodules and its correlation with CEACAM5 glycoprotein expression by the tumor as quantified by tumor and normal pulmonary parenchymal fluorescence.

RESULTS Ten patients (5 per group; 5 male and 5 female; median [IQR] age, 66 58-69 years) with 14 total lesions (median [range] lesion size, 0.91 [0.90-2.00] cm) were enrolled in the study. In the control group of 4 patients (1 patient did not undergo surgical resection because of abnormal preoperative cardiac clearance findings that were not deemed related to SGM-101 infusion), the mean (SD) lesion size was 1.33 (0.48) cm, 2 patients had elevated serum CEA markers, and 2 patients had normal serum CEA levels. Of the 4 patients who underwent surgical intervention, those with 2+ and 3+ tissue CEACAM5 expression had excellent tumor fluorescence, with a mean (SD) tumor to background ratio of 3.11 (0.45). In the patient cohort, the mean (SD) lesion size was 0.68 (0.22) cm, and no elevations in serum CEA levels were found. Lack of SGM-101 fluorescence was associated with benign lesions and with lack of CEACAM5 staining.

CONCLUSIONS AND RELEVANCE This in-human proof-of-principle nonrandomized controlled trial demonstrated SGM-101 localization to CEACAM5-positive tumors with the detection of real-time near-infrared fluorescence in situ, *ex vivo*, and by immunofluorescence microscopy. These findings suggest that SGM-101 is a safe, receptor-specific, and feasible intraoperative molecular imaging fluorochrome that should be further evaluated in randomized clinical trials.

Introduction

Lung cancer, particularly non-small cell lung cancer (NSCLC), carries one of the highest rates of cancer-related morbidity and mortality worldwide.[1] Although implementation of screening programs in high-risk patient groups and education around tobacco use prevention have made an impact over the past few decades, NSCLC still inflicts significant strains on the general population.[2] Despite the introduction of advanced immune checkpoint treatments and targeted radiotherapy regimens, surgery remains the best tool in the armamentarium against the disease.[3,4] Stage by stage, surgery confers the highest survival probability in non-disseminated disease.[5] However, success of surgical intervention is intimately related to oncologically sound disease removal by ensuring negative margins and identification of occult synchronous or metachronous lesions. Recurrence after surgery is correlated with inferior survival outcomes.[6]

Therefore, thoracic surgeons continually strive for R0 oncologic disease clearance at index operation.[7] Surgeons have traditionally relied on sensory feedback, such as visualization and tactile assessment, to confirm lesion localization and removal. However, with the increasing use of minimally invasive techniques, these core techniques have been continually challenged, as the surgeon has to rely on the visual field achieved via a thoracoscope or assess lesion characteristics *ex vivo* on the back table.[7] Intraoperative molecular imaging (IMI) has recently emerged as a potential solution to circumvent the current challenges.[7-9] This technology involves systemic delivery of tumor-targeted fluorochrome, which is then visualized using specialized near-infrared (NIR)

(700- 2526 nm) camera systems.[7] Several types of fluorochromes have been approved for a variety of clinical uses by the US Food and Drug Administration (FDA). These fluorochromes include indocyanine green, pafolacianine, and gleolan, which improve outcomes in various solid organ malignant tumors, including sarcomas, lung cancer, colorectal cancer, breast cancer, intracranial tumors, and ovarian cancer. However, due to the large heterogeneity that exists within various NSCLC tumors, particularly lung adenocarcinomas, not all patients benefit from currently available NIR tracers.[8,10-15]

A promising target is the glycoprotein carcinoembryonic antigen-related cell adhesion molecule type 5 (CEACAM5), also known as carcinoembryonic antigen (CEA). Although the glycoprotein has been extensively studied and used for screening, diagnosis, and prognosis in gastrointestinal malignant neoplasms, it has been relatively underused in lung cancer, although 30% to 80% of lung adenocarcinomas express this surface receptor.[16-20] In addition, the surface glycoprotein expression in CEACAM5-positive tumors is significantly higher than that in normal tissue, making it an attractive antigen to be explored (106 surface antigens per cell).[21-23] Targeted delivery of anti-CEACAM5- conjugated NIR fluorochromes, such as SGM-101 (Surgimab), has been demonstrated in colorectal and pancreatic adenocarcinomas, with encouraging results.[21,24-26] SGM-101 is an anti-CEACAM5 antibody conjugated to the NIR BM-104 fluorochrome that specifically emits fluorescence once it binds to CEACAM5-expressing tumors. Given the specificity of the fluorochrome, the ability to readily determine CEACAM5 tumor expression from preoperative biopsies, and the serum detection of glycoprotein, SGM-101 presents an intriguing area to explore in IMI-guided lung cancer resections.

In this study, we explored the safety, efficacy, and specificity of SGM-101 during IMI-guided lung nodule resections. First, we explored a large national cancer database for CEACAM5 RNA expression levels in various lung cancers. Second, we assessed glycoprotein expression levels in 33 patients diagnosed with lung adenocarcinoma from our institution to assess local rates of CEACAM5 tumor presence. Third, we performed an open-label nonrandomized controlled trial in patients with gastrointestinal tumors who presented with lung metastases based on serum CEA levels as a control and compared the results in subsequent patients who underwent SGM-101-guided primary lung cancer resection. We hypothesized that SGM-101 would specifically localize to CEACAM5-positive lung nodules and allow lesion localization *in vivo*, *ex vivo*, and on immunohistopathologic assessment.

Methods

STUDY DESIGN AND PATIENT SELECTION

The current study was an open-label, nonblinded, proof-of-principle, phase 1 nonrandomized controlled trial performed in patients 18 years or older at the Hospital of the University of Pennsylvania in Philadelphia from August 1, 2020, to January 31, 2022. The trial protocol appears in Supplement 1. Details on immunohistochemistry, The Cancer Genome Atlas analysis, inclusion and exclusion criteria, fluorochrome parameters, camera systems used, and outcomes analyzed are detailed in the eMethods in Supplement 2. Data on race and ethnicity were not collected because this was a cellular molecular study and such data would not be informative. The study was reviewed and approved by the University of Pennsylvania Institutional Review Board in accordance with Good Clinical Practice guidelines as outlined by the International Council of Harmonization of Technical Requirements for Pharmaceuticals for Human Use in addition to laws and regulations for human research by the state of Pennsylvania and the FDA. All patients were informed of the risks, benefits, and alternatives regarding the interventions in the study. Participants enrolled in the study signed written informed consent forms approved by the University of Pennsylvania Institutional Review Board before initiation of the trial. The rationale, background, methods, design, analysis, and interpretation of the study follow the recommendations set by the Transparent Reporting of Evaluations With Nonrandomized Designs (TREND) reporting guideline.

STUDY GROUPS

In this nonrandomized controlled trial, the first group (positive control) included patients with known primary or recurrent gastrointestinal adenocarcinoma (colon, rectal, and pancreatic adenocarcinoma) with or without elevated serum CEA levels who were found to have nodules suggestive of pulmonary metastases. The second group included patients with nodules suggestive of malignant primary pulmonary disease on screening imaging who were scheduled for surgical resection regardless of serum CEA status. Of note, our institutional practice does not include preoperative nodule sampling.

NIR TRACER

SGM-101 was manufactured in accordance with Good Laboratory Practice guidelines and supplied by Surgimab. The SGM-101 active ingredient is a

covalent conjugate of the SGM-Ch511 anti-CEACAM5 chimeric monoclonal antibody with the fluorochrome BM-104. Patients in this study were administered 10 mg of SGM-101 intravenously for 30 minutes followed by a 50-mL flush of isotonic saline to account for the dead volume of the tubing. Patients were administered SGM-101 3 to 5 days (±1 day) before surgery at the Center for Health and Precision Surgery and monitored for a minimum of 1-hour after infusion.

SURGICAL PROCEDURES

Surgical procedures were performed by a thoracic surgeon (J.K. and S.S.). During surgery, surgeons used standard visualization and finger palpation (when applicable) to identify known tumors. After identification of the tumor, NIR imaging was used to confirm lesion fluorescence. If the preoperatively identified nodule was unidentifiable by white-light visualization or palpation, localization using fluorescence guidance was attempted. After the primary lesions were identified, fluorescence imaging was used to assess the hemithorax for occult lesions. After resection of the nodules, the specimen was analyzed *ex vivo* on a back table using an NIR camera system to assess nodule fluorescence and margin assessment. All samples were analyzed in triplicate by Pearl and Odyssey NIR Imager (LI-COR Biosciences) as well as ImageJ, version 1.53t (National Institutes of Health). The sample was then sent for frozen section analysis by a board-certified thoracic pathologist.

STATISTICAL ANALYSIS

Data are presented as mean (SD) unless otherwise noted. Data were analyzed for parametric distribution. An unpaired t test was used to compare continuous variables across 2 groups, whereas analysis of variance was used to compare continuous variables across more than 2 groups. Univariate statistical significance between groups were confirmed using the Fisher exact test. A 1-sided $P < .05$ was considered statistically significant.

Results

DEMOGRAPHIC CHARACTERISTICS

A total of 35 patients were eligible for enrollment in the study, of whom 10 (5 per group; 5 male and 5 female; median [IQR] age, 66^{58-69} years) with 14 total lesions (median range lesion size, 0.91 [0.90-2.00] cm) consented to undergo a proof-of-principle SGM-101-guided lung resection clinical trial (eTables 1 and 2 in Supplement 2). There was no loss of follow-up in the study. Given that SGM-101 was successful in the localization of pancreatic and colorectal malignant neoplasms, we selected 5 patients with malignant neoplasms suggestive of colorectal or pancreatic cancer as a control group in the study before use of the tracer in the primary lung cancer group (eTable 2 in Supplement 2).[21,26] After selection of the control group, we selected 5 patients for the primary lung malignant neoplasm cohort. All patients received 10 mg of SGM-101, with a median (range) time from infusion to surgery of 92.88 (91.2-94.67) hours. The median (range) preoperative serum CEA level was 3.0 ng/mL (2.0-3.5 ng/mL) (to convert to micrograms per liter, multiply by 1), with the metastasis cohort having an elevated median (range) CEA level of 5.11 ng/mL (3.10-9.18 ng/mL) ($P = .03$).

No SGM-101 infusion-related complications and no severe (Clavien-Dindo classification higher than 3) postoperative complications occurred. Patient 5 in the metastasis control cohort underwent infusion of SGM-101 but had abnormal electrocardiographic findings during preoperative clearance and did not undergo surgery. Demographic details and complication profiles are provided in eTables 2 and 3 in Supplement 2.

LOCALIZATION OF CEACAM5-POSITIVE METASTATIC NODULES

A total of 5 patients were recruited for the control group. One patient (patient 5) did not undergo surgical resection because of abnormal preoperative cardiac clearance findings that were not deemed related to SGM-101 infusion. The mean (SD) lesion size in the control cohort was 1.33 (0.48) cm. Patients 1 and 2 had elevated serum CEA markers, whereas patients 3 and 4 had normal serum CEA levels. Of the 4 patients who underwent surgical intervention, those with 2+ and 3+ tissue CEACAM5 expression had excellent tumor fluorescence, with a mean (SD) tumor to background ratio (TBR) of 3.11 (0.45) (Figure 1 and Figure 2; eFigures 1 and 2 in Supplement 2).

Patient 1 had 2 concerning nodules on preoperative workup (Figure 1 and Figure 2; eFigures 1, 3, and 4 in Supplement 2). SGM-101 identified 1 nodule *in vivo* and *ex vivo* by fluorescence microscopy (Video). The mean (SD) TBR for nodule 1 was 3.12 (0.38). Nodule 2 was visualized *in vivo* but did not demonstrate any fluorescence *in vivo* or *ex vivo* (Video). The CEACAM5 staining demonstrated a 3+ score for nodule 1, and no staining was observed for nodule 2. Nodule 1 was confirmed to be a metastatic lesion associated with primary pathology (Figure 2 and Figure 3), whereas nodule 2 was a lymphoid aggregate. Similar observations were noted in patient 2, whereas serum CEA levels were elevated and

demonstrated excellent fluorescence *in vivo*, *ex vivo*, and on histologic assessment (Video). The mean (SD) TBR was 2.89 (0.51) for the fluorescent nodule for patient 2. SGM-101 fluorescence correlated with 3+ CEACAM5 staining (Video; Figure 2; eFigures 2, 4, and 5 in Supplement 2).

FIGURE 1 SGM-101-guided lung nodule resection in a control patient.
A. Computed tomography images of the tumor (yellow arrowheads indicate tumor).
B. Nodule 1. **C.** Nodule 2. NIR indicates near infrared.

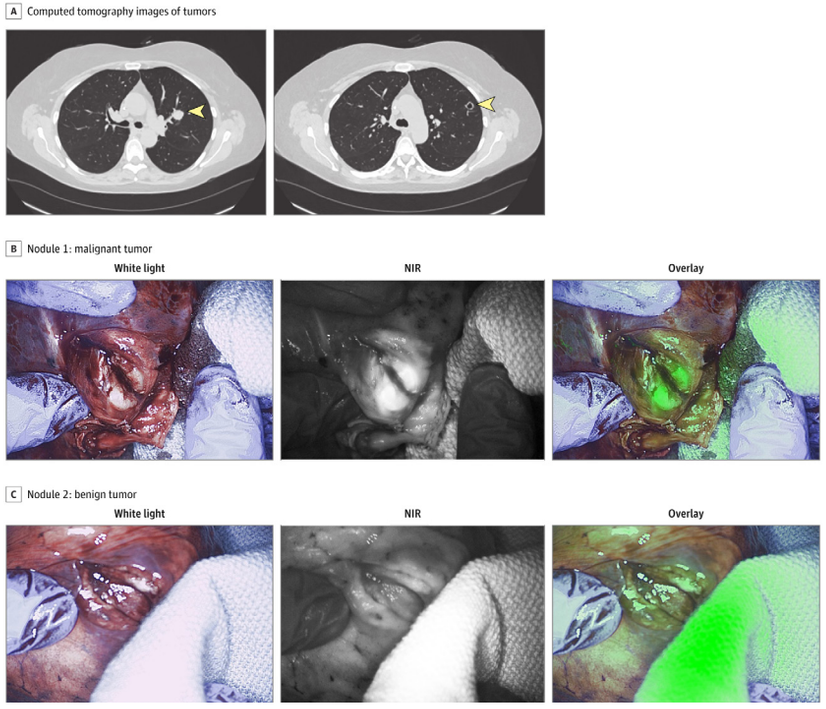

Patient 3 had known stage 3 ($T_2N_3M_0$) pancreatic adenocarcinoma that was operated on 6 months earlier. This patient had no serum CEA elevation. The nodule was not visualized *in vivo* but demonstrated mild CEACAM5 (1+) staining with fluorescence that was detected on *ex vivo* assessment. Retrospective analysis of the index operation revealed a normal serum CEA level at the time of pancreaticoduodenectomy with mild CEACAM5 staining on uncinate tumors.

Conversely, in patient 4 with colorectal adenocarcinoma, who never had serum CEA elevation but had strong CEACAM5 staining at the time of index operation, nodules suggestive of disease were visualized *in vivo* and *ex vivo* and were associated with CEACAM5 staining (2+). Compared with patients 1 and 2, the nodule was significantly smaller (0.51 cm) and produced visible but statistically significantly lower fluorescence emission (mean [SD] TBR, 1.89 [0.33]; P = .04) (eFigure 5 in Supplement 2).

FIGURE 2 Association of SGM-101 fluorescence with carcinoembryonic antigen-related cell adhesion molecule type 5 (CEACAM5) presence by immunohistochemical analysis.
Scale bars = 100 µm.

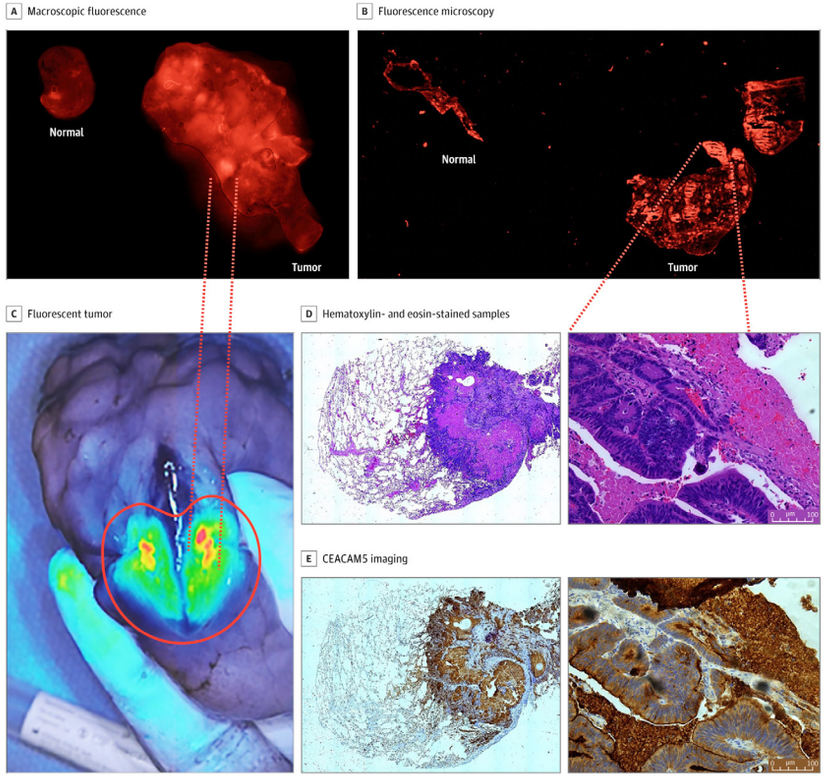

FIGURE 3 Localization of SGM-101 to carcinoembryonic antigen-related cell adhesion molecule type 5 (CEACAM5) tumors.

Patient 8 with invasive adenocarcinoma demonstrated a tumor with a large necrotic core (>80%) but had high CEACAM5 staining correlating with the thyroid transcription factor 1 (TTF-1) score (scale bar = 100 µm). Tumors were able to localize *in vivo*, *ex vivo*, and on a near-infrared scanner. AU indicates absorbance units; CK5/6, cytokeratin 5/6.

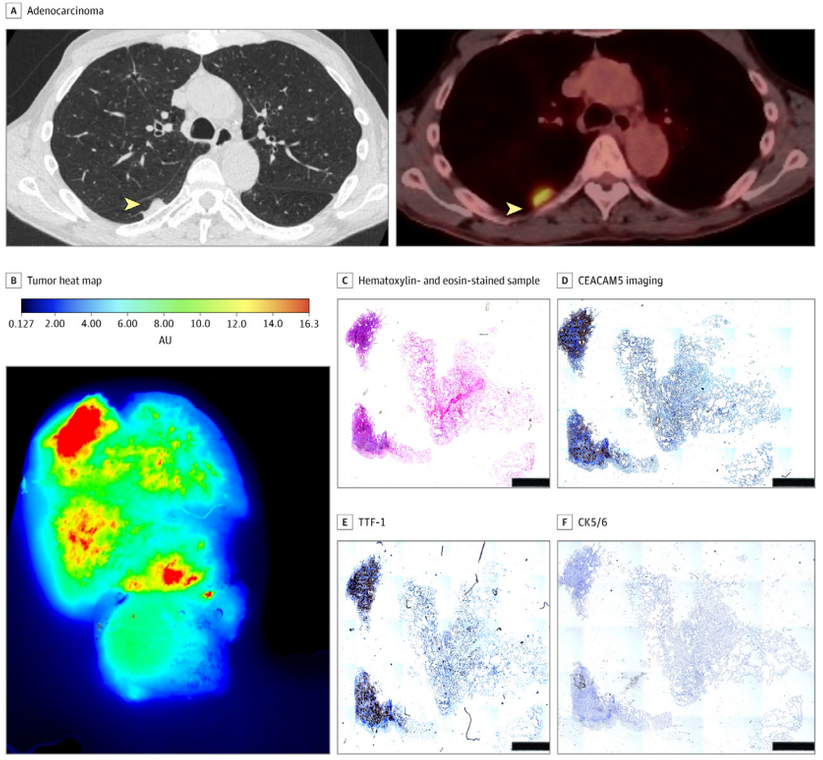

SGM-101 FLUORESCENT LABELING OF CEACAM5-POSITIVE LUNG TUMORS

Five patients with primary nodules were selected for a proof-of-principle study. No elevation in serum CEA levels were found in this patient cohort. The mean (SD) lesion size was 0.68 (0.22) cm. Lack of SGM-101 fluorescence was associated with benign lesions and with lack of CEACAM5 staining. Benign lesions lacked any fluorescence in *ex vivo* and histologic analyses (Figure 4). Patient 1 demonstrated an abscess cavity that was positive on positron emission tomography at preoperative assessment. No SGM-101 fluorescence, no CEACAM5 staining, and no other immunohistochemical staining were associated with markers of lung malignant neoplasms, including thyroid transcription factor 1 (TTF-1), cytokeratin 5/6 (CK 5/6), and p63 (Figure 4; eFigure 6 in Supplement 2). The presence of CEACAM5, particularly strong (>2+), was associated with the detection of SGM-101 fluorescence *in vivo* (Figure 4; eTables 4-6 in Supplement 2).

FIGURE 4 Fluorescence microscopy assessment of primary lung nodules analyzed in the study.

The benign lesion (A) demonstrates no uptake of SGM-101 fluorescence, which corresponded with a lack of carcinoembryonic antigen, p63, and thyroid transcription factor 1 (TTF-1) staining (scale bar = 100 µm). Conversely, malignant lesions (primary lung adenocarcinoma) (B) demonstrate areas of fluorescence corresponding to areas of carcinoembryonic antigen-related cell adhesion molecule type 5 (CEACAM5) staining that were also congruent with areas of TTF-1 expression, demonstrating CEACAM5- dependent SGM-101 labeling. Adjacent normal lung parenchyma (inset, C) demonstrates a lack of fluorescence and a lack of CEACAM5 staining. H&E indicates hematoxylin-eosin.

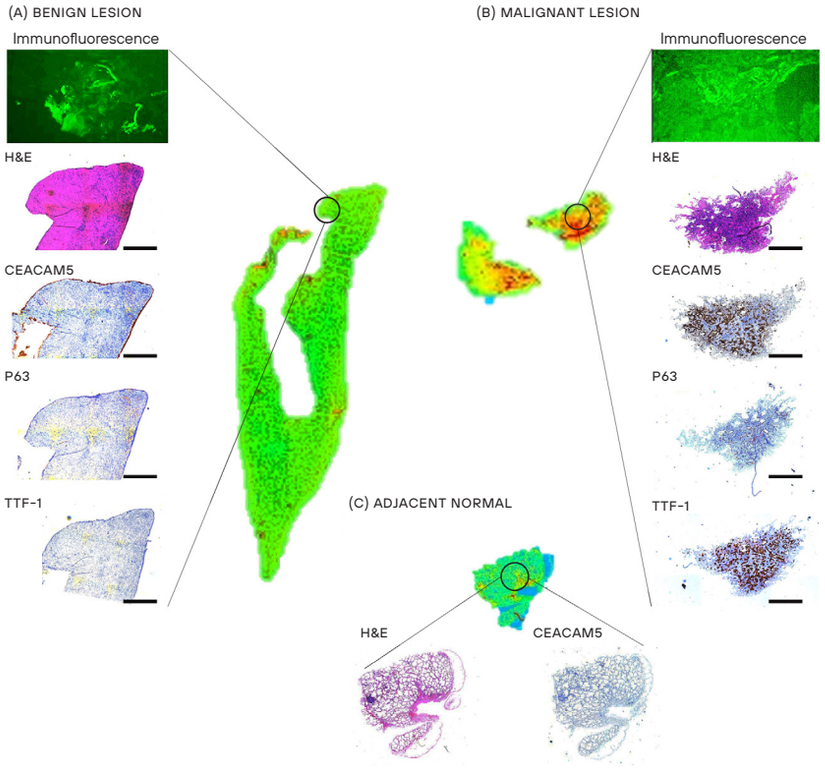

The area of fluorescence in patient 8 was lower than the lesion size, but on inspection, the tumor had a significant area of necrosis (>80%); however, the viable areas demonstrated fluorescence with a strong association with areas of TTF-1 and CEACAM5 and a lack of CK 5/6 and p63 staining, indicating adenocarcinoma spectrum lesions. Similarly, CEACAM5 staining was associated with SGM-101 fluorescence emission in this cohort (eFigure 7 in Supplement 2). Four of 5 patients in this cohort had lesions deeper than 12 mm from the pleural surface, indicating a lack of *in vivo* fluorescence (1.2 cm in patient 7 vs 0.33 cm in patient 8). SGM-101 allowed the assessment of CEACAM5-positive nodules, margins, and normal tissue (eFigures 7-9 in Supplement 2). Malignant nodules with the highest antigenic concentration of CEACAM5, as demonstrated with immunohistochemical staining, had the highest fluorescence emission compared with the margin of the tumor and normal lung and distant normal lung. In addition, none of the lymph nodes examined during the procedures demonstrated fluorescence, which was concordant with final pathology demonstrating the absence of lymphatic metastases.

Discussion

Intraoperative molecular imaging-guided resections have been increasingly added to the armamentarium of solid organ malignant neoplasm resections. However, malignant tumors, particularly in the lung, are heterogonous, which requires exploration of different cellular targeting agents. One such target we explored in this study was the CEACAM5 cell surface glycoprotein, which is expressed in various adenocarcinomas, including colon, rectum, pancreas, esophagogastric, and lung adenocarcinomas.[16] We hypothesized that SGM-101, which is an anti-CEACAM5 antibody-conjugated fluorochrome, will specifically fluorescently label CEACAM5-positive lung nodules. To our knowledge, this is the first study in the literature that explores CEACAM5 glycoprotein as a potential target in IMI-guided lung nodule resections.

The feasibility and applicability of IMI tracers rely significantly on the clinical utility and ability to use the product in practice daily. Although the CEACAM5 glycoprotein has been extensively studied and validated in the management of various gastrointestinal malignant neoplasms, the same cannot be said in lung cancer.[21,25] Literature reports[17,18,23,27,28] demonstrate variable expression of the glycoprotein in lung cancer, and significant geographic variables are associated with the data. Therefore, we initially wanted to explore CEACAM5 as a potential target in our overall patient population.

Twenty-two of 33 lung adenocarcinomas (67%) analyzed in our cohort demonstrated CEACAM5 expression by immunohistochemistry, and glycoprotein expression was largely detected in the tumor core itself rather than adjacent normal tissue, which is significant in developing targeted tracers to avoid false positivity (eFigures 1 and 2 and eTable 1 in Supplement 2). Analysis of a large national cancer database similarly demonstrated NSCLC to have a high messenger RNA expression of CEACAM5 compared with normal and in line with pancreatic, gastric, and esophageal cancers for which glycoprotein is an established clinical diagnostic and prognostic marker (eFigure 3 in Supplement 2).[16,29] In addition, although the sample size was small, higher CEACAM5 expression was noted in higher-stage disease.

In the control group of patients with metastatic pulmonary nodules, SGM-101 allowed for the *in vivo* and *ex vivo* localization of CEACAM5-positive tissues (eTable 6 in Supplement 2). Serum CEA levels had a good positive predictive value, but negative or normal values did not necessarily exclude fluorescence detection (Figure 1 and Figure 2). These results corroborate previous findings of SGM-101 and indicate the glycoprotein targeting and specificity of the antibody fluorochrome conjugate, which does not change behavior in the pulmonary parenchyma.[30] The CEACAM5 expression levels at index primary lesion resection also appear to be correlated with metastatic CEACAM5 expression, which can further inform thoracic surgeons about the feasibility of using SGM-101 during metastasectomy.

With the observation that lung parenchyma does not hinder SGM-101's ability to penetrate pulmonary parenchyma, we explored NIR tracer lesion labeling in patients with pulmonary nodules suggestive of disease. It is our routine institutional practice not to perform diagnostic biopsy for patients with lesions concerning for primary lung cancer and unlike the control cohort did not have preoperative CEACAM5 or diagnosis status. Nevertheless, none of the 2 patients with benign tumors had any fluorescence *in vivo*, *ex vivo*, or in histologic assessment. This finding was associated with a lack of CEACAM5, TTF-1, CK 5/6, p63, and Ki-67 staining (Figure 3 and Figure 4).

Conversely, patients with strong CEACAM5 expression demonstrated fluorescence similar to that of the control group. SGM-101 could be detected in *ex vivo* analysis colocalized with CEACAM5 staining. Tumors with no CEACAM5 expression as predicted did not demonstrate any fluorescence in any setting. Unlike the control group, most lesions were smaller than 0.75 cm and tended to be deeper in the pulmonary parenchyma. The depth of lesion localization is a known challenge for NIR tracers and correlates with the emission

wavelength of the target fluorochrome. With the increasing developments of new fluorochromes that operate in the NIR-II range (>1000 nm), it is expected that deeper parenchyma in solid organ malignant neoplasms can be explored. We demonstrated that the targeted antibody in SGM-101 is highly specific and can potentially be conjugated to a different validated fluorochrome once NIR-II tracers become accessible.

LIMITATIONS

There are several limitations that need to be addressed in this proof-of-principle study. The sample size in each arm of the study was small, with a total of 9 patients with 14 total lesions undergoing SGM-101-guided resection. Larger clinical phase 2 and 3 randomized controlled studies are needed to discern the benefit of SGM-101 in IMI-guided lung cancer resections. In addition, in this early exploratory cohort, the selection of patients with positive serum CEA levels and/or preoperative biopsy with CEACAM5 immunohistochemical assessment can identify optimal patients who would benefit from SGM-101. Ideal patients who could benefit would be those with lesions greater than 1 cm that are closer to the pleural surface. Although the tracer adds additional cost to surgical care, potential benefits can be derived from SGM-101-guided resections. In optimally selected patients, the NIR tracer can confirm the detection of primary tumors, assess margins, and potentially identify occult lesions that would otherwise be missed by conventional means. These benefits would also facilitate surgery progression in cases of lesion fluorescence because the surgeon would not have to wait for frozen section confirmation, which can take up to 1 hour in certain facilities, therefore decreasing the time the patient is under anesthesia and operating room costs. Additional trials with larger cohorts can address these claims and challenges.

Conclusions

This proof-of-principle, phase 1 nonrandomized controlled trial demonstrates that the CEACAM5- targeted NIR tracer SGM-101 can detect CEACAM5 glycoprotein-positive lung tumors. Ideal patients are those with lesions larger than 1.0 cm who are CEACAM5 positive or patients with positive serum CEA levels. Additional, larger-scale trials are needed to validate the study findings, but the current results demonstrate that CEACAM5 surface glycoprotein targeting is a feasible target with clinical utility.

REFERENCES

1 Torre LA, Siegel RL, Jemal A. Lung cancer statistics. Adv Exp Med Biol. 2016;893:1-19. doi:10.1007/978-3-319- 24223-1_1

2 Young RP, Hopkins RJ. Measures of outcome in lung cancer screening: maximising the benefits. J Thorac Dis. 2016;8(10):E1317-E1320. doi:10.21037/jtd.2016.10.49

3 Owen D, Chaft JE. Immunotherapy in surgically resectable non-small cell lung cancer. J Thorac Dis. 2018; 10(suppl 3):S404-S411. doi:10.21037/jtd.2017.12.93

4 Montagne F, Guisier F, Venissac N, Baste J-M. The role of surgery in lung cancer treatment: present indications and future perspectives-state of the art. Cancers (Basel). 2021;13(15):3711. doi:10.3390/cancers13153711

5 Hirsch FR, Scagliotti GV, Mulshine JL, *et al.* Lung cancer: current therapies and new targeted treatments. Lancet. 2017;389(10066):299-311. doi:10.1016/S0140-6736(16)30958-8

6 Masai K, Sakurai H, Sukeda A, *et al.* Prognostic impact of margin distance and tumor spread through air spaces in limited resection for primary lung cancer. J Thorac Oncol. 2017;12(12):1788-1797. doi:10.1016/j.jtho.2017.08.015

7 Azari F, Kennedy G, Singhal S. Intraoperative detection and assessment of lung nodules. Surg Oncol Clin N Am. 2020;29(4):525-541. doi:10.1016/j.soc.2020.06.006

8 Azari F, Kennedy G, Bernstein E, *et al.* Intraoperative molecular imaging clinical trials: a review of 2020 conference proceedings. J Biomed Opt. 2021;26(5):050901. doi:10.1117/1.JBO.26.5.050901

9 Kennedy GT, Azari FS, Bernstein E, *et al.* Targeted intraoperative molecular imaging for localizing nonpalpable tumors and quantifying resection margin distances. JAMA Surg. 2021;156(11):1043-1050. doi:10.1001/jamasurg. 2021.3757

10 Hadjipanayis CG, Stummer W. 5-ALA and FDA approval for glioma surgery. J Neurooncol. 2019;141(3): 479-486. doi:10.1007/s11060-019-03098-y

11 Azari F, Kennedy GT, Zhang K, *et al.* Impact of intraoperative molecular imaging after fluorescent-guided pulmonary metastasectomy for sarcoma. J Am Coll Surg. 2022;234(5):748-758. doi:10.1097/XCS.0000000000000132

12 Lee JYK, Cho SS, Stummer W, *et al.* Review of clinical trials in intraoperative molecular imaging during cancer surgery. J Biomed Opt. 2019;24(12):1-8. doi:10.1117/1.JBO.24.12.120901

13 Randall LM, Wenham RM, Low PS, Dowdy SC, Tanyi JL. A phase II, multicenter, open-label trial of OTL38 injection for the intra-operative imaging of folate receptor-alpha positive ovarian cancer. Gynecol Oncol. 2019;155 (1):63-68. doi:10.1016/j.ygyno.2019.07.010

14 Zeh R, Sheikh S, Xia L, *et al.* The second window ICG technique demonstrates a broad plateau period for near infrared fluorescence tumor contrast in glioblastoma. PLoS One. 2017;12(7):e0182034. doi:10.1371/journal.pone. 0182034

15 Azari F, Kennedy G, Zhang K, *et al.* Effects of light-absorbing carbons in intraoperative molecular imaging- guided lung cancer resections. Mol Imaging Biol. Published online March 15, 2022. doi:10.1007/s11307-021- 01699-6

16 Blumenthal RD, Leon E, Hansen HJ, Goldenberg DM. Expression patterns of CEACAM5 and CEACAM6 in primary and metastatic cancers. BMC Cancer. 2007;7:2. doi:10.1186/1471-2407-7-2

17 Gao Y, Song P, Li H, Jia H, Zhang B. Elevated serum CEA levels are associated with the explosive progression of lung adenocarcinoma harboring EGFR mutations. BMC Cancer. 2017;17(1):484. doi:10.1186/s12885-017-3474-3

18 Klaile E, Klassert TE, Scheffrahn I, *et al.* Carcinoembryonic antigen (CEA)-related cell adhesion molecules are co-expressed in the human lung and their expression can be modulated in bronchial epithelial cells by non-typable Haemophilus influenzae, Moraxella catarrhalis, TLR3, and type I and II interferons. Respir Res. 2013;14(1):85. doi: 10.1186/1465-9921-14-85

19 Muley T, Dienemann H, Herth FJF, Thomas M, Meister M, Schneider J. Combination of mesothelin and CEA significantly improves the differentiation between malignant pleural mesothelioma, benign asbestos disease, and lung cancer. J Thorac Oncol. 2013;8(7):947-951. doi:10.1097/JTO.0b013e31828f696b

20 Arrieta O, Villarreal-Garza C, Martínez-Barrera L, *et al.* Usefulness of serum carcinoembryonic antigen (CEA) in evaluating response to chemotherapy in patients with advanced non small-cell lung cancer: a prospective cohort study. BMC Cancer. 2013;13:254. doi:10.1186/1471-2407-13-254

21 de Valk KS, Deken MM, Schaap DP, *et al.* Dose-finding study of a CEA-targeting agent, SGM-101, for intraoperative fluorescence imaging of colorectal cancer. Ann Surg Oncol. 2021;28(3):1832-1844. doi:10.1245/ s10434-020-09069-2

22 Zheng J, Ye X, Liu Y, Zhao Y, He M, Xiao H. The combination of CTCs and CEA can help guide the management of patients with SPNs suspected of being lung cancer. BMC Cancer. 2020;20(1):106. doi:10.1186/s12885-020- 6524-1

23 Huo YR, Glenn D, Liauw W, Power M, Zhao J, Morris DL. Evaluation of carcinoembryonic antigen (CEA) density as a prognostic factor for percutaneous ablation of pulmonary colorectal metastases. Eur Radiol. 2017;27(1):128-137. doi:10.1007/s00330-016-4352-0

24 Boogerd LSF, Hoogstins CES, Schaap DP, *et al*. Safety and effectiveness of SGM-101, a fluorescent antibody targeting carcinoembryonic antigen, for intraoperative detection of colorectal cancer: a dose-escalation pilot study. Lancet Gastroenterol Hepatol. 2018;3(3):181-191. doi:10.1016/S2468-1253(17)30395-3
25 Gutowski M, Framery B, Boonstra MC, *et al*. SGM-101: An innovative near-infrared dye-antibody conjugate that targets CEA for fluorescence-guided surgery. Surg Oncol. 2017;26(2):153-162. doi:10.1016/j.suronc.2017.03.002
26 Hoogstins CES, Boogerd LSF, Sibinga Mulder BG, *et al*. Image-guided surgery in patients with pancreatic cancer: first results of a clinical trial using SGM-101, a novel carcinoembryonic antigen-targeting, near-infrared fluorescent agent. Ann Surg Oncol. 2018;25(11):3350-3357. doi:10.1245/s10434-018-6655-7
27 Triphuridet N, Vidhyarkorn S, Worakitsitisatorn A, *et al*. Screening values of carcinoembryonic antigen and cytokeratin 19 fragment for lung cancer in combination with low-dose computed tomography in high-risk populations: Initial and 2-year screening outcomes. Lung Cancer. 2018;122:243-248. doi:10.1016/j.lungcan.2018. 05.012
28 Yang Y, Xu M, Huang H, *et al*. Serum carcinoembryonic antigen elevation in benign lung diseases. Sci Rep. 2021;11(1):19044. doi:10.1038/s41598-021-98513-8
29 Cerami E, Gao J, Dogrusoz U, *et al*. The cBio cancer genomics portal: an open platform for exploring multidimensional cancer genomics data. Cancer Discov. 2012;2(5):401-404. doi:10.1158/2159-8290.CD-12-0095
30 Azari F, Kennedy GT, Chang A, *et al*. Glycoprotein receptor CEACAM5-targeted intraoperative molecular imaging tracer in non-small cell lung cancer. Ann Thorac Surg. 2022;S0003-4975(22)00731-7. doi:10.1016/j. athoracsur.2022.05.019

PART 3

NEW WAYS FOR IDENTIFICATION OF NOVEL TARGETS FOR NIR FLUORESCENCE IMAGING

CHAPTER X

DATA-DRIVEN IDENTIFICATION OF TARGETS FOR FLUORESCENCE-GUIDED SURGERY IN NON-SMALL CELL LUNG CANCER

Ruben P. J. Meijer*, Lisanne K. A. Neijenhuis*, Annette P. Zeilstra, Sophie F. Roerink, Shadhvi S. Bhairosingh, Denise E. Hilling, J. Sven D. Mieog, Peter J. K. Kuppen, Cornelis F. M. Sier, Jerry Braun, Jacobus Burggraaf, Alexander L. Vahrmeijer, Danielle Cohen, Merlijn Hutteman

**Both authors contributed equally to the manuscript*

Mol Imaging Biol. 2023 Feb;25(1):228-239

Abstract

PURPOSE Intraoperative identification of lung tumors can be challenging. Tumor-targeted fluorescence-guided surgery can provide surgeons with a tool for real-time intraoperative tumor detection. This study evaluated cell surface biomarkers, partially selected via data-driven selection software, as potential targets for fluorescence-guided surgery in non-small cell lung cancers: adenocarcinomas (ADC), adenocarcinomas in situ (AIS), and squamous cell carcinomas (SCC).

PROCEDURES Formalin-fixed paraffin-embedded tissue slides of resection specimens from 15 patients with ADC and 15 patients with SCC were used and compared to healthy tissue. Molecular targets were selected based on two strategies: (1) a data-driven selection using > 275 multi-omics databases, literature, and experimental evidence; and (2) the availability of a fluorescent targeting ligand in advanced stages of clinical development. The selected targets were carbonic anhydrase 9 (CAIX), collagen type XVII alpha 1 chain (COLLAGEN XVII), glucose transporter 1 (GLUT-1), G protein-coupled receptor 87 (GPR87), transmembrane protease serine 4 (TMPRSS4), carcinoembryonic antigen (CEA), epithelial cell adhesion molecule (EPCAM), folate receptor alpha (FRα), integrin αvβ6 (αVβ6), and urokinase-type plasminogen activator receptor (UPAR). Tumor expression of these targets was assessed by immunohistochemical staining. A total immunostaining score (TIS, range 0–12), combining the percentage and intensity of stained cells, was calculated. The most promising targets in ADC were explored in six AIS tissue slides to explore its potential in non-palpable lesions.

RESULTS Statistically significant differences in TIS between healthy lung and tumor tissue for ADC samples were found for CEA, EPCAM, FRα, αVβ6, CAIX, COLLAGEN XVII, GLUT-1, and TMPRSS4, and of these, CEA, CAIX, and COLLAGEN XVII were also found in AIS. For SCC, EPCAM, UPAR, CAIX, COLLAGEN XVII, and GLUT-1 were found to be overexpressed.

CONCLUSIONS EPCAM, CAIX, and COLLAGEN XVII were identified using concomitant use of data-driven selection software and clinical evidence as promising targets for intraoperative fluorescence imaging for both major subtypes of non-small cell lung carcinomas.

Introduction

Non-small cell lung cancer (NSCLC) is the leading cause of cancer-related deaths worldwide.[1] Most NSCLC patients are diagnosed with disseminated disease, leaving only palliative treatment options. Therefore, much attention is given to screening programs to identify patients with early-stage tumors.[2-4] This may change the treatment options for instance by lung parenchyma sparing resections, potentially resulting in more residual lung tissue and better postoperative lung function.

Although lung parenchyma sparing resections (e.g., segmentectomies), as treatment of small-sized pulmonary nodules, have good clinical outcomes in terms of disease-free and overall survival, these may be technically difficult, particularly for small nodules.[5-7] Especially adenocarcinomas in situ (AIS) are difficult to identify as they are barely palpable. In addition, more lung resections are performed minimally invasive, using video-assisted thoracoscopic surgery (VATS) or robotic-assisted thoracoscopic surgery (RATS), and the diminished or absent tactile feedback increases the risk of missing synchronous local metastases.[8,9] Also, in patients with more advanced tumor stages, there may be challenges albeit from a different nature. Namely, tumor-positive resection margins are found at histopathologic assessment in 20% of the patients with T3 or T4 lung cancer,[10,11] which negatively affect prognosis and approximately halves the 5-year survival rate.[11-13] Moreover, up to 60% of patients develop a recurrence despite curatively intended surgeries of early-stage NSCLC.[14-16] It is hypothesized that a significant portion of these local recurrences is explained by occult local metastases that are already present during primary surgery. Tumor-targeted fluorescence-guided surgery has the potential to overcome several of these challenges.

Near-infrared (NIR) fluorescence imaging is a real-time imaging technique, which requires a dedicated camera system and a fluorescent agent.[17] These agents can be divided into two groups: non-targeted and targeted, binding to a specific ligand, which is upregulated in tumor cells or activated by the tumor-specific environment. Light in the NIR spectrum (700–900 nm) has better depth penetration, up to 10 mm, compared to visible light. Moreover, this light is invisible to the human eye and will thereby not interfere with the standard surgical field.[18] The potentially added value of tumor-targeted fluorescence imaging in lung parenchyma sparing resections of NSCLC is threefold: detection of the surgical target, identification of synchronous additional, mostly small malignant lesions, and reduction of tumor-positive resection margins.

Optimal target characteristics for fluorescence-guided surgery include target localization on the cell membrane, evenly distribution throughout the tumor tissue, low expression in surrounding normal tissue, and upregulation in a majority percentage of patients.[19] Potential targets are often identified by reviewing key publications from recent literature. Currently, a data-driven selection method is available that combines multiple databases and interlinks literature. It provides researchers with unique insights and has the potential to dramatically reduce the time required compared to a conventional literature search. This study aims to identify potentially suitable targets for fluorescence-guided surgery in NSCLC, both using conventional strategies, and with the use of a data-driven selection platform, combining public data on gene expression and protein localization.

Material and methods

PATIENTS

Formalin-fixed paraffin-embedded tissue blocks from 30 patients (15 adenocarcinomas (ADC) and 15 squamous cell carcinomas (SCC)) who underwent surgical resection of a primary NSCLC between 2000 and 2017 and without previous neoadjuvant therapy were randomly selected from the Department of Pathology, Leiden University Medical Center (LUMC), the Netherlands. Medical records and pathology reports were retrospectively reviewed. A board-certified pathologist (DC) reviewed all tissue samples before inclusion in the study. After analysis of the immunohistochemistry (IHC) staining results of the ADC and SCC slides, additional analysis on a random selection of 6 AIS was performed. AIS tissue slides were stained for the most promising targets, based on the immunostaining results in ADC.

Tissue samples were used in accordance with the code for secondary use of human tissue as prescribed by the Dutch Federation of Medical Scientific Societies, which does not require additional informed consent. The study was approved by the Institutional Ethics Review Board of the Leiden University Medical Center (Leiden, The Netherlands).

TARGET SELECTION

In this study, a selection of ten potential targets was chosen based on two different strategies. The first 5 targets were chosen after an unbiased search using data-driven selection software (Euretos, Utrecht, the Netherlands) integrating more than 275 multi-omics databases along with literature and experimental evidence. This data-driven selection platform compares the RNA expression of genes between different types of tissues. In our search, we compared RNA expression in lung cancer to healthy lung and lymph node tissue. RNA expression data on primary NSCLC were derived from the TCGA-LUAD and TCGA-LUSC datasets.[20,21] Expression data on healthy lymph node tissue and healthy lung tissue was derived from the GTEX-project.[22] All expression values were normalized to transcripts per million (TPM), which is the most effective normalization in reducing non-biological variability in transcriptomic data.[23] To predict whether encoded proteins are present on the cell surface, we explored presence in the experimentally derived cell surface protein atlas (CSPA)[24] or bioinformatically predicted sets of cell surface proteins.[25,26] We performed an exhaustive search for targets by applying the following criteria: (1) median expression in tumor exceeding expression in the healthy lung or lymph nodes and (2) surface expression predicted or experimentally confirmed. The different proteins for ADC (56 results) and SCC (114 results) were presented with multiple parameters per gene. A log2- fold change of tumor vs normal tissue was calculated by converting the TPM-values to log2-values and analyzed with the limma-package in R.[27] Log2-fold changes were then obtained from the topTable-function. From this gene list, only genes that are abundantly expressed in both ADC and SCC but minimally in healthy lung tissue or lymph nodes were included, resulting in a set of 30 genes. The five genes with the highest log2-fold change of tumor in comparison to normal were then selected for immunohistochemical analysis: carbonic anhydrase 9 (CAIX), collagen type XVII alpha 1 chain (COLLAGEN XVII), glucose transporter 1 (GLUT-1), G protein-coupled receptor 87 (GPR87), and transmembrane protease serine 4 (TMPRSS4).

In addition to the data-driven selection-derived targets, 5 targets were included, based on the availability of a fluorescent targeting ligand in advanced stages of clinical development for the detection of various cancer types: carcinoembryonic antigen (CEA), epithelial cell adhesion molecule (EPCAM), folate receptor alpha (FRα), integrin αvβ6 (αVβ6), and urokinase-type plasminogen activator receptor (UPAR).

IMMUNOHISTOCHEMISTRY STAINING

Formalin-fixed and paraffin-embedded tissue blocks were cut in sections with a thickness of 4 µm and mounted on adhesive Starfrost slides (Waldemar Knittel Glasbearbeitungs GmbH, Braunschweig, Germany). Subsequently, the slides were deparaffinized with xylene and rehydrated in decreasing concentrations

of diluted ethanol (100%, 70%, and 50%). Then slides were rinsed with demineralized water, and endogenous peroxidase was blocked with 0.3% hydrogen peroxide (Merck Millipore, Darmstadt, Germany) for 20 min at room temperature. The method used for antigen retrieval was dependent on the protocol of the antibody (Supplementary Table 1). Antigen retrieval for uPAR, CEA, FRα, GLUT-1, CAIX, COLLAGEN XVII, and GPR87 was performed by heat induction at 95 °C during 10 min using PT Link (Dako) with low-pH (pH 6.0). For TMPRSS4, PT Link with high-pH (pH 9.0) was used. For αVβ6, antigen retrieval was performed with 0.4% pepsin at 37 °C using a water bath for 10 min, and for EPCAM, trypsin was used during 20 min. The sections were incubated overnight at room temperature with primary antibody (diluted in 1% BSA/PBS). The negative control was incubated with 1% BSA/PBS. Tumor sections known to express the target(s) were used as positive controls. The slides were washed with PBS followed by incubation with HRP-labelled secondary antibody (either anti-mouse or anti-rabbit (both Dako)) for 30 min at room temperature. For staining, DAB substrate was applied for 10 min, and for counterstaining, hematoxylin (VWR international, Amsterdam, the Netherlands) was applied for 15 s. Lastly, the tissue sections were dehydrated at 37 °C for 60 min and mounted in Pertex (Histolab, Askim, Sweden).

IMMUNOHISTOCHEMISTRY STAINING SCORING

Two authors (AZ and DC) evaluated the stained slides independently. In case of discrepancy, rescoring was done until consensus was achieved. Total immunostaining score (TIS) was used for tumor and normal tissue. TIS is the mathematical product of a proportion score (PS) and an intensity score (IS) with a maximum score of 12. The PS describes the estimated fraction of positively stained tumor cells (0 = none, 1 = < 10%, 2 = 10-50%, 3 = 51-80%, 4 = > 80%), and the IS represents the estimated staining intensity (0 = no staining, 1 = weak, 2 = moderate, 3 = strong). The calculated TIS was then defined as no expression (0), weak expression (1-4), moderate expression (6-8), or intense (9-12) expression.

STATISTICAL ANALYSIS

For statistical analysis, IBM SPSS Statistics version 25 (IBM Corp., Armonk, NY, USA) and GraphPad Prism 6 (GraphPad Software Inc., La Jolla, CA, USA) were used. Paired differences in expression level between normal and tumor tissue were calculated using the Wilcoxon signed rank test. Test results were considered statistically significant at the level of $p < 0.05$.

Results

Patient and tumor characteristics are summarized in Table 1. Histological subtyping showed heterogeneity within the ADC group; all SCC samples were non-keratinizing tumors. Representative images of tissue samples are presented in figure 1 (ADC), figure 2 (AIS), and figure 3 (SCC). In the case of tumor-positive staining, a predominant cell membrane pattern was seen in both ADC and SCC for CEA, EPCAM, FRα, αVβ6, CAIX, COLLAGEN XVII, GLUT-1, and GPR87. The staining pattern of uPAR was dominant in the extracellular matrix, whereas TMPRSS4 showed positive staining for both the cell membrane as the extracellular matrix.

TABLE 1 Patient and tumor characteristics.

Characteristics	ADC (n=15)	AIS (n=6)	SCC (n=15)
Age at surgery median years (range)	69 (53-79)	65.5 (47-72)	66 (57-78)
Gender			
Male	9	2	11
Female	6	4	4
Tumor size (cm) median (range)	2.9 (1.2-5.2)	1.3 (0.6-2.6)	4.2 (1.8-8.2)
Histological subtype			
Acinar	9		
Lepidic	6	6	
Mucinous	2		
Micropapillary	3		
Papillary	4		
Solid	5		
Keratinized			0
Non-keratinized			15
TNM staging			
Tumour stage (T)			
1	5	5	5
2	7	0	4
3	1	0	3
4	2	1	3
Nodal stage (N)			
0	13	6	10
1	2	0	5
2	0	0	0
3	0	0	0
Metastatic stage (M)			
0	15	6	14
1	0	0	1

Abbreviations: ADC Adenocarcinoma, AIS adenocarcinoma in situ, SCC Squamous Cell Carcinoma, cm centimeter

ADENOCARCINOMA

Based on the TIS, normal tissue had low (no to weak) expression in all of the samples for CEA, EPCAM, FRα, UPAR, COLLAGEN XVII, GLUT-1, and GPR87, whereas 86.7% of the samples were low for CAIX (figure 4, Supplementary Table 2). Tumor tissue showed high expression (moderate to intense) in 100% of the samples for TMPRSS4 and in 93.3% for αVβ6, CAIX, and COLLAGEN XVII. Matched sampling using the Wilcoxon-signed rank test showed significantly higher expression in the tumor compared to the adjacent normal lung tissue for CEA, EPCAM, FRα, αVβ6, CAIX, COLLAGEN XVII, GLUT-1, and TMPRSS4 (respectively p = 0.003, 0.003, 0.005, 0.006, 0.001, 0.000, 0.007, and 0.035; figure 5). No significant difference in staining intensity was found for UPAR and GPR87 (both p = 0.066). Multiple samples showed CAIX and COLLAGEN XVII expression in necrotic tumor fields. The UPAR staining pattern for all samples was dominant in stromal tissue, as was staining GLUT-1 in erythrocytes and nerve sheath branches and for TMPRSS4 in lung epithelium.

FIGURE 1 Representative slides of adenocarcinoma cases stained for different markers.
A representative lung tumor sample (first row), detailed tumor sample (second row), and detailed normal lung tissue (third row) are shown for each marker. The area of the detailed tumor staining is indicated with a rectangle in the tumor overview. The black bar represents 1 mm in the overview pictures and 100 µm in the detailed pictures.

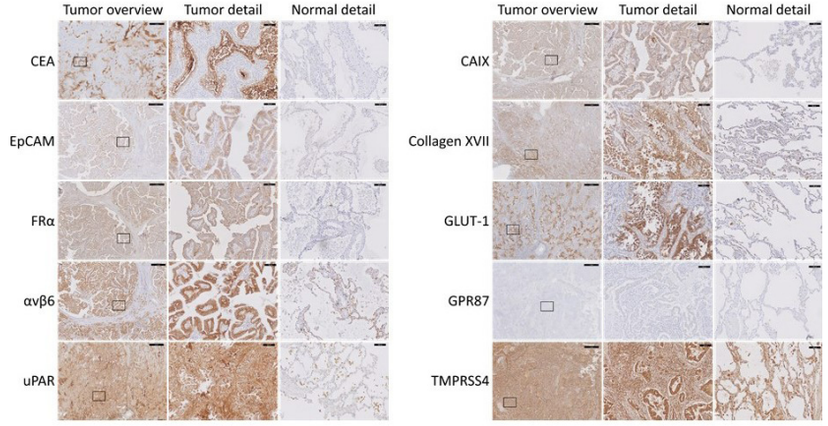

Abbreviations: CEA, carcinoembryonic antigen; EPCAM, epithelial cell adhesion molecule; FRα, folate receptor alpha; αVβ6, integrin αvβ6; UPAR, urokinase-type plasminogen activator receptor; CAIX, carbonic anhydrase 9; COLLAGEN XVII, collagen type XVII alpha 1 chain; GLUT-1, glucose transporter 1; GPR87, G protein-coupled receptor 87; TMPRSS4, transmembrane protease serine 4.

FIGURE 2 Representative slides of adenocarcinoma in situ cases stained for different markers.
A representative lung tumor sample (first row), detailed tumor sample (second row), and detailed normal lung tissue (third row) are shown for each marker. The area of the detailed tumor staining is indicated with a rectangle in the tumor overview. The black bar represents 1 mm in the overview pictures and 100 µm in the detailed pictures.

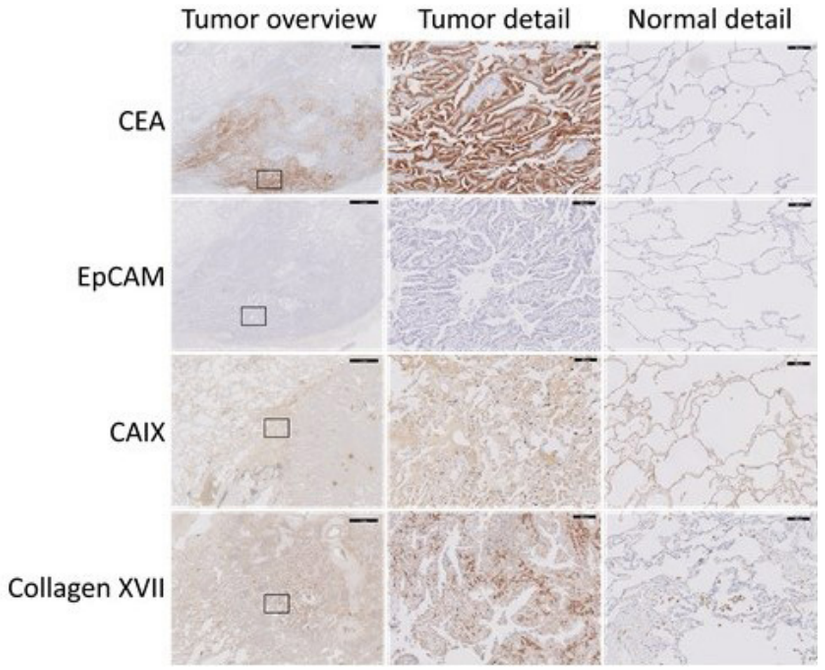

Abbreviations: CEA, carcinoembryonic antigen; EPCAM, epithelial cell adhesion molecule; CAIX, carbonic anhydrase 9; COLLAGEN XVII, collagen type XVII alpha 1 chain.

FIGURE 3 Representative slides of squamous cell carcinoma cases stained for different markers.

A representative lung tumor sample (first row), detailed tumor sample (second row), and detailed normal lung tissue (third row) are shown for each marker. The area of the detailed tumor staining is indicated with a rectangle in the tumor overview. The black bar represents 1 mm in the overview pictures and 100 µm in the detailed pictures.

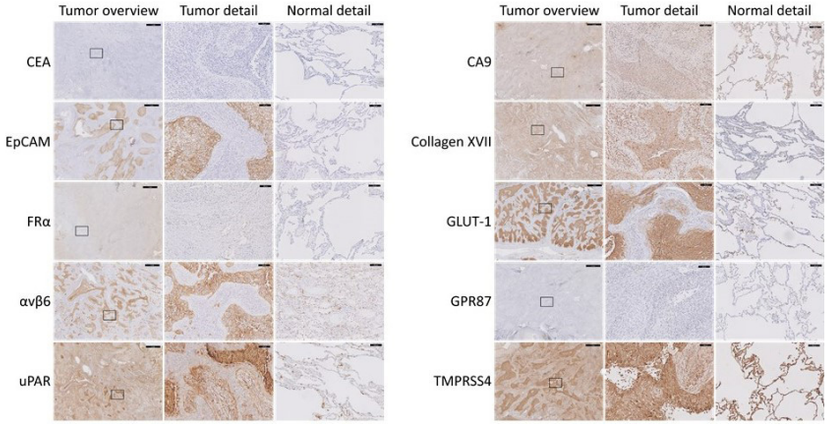

Abbreviations: CEA, carcinoembryonic antigen; EPCAM, epithelial cell adhesion molecule; FRα, folate receptor alpha; αVβ6, integrin αvβ6; UPAR, urokinase-type plasmino- gen activator receptor; CAIX, carbonic anhydrase 9; COLLAGEN XVII, collagen type XVII alpha 1 chain; GLUT-1, glucose transporter 1; GPR87, G protein-coupled receptor 87; TMPRSS4, transmembrane protease serine 4.

FIGURE 4 Target expression in adenocarcinomas.

This figure shows per target the percentage of adenocarcinoma tissue slides and healthy tissue slides that had high target expression with IHC staining. High expression was defined as a total immunostaining score of 6 or higher. The TIS is a product of a proportion score (0 = none, 1 = < 10%, 2 = 10-50%, 3 = 51-80%, 4 = > 80%) and intensity score (0 = no staining, 1 = weak, 2 = moderate, 3 = strong). Abbreviations: TIS, total immunostaining score; CEA, carcinoembryonic antigen; EPCAM, epithelial cell adhesion molecule; FRα, folate receptor alpha; αVβ6, integrin αvβ6; UPAR, urokinase-type plasminogen activator receptor; CAIX, carbonic anhydrase 9; COLLAGEN XVII, collagen type XVII alpha 1 chain; GLUT-1, glucose transporter 1; GPR87, G protein-coupled receptor 87; TMPRSS4, transmembrane protease serine 4.

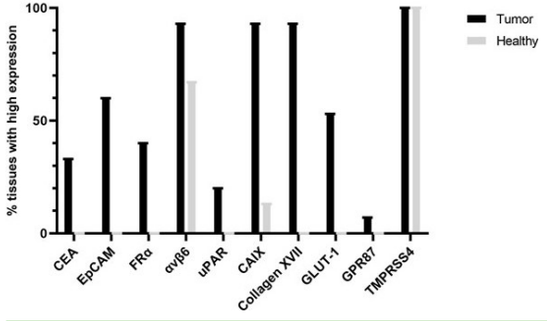

FIGURE 5 Target expression of adjacent normal lung compared to adeno-carcinoma tissue.

Shown are the total immunostaining scores of the normal lung and tumor tissue in adenocarcinomas, per patient and per biomarker. The horizontal line indicates the median TIS.

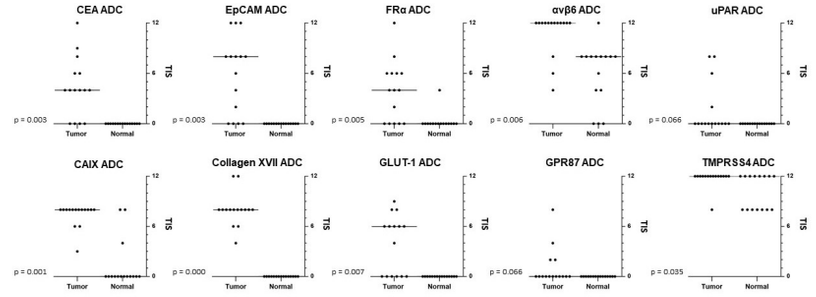

Abbreviations: CEA, carcinoembryonic antigen; EPCAM, epithelial cell adhesion molecule; FRα, folate receptor alpha; αVβ6, integrin αvβ6; UPAR, urokinase-type plasminogen activator receptor; CAIX, carbonic anhydrase 9; COLLAGEN XVII, collagen type XVII alpha 1 chain; GLUT-1, glucose transporter 1; GPR87, G protein-coupled receptor 87; TMPRSS4, transmembrane protease serine 4.

FIGURE 6 Target expression in adenocarcinomas in situ.

This figure shows per target the percentage of adenocarcinoma in situ tissue slides and healthy tissue slides that had high target expression with IHC staining. High expression was defined as a total immunostaining score of 6 or higher. The TIS is a product of a proportion score (0 = no staining, 1 = weak, 2 = moderate, 3 = strong).

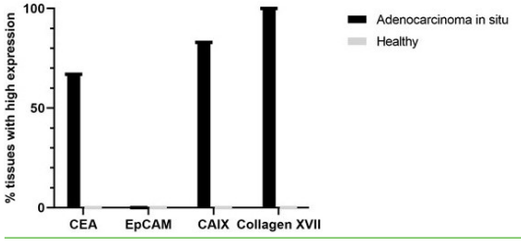

Abbreviations: TIS, total immunostaining score; CEA, carcinoembryonic antigen; EPCAM, epithelial cell adhesion molecule; CAIX, carbonic anhydrase 9; COLLAGEN XVII, collagen type XVII alpha 1 chain.

FIGURE 7 Target expression of adjacent normal lung compared to adenocarcinoma in situ tissue.
Shown are the total immunostaining scores of the normal lung and adenocarcinoma in situ tissue, per patient and per biomarker. The horizontal line indicates the median TIS.

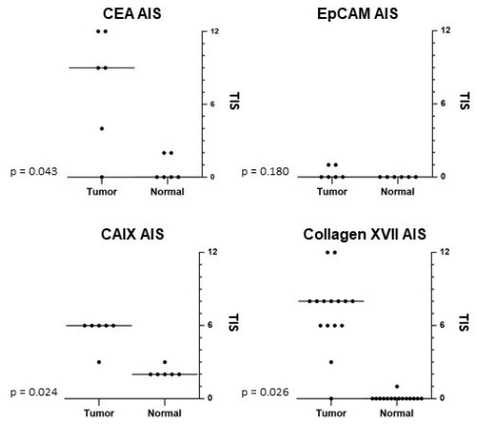

Abbreviations: CEA, carcinoembryonic antigen; EPCAM, epithelial cell adhesion molecule; CAIX, carbonic anhydrase 9; COLLAGEN XVII, collagen type XVII alpha 1 chain

FIGURE 8 Target expression in squamous cell carcinomas.
This figure shows per target the percentage of squamous cell carcinoma tissue slides and healthy tissue slides that had high target expression with IHC staining. High expression was defined as a total immunostaining score of 6 or higher. The TIS is a product of a proportion score (0 = none, 1 = < 10%, 2 = 10-50%, 3 = 51-80%, 4 = > 80%) and intensity score (0 = no staining, 1 = weak, 2 = moderate, 3 = strong).

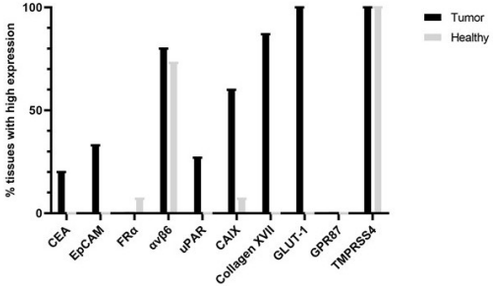

Abbreviations: TIS, total immunostaining score; CEA, carcinoembryonic antigen; EPCAM, epithelial cell adhesion molecule; FRα, folate receptor alpha; αVβ6, integrin αvβ6; UPAR, urokinase-type plasminogen activator receptor; CAIX, carbonic anhy- drase 9; COLLAGEN XVII, collagen type XVII alpha 1 chain; GLUT-1, glucose transporter 1; GPR87, G protein-coupled receptor 87; TMPRSS4, transmembrane protease serine 4.

FIGURE 9 Target expression of adjacent normal lung compared to squamous cell carcinoma tissue.
Shown are the total immunostaining scores of the normal lung and tumor tissue in squamous cell carcinomas, per patient and per biomarker. The horizontal line indicates the median TIS.

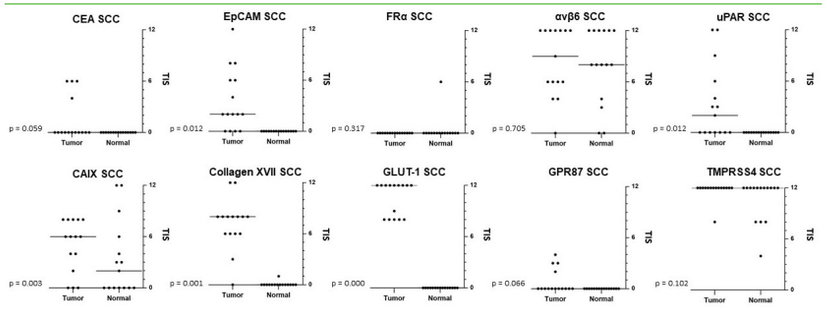

Abbreviations: CEA, carcinoembryonic antigen; EPCAM, epithelial cell adhesion molecule; FRα, folate receptor alpha; αVβ6, integrin αvβ6; UPAR, urokinase-type plasminogen activator receptor; CAIX, carbonic anhydrase 9; COLLAGEN XVII, collagen type XVII alpha 1 chain; GLUT-1, glucose transporter 1; GPR87, G protein-coupled receptor 87; TMPRSS4, transmembrane protease serine 4 Adenocarcinoma in situ

ADENOCARCINOMA IN SITU

Since AIS in particular are barely palpable, 6 additional AIS were stained for the four most promising targets in ADC. Low target expression in normal lung tissue was seen for all CEA, EPCAM, CAIX, and COLLAGEN XVII samples (figure 6, Supplementary Table 3). Tumor expression was high in 66.7%, 0%, 83.3%, and 100% of the samples for respectively CEA, EPCAM, CAIX, and COLLAGEN XVII. Differences in staining intensity between AIS and healthy lung were significant for CEA, CAIX, and COLLAGEN XVII (respectively p = 0.043, 0.024, and 0.026) (figure 7). No statistical difference was found for EPCAM (p = 0.180).

SQUAMOUS CELL CARCINOMA

The TIS value for CEA, EPCAM, UPAR, COLLAGEN XVII, GLUT-1, and GPR87 was low in all normal tissue samples. Expression of FRα and CAIX was low in 93.3% of normal tissue samples (figure 8, Supplementary Table 4). A high TIS value in tumor tissue was seen in 100% of the samples for GLUT-1 and TMPRSS4 and in 86.7% of the samples for COLLAGEN XVII. Differences in staining intensity between tumor and healthy lung were significant for EPCAM, UPAR, CAIX, COLLAGEN XVII, and GLUT-1 (respectively p=0.003, 0.012, 0.003, 0.001, and 0.000; figure 9). No statistical difference was found for CEA, FRα, αVβ6, GPR87, and TMPRSS4 (respectively

p=0.059, 0.317, 0.705, 0.066, and 0.102). Necrotic tumor fields were positive for CEA, αVβ6, UPAR, and GLUT-1 in multiple samples. UPAR showed high expression in the stromal tissue of all samples. A substantial number of samples showed staining for GLUT-1 in erythrocytes and nerve sheath branches and TMPRSS4 in lung epithelium.

Discussion

A suitable molecular target for fluorescence-guided surgery (FGS) in NSCLC should be overexpressed in the tumor compared to adjacent normal lung tissue. As NSCLC comprises various subtypes, it would be beneficial if a potential agent is suitable for multiple types of NSCLC, hence overexpressed in ADC, AIC, and SCC.

In this study, ten cell surface targets in NSCLC were investigated with IHC staining to find a suitable target for tumor-targeted fluorescence imaging. Five targets were selected using an extensive multiomics database search using data-driven selection software, and those were compared with five targets chosen based on the availability of fluorescent targeting ligands in advanced stages of clinical development in other cancer types.

Following this strategy, EPCAM, CAIX, COLLAGEN XVII, and GLUT-1 are significantly overexpressed in both ADC and SCC. However, in contrast to EPCAM, CAIX, and COLLAGEN XVII, GLUT-1's high expression on erythrocytes makes it an unsuitable target for FGS as this will most likely provide high background fluorescence. Resulting in a high false positive rate using fluorescence imaging during surgery. Even though the expression of GLUT-1 on erythrocytes has been described in previous publications, it was reported as a promising option after our data-driven selection.[28] This was not an error of the platform itself, but a consequence of an incomplete search strategy. To perform a search in the platform, you have to decide between which tissue types you want to compare RNA expression in genes. In our research, we chose to compare lung tumor tissue to normal lung and lymph node tissue. Besides tumor tissue and normal lung tissue, this data-driven selection did not include target expression in other cell types present in the healthy lung (e.g., blood). This emphasizes the importance of a relevant and complete research question before starting a search.

Data-driven selection software identified 2 out of the 3 most promising targets (CAIX and COLLAGEN XVII).

EPCAM, chosen based on our institution's experience in colorectal cancer, was also identified as a potential target for ADC in the initial results of the data-driven selection software. Due to the absence in the SCC results and, according to the data-driven selection, the relatively high expression on normal lung tissue, it was excluded in the final selection. These conflicting results between the results of the data-driven selection and IHC demonstrate the value of IHC confirmation of the data-driven selection. It must be stated that data-driven selection software is a discovery tool and can therefore be beneficial to discover new targets, but cannot replace current validation tools as IHC. A possible explanation for the difference between the results of the data-driven selection and IHC could be that the data-driven selection platform uses RNA expression of genes, and this does not always correspond to the protein expression of genes.

Not only suitable targets for fluorescence imaging in invasive ADC and SCC were assessed, but also for AIS. Significantly overexpressed targets in AIS are CEA, CAIX, and COLLAGEN XVII. Preferably, a target is used that is overexpressed in all types of lung cancer (ADC, SCC, and AIS); therefore, CAIX and COLLAGEN XVII are the most favorable targets, given the results in ADC (including early stage) and SCC. CEA and CAIX had similar expression in ADC and AIS; EPCAM was not expressed in AIS samples, while 60% of ADC samples had high expression of EPCAM. This might be due to the fact that EPCAM is involved in tumor initiation and tumor cell invasion.[29] A difference in target expression between carcinoma in situ and invasive carcinoma has been described previously.[30]

NSCLC is genetically and phenotypically known to be highly heterogenic, both across individuals as well as within individual tumors.[31,32] Therefore, it is not remarkable that none of the targets had a perfect score concerning higher expression in the tumor compared to normal lung tissue. To counteract this heterogeneity, we expect the long-term clinical application of this technology to include a tumor-tailored selection of different targets resulting in the use of multiple fluorescent agents in one patient.

OTL-38, targeting FRα, is the only tumor-targeting agent of which clinical results in NSCLC patients have been published. Intraoperative tumor detection using OTL-38 was successful in 81% of the ADC and 54% of the SCC. During back table imaging (*ex vivo*), fluorescence imaging with OTL-38 was able to visualize 100% of the ADC and 69% of the SCC.[33,34] Several studies have evaluated the expression of FRα in lung cancer. FRα was found to be expressed in 72-87% of the ADC and in 13-57% of the SCC.[35,36] Our study report supports these results in ADC and corroborates the finding of high variability in the expression of FRα in SCC tumor tissue. The IHC staining rates for FRα are lower as compared with fluorescence imaging rates with OTL-38 in tumor tissue. There is no explanation

for this difference. There has been suggested that IHC is only able to detect large differences in amounts of FRα molecules, while a smaller difference could be enough to discriminate normal from tumor tissue using fluorescence imaging.[37] However, this needs to be further confirmed with subsequent research.

Roughly, there are two methods for fluorescent agent administration: locally (e.g., topically and inhalation) or systemic (intravenously). CT-guided intraparenchymal injection of indocyanine green into lung tumors has been performed successfully in the past.[38] However, this is an invasive method and carries the risk for several complications, such as pulmonary hemorrhage or pneumothorax. In addition, this method can only be used to intraoperatively localize known tumors, as it cannot identify additional lesions. Inhalation of non-targeted contrast agents has been evaluated, but not yet in a clinical setting.[39] At present, most clinical and preclinical studies use intravenous administration of fluorescent agents. To use this administration route, it is important that there is blood flow to the tumor. Intravenous administration appears to be feasible in lung tumors, since it has been shown that these tumors even have increased blood flow.[40] This is supported by the observation that tumors were visible after the administration of the agent OTL-38 intravenously.

Currently, there are clinical trials recruiting lung cancer patients scheduled for resection aided by fluorescence-guided surgery. Among the fluorescent agents used in these studies are panitumumab-IRDye800 and IRDye800CW-nimotuzumab, both targeting the epidermal growth factor receptor (EGFR).[41,42] EGFR is upregulated in most cancer types and is a popular target for fluorescence-guided surgery, because of the clinical availability of EGFR antibodies. According to our search with the data-driven selection platform, the expression of EGFR in NSCLC is lower compared to our selected targets with the platform. However, we did show that IHC scorings in these targets were not always correlated to what was expected with the search. Another study, recruiting patients with different tumor types, including NSCLC, investigates ONM-100, a pH-activable fluorescent agent that does not bind to a target, but exploits the acid microenvironment of solid tumors.[43] Moreover, SGM-101, targeting CEA, is being investigated not only in primary lung cancer, but also in colorectal lung metastases.[44,45] A common endpoint in all these studies is the tumor-to-background ratio (TBR). This ratio of the mean fluorescence intensity of the tumor and the surrounding tissue (background) is the most used semiquantitative parameter in FGS. Although IHC serves as an indicator for potential clinically useful fluorescent agents, its correlation with the TBR is unknown.

Targets suitable for ADC, SCC, and AIS are CAIX and COLLAGEN XVII. A fluorescent-labeled contrast agent, ^{111}In-DOTA-girentuximab-IRDye800CW, targeting CAIX, has already been clinically investigated and shown to be safe and able to detect all CAIX-positive clear cell renal cell carcinomas.[46] Although EPCAM does not seem to be an optimal target for AIS, it is still a promising target for NSCLC in general. Firstly, it is suitable for ADC and SCC, and these are the most common subtypes of NSCLC. Moreover, a fluorescence-labeled contrast agent VB$_5$-845D- 800CW, a fluorescent agent targeting EPCAM, is currently being tested in healthy volunteers and colorectal cancer patients.[47] The fact that these agents targeting CAIX and EPCAM have already been tested and proven to be safe in patients could facilitate a clinical trial using these agents for the visualization of NSCLC in the short term.

Conclusion

Data-driven selection has proven to be a valuable tool for the identification of novel targets in NSCLC. After histological evaluation, EPCAM, CAIX, and COLLAGEN XVII have been shown to be the most promising targets for NSCLC. However, the clinical potential of these targets for fluorescence-guided surgery has to be confirmed in clinical trials.

REFERENCES

1 Global Burden of Disease Cancer C, Fitzmaurice C, Abate D, Abbasi N, Abbastabar H, Abd-Allah F, Abdel-Rahman O, Abdelalim A, Abdoli A, Abdollahpour I and others. Global, Regional, and National Cancer Incidence, Mortality, Years of Life Lost, Years Lived With Disability, and Disability-Adjusted Life-Years for 29 Cancer Groups, 1990 to 2017: A Systematic Analysis for the Global Burden of Disease Study. JAMA Oncol 2019.

2 National Lung Screening Trial Research T, Aberle DR, Adams AM, Berg CD, Black WC, Clapp JD, Fagerstrom RM, Gareen IF, Gatsonis C, Marcus PM and others. Reduced lung-cancer mortality with low-dose computed tomographic screening. N Engl J Med 2011;365(5):395-409.

3 Walter JE, Heuvelmans MA, de Jong PA, Vliegenthart R, van Ooijen PMA, Peters RB, Ten Haaf K, Yousaf-Khan U, van der Aalst CM, de Bock GH and others. Occurrence and lung cancer probability of new solid nodules at incidence screening with low-dose CT: analysis of data from the randomised, controlled NELSON trial. Lancet Oncol 2016;17(7):907-916.

4 de Koning HJ, van der Aalst CM, de Jong PA, Scholten ET, Nackaerts K, Heuvelmans MA, Lammers JJ, Weenink C, Yousaf-Khan U, Horeweg N and others. Reduced Lung-Cancer Mortality with Volume CT Screening in a Randomized Trial. N Engl J Med 2020;382(6):503-513.

5 Yamato Y, Tsuchida M, Watanabe T, Aoki T, Koizumi N, Umezu H, Hayashi J. Early results of a prospective study of limited resection for bronchioloalveolar adenocarcinoma of the lung. Ann Thorac Surg 2001;71(3):971-4.

6 Chen T, Luo J, Wang R, Gu H, Gu Y, Huang Q, Wang Y, Zheng J, Yang Y, Zhao H. Prognosis of limited resection versus lobectomy in elderly patients with invasive lung adenocarcinoma with tumor size less than or equal to 2 cm. J Thorac Dis 2018;10(4):2231-2239.

7 Yoshizawa A, Motoi N, Riely GJ, Sima CS, Gerald WL, Kris MG, Park BJ, Rusch VW, Travis WD. Impact of proposed IASLC/ATS/ERS classification of lung adenocarcinoma: prognostic subgroups and implications for further revision of staging based on analysis of 514 stage I cases. Mod Pathol 2011;24(5):653-64.

8 Cerfolio RJ, Bryant AS. Is palpation of the nonresected pulmonary lobe(s) required for patients with non-small cell lung cancer? A prospective study. J Thorac Cardiovasc Surg 2008;135(2):261-8.

9 Ellis MC, Hessman CJ, Weerasinghe R, Schipper PH, Vetto JT. Comparison of pulmonary nodule detection rates between preoperative CT imaging and intraoperative lung palpation. Am J Surg 2011;201(5):619-22.

10 Orosco RK, Tapia VJ, Califano JA, Clary B, Cohen EEW, Kane C, Lippman SM, Messer K, Molinolo A, Murphy JD and others. Positive Surgical Margins in the 10 Most Common Solid Cancers. Sci Rep 2018;8(1):5686.

11 Osarogiagbon RU, Lin CC, Smeltzer MP, Jemal A. Prevalence, Prognostic Implications, and Survival Modulators of Incompletely Resected Non-Small Cell Lung Cancer in the U.S. National Cancer Data Base. J Thorac Oncol 2016;11(1):e5-16.

12 Wind J, Smit EJ, Senan S, Eerenberg JP. Residual disease at the bronchial stump after curative resection for lung cancer. Eur J Cardiothorac Surg 2007;32(1):29-34.

13 Riquet M, Achour K, Foucault C, Le Pimpec Barthes F, Dujon A, Cazes A. Microscopic residual disease after resection for lung cancer: a multifaceted but poor factor of prognosis. Ann Thorac Surg 2010;89(3):870-5.

14 al-Kattan K, Sepsas E, Fountain SW, Townsend ER. Disease recurrence after resection for stage I lung cancer. Eur J Cardiothorac Surg 1997;12(3):380-4.

15 Roth K, Nilsen TI, Hatlen E, Sorensen KS, Hole T, Haaverstad R. Predictors of long time survival after lung cancer surgery: a retrospective cohort study. BMC Pulm Med 2008;8:22.

16 Uramoto H, Tanaka F. Recurrence after surgery in patients with NSCLC. Transl Lung Cancer Res 2014;3(4):242-9.

17 Vahrmeijer AL, Hutteman M, van der Vorst JR, van de Velde CJ, Frangioni JV. Image-guided cancer surgery using near-infrared fluorescence. Nat Rev Clin Oncol 2013;10(9):507-18.

18 Frangioni JV. New technologies for human cancer imaging. J Clin Oncol 2008;26(24):4012-21.

19 van Oosten M, Crane LM, Bart J, van Leeuwen FW, van Dam GM. Selecting Potential Targetable Biomarkers for Imaging Purposes in Colorectal Cancer Using TArget Selection Criteria (TASC): A Novel Target Identification Tool. Transl Oncol 2011;4(2):71-82.

20 Cancer Genome Atlas Research N. Comprehensive genomic characterization of squamous cell lung cancers. Nature 2012;489(7417):519-25.

21 Cancer Genome Atlas Research N. Comprehensive molecular profiling of lung adenocarcinoma. Nature 2014;511(7511):543-50.

22 Consortium GT. The Genotype-Tissue Expression (GTEx) project. Nat Genet 2013;45(6):580-5.

23 Abrams ZB, Johnson TS, Huang K, Payne PRO, Coombes K. A protocol to evaluate RNA sequencing normalization methods. BMC Bioinformatics 2019;20(Suppl 24):679.

24 Bausch-Fluck D, Hofmann A, Bock T, Frei AP, Cerciello F, Jacobs A, Moest H, Omasits U, Gundry RL, Yoon C and others. A mass spectrometric-derived cell surface protein atlas. PLoS One 2015;10(3):e0121314.

25 Bausch-Fluck D, Goldmann U, Muller S, van Oostrum M, Muller M, Schubert OT, Wollscheid B. The in silico human surfaceome. Proc Natl Acad Sci U S A 2018;115(46):E10988-E10997.

26 Fonseca AL, da Silva VL, da Fonseca MM, Meira IT, da Silva TE, Kroll JE, Ribeiro-Dos-Santos AM, Freitas CR, Furtado R, de Souza JE and others. Bioinformatics Analysis of the Human Surfaceome Reveals New Targets for a Variety of Tumor Types. Int J Genomics 2016;2016:8346198.

27 Ritchie ME, Phipson B, Wu D, Hu Y, Law CW, Shi W, Smyth GK. limma powers differential expression analyses for RNA-sequencing and microarray studies. Nucleic Acids Res 2015;43(7):e47.

28 Zhang JZ, Ismail-Beigi F. Activation of Glut1 glucose transporter in human erythrocytes. Arch Biochem Biophys 1998;356(1):86-92.

29 Imrich S, Hachmeister M, Gires O. EpCAM and its potential role in tumor-initiating cells. Cell Adh Migr 2012;6(1):30-8.

30 Lonergan KM, Chari R, Coe BP, Wilson IM, Tsao MS, Ng RT, Macaulay C, Lam S, Lam WL. Transcriptome profiles of carcinoma-in-situ and invasive non-small cell lung cancer as revealed by SAGE. PLoS One 2010;5(2):e9162.

31 Zito Marino F, Bianco R, Accardo M, Ronchi A, Cozzolino I, Morgillo F, Rossi G, Franco R. Molecular heterogeneity in lung cancer: from mechanisms of origin to clinical implications. Int J Med Sci 2019;16(7):981-989.

32 Carnio S, Novello S, Papotti M, Loiacono M, Scagliotti GV. Prognostic and predictive biomarkers in early stage non-small cell lung cancer: tumor based approaches including gene signatures. Transl Lung Cancer Res 2013;2(5):372-81.

33 Predina JD, Newton AD, Xia L, Corbett C, Connolly C, Shin M, Sulyok LF, Litzky L, Deshpande C, Nie S and others. An open label trial of folate receptor-targeted intraoperative molecular imaging to localize pulmonary squamous cell carcinomas. Oncotarget 2018;9(17):13517-13529.

34 Predina JD, Newton AD, Keating J, Dunbar A, Connolly C, Baldassari M, Mizelle J, Xia L, Deshpande C, Kucharczuk J and others. A Phase I Clinical Trial of Targeted Intraoperative Molecular Imaging for Pulmonary Adenocarcinomas. Ann Thorac Surg 2018;105(3):901-908.

35 O'Shannessy DJ, Yu G, Smale R, Fu YS, Singhal S, Thiel RP, Somers EB, Vachani A. Folate receptor alpha expression in lung cancer: diagnostic and prognostic significance. Oncotarget 2012;3(4):414-25.

36 Cagle PT, Zhai QJ, Murphy L, Low PS. Folate receptor in adenocarcinoma and squamous cell carcinoma of the lung: potential target for folate-linked therapeutic agents. Arch Pathol Lab Med 2013;137(2):241-4.

37 Boogerd LS, van der Valk MJ, Boonstra MC, Prevoo HA, Hilling DE, van de Velde CJ, Sier CF, Fariña Sarasqueta A, Vahrmeijer AL. Biomarker expression in rectal cancer tissue before and after neoadjuvant therapy. Onco Targets Ther 2018;11:1655-1664.

38 Li X, Xu K, Cen R, Deng J, Hao Z, Liu J, Takizawa H, Ng CSH, Marulli G, Kim MP and others. Preoperative computer tomography-guided indocyanine green injection is associated with successful localization of small pulmonary nodules. Transl Lung Cancer Res 2021;10(5):2229-2236.

39 Quan YH, Oh CH, Jung D, Lim JY, Choi BH, Rho J, Choi Y, Han KN, Kim BM, Kim C and others. Evaluation of Intraoperative Near-Infrared Fluorescence Visualization of the Lung Tumor Margin With Indocyanine Green Inhalation. JAMA Surg 2020;155(8):732-740.

40 Huang C, Liang J, Lei X, Xu X, Xiao Z, Luo L. Diagnostic Performance of Perfusion Computed Tomography for Differentiating Lung Cancer from Benign Lesions: A Meta-Analysis. Med Sci Monit 2019;25:3485-3494.

41 Bharadwaj S. Evaluation of IRDye800CW-nimotuzumab in Lung Cancer Surgery

42 Rosenthal E. A Phase I/II Study Evaluating the Safety and Pharmacokinetics of Panitumumab-IRDye800 as an Optical Imaging Agent to Detect Lung Cancer During Surgical Procedures

43 A Phase 2a, Single-dose, Open-label Study to Evaluate Diagnostic Performance, Safety & Timing of Postdose Imaging of ONM-100, an Intraoperative Fluorescence Imaging Agent for the Detection of Cancer, in Patients With Solid Tumors Undergoing Routine Surgery

44 S. S. Intraoperative Imaging of Pulmonary Nodules by SGM-101.

45 A.L. V. Intraoperative Molecular Imaging Of Pulmonary Nodules By SGM-101, A Fluorochrome-Labeled Anti-Carcino-Embryonic Antigen (CEA) Monoclonal Antibody

46 Hekman MC, Rijpkema M, Muselaers CH, Oosterwijk E, Hulsbergen-Van de Kaa CA, Boerman OC, Oyen WJ, Langenhuijsen JF, Mulders PF. Tumor-targeted Dual-modality Imaging to Improve Intraoperative Visualization of Clear Cell Renal Cell Carcinoma: A First in Man Study. Theranostics 2018;8(8):2161-2170.

47 A.L. V. A phase I study assessing the safety and performance of VB5-845D-800CW, an anti-Epcam fluorescent agent, for the intraoperative detection of gastrointestinal cancer.

SUMMARY, DISCUSSION AND FUTURE PERSPECTIVES

The rapidly evolving field of near-infrared (NIR) fluorescence-guided surgery is gradually finding its way into the clinic. Before becoming standard of care patient benefit needs to be unequivocally demonstrated. This thesis primarily focuses on clinical applications for NIR fluorescence-guided surgery in colorectal surgery. Both targeted and non-targeted fluorescent agents are addressed.

PART I: NIR FLUORESCENCE IMAGING IN COLORECTAL CANCER SURGERY

The first part of this thesis focuses on the use of NIR fluorescence imaging in colorectal cancer patients. It includes an extensive review followed by three chapters that detail studies involving non-targeted fluorescent agents.

Chapter 2 comprises a comprehensive overview of fluorescence-guided surgery in colorectal cancer. It displays current clinically available applications, and focuses on promising future modalities. The discussed applications encompass the imaging of primary and recurrent colorectal tumors, sentinel lymph node imaging, visualization of peritoneal and liver metastases, nerve imaging, urinary tract imaging, as well as perfusion assessment. The first studies show additional value of this technique regarding change in surgical management. Future trials should focus on patient related outcomes such as quality of life, complication rates, disease free survival, and overall survival.

In **chapter 3** of this thesis, the literature on the application of NIR fluorescence imaging for sentinel lymph node (SLN) mapping in colorectal surgery is examined. SLN mapping shows promise as a valuable tool in the treatment of colorectal cancer patients. Nevertheless, conventional lymph node mapping methods using a combination of a radiocolloid tracer and patent blue, face limitations because of poor depth penetration of patent blue, while the logistical challenges associated with radiocolloid tracer pose additional hurdles. With NIR fluorescence imaging, the SLN can be accurately identified in most patients resulting in more accurate lymph node staging. Despite its potential benefits, current technical challenges (like endoscopic dye injection and the low negative predictive value of the SLN) withhold surgeons from incorporating this application into routine practice.

Despite the promising results on indocyanine green (ICG) perfusion analysis there is still debate about the interpretation of the observed fluorescence signal. The current visual interpretation is subjective and therefore hampers standardisation. In **Chapter 4**, a case study, four patients are described with possible compromised bowel perfusion after mesenteric resection, revealing challenges in interpreting uncorrected fluorescence signals. This study emphasizes the importance of quantifying NIR fluorescence signals for assessing tissue perfusion during surgery. Bowel perfusion, as assessed clinically by independent surgeons based on NIR fluorescence imaging, resulted in different treatment strategies, three with excellent clinical outcome, but one with a perfusion related complication, highlighting the complexities of interpreting uncorrected fluorescence signals. Post- surgery quantitative analysis of fluorescence dynamics showed different patterns in the affected bowel segment compared to the unaffected reference segments for the four patients. The study suggests that real-time standardized quantification of NIR fluorescence imaging could improve surgical decision-making in the future. However, few studies explore the use of quantification software beyond feasibility due to method limitations.[1]

Chapter 5 introduces a protocol for a multicenter, randomized controlled clinical trial evaluating the effectiveness of NIR fluorescence imaging with ICG in reducing anastomotic leakage (AL) rate in colorectal surgery. In the final study, 931 patients were randomized between the Fluorescence Guided Bowel Anastomosis group and the Conventional Bowel Anastomosis group.[2] There was no significant differences in overall AL rate. However, subgroup analysis showed a significantly lower AL rate in patients undergoing left-sided colorectal surgery, especially for patients who underwent rectosigmoid resection. It underlines the value of NIR fluorescence imaging with ICG in reducing anastomotic leakage rates in colorectal surgery.

PART II: INTRAOPERATIVE IMAGING USING SGM-101; A TUMOR TARGETED NIR FLUOROPHORE

The second part of this thesis focusses on the clinical results of the carcinoembryonic antigen (CEA) specific antibody SGM-101. This anti-CEA fluorescent antibody is primarily used in colorectal cancer, but other malignancies have been studied as well.

The process of clinical translation of novel fluorescent agents is an essential part in the evolution of NIR fluorescence guided surgery. **Chapter 6** gives an overview of the clinical translation of SGM-101, a novel fluorescent anti-CEA monoclonal antibody.

SGM-101 can aid in improving detection and complete resection for CEA-positive tumors. In **chapter 7**, the performance of SGM-101 for the detection of colorectal and pancreatic liver metastases was investigated. In this pilot study,

all clinically suspected malignant lesions were detected with NIR fluorescence-guided surgery. These findings show that SGM-101 can facilitate real-time detection of liver metastases, potentially aiding surgeons in achieving more precise and complete tumor removal.

On the contrary, only 31% of the colorectal lung metastases were intraoperatively detected (**chapter 8**). In this chapter we have explored the feasibility of NIR fluorescence-guided surgery, using SGM-101, for the detection of colorectal lung metastases. Metastasectomy is a common treatment option for patients with colorectal lung metastases (CLM). Challenges exist with margin assessment and identification of small nodules, especially during minimally invasive surgery. Intraoperative fluorescence imaging has the potential to overcome these challenges. The study focuses on *in vivo*, back table, and closed-field bread loaf imaging. It demonstrated the potential of fluorescence imaging of CLM with SGM-101. CEA expression was observed in all tumors and closed-field imaging showed excellent CEA specific targeting of the tracer to the tumor nodules. The full potential of SGM-101 for *in vivo* detection of the tracer can be achieved with improved minimal invasive imaging systems and optimal patient selection.

The difference between colorectal liver and lung metastases may be a consequence of the use of minimal invasive NIR fluorescence imaging systems, as this was used in most lung metastases cases (85%), but in only 1 (9,1%) of the liver procedures. Moreover, closed-field imaging showed excellent results for colorectal lung metastases. This confirms the hypothesis that improving minimal invasive NIR systems should lead to better intraoperative imaging results. The promising results from those phase I/II studies served as the basis for a phase III multicentre trial (NCT03659448), including patients in Europe and the US. This trial focuses on primary, recurrent and abdominal metastatic colorectal cancer, aiming to demonstrate added value of fluorescence guided surgery regarding resection margins and the detection of additional lesions.

Chapter 9 reports on the first in-human surgical trial using SGM-101 to evaluate the suitability for molecular imaging-guided lung cancer resections, along with its correlation with the expression of carcinoembryonic antigen-related cell adhesion molecule type 5 (CEACAM5) glycoprotein. Among the 4 patients undergoing surgery, lesions with 2+ and 3+ tissue CEACAM5 expression had outstanding tumor fluorescence, displaying a mean tumor-to-background ratio of 3.1. Conversely, the absence of SGM-101 fluorescence was linked to benign lesions and a lack of CEACAM5 staining. This study demonstrated SGM-101 localization to CEACAM5-positive tumors with the detection of real-time near-infrared fluorescence in situ, *ex vivo*, and by immunofluorescence microscopy. These findings suggest that SGM-101 is a receptor-specific, and feasible intraoperative molecular imaging fluorochrome that should be further evaluated in randomized clinical trials.

PART III: NEW WAYS FOR IDENTIFICATION OF NOVEL TARGETS FOR NIR FLUORESCENCE IMAGING

The final section of this thesis focuses on the future: finding new targets for NIR fluorescence imaging.

Selection of novel cell surface biomarkers for fluorescence-guided surgery is conventionally done by reviewing key publications from recent literature. Unfortunately, this is time consuming. Nowadays a data driven selection method is available that combines multiple databases and interlinks literature (**chapter 10**). This chapter encompasses a study assessing cell surface biomarkers for non-small cell lung cancer that are potentially suitable for fluorescence-guided surgery. The selection of these biomarkers involves a data driven selection using >275 multi-omics databases, literature, and experimental evidence. Ten biomarkers were selected, and tumor expression was assessed by immunohistochemical staining. Epithelial cell adhesion molecule (EPCAM), carbonic anhydrase 9 (CAIX), and collagen type XVII alpha 1 chain (COLLAGEN XVII) were identified as promising targets for intraoperative fluorescence imaging for both major subtypes of non-small cell lung carcinomas and should be investigated further in future studies. This approach offers researchers unique insights and has the potential to significantly reduce the time required compared to a conventional literature search. On the other hand, data driven selection can lead to new targets, for which no clinical fluorescent target ligands are yet available. These completely new targets will therefore require more research, probably including immunohistochemistry (IHC). Although IHC serves as an indicator for potential clinically useful fluorescent agents, its correlation with NIR fluorescence-guided surgery endpoints, like the tumor-to-background ratio, is unknown.

In conclusion, this thesis underscores the burgeoning potential of NIR fluorescence-guided surgery, especially in colorectal cancer. Through comprehensive analyses of both targeted and non-targeted fluorescent agents, significant advancements have been identified that could transform surgical precision and patient outcomes. Despite promising preliminary results,

challenges such as standardization of fluorescence signal interpretation and technical limitations of current imaging systems persist. Future research should focus on large-scale clinical trials to unequivocally demonstrate patient benefits, refine imaging techniques, and explore new biomarkers for a broader range of malignancies. Ultimately, the integration of NIR fluorescence-guided surgery into routine practice hinges on continuous innovation and robust clinical validation to enhance surgical accuracy and patient care.

REFERENCES

1 Van Den Hoven P, Osterkamp J, Nerup N, Svendsen MBS, Vahrmeijer A, Van Der Vorst JR, *et al.* Quantitative perfusion assessment using indocyanine green during surgery-current applications and recommendations for future use. Langenbecks Arch Surg. 2023;408(1):67.

2 Faber RA, Meijer RPJ, Droogh DHM, Jongbloed JJ, Bijlstra OD, Boersma F, *et al.* Indocyanine green near-infrared fluorescence bowel perfusion assessment to prevent anastomotic leakage in minimally invasive colorectal surgery (AVOID): a multicentre, randomised, controlled, phase 3 trial. Lancet Gastroenterol Hepatol. 2024.

APPENDICES

Nederlandse samenvatting

Met bijna 2 miljoen nieuwe gevallen per jaar is het colorectaal carcinoom een van de meest voorkomende vormen van kanker wereldwijd. Ondanks screeningprogramma's en verbeterde niet-invasieve behandelingsopties blijft chirurgie de hoeksteen van de behandeling. Twee belangrijke factoren bepalen het succes van chirurgie: complete tumorresectie inclusief metastasen en het minimaliseren van chirurgische complicaties.

DEEL I: NIR-FLUORESCENTIEBEELDVORMING BIJ ONCOLOGISCHE COLORECTALE CHIRURGIE

Het eerste deel van dit proefschrift richt zich op de toepassing van nabij-infrarood (NIR) fluorescentiebeeldvorming bij oncologische colorectale chirurgie. Dit deel begint met een uitgebreide literatuurreview, gevolgd door klinische studies waarin zowel niet-specifieke (non-targeted) als tumor-specifieke (targeted) fluorescentiemiddelen worden onderzocht.

In **hoofdstuk 2** wordt een overzicht gegeven van de huidige klinische toepassingen van fluorescentiegeleide chirurgie bij colorectale kanker. De besproken toepassingen omvatten beeldvorming van primaire en recidiverende tumoren, schildwachtklierprocedures, visualisatie van peritoneale en levermetastasen, zenuw- en urinewegbeeldvorming, en beoordeling van weefselperfusie. De eerste klinische studies tonen aan dat deze technieken bijdragen aan veranderingen in het chirurgisch beleid. Toekomstig onderzoek moet zich richten op patiëntgerelateerde uitkomsten zoals kwaliteit van leven, complicaties, ziektevrije overleving en algehele overleving.

Hoofdstuk 3 richt zich op NIR-fluorescentiebeeldvorming voor schildwachtklierdetectie in colorectale chirurgie. De conventionele methoden, zoals patent blauw en radiocolloïden, hebben beperkingen door respectievelijk een beperkte weefselpenetratie en logistieke uitdagingen. NIR-fluorescentie kan de schildwachtklier nauwkeurig identificeren en de lymfeklierstadiering verbeteren. Technische uitdagingen, zoals de noodzaak van endoscopische injectie en een lage negatief voorspellende waarde, beperken echter de implementatie in de klinische praktijk.

In **hoofdstuk 4** wordt een casusstudie beschreven waarin de interpretatie van fluorescentiesignalen bij darmperfusie wordt onderzocht. Bij vier patiënten met een mogelijk verminderde darmperfusie na mesenteriale resectie blijkt dat subjectieve beoordeling van fluorescentiesignalen kan leiden tot variatie in behandelstrategieën. Dit hoofdstuk benadrukt het belang van een gestandaardiseerde en kwantitatieve benadering van fluorescentiesignalen voor een beter onderbouwde chirurgische besluitvorming.

Hoofdstuk 5 introduceert een protocol voor een multicenter, gerandomiseerde klinische studie waarin de effectiviteit van indocyanine groen (ICG)-fluorescentiebeeldvorming bij het verminderen van naadlekkage in colorectale chirurgie wordt onderzocht. In de uiteindelijke studie werden 931 patiënten gerandomiseerd tussen een fluorescentiegeleide anastomosegroep en een conventionele anastomosegroep. Hoewel er geen significant verschil werd gevonden in het totale percentage naadlekkages, toonde subgroepanalyse een lager risico bij patiënten die een linkszijdige colorectale resectie ondergingen, vooral bij rectosigmoïdresecties.

DEEL II: INTRA-OPERATIEVE BEELDVORMING MET SGM-101; EEN TUMOR-SPECIFIEKE NIR-FLUOROFOOR

Het tweede deel van dit proefschrift richt zich op de klinische resultaten van SGM-101, een fluorescerend antilichaam dat zich specifiek richt op het carcino-embryonaal antigeen (CEA). Dit middel wordt voornamelijk gebruikt voor de beeldvorming van colorectale kanker, maar er wordt ook onderzoek gedaan naar toepassingen bij andere maligniteiten.

Hoofdstuk 6 beschrijft de klinische vertaling van SGM-101 van laboratoriumonderzoek naar toepassing in klinische trials. SGM-101 heeft de potentie om de detectie en complete resectie van CEA-positieve tumoren te verbeteren door middel van intra-operatieve fluorescentiegeleide chirurgie.

In **hoofdstuk 7** wordt het vermogen van SGM-101 om levermetastasen van een pancreas- of coloncarcinoom te detecteren onderzocht. In een pilotstudie werden alle klinisch verdachte metastasen geïdentificeerd met fluorescentiegeleide chirurgie, wat suggereert dat SGM-101 kan bijdragen aan nauwkeurigere tumorresecties.

Hoofdstuk 8 richt zich op de haalbaarheid van NIR-fluorescentiegeleide chirurgie met SGM-101 voor de detectie van colorectale longmetastasen. De detectiegraad *in vivo* bleek lager (31%) dan bij levermetastasen, waarschijnlijk door het gebruik van minimaal invasieve NIR-systemen. Dit resultaat suggereert dat verbeterde laparoscopische NIR-systemen en een zorgvuldige patiëntselectie nodig zijn om het volledige potentieel van SGM-101 te benutten.

In **hoofdstuk 9** wordt de eerste klinische studie beschreven waarin SGM-101 wordt gebruikt voor moleculaire beeldvorming bij longkanker. De resultaten tonen aan dat SGM-101 zich specifiek richt op CEACAM5-positieve tumoren met een hoge tumor-achtergrond ratio. Deze bevindingen bevestigen de

haalbaarheid van SGM-101 als intraoperatieve fluorescerende tracer en vormen de basis voor verdere klinische trials.

DEEL III: IDENTIFICATIE VAN NIEUWE BIOMARKERS VOOR FLUORESCENTIEGELEIDE CHIRURGIE

Het laatste deel van dit proefschrift richt zich op de toekomst van NIR-fluorescentiebeeldvorming en de ontwikkeling van nieuwe biomarkers.

In **hoofdstuk 10** wordt een data-gedreven methode geïntroduceerd voor het selecteren van nieuwe moleculaire doelwitten voor fluorescentiegeleide chirurgie. Met behulp van meer dan 275 multi-omics databases worden potentiële biomarkers voor het niet-kleincellig longcarcinoom geïdentificeerd. Dit resulteert in de selectie van tien kandidaat-biomarkers, waarvan epithelial cell adhesion molecule (EPCAM), carbonic anhydrase 9 (CAIX) en collagen type XVII alpha 1 chain (COLLAGEN XVII) als veelbelovende doelen worden aangemerkt. Dit hoofdstuk benadrukt dat bio-informatica kan bijdragen aan een snellere en efficiëntere ontwikkeling van nieuwe fluorescentiemiddelen.

CONCLUSIE EN TOEKOMSTPERSPECTIEF

Dit proefschrift laat zien dat NIR-fluorescentiegeleide chirurgie een veelbelovende techniek is voor het verbeteren van chirurgische precisie en oncologische uitkomsten bij het colorectaal carcinoom. Zowel niet-specifieke als tumor-specifieke fluorescentiemiddelen dragen bij aan een betere intra-operatieve detectie van tumoren, verbeterde beoordeling van weefselperfusie en optimalisatie van chirurgische beslissingen. De studies tonen aan dat technieken met SGM-101 en ICG waardevolle hulpmiddelen kunnen zijn, maar dat verdere standaardisatie en validatie in grootschalige klinische trials noodzakelijk is.

Toekomstige onderzoeken moeten zich richten op de integratie van geavanceerde beeldvormingssystemen, zoals verbeterde minimaal invasieve NIR-camera's, en de ontwikkeling van nieuwe biomarkers die nog beter onderscheid maken tussen tumor- en gezond weefsel. Daarnaast zal kwantitatieve analyse van fluorescentiesignalen bijdragen aan een meer objectieve en reproduceerbare interpretatie van de beeldvorming.

Hoewel er nog uitdagingen bestaan, bieden de bevindingen uit dit proefschrift een solide basis voor verdere klinische implementatie van NIR-fluorescentiegeleide chirurgie. De uiteindelijke doelstelling is om deze technologie te integreren in de standaardzorg, zodat patiënten profiteren van nauwkeurigere operaties, minder complicaties en verbeterde oncologische uitkomsten.

CURRICULUM VITAE

Ruben Petrus Johannes Meijer werd op 26 april 1990 geboren te Voorburg. Hij groeide op in Rijswijk en behaalde in 2008 zijn VWO-diploma aan het Huygenslyceum in Voorburg. Vervolgens startte hij de studie Geneeskunde aan de Erasmus Universiteit Rotterdam. Gedurende zijn studie werkte Ruben onder andere in het Sophia Kinderziekenhuis, waar hij actief betrokken was bij wetenschappelijk onderzoek.

Na het behalen van zijn masterdiploma begon Ruben als arts-assistent (ANIOS) orthopedie van het Reinier de Graaf Gasthuis. Vervolgens werkte hij als ANIOS bij de orthopedie van het Alrijne Ziekenhuis en bij de heelkunde van het Haaglanden Medisch Centrum. In 2018 begon Ruben als promovendus binnen de Green Light Leiden-groep, onder leiding van Prof. dr. J. Burggraaf, Prof. dr. A.L. Vahrmeijer (promotoren) en dr. D.E. Hilling (copromotor). Zijn onderzoek richtte zich voornamelijk op het opzetten en uitvoeren van (inter)nationale fase 3-studies binnen de fluorescentie-geleide chirurgie.

Na zijn fulltime onderzoeksperiode werkte Ruben als ANIOS bij de heelkunde van het Alrijne Ziekenhuis en bij de acute psychiatrie van GGZ Rivierduinen. In 2023 startte hij met de opleiding tot huisarts, die hij naar verwachting in augustus 2025 zal afronden.

LIST OF PUBLICATIONS

Feb. 2025 **Meijer RPJ**, Silven AV, Borgdorff H. 'Effect acupunctuur bij aspecifieke lagerugpijn twijfelachtig'; Huisarts & Wetenschap

Oct. 2024 Faber RA, **Meijer RPJ**, Droogh DHM, Jongbloed JJ, Bijlstra OD, Boersma F, Braak JPBM, Meershoek-Klein Kranenbarg E, Putter H, Holman FA, Mieog JSD, Neijenhuis PA, van Staveren E, Bloemen JG, Burger JWA, Aukema TS, Brouwers MAM, Marinelli AWKS, Westerterp M, Doornebosch PG, van der Weijde A, Bosscha K, Handgraaf HJM, Consten ECJ, Sikkenk DJ, Burggraaf J, Keereweer S, van der Vorst JR, Hutteman M, Peeters KCMJ, Vahrmeijer AL, Hilling DE. 'Indocyanine green near-infrared fluorescence bowel perfusion assessment to prevent anastomotic leakage in minimally invasive colorectal surgery (AVOID): a multicentre, randomised, controlled, phase 3 trial'; Lancet Gastroenterol. Hepatol.-PMID: 39151436

Aug. 2024 **Meijer RPJ**, Galema HA, Faber RA, Bijlstra OD, Maat APWM, Cailler F, Braun J, Keereweer S, Hilling DE, Burggraaf J, Vahrmeijer AL, Hutteman M 'Intraoperative molecular imaging of colorectal lung metastases with SGM-101: a feasibility study'; Eur J Nucl Med Mol Imaging-PMID: 37552367

Jan. 2023 Azari F, **Meijer RPJ**, Kennedy GT, Chang A, Nadeem B, Din A, Marfatia I, Pèlegrin A, Framery B, Cailler F, Sullivan NT, Kucharczuk J, Martin L, Vahrmeijer AL, Singhal S. 'CEACAM5 Receptor Targeted Fluorescent Intraoperative Molecular Imaging Tracer Localizes to Carcinoembryonic Antigen Expressing Malignant Lung Nodules: Results from First In-Human SGM-101 Guided Lung Cancer Surgical Trial'; JAMA Network Open-PMID: 36705924

Feb. 2023 **Meijer RPJ**, Neijenhuis LKA, Zeilstra AP, Roerink SF, Bhairosingh SS, Hilling DE, Mieog JSD, Kuppen PJK, Sier CFM, Braun J, Burggraaf J, Vahrmeijer AL, Cohen D, Hutteman M. 'Data-Driven Identification of Targets for Fluorescence-Guided Surgery in Non-Small Cell Lung Cancer'; Mol Imaging Biol.-PMID: 36575340

Apr. 2022 **Meijer RPJ**, Faber RA, Bijlstra OD, Braak JPBM, Meershoek-Klein Kranenbarg E, Putter H, Mieog JSD, Burggraaf K, Vahrmeijer AL, Hilling DE, AVOID study group. 'AVOID; a phase III, randomised controlled tirla using indocyanine green for the prevention of anastomotic leakage in colorectal surgery'; BMJ open-PMID: 35365509

Mar. 2022 Kalisvaart GM, **Meijer RPJ**, Bijlstra OD, Galema HA, de Steur WO, Hartgrink HH, Verhoef C, de Geus-Oei LF, Grünhagen DJ, Schrage YM, Vahrmeijer AL, van der Hage JA. 'Intraoperative near-infrared fluorescence imaging with indocyanine green for identification of gastrointestinal stromal tumors (GISTs), a feasibility study'; Cancers-PMID: 35326721

Oct. 2021 Galema HA, **Meijer RPJ**, Lauwerends LJ, Verhoef C, Burggraaf J, Vahrmeijer AL, Hutteman M, Keereweer S, Hilling DE. 'Fluorescence-guided surgery in colorectal cancer; A review on clinical results and future perspectives'; European Journal of Surgical Oncology-PMID: 34657780

Aug. 2021 van Schie P, Gerritsen M, van der Lelij TJN, **Meijer RPJ**, van Arkel ERA, Fiocco M, Swen JA, Vahrmeijer AL, Hazelbag HM, Keereweer S, van Driel PBAA. 'Intra-operative assessment of the vascularisation of a cross section of the meniscus using near-infrared fluorescence imaging'; Knee Surgery, Sports Traumatology, Arthroscopy-PMID: 34347140

Jun. 2021 **Meijer RPJ**, van Manen L, Hartgrink HH, Burggraaf J, Gioux S, Vahrmeijer AL, Mieog JSD. 'Quantitative dynamic near-infrared fluorescence imaging using indocyanine green for analysis of bowel perfusion after mesenteric resection'; Journal of

Biomedical Optics-PMID: 34109769

Nov. 2020 **Meijer RPJ**, de Valk KS, Deken MM, Boogerd LSF, Hoogstins CES, Bhairosingh SS, Swijnenburg R, Bonsing BA, Framery B, Fariña Sarasqueta A, Putter H, Hilling DE, Burggraaf J, Cailler F, Mieog JSD, Vahrmeijer AL. 'Intraoperative detection of colorectal and pancreatic liver metastases using SGM-101, a fluorescent antibody targeting CEA'; European Journal of Surgical Oncology-PMID: 33158638

Nov. 2020 Achterberg FB, Sibinga Mulder BG, **Meijer RPJ**, Bonsing BA, Hartgrink HH, Mieog JSD, Zlitni A, Park S, Fariña Sarasqueta A, Vahrmeijer AL, Swijnenburg R. 'Real-time surgical margin assessment using ICG-fluorescence during laparoscopic and robot-assisted resections of colorectal liver metastases'; Annals of Translational Medicine-PMID: 33313193

Oct. 2020 de Valk KS, Deken MM, Schaap DP, **Meijer RPJ**, Boogerd LSF, Hoogstins CES, van der Valk MJ, Kamerling IM, Bhairosingh SS, Framery B, Hilling DE, Peeters K, Holman FA, Kusters M, Rutten HJ, Cailler F, Burggraaf J, Vahrmeijer AL. 'Dose-Finding Study of a CEA-Targeting Agent, SGM-101, for Intraoperative Fluorescence Imaging of Colorectal Cancer'; Annals of Surgical Oncology-PMID: 33034788

Aug. 2020 Achterberg FB, Deken MM, **Meijer RPJ**, Mieog JSD, Burggraaf J, van de Velde CJH, Swijnenburg RJ, Vahrmeijer AL. 'Clinical translation and implementation of optical imaging agents for precision image-guided cancer surgery'; European Journal of Nuclear Medicine and Molecular Imaging-PMID: 32783112

Mar. 2020 Schaap DP, de Valk KS, Deken MM, **Meijer RPJ**, Burggraaf J, Vahrmeijer AL, Kusters M. 'Carcinoembryonic antigen-specific, fluorescent image-guided cytoreductive surgery with hyperthermic intraperitoneal chemotherapy for metastatic colorectal cancer'; British Journal of Surgery-PMID: 31960953

Feb. 2020 **Meijer RPJ**, de Valk KS, Framery B, Gutowski M, Pèlegrin A, Cailler F, Hilling, DE, Vahrmeijer AL. 'The clinical translation of a near-infrared fluorophore for fluorescence guided surgery: SGM-101 from the lab to a phase III trial'; SPIE proceedings

Apr. 2018 van Leeuwen C, **Meijer RPJ**, Sala M, Eefting D. 'Een Pijnloze Rode Zwelling in de Lies'; Medisch Contact

Apr. 2017 **Meijer RPJ**, Halm JA, Schepers T. 'Unstable Fragility Fractures of the Ankle in the Elderly; Transarticular Steinmann Pin or External Fixation'; The Foot-PMID: 28672133

Apr. 2017 **Meijer RPJ**, Jasper J, Snoeker B, Jansen J. 'A pseudotumour of the thigh: tensor fasciae latae muscle hypertrophy due to an underlying abductor tendon tear'; BMJ Case Reports-PMID: 28442457

Sep. 2014 den Boer SL, **Meijer RPJ**, van Iperen GG , ten Harkel AD, du Marchie Sarvaas GJ, Straver B, Rammeloo LA, Tanke RB, van Kampen JJ, Dalinghaus M. 'Evaluation of the diagnostic work-up in children with myocarditis and idiopathic dilated cardiomyopathy'; Pediatric Cardiology-PMID: 25194576

DANKWOORD

Lieve patiënten, dank voor jullie vertrouwen en onbaatzuchtige deelname. Jullie keuze voor de toekomst van anderen in tijden van onzekerheid is indrukwekkend.

Prof. dr. Burggraaf, beste Koos, kritisch, maar altijd onderbouwd was je er altijd precies wanneer het nodig was. Vaak de laatste stok achter de deur, dank daarvoor.

Prof. dr. Vahrmeijer, beste Lex, wat een eer om de eerste te zijn die je professor mag noemen. Ik heb mogen leren van jouw manier van netwerken, erg bijzonder hoe je over heel de wereld vrienden hebt.

Dr. Hilling, beste Denise, benaderbaar en daarom van onschatbare waarde. Dank voor je aanstekelijke enthousiasme.

Merlijn, zonder jou had ik nooit tegenover Lex gezeten, waarvoor eeuwige dank. En ik zal het missen, niemand noemt me 'Meijertje' zoals jij dat doet.

Sven, zijdelings betrokken, maar juist daarom was jouw steun op het juiste moment erg waardevol.

Het was een voorrecht om deel uit te maken van Green Light Leiden. Marion, samen in een Canadees tentje en lunchen om half 11, heerlijk. Maar bovenal koester ik de band, ook met 200 kilometer afstand. Kim, jouw quotes zijn ongeëvenaard, ik mis ze. Friso, van samen op 11A/B naar samen op J3, dank voor de mooie tijd. Judith, ik heb genoten die verfrissende energie in de laatste periode.

Hidde, ouwe Rotterdammer, dank voor de vlekkeloze samenwerking.

Chères Françoise et Bérénice, merci pour votre confiance dans le grand projet de l'étude de phase III. J'espère sincèrement que ce projet aidera à la fois les patients et SurgiMab à avancer.

Graziella en Dorien, infuusdagen zijn lang, maar jullie maakten ze vrolijk en zorgeloos. Jeffrey en Elma, dank voor het vergemakkelijken van mijn PhD-leven.

Lang niet gedacht ooit een afdeling psychiatrie te bedanken. Echter, oud-collega's van de crisisdienst GGZ Rivierduinen, dank voor de zachte landing in een tijd van enorme teleurstelling.

Hans en Ingrid, elke dag met jullie in de praktijk voelde vertrouwd. Dank voor de rotsvaste basis als huisarts. Paul en Meike, in Zoetermeer leer ik de fijne kneepjes van het vak en ben ik er klaar voor.

Jor en Anouk, een stevig vangnet waar ik vaak mee heb gelachen, maar soms een traan heb kunnen laten. Zonder jullie had dit boekje veel meer moeite gekost.

Maat, onderuitgezakt een film en comfortfood, je weet zelf misschien niet eens hoe fijn ik dat vond. Laten we dat blijven doen.

Bart en Martijn, het begon zo mooi met een blinddate. Dank dat jullie vandaag naast mij wilden staan. Bart, stoom afblazen met jou is een makkie. Het idee van jou, in een rokkostuum naast mij, heeft het laatste duwtje gegeven aan dit boekwerk. Martijn, ik had een enorme omweg nodig om erachter te komen dat ik je collega wil blijven. Hoe innig deze samenwerking wordt moet nog blijken, maar als vriend waardeer ik je enorm. Jouw warme en open houding is ongeëvenaard.

Timmy en Lau, maar weinigen waren altijd zo oprecht geïnteresseerd als jullie. En dank voor die onuitputbare energie met de kids.

Rik, een nabij voorbeeld. Vaak motiverend én kritisch. Gelukkig was Jolanda er voor de zachte nuancering. Dank voor jullie warme basis. En oma Limbo, altijd liefdevol steunend en ik weet zeker dat ook opa Huub fier is.

Opa Piet, uw stimulans gaf mij kansen die u nooit kreeg. Oma Bep, een voorbeeld-oma, een goed kleinkind bouw je op pannenkoeken en tomatensoep. Dank voor jullie oprechte trots.

Opa en oma Meijer, bedankt voor jullie betrokkenheid. Fijn dat jullie er voor me zijn.

Maybs, zusje. Niet altijd makkelijk, maar vol bewondering zie ik je steeds meer jezelf worden. Ga zo door. En Ramon, broertje, heerlijk om met jou de mooiste hobby van de wereld te delen en een genuanceerdere versie van mezelf voorgeschoteld te krijgen. Dank dat je in alles mijn broer en vriend bent!

Sven, nu ik vader ben bewonder ik des te meer hoe jij in die rol bent gestapt. Jouw invloeden geven het leven kleur, zeker het mijne.

Pa, wat herken ik mezelf in jou; bloedfanatiek en eigenwijs. Eigenschappen die m'n promotie (on)mogelijk hebben gemaakt. Andrea, wat ben jij een geschenk, de lijm van het gezin. Dank voor jullie

Mam, jij liet mij al vroeg zien wat doorzetten is. Jouw onvoorwaardelijke steun legde de basis waarop dit boekje is gebouwd. De rots in de branding waar ik, Nienke en de kids altijd op terug kunnen vallen. Wees trots op jezelf! En Ray, ik waardeer dat je af en toe op de rem drukt, bij haar en bij mij.

Lieve Nienke, het slotstuk van dit dankwoord is natuurlijk voor jou. Jouw enorme steun en kritische gesprekken hebben mij door de diepste dalen van het promoveren weten te leiden. Opgerakeld uit de krochten van het 'carrière maken' wist je me altijd weer te motiveren. Maar veel belangrijker dan dit alles, is de liefde voor elkaar. Jij maakt mij beter.